PLANT-SOIL INTERACTIONS AND REDOX STATE SHAPE CARBON TRANSFORMATIONS AND METHANE CYCLING IN COASTAL MARSHES

CLARISSE KOKOÉ ELISABETH GÖSELE | HAMBURG 2025

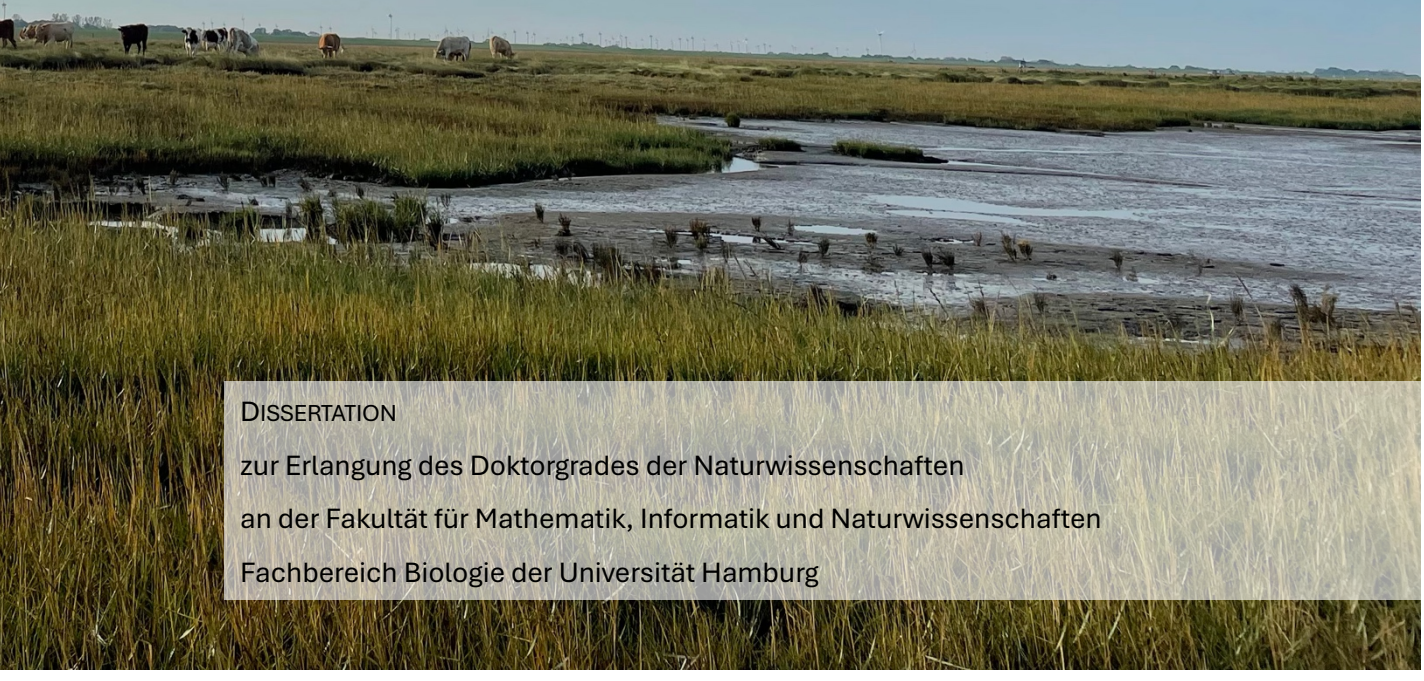

DISSERTATION

zur Erlangung des Doktorgrades der Naturwissenschaften

an der Fakultät für Mathematik, Informatik und Naturwissenschaften

Fachbereich Biologie der Universität Hamburg

Plant-soil interactions and redox state shape carbon transformations and methane cycling in coastal marshes

DISSERTATION

zur Erlangung des Doktorgrades der Naturwissenschaften

an der Fakultät für Mathematik, Informatik und Naturwissenschaften

Fachbereich Biologie

der Universität Hamburg

Vorgelegt von **Clarisse Kokoé Elisabeth Gösele**

Dezember 2025

Hamburg

Supervision: Prof. Dr. Kai Jensen, Prof. Dr. Peter Müller

Submission date: 15.12.2025

Disputation date: 10.04.2026

CONTENTS

ABSTRACT

Coastal marshes play a vital role in regulating the global climate by storing large amounts of carbon. At the same time, they are important natural sources of methane, a potent greenhouse gas. Both carbon storage and methane fluxes are closely linked to soil redox conditions, which vary widely across space and time due to environmental drivers such as salinity, hydrology, and soil organic matter inputs. These drivers not only shape microbial communities that determine redox dynamics but also influence plant species composition. Through their root traits – such as root exudation, turnover, and root oxygen loss – plants actively regulate soil redox conditions and, consequently, control carbon turnover processes and methane cycling. Because plant functional traits respond to the same environmental drivers that control redox states, interactions between plants and their environment are central to understanding variability in methane production and emission. However, the mechanisms linking plant-mediated redox regulation to methane fluxes across contrasting environmental settings and global change pressures (e.g., land-use change, warming) remain poorly understood. This dissertation tests the assumption that coastal marsh plants control soil redox dynamics and thereby regulate carbon transformations and methane emissions across environmental gradients and under global change scenarios. Specifically, it examines how species-specific root traits, represented by belowground biomass and root exudation, shape soil redox conditions that control carbon transformation and methane emissions from coastal marshes.

To address these objectives, Chapter 2 provides an overview of the in this dissertation studied environmentally contrasting coastlines, including the first comprehensive study quantifying soil organic carbon stocks in grazed and ungrazed coastal marshes: the Baltic Sea and the North Sea coasts. Despite comparable soil organic carbon stocks to one meter depth, the contrasting tidal and sedimentary regimes led to higher topsoil soil organic carbon accumulation in the Baltic Sea. Livestock grazing enhanced topsoil soil organic carbon in North Sea marshes, presumably through trampling-induced alterations of soil biogeochemistry, whereas soil organic carbon dynamics in Baltic Sea marshes were primarily controlled by belowground plant productivity.

Chapter 3 deepens the mechanistic understanding of plant-soil interactions, demonstrating that continuously anoxic background soil-redox conditions promote the persistence of root exudate–derived carbon, whereas fluctuating oxic–anoxic conditions accelerate its mineralization. Box A extends this analysis, showing that background soil-redox state and species identity jointly determine the potential of root exudates to fuel methane production.

Building on these mechanistic insights, Chapters 4 and 5 scale up to ecosystem-level methane cycling under global change pressures. Chapter 4 shows that livestock grazing generally reduced methane emissions, though responses varied strongly across sites due to vegetation-mediated shifts in plant–soil interactions. Chapter 5 finds that warming intensified soil reduction, particularly in pioneer zones, resulting in increased methane emissions and reduced methane uptake in higher

marsh zones. These effects were linked to enhanced methanogen (methylotrophic) abundance and declining methanotrophic activity, indicating a greater temperature sensitivity of methane production than oxidation. Box B expands the perspective by revealing that wetland plants can host both methanogenic and methanotrophic microorganisms within their tissues yet may act as net methane sinks depending on background soil-redox conditions.

Given the large variability of measured methane fluxes featured throughout this dissertation, Box C introduces a transferable flux quality-control approach combining R^2 and RMSE as a filter criterion to improve the reliability and comparability of methane flux estimates across coastal marsh environments.

Finally, Chapter 6 synthesizes the findings into a unifying conceptual framework – the **root-redox-methane framework** – which confirms that coastal marsh plants, in interaction with their environment, regulate soil-redox dynamics and thereby control carbon transformation and methane cycling across environmental gradients and under global change scenarios.

ZUSAMMENFASSUNG

Die Marschen spielen eine entscheidende Rolle bei der Regulierung des globalen Klimas, da sie große Mengen an Kohlenstoff speichern. Gleichzeitig sind sie wichtige natürliche Quellen für Methan, welches ein starkes Treibhausgas ist. Sowohl Kohlenstoffspeicherung als auch Methanflüsse sind eng mit Bodenredoxbedingungen verknüpft, die aufgrund von Umwelteinflüssen wie Salzgehalt, Hydrologie und Einträgen an organischem Material räumlich und zeitlich stark variieren. Diese Umweltfaktoren prägen nicht nur mikrobielle Gemeinschaften, welche die Bodenredoxdynamik bestimmen, sondern beeinflussen auch die Zusammensetzung der Pflanzenarten. Durch ihre Wurzeleigenschaften – wie Wurzelexsudation, -umsatz und Wurzel-Sauerstofffreisetzung – regulieren Pflanzen aktiv die Bodenredoxbedingungen und steuern somit Kohlenstoffumsetzungsprozesse und den Methankreislauf. Da funktionelle Pflanzenmerkmale auf dieselben Umweltfaktoren reagieren, die auch die Bodenredoxbedingungen steuern, sind Wechselwirkungen zwischen Pflanzen und ihrer Umwelt zentral für das Verständnis der Variabilität von Methanproduktion und -emission. Die Mechanismen, welche die pflanzenvermittelte Bodenredoxregulation mit Methanflüssen unter unterschiedlichen Umweltbedingungen und Einflüssen des globalen Wandels (z. B. Landnutzungsänderung, Erwärmung) verbinden, sind jedoch bislang nur unzureichend verstanden. Diese Dissertation überprüft die Annahme, dass Marschpflanzen Bodenredoxdynamiken steuern und dadurch die Kohlenstoffumwandlung und die Methanemissionen über Umweltgradienten hinweg und unter Einfluss des Klimawandels regulieren. Im Besonderen wird untersucht, wie artspezifische Wurzeleigenschaften, dargestellt durch die unterirdische Biomasse und Wurzelexsudation, die Bodenredoxbedingungen prägen, welche wiederum die Kohlenstoffumwandlung und Methanemissionen von Marschen steuern.

Kapitel 2 gibt einen Überblick über die in dieser Dissertation untersuchten, ökologisch kontrastreichen Küstenstandorte und ist die erste umfassende Studie zur Quantifizierung der organischen Kohlenstoffvorräte in beweideten und unbeweideten Marschen an den Ostsee- und der Nordseeküste. Trotz vergleichbarer Vorräte an organischem Bodenkohlenstoff bis zu einer Tiefe von einem Meter führten die unterschiedlichen Gezeiten- und Sedimentationsregime zu einer höheren Anreicherung von organischem Kohlenstoff in den Oberböden der Ostsee. Viehbeweidung erhöhte den organischen Kohlenstoffgehalt der Oberböden in den Nordseemarschen, vermutlich durch tritthervorgerufene Veränderungen der Bodenbiogeochemie, während die Dynamik des organischen Bodenkohlenstoffs in den Ostseemarschen hauptsächlich durch die unterirdische Pflanzenproduktivität bestimmt wurde.

Kapitel 3 vertieft das mechanistische Verständnis der Pflanzen-Boden-Interaktionen und zeigt, dass dauerhaft anoxische Hintergrund-Bodenredoxbedingungen die Persistenz von aus Wurzelexsudaten stammendem Kohlenstoff fördern, während schwankende oxisch–anoxische Bedingungen dessen Mineralisierung beschleunigen. Box A erweitert diese Analyse und zeigt, dass Hintergrund-Bodenredoxbedingungen und die Pflanzenart gemeinsam bestimmen, in welchem Maße Wurzelexsudate die Methanproduktion fördern können.

Aufbauend auf diesen mechanistischen Erkenntnissen skalieren Kapitel 4 und 5 die Betrachtung auf den Ökosystemmaßstab des Methankreislaufs unter dem Einfluss des Klimawandels. Kapitel 4 zeigte, dass Viehbeweidung die Methanemissionen im Allgemeinen verringerte, Methanflüsse jedoch stark zwischen den Standorten variierten, bedingt durch vegetationvermittelte Veränderungen in den Pflanzen-Boden-Interaktionen. Kapitel 5 zeigt, dass Erwärmung die Bodenreduktion, insbesondere in der Pionierzone, verstärkte, was zu erhöhten Methanemissionen und einer verminderten Methanaufnahme in der oberen Marsch führte. Diese Effekte waren mit einer erhöhten Abundanz methanogener (methylotropher) Mikroorganismen und einer abnehmenden Aktivität methanotropher Mikroben verbunden, was auf eine höhere Temperaturempfindlichkeit der Methanproduktion im Vergleich zur Methanoxidation hinweist. Box B erweitert die Perspektive, indem sie zeigt, dass Feuchtgebietspflanzen sowohl methanogene als auch methanotrophe Mikroorganismen in ihrem Gewebe beherbergen können, je nach Bodenredoxbedingungen jedoch als netto Methansenke wirken können.

Angesichts der großen Variabilität der in dieser Dissertation gemessenen Methanflüsse führt Box C einen übertragbaren Ansatz zur Qualitätssicherung von Flussmessungen ein, der die Kombination aus R^2 und RMSE als Filterkriterium nutzt, um die Zuverlässigkeit und Vergleichbarkeit von Methanflüssen in Küstenmarschen zu verbessern.

Abschließend integriert Kapitel 6 die Ergebnisse in einen konzeptionellen Rahmen – das **root-redox-methane framework** –, welches bestätigt, dass Marschpflanzen in Wechselwirkung mit ihrer Umwelt die Bodenredoxbedingungen regulieren und dadurch die Kohlenstoffumwandlung

und den Methankreislauf über Umweltgradienten hinweg und unter Einfluss des Klimawandels regulieren.

PREFACE

This doctoral thesis has been written under the umbrella of the three following research missions:

- **CDRmare** (**C**arbon **D**ioxide **R**emoval through **marine** carbon sinks in decarbonization pathways) Research Mission of the German Marine Research Alliance (DAM), funded by the BMBF (Bundesministerium für Bildung und Forschung)
- **GREENTRIALS** (**G**reenhouse-gas fluxes in Wadden Sea Tidal Marshes – A **Tri**lateral (NL, DE, DK) Assessment of N**a**tural C**l**imate **S**olutions), funded by the BEN Postdoc-Programm 2020
- **RTG 2530** (Biota-mediated effects on Carbon cycling in Estuaries), funded by the DFG (Deutsche Forschungsgemeinschaft)

Further projects and respective funding agencies are stated at the end of each manuscript in chapters two, three, four and five.

Sorted in projects:

CDRmare's research mission was to investigate six distinct approaches of marine CO_2 sequestration and storage. One of the six consortia was **sea4soCiety**, investigating the carbon storage potential of vegetated coastal ecosystems (VCE) as a natural-based solution. The research rationale that was answered by this thesis was the *blue carbon* stock quantification in four coastal wetland types: mangrove forests, salt marshes, seagrass beds, unvegetated areas. Carbon stocks were analyzed from the coasts of the German North Sea, the German Baltic Sea, the Colombian Caribbean Sea, and the eastern and western coasts of Malaysia.

GREENTRIALS assessed the impact of livestock grazing on methane fluxes. An understudied topic, highly important for German coastlines, since it is the dominant form of land management along the two German coastlines.

RTG 2530 investigated how biotic interactions – from microbes to food webs – mediates carbon cycling in estuaries across marshes, tidal flats and channels. This dissertations work was associated with the RTG 2530 and assessed greenhouse gas fluxes in coastal marshes.

THESIS MANUSCRIPTS AND FURTHER CONTRIBUTIONS

This monographic doctoral thesis comprises the content of one publication and five manuscripts – the publication and three of the manuscripts are included as Chapters (2-5) and two manuscripts as Boxes (B, C). The manuscript Chapters represent work that is substantially complete, and the Boxes are earlier-stage manuscripts. The data acquisition underlying all six components has been finalized. For consistency throughout this thesis, the figures and tables of the manuscripts were renumbered, and all references were summarized at the end of the thesis.

In Chapter 3, 4, 5, Box B, and C I contributed as a first author, including study conceptualization and design, fieldwork and lab work organization and implementation, data assessment and evaluation, article conceptualization and visualization, and article writing, review and editing. As a co-author I contributed to study conceptualization and design, fieldwork and lab work organization and implementation, data assessment and evaluation, and article reviewing and editing.

Chapter 2:

Logemann, E. L., **Goesele, C.**, Jensen, K., and Mueller, P. (2025). Soil Organic Carbon Stocks of German Salt Marshes: A Comparative Study Along Low- and High-Energy Coastlines. *Journal of Geophysical Research-Biogeosciences*. https://doi.org/10.1029/2025JG008797

Chapter 3:

Tang, H. & **Goesele, C.**, Krueger, N., Dou, X., Lu, M., Jensen, K., and Mueller, P. (in preparation). Redox controls exudate-derived carbon stability in coastal wetland soils. To be submitted to *Soil Biology and Biogeochemistry*.

Chapter 4:

Goesele, C, Logemann, E. L., Chen, C., Kutzbach, L., Jensen, K., and Mueller, P. (in preparation). Vegetation control on soil redox determines grazing effects on methane emissions from coastal marshes. To be submitted to *Journal of Applied Ecology*.

Chapter 5:

Goesele, C. & Mittmann-Goetsch, J., Unger, V., Jensen, K., Liebner, S., Thomsen, S., Rich, R., Kutzbach, L., Chen, C., Bartholomäus, A., and Mueller, P. (in preparation). Warming stimulates soil reduction and methane production in salt marshes. To be submitted to *Global Change Biology*.

Box B:

Goesele, C. & Mittmann-Goetsch, J., Hessler, L., Chen, C., Unger, V., Jensen, K., Liebner, S., Mueller, P., and Täumer, J. (in preparation). Hidden methane oxidation within wetland plant tissues. To be submitted in 2026.

Box C:

Goesele, C. & Kutzbach, L. (in preparation): Balancing R^2 and RMSE as filter criterion for quality control of methane flux across magnitudes. To be submitted in 2026-2027.

Further Contributions

Hauschild, N., **Goesele, C.**, Jensen, K., and Mueller, P. (in preparation): Tidal inundation effects on methane fluxes in a temperate salt marsh. To be submitted in 2026.

Williamson, M. F., **Goesele, C.**, Jilbert; T., Geilfus, N. X., Norkko A., and Gustafsson, C. (in preparation): Greenhouse Gas Emissions in Coastal Reed Ecosystems. To be submitted in 2026-2027.

ABBREVIATIONS AND DEFINITIONS

Abbreviations

IRIS (stick, method)	Indicator of Reduction In Soils
PSU	Practical Salinity Unit
ROL	root oxygen loss
SOC	soil organic carbon
(S)OM	(soil) organic matter
SRB	sulfate reducing bacteria
VWC	volumetric water content

Definitions

Methane emission	Refers to the net release of methane from a source to the atmosphere. This occurs when methane production outweighs methane oxidation and/or when produced methane bypasses zones of oxidation or is produced elsewhere, i.e. positive methane flux.
Methane flux	Measured rate of methane transfer per unit area per time from a source to the atmosphere; reported in this thesis as methane (µmol) per square meter (m^2) per day.
Methane uptake	Refers to the net uptake of atmospheric methane into soil when rates of methane oxidation are greater than methane production, producing a negative methane flux.
Methane oxidation	Microbial conversion of methane to carbon dioxide by methanotrophic bacteria and sometimes archaea, reduces the amount of methane available for emission to the atmosphere and can lead to uptake of atmospheric methane.
Methane production	Microbial production of methane, primarily by methanogenic archaea using substrates such as acetate, hydrogen, carbon dioxide and methylated compounds.

CHAPTER ONE | GENERAL INTRODUCTION

1.1 | COASTAL WETLANDS AND THEIR ROLE IN THE GLOBAL CARBON CYCLE

Coastal wetlands – such as marshes, mangroves, and seagrass beds – are vital ecosystems that provide myriad ecosystem services (Barbier 2013, Taillardat et al. 2020). They serve as reproductive habitats for a diverse array of plant and animal species, function as nursery grounds for fish, and contribute to human livelihoods through fisheries, tourism, and recreation. Additionally, they protect against coastal erosion by attenuating energy from waves and storm surges (Stark et al. 2015). Given that 60 % of the global human population resides along the coastline, coastal wetlands are both ecologically and economically important (Barbier 2013, Davidson and Finlayson 2019). In recent years, coastal wetlands have been recognized for their role in buffering the impacts of multiple climate change pressures, including accelerated sea-level rise and increasing atmospheric greenhouse gas concentrations. Their exceptional ability to sequester large amounts of greenhouse gases as soil organic carbon (SOC) makes them critical for climate change regulation and has led to their designation as *blue carbon* ecosystems (Nellemann et al. 2009, McLeod et al. 2011, Macreadie et al. 2021, Temmink et al. 2022).

Coastal wetland vegetation removes the greenhouse gas carbon dioxide (CO_2) from the atmosphere through photosynthesis, converting it to plant biomass and organic assimilates (Zhang et al. 2025). This photosynthetically fixed carbon is subsequently transferred into predominantly anoxic soils through the deposition of plant litter and root exudates, where it can be preserved and sequestered for millennia (McLeod et al. 2011, Duarte 2017, Howard et al. 2017, Macreadie et al. 2019, Zhang et al. 2025). Indeed, the amount of carbon stored long term in coastal wetland soils is substantially greater than that of terrestrial forests with mangroves, coastal marshes, and seagrass meadows storing ~330-900 Mg C ha^{-1} compared to ~150-230 Mg C ha^{-1} in terrestrial forests (Temmink et al. 2022). Coastal marshes in particular have the highest carbon sequestration rates of all *blue carbon* ecosystems, averaging ~250 g C m^{-2} yr^{-1}. In comparison, sequestration rates in mangroves and seagrass meadows average ~200 g C m^{-2} yr^{-1} and ~150 g C m^{-2} yr^{-1}, respectively (Temmink et al. 2022). However, they also exhibit high variability in SOC sequestration rates and stocks within and across marshes (Alongi 2020, Macreadie et al. 2021, Maxwell et al. 2023), reflecting both a highly effective carbon sink function and the complexity of the factors that regulate it. Many questions regarding the drivers of carbon stabilization and ultimately sequestration across multiple spatial scales remain unresolved.

While the carbon sink function of coastal marshes is well-established, studies have shown that following disturbance, coastal marshes can become sources of greenhouse gases (Lovelock et al. 2017, McTigue et al. 2021). However, most studies to date have focused on CO_2, as methane (CH_4) emissions have long been assumed to be negligible in coastal marshes (Laanbroek 2010). The potential for methane emissions in coastal marshes to offset the carbon sink function of wetlands has only recently been highlighted (Rosentreter et al. 2021a, Rosentreter et al. 2021b). As such,

there is a dearth of information regarding carbon turnover in coastal marshes in the context of methane cycling. Methane is approximately 28 times more potent than CO_2 on a 100-year time scale (Myhre et al. 2013, Neubauer and Megonigal 2015, Saunois et al. 2020). Thus, even small changes in methane emission rates may be climate relevant.

Methane is produced by methanogenic archaea in waterlogged soils during the terminal step of organic matter decomposition when oxygen and all other alternative electron acceptors have been depleted (Segers 1998). Wetlands are therefore the largest natural source of atmospheric methane, accounting for 4-6 % of global land area while contributing up to 53 % of global methane emissions (Rosentreter et al. 2021b). In salt marshes, methane fluxes range between -1.5 and 1510 mg CH_4 m^{-2} day^{-1} (Rosentreter et al. 2021a).

Methane emissions are highly dependent on the soil redox state, which in turn is highly sensitive to both abiotic and biotic factors (Sutton-Grier et al. 2011, Mueller et al. 2020b, Sulman et al. 2022). Methane is produced under reducing conditions but may be oxidized to CO_2 by aerobic and/or anaerobic methanotrophs — bacteria and archaea that utilize methane as an energy source (Martinez-Cruz et al. 2017, Guerrero-Cruz et al. 2021). Despite clear links between redox state and methane production and oxidation, the mechanisms through which redox dynamics control methane production, oxidation, and ultimately methane emission and uptake in coastal marshes are still poorly understood. Plants have also been recognized as significant control over methane emissions in wetlands (Sutton-Grier and Megonigal 2011, Bridgham et al. 2013, Bhullar et al. 2014, Mueller et al. 2020b). However, the degree to which they enhance or inhibit methane emissions and the associated mechanisms are not well resolved.

In the following sections, I elaborate on how environmental factors and plant-mediated processes interact to regulate soil-redox conditions, that control carbon transformation, specifically carbon stabilization and methane production and oxidation, as well as the resulting methane fluxes.

1.2 | ENVIRONMENTAL FACTORS CONTROL SOIL-REDOX STATE OF COASTAL MARSH SOILS

Hydrology is the primary environmental driver of soil-redox conditions in coastal marshes. The frequency and duration of flooding regulate oxygen availability in surface and subsurface soils, thereby shaping the biogeochemical setting in which carbon transformation processes occur. Due to frequent tidal inundation and the rapid consumption of oxygen (O_2) by aerobic respiration and organic matter degradation, coastal marsh soils are generally reducing environments. As oxygen becomes depleted, anaerobic microbial respiration proceeds through a predictable cascade of terminal electron acceptors—nitrate (NO_3^-), manganese oxides (MnO_2), iron hydroxides [$Fe(OH)_3$], sulfate (SO_4^{2-}), and finally CO_2 – each associated with a progressive decline in redox potential (Eh).

Once the available electron acceptors are exhausted, Eh values can drop below −200 mV, indicating strongly reduced conditions favorable for methane production (Schlesinger and Bernhardt 2020). Because seawater sulfate concentrations scale linearly with salinity, at approximately 0.8 mmol SO_4^{2-} L^{-1} per PSU, periodic flooding with sulfate-rich tidal waters promotes sulfate reduction as the dominant anaerobic metabolic pathway following oxygen depletion (Böttcher et al. 2007, Dubinin et al. 2022, Leydena et al. 2023). This makes salinity a central determinant of soil redox state and a key regulator of methane production, as sulfate reducers outcompete methanogens for shared substrates when sulfate is abundant (Sela-Adler et al. 2017). Consequently, spatial and temporal variations in salinity interact with hydrological patterns to influence both the magnitude and variability of soil reduction across coastal marshes.

While hydrology and salinity directly regulate the availability of electron acceptors, their influence on soil-redox conditions also extends indirectly through effects on plant communities. Abiotic drivers determine plant species composition, which in turn shapes root structure, biomass allocation, and rhizosphere activity—all of which modify oxygen supply and organic carbon inputs at the microscale (Sutton-Grier and Megonigal 2011). Wetland vegetation can also influence soil-redox conditions by acting as both a source of electron donors via root exudates and litter inputs and, in some species, as a source of electron acceptors through root oxygen loss from roots (Turner et al. 2020, Koop-Jakobsen et al. 2021, Mittmann-Goetsch et al. 2024). These plant-mediated feedbacks add substantial spatiotemporal heterogeneity to soil redox dynamics.

Frequent flooding and prolonged soil saturation in coastal marshes create anoxic, reducing conditions that slow down organic matter decomposition and promote long-term stabilization of soil organic carbon (Stagg et al. 2017). At the same time, these environments create conditions conducive to methane production, positioning soil redox processes as a mechanistic link between the dual carbon sink and source functions of coastal marsh ecosystems (Cui et al. 2024).

1.3 | CARBON SINK FUNCTION OF COASTAL MARSHES – CARBON ACCUMULATION

Anoxic soil-redox conditions are the main driver of soil organic carbon accumulation in coastal marshes. Under these anoxic conditions, decomposition rates can be reduced by up to an order of magnitude compared to aerated soils, because oxygen limitation constrains aerobic respiration and forces microbes to rely on energetically less favorable anaerobic pathways, thereby lowering overall mineralization rates (Keiluweit et al. 2017, Stagg et al. 2017). These hydrologically driven redox conditions underpin the exceptionally high carbon storage potential of coastal marsh soils.

In coastal marshes organic carbon accumulation occurs via allochthonous and autochthonous carbon inputs. Allochthonous carbon includes externally derived organic materials such as suspended sediments and aquatic primary producers, whose delivery and retention are governed by hydrological and geomorphological processes that control sediment deposition and vertical

accretion (Needelman et al. 2018). At the same time, hydrology influences plant occurrence while the vegetation itself further modifies sedimentation processes, as canopy height and density regulate sediment trapping (Allen 2000). Autochthonous carbon is mainly derived from wetland vegetation, whereby plant productivity controls the inputs of leaves, roots, rhizomes, and root exudates to the soil organic carbon pool (Duarte et al. 2005). The relative dominance of allochthonous versus autochthonous inputs is fundamental for distinguishing coastal marsh soil types, with minerogenic marshes characterized by high allochthonous mineral and organic inputs and organogenic marshes dominated by autochthonous plant production and organic carbon accumulation (Allen 2000).

Once deposited into saturated, reducing soils, both allochthonous and autochthonous organic carbon can be stabilized over decadal to millennial timescales (McLeod et al. 2011). However, this stabilized carbon pool also constitutes the primary substrate for anaerobic microbial metabolisms, including methanogenesis, which become increasingly important as alternative electron acceptors are depleted (Sutton-Grier et al. 2011, Candry et al. 2023). Thus, the same hydrological and redox regimes that underlie the carbon sink function of coastal marshes also regulate the availability and quality of organic carbon as a substrate for methane production, directly linking carbon stabilization processes to the potential carbon source function discussed in the following section.

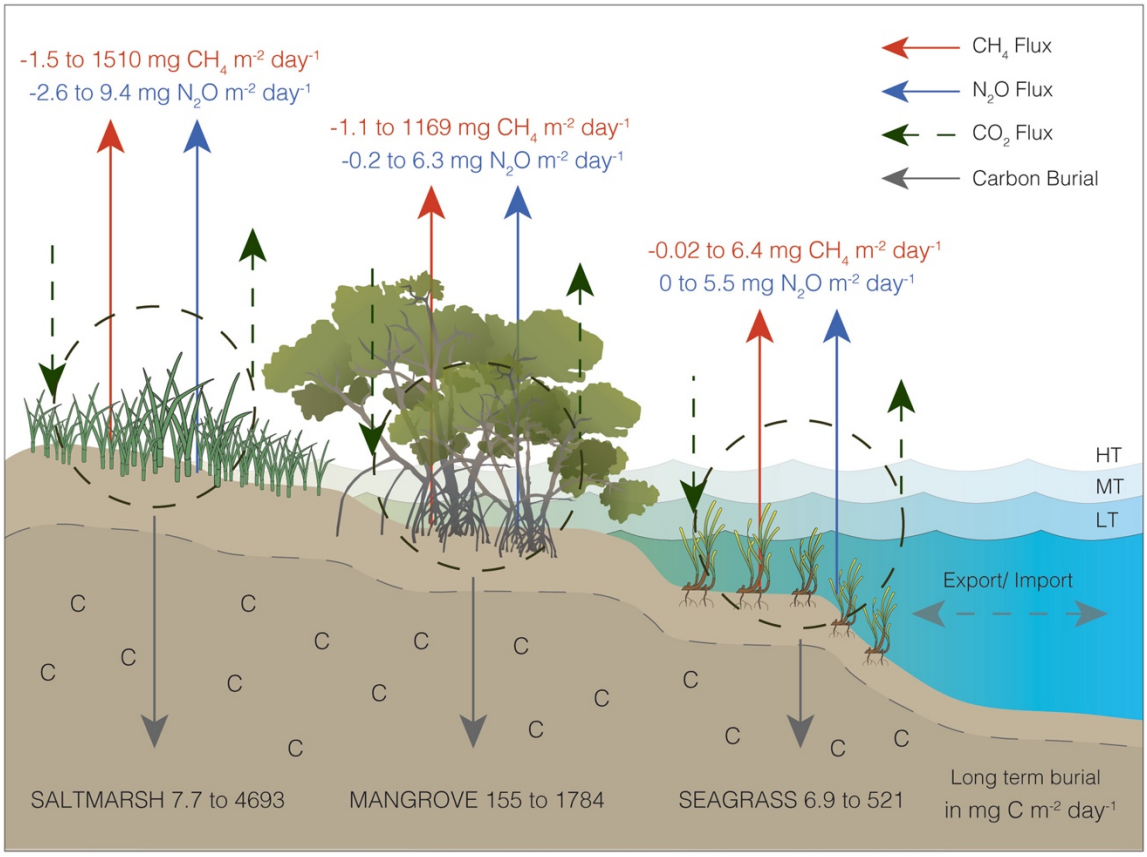

***FIGURE 1.1** | Summary of methane (CH_4) and nitrous oxide (N_2O) flux variability in coastal blue carbon ecosystems. The range is shown for lowest to highest literature values (mg CH_4 m^{-2} day^{-1}) for site-specific measurements in saltmarsh, mangrove and seagrass ecosystems. The minimum to maximum range is also given for long-term carbon burial, noting that methods used for such values are inconsistent. The CO_2 recycling pathway and the lateral export or import of inorganic and organic carbon components are indicated but not quantified (dashed arrows). The lateral export of dissolved inorganic carbon components can provide an additional long-term carbon sink (Maher et al. 2018). HT (high tide), MT (mid tide) and LT (low tide) indicate the tidal cycle. Data for CH_4 and N_2O fluxes are from Al-Haj and Fulweiler (2020), Maher et al. (2016), and Murray et al. (2015). Carbon burial rates are from McLeod et al. (2011), Rosentreter et al. (2018), Ruiz-Fernandez et al. (2018), and Ruiz-Fernández et al. (2020). Source: Rosentreter et al. (2021a).*

1.4 | CARBON SOURCE FUNCTION OF COASTAL MARSHES – METHANE EMISSION

Despite their high capacity for organic carbon sequestration, coastal marshes can simultaneously act as sources of greenhouse gases. Greenhouse gases, include e.g. carbon-based gases such as CO_2 and methane, and nitrogen-based gas nitrous oxide (N_2O). All of these fluxes can be expressed in CO_2 equivalents (CO_2e) (Myhre et al. 2013), allowing direct comparison with carbon accumulation rates, and thus allowing assessment of whether a given marsh functions as a net carbon sink or source (Rosentreter et al. 2021a). As long as the rate of carbon sequestration exceeds the combined greenhouse gas emissions and carbon export, coastal marshes act as net carbon sinks, therefore providing a net climate cooling effect, whereas environmental change can tips this balance and potentially shift them toward a net carbon source resulting in a climate warming effect (Neubauer and Megonigal 2015, Lovelock et al. 2017, McTigue et al. 2021).

Soil redox potential generally correlates negatively with methane fluxes, because oxygen is rapidly depleted in coastal wetland soils and anaerobic respiration processes quickly become dominant (Cui et al. 2024). Methane is produced via three major microbial pathways: acetoclastic methanogenesis, which consumes acetate derived from the breakdown of complex organic compounds; hydrogenotrophic methanogenesis, which uses hydrogen and CO_2; and methylotrophic methanogenesis, which metabolizes non-competitive methylated substrates such as methanol, methylamine, and methyl sulfides (Oremland and Polcin 1982, Capooci et al. 2024). The relative importance of these pathways depends strongly on substrate availability and on the salinity and sulfate regime imposed by tidal inundation (Oremland et al. 1982, Le Mer and Roger 2001, Capooci et al. 2024).

Regular flooding with sulfate-rich seawater fuels microbial sulfate reduction, a thermodynamically more favorable process than CO_2 reduction, leading sulfate-reducing microorganisms to outcompete methanogens for shared substrates such as hydrogen and acetate (Oremland and Polcin 1982). This suppresses hydrogenotrophic and acetoclastic methanogenesis, especially in settings with higher salinity, and helps explain why methane emissions from many tidal salt marshes are lower than from freshwater wetlands (Poffenbarger et al. 2011). In contrast, methylotrophic methanogenesis can proceed on non-competitive substrates, and has been suggested to contribute to methane emissions from coastal marshes (Oremland and Polcin 1982, Xiao et al. 2018, Capooci et al. 2024).

Wetland plants modulate microbial controls on greenhouse gas emissions. Through primary production, litter inputs, ROL, and root exudation, vegetation creates fine-scale redox heterogeneity that regulates the balance between methane production and oxidation, making plant functional traits a key determinant of the net greenhouse gas balance of coastal wetlands.

1.5 | PLANT-MEDIATION OF SOIL-REDOX CONDITIONS – ROOT OXYGEN LOSS AND ROOT EXUDATION

Wetland plants exert important control on methane emissions by functioning as sources of both electron donors and electron acceptors to the rhizosphere (Turner et al. 2020, Koop-Jakobsen et al. 2021, Mittmann-Goetsch et al. 2024). Through their aerenchyma tissues, they facilitate a bi-directional gas exchange, releasing oxygen into the rhizosphere and transporting methane from the soil to the atmosphere (Dacey and Klug 1979, Armstrong et al. 2000, Bezbaruah and Zhang 2005, Vroom et al. 2022).

In the anaerobic soils of coastal marshes, root oxygen loss (ROL) represents one of the main drivers of aerobic microbial processes, because ROL increases the electron acceptor availability and fosters redox conditions favorable to aerobic respiration, following increases in SOM decomposition (Wolf et al. 2007, Spivak et al. 2019), but also methane oxidation by methanotrophic microorganisms

(Colmer 2003, Keiluweit et al. 2016, Noyce et al. 2023). ROL further supports root respiration, nutrient uptake, and detoxification from reduced compounds, enhancing plant performance under waterlogged conditions (Bradley and Morris 1990, Lai et al. 2012). The magnitude and spatial extent of ROL depend on plant root traits, including aerenchyma development, root porosity, and root length and architecture (Armstrong et al. 2000, Colmer 2003, Bezbaruah and Zhang 2005). These root characteristics differ between plant species, indicating that plant species composition plays a key role in influencing soil-redox states. Consequently, Noyce et al. (2023) showed that species that exhibit strong ROL and efficient internal gas transport can promote methane oxidation. Plants also supply electron donors to the soil through root turnover and root exudation, whereby root exudation – the release of recently photosynthetically fixed carbon into the rhizosphere (Jones et al. 2004, Badri and Vivanco 2009, Jones et al. 2009) – rapidly alters soil redox conditions (Sutton-Grier et al. 2011). Exudates are primarily composed of low-molecular weight organic compounds such as sugars, amino acids, fatty acids, organic acids and secondary metabolites (Canarini et al. 2019, Ritter et al. 2025). Once released, these compounds undergo rapid microbial turnover (Phillips et al. 2011, Koyama et al. 2025), which quickly depletes electron acceptors and creates reducing microsites (Lacroix et al. 2025). These plant-microbe interactions slow down organic matter decomposition while simultaneously favoring anaerobic pathways including methanogenesis (Turner et al. 2020, Haviland and Noyce 2024, Girkin et al. 2025).

Research on root exudation is still an emerging field, but evidence from upland terrestrial ecosystems demonstrates that root exudation contributes significantly to SOC (Guyonnet et al. 2018, Panchal et al. 2022, Wen et al. 2022, Lei et al. 2023, Chari et al. 2024). That is, exudate classes such as phenols, are known to inhibit soil microbial activity ((Hamer and Marschner 2005); and see wetland study: (Sogin et al. 2022)) and others bind with minerals (Hamer and Marschner 2002). While knowledge of root exudate functions in carbon cycling is growing for upland terrestrial soils, the role of root exudates in coastal marsh carbon stabilization remains poorly explored.

In wetland soils, studies indicate that root exudation can contribute to methane production and emission by supplying labile carbon substrates to methanogenic communities in anoxic zones (Waldo et al. 2019, Turner et al. 2020, Haviland and Noyce 2024, Girkin et al. 2025). At the same time, exudation patterns and compositions vary among plant species, suggesting that root exudate traits are critical for understanding species-specific effects on carbon stabilization and methane cycling (Yuan et al. 2019, Kim et al. 2020a, Kim et al. 2020b, Haviland and Noyce 2024).

Taken together, the high spatial and species-specific variability in root exudation and ROL and its effects on soil redox dynamics underline the pivotal yet still poorly understood role of plant mediation in coastal marsh carbon stabilization and methane cycling. How these plant-driven redox processes interact with environmental controls to influence carbon transformation remains largely unresolved. Moreover, the response of this plant-mediated redox regulation, and its consequences

for carbon storage and greenhouse gas fluxes, to global change pressures such as land use change, and climate warming is not understood.

1.6 | GLOBAL CHANGE IMPACTS ON CARBON TRANSFORMATION AND METHANE CYCLING

Land use such as livestock grazing, other agricultural practices, drainage, or damming can alter both biotic and abiotic ecosystem processes in coastal marshes, with potentially important consequences for carbon stabilization and methane cycling (Kroeger et al. 2017). Livestock grazing is a globally relevant land use in these systems and particularly common in large parts of Europe (Tessier et al. 2003, Nolte et al. 2014, Barr and Bell 2017). Grazing alters soil-redox conditions and vegetation properties through trampling-induced compaction (Davidson et al. 2017, Mueller et al. 2017, Ford et al. 2019, Harvey et al. 2019, Leiva-Dueñas et al. 2024, Logemann et al. 2025), which can promote reducing soil conditions. At the same time, plants often respond to grazing with increased belowground carbon allocation (Elschot et al. 2015, Graversen et al. 2022), resulting in higher root turnover and most likely also exudation, processes that further lower soil redox potential. These combined effects suggest that livestock grazing may promote carbon storage and increase methane emissions through plant-mediated soil redox potentials, yet the link has been previously overlooked.

Climate change and especially global warming influence both biotic and abiotic processes in coastal marsh soils, with potentially important consequences for carbon stabilization and methane cycling (Noyce and Megonigal 2021, Heinzle et al. 2023, Tang et al. 2023). Warming reduces soil redox conditions (Noyce et al. 2023, Lee et al. 2025), and under these reducing conditions warming does not decrease carbon stabilization in coastal marsh soils (Tang et al. 2023). Furthermore, warming has been shown to increase methane emissions from coastal wetlands, largely by altering soil redox conditions through shifts in plant productivity and microbial activity (Noyce and Megonigal 2021). Higher plant productivity enhances belowground carbon allocation, root turnover, and exudation, further lowering soil redox potential. These combined effects suggest that warming may promote carbon storage and increase CH_4 emissions through plant-mediated soil redox conditions under warming, yet the link has been previously overlooked.

1.7 | THESIS OUTLINE

Previous studies have established that soil redox conditions, governed by hydrology and biochemistry, critically regulate carbon transformation and methane cycling in coastal marshes (Cui et al. 2024). Within these biogeochemical settings, wetland plants exert strong control over soil-redox conditions through ROL and root exudation (Haviland and Noyce 2024), shaping microbial

communities (Eisenhauer et al. 2017) and biogeochemical processes. However, the spatial and temporal generalizability and mechanisms of plant-mediated redox regulation remain uncertain across species, environments, and scales. Furthermore, how these plant-driven soil redox processes respond to global change pressures such as land-use and global warming remains poorly understood. Addressing these gaps, this dissertation tests the central assumption that wetland plants regulate soil-redox dynamics and thereby control carbon transformations and methane cycling across contrasting environmental gradients and under global change scenarios.

To test this assumption, this dissertation is built around two coastal marsh regions with contrasting environmental settings initially shaped by hydrological differences: the Baltic Sea and the North Sea coast. The low-energy, microtidal Baltic Sea marshes are characterized by prolonged inundation, organic-rich soils, and lower salinity, while the high-energy mesotidal North Sea marshes are marked by rapid sedimentation, well-aerated soils, and higher salinity (Mueller et al.; Granse et al., 2024; Kirwan & Megonigal, 2013). These contrasting hydrological and geochemical contexts influence soil properties such as SOC stocks (Fig. 1.2), soil-redox states, and plant community composition. Therefore, these two coastlines provided a natural experiment to test the roles of plant-mediated soil-redox controls in contrasting environmental settings and under global change pressures such as global warming and livestock grazing.

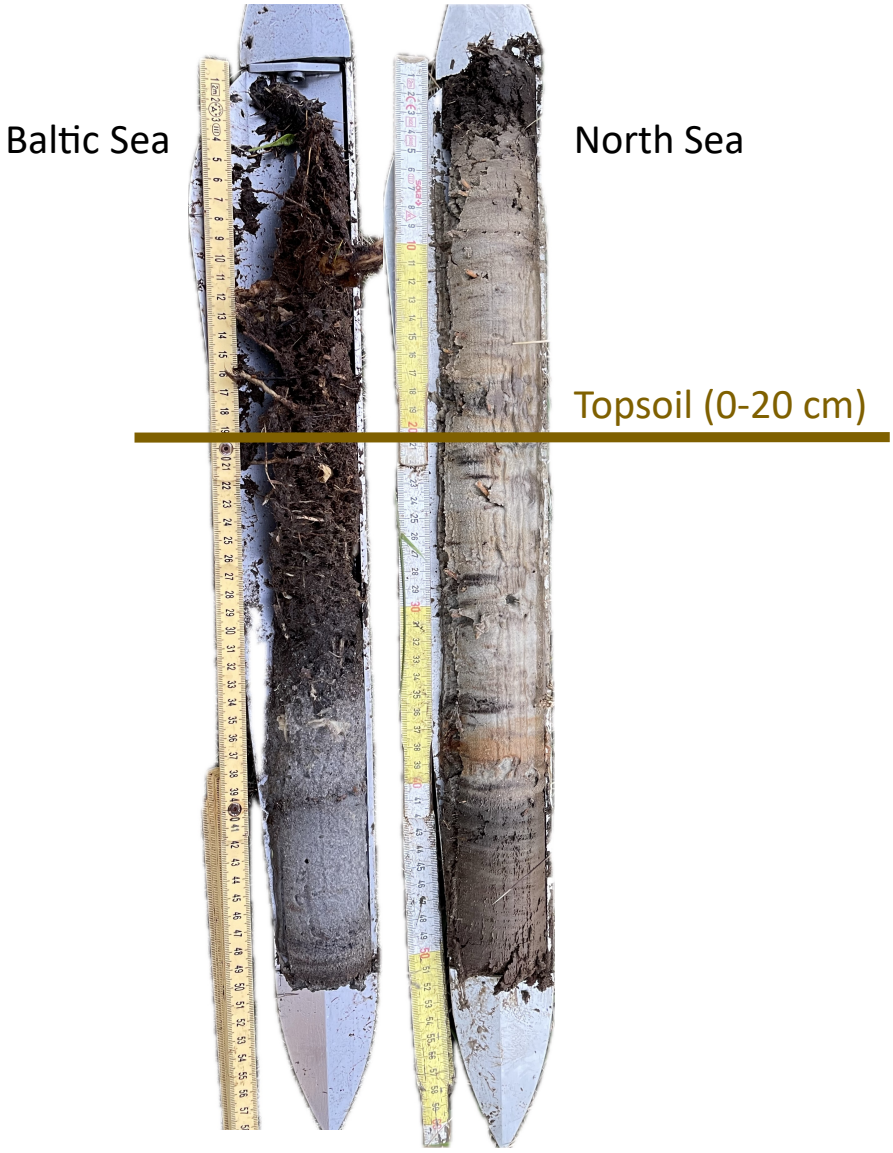

***FIGURE 1.2** | Example for organic-rich Baltic and organic-poor North Sea topsoil. Photo: Clarisse Gösele.*

With **Chapter 2** I provide an overview of these environmental contrasts, including the first comprehensive study quantifying SOC stocks in grazed and ungrazed Baltic and North Sea marshes. These environmental background settings underpin all later interpretations of plant–soil interactions within these characteristic coastal settings. Building on the environmental context I established in Chapter 2, the following two sections deepen the mechanistic understanding of plant-soil interactions in coastal marshes, by examining how the fate of root exudates from two characteristic salt-marsh plants *Spartina anglica* and *Elymus athericus* depends on background soil-redox conditions. I explore how background soil-redox conditions influence both the stabilization of this root-derived carbon (**Chapter 3**) and the potential of root exudates to fuel methane production (**Box A**).

Having established these mechanistic links between background- and plant-mediated soil-redox conditions and carbon turnover, Chapters 4 and 5 focus on ecosystem-scale expressions of methane

cycling. In these chapters, I examine how two global-change pressures influence plant–soil interactions and how such effects translate into altered methane cycling and methane fluxes from coastal marshes. **Chapter 4** focuses on how livestock grazing affects soil properties and vegetation composition and thereby influences plant-soil interactions that control methane emissions from marshes along the two coastlines. **Chapter 5** presents results from a warming experiment conducted in a North Sea coastal marsh. Here I highlight how increased temperatures influence methane cycling in coastal marshes through alterations of plant-soil and microbe-soil interactions. With **Box B** I expand the perspective from soils and roots to other plant compartments and explore the role of wetland plant tissues as an overlooked site of methane cycling.

The methane flux data featured throughout this dissertation, including in Chapters 4, 5, Box B, and Chapter 6, exhibits considerable variation in magnitudes, posing a methodological challenge of evaluating fluxes spanning such a wide range. In **Box C**, I therefore briefly elaborate on this challenge and propose a simple and transferable flux quality control approach that uses a combination of R^2 and RMSE as a filter criterion to improve comparability and the reliability of methane flux estimates across diverse coastal marsh environments. Finally with **Chapter 6** I synthesize the results of the previous Chapters and Boxes in a conceptual framework (the root-redox-methane framework**)** to validate my assumption that wetland plants regulate_soil-redox dynamics and thereby control carbon transformations and methane cycling across contrasting environmental gradients and under global change scenarios.

CHAPTER TWO | SOIL ORGANIC CARBON STOCKS OF GERMAN SALT MARSHES: A COMPARATIVE STUDY ALONG LOW- AND HIGH-ENERGY COASTLINES

Soil Organic Carbon Stocks of German Salt Marshes: A Comparative Study along Low- and High-Energy Coastlines

Published in *Journal of Geophysical Research-Biogeosciences*.

Ella L. Logemann [1], **Clarisse Goesele** [1], Kai Jensen[1], and Peter Mueller[2,3]

[1] University of Hamburg

[2] University of Münster

[3] University of Kaiserslautern-Landau

Corresponding author: Ella Logemann (ella.logemann@uni-hamburg.de)

Key Points:

- The low-energy Baltic Sea salt marshes have greater SOC stocks on average than the high-energy North Sea salt marshes.
- Grazing increased SOC density by enhancing soil compaction and inducing changes in plant productivity. Drivers differed between coasts.
- The highest SOC density was found in the low marsh, most likely due to organic carbon loss under increased aeration of the high marsh soils.

2.1 | ABSTRACT

Blue carbon ecosystems, such as salt marshes, store comparably large amounts of organic carbon in their soils and function more effectively as carbon sinks than most other terrestrial ecosystems. Here we provide the first comprehensive study, quantifying soil organic carbon (SOC) stocks in grazed and non-grazed German salt marshes. In Germany, salt marshes are found along the low-energy, microtidal coastline of the Baltic Sea as organogenic ecosystems and along the high-energy, mesotidal coastlines of the North Sea as minerogenic ecosystems. One-meter soil cores were taken across 14 sites covering three distinct salt marsh types: Baltic Sea, North Sea mainland and North Sea island. Baltic salt marshes held on average the greatest SOC stocks with 221±56.3 (mean±SE) Mg SOC/ha followed by North Sea mainland salt marshes with 187±24.9 Mg SOC/ha and North Sea island salt marshes with 78±9 Mg SOC/ha. Our findings indicate that livestock grazing resulted in a 1.5-fold increase in SOC density. The microtidal Baltic salt marshes store more SOC in their topsoil than mesotidal North Sea salt marshes, most likely due to the higher sediment deposition rates in North Sea mainland salt marshes causing SOC dilution through mineral inputs. We conclude greater aeration in high-marsh soils might counterbalance SOC accumulation under proceeding succession. Positive livestock grazing effects were relatively consistent within North Sea salt marshes, likely caused by trampling-induced changes in soil biogeochemistry. By contrast, grazing had variable effects on SOC in Baltic Sea salt marshes, with belowground plant productivity identified as the primary driver.

Plain Language Summary

Blue carbon ecosystems, such as salt marshes, are important carbon sinks. Here, we provide budgets of the soil organic carbon stocks of German salt marshes. We sampled salt marshes along the Baltic Sea and North Sea coast, at both islands and mainland coasts. The salt marsh types (Baltic Sea, North Sea mainland and North Sea island) differ in morphology and tidal dynamics. The low-energy Baltic salt marshes stored the most organic carbon in their soils. Additionally, we found that grazing increased soil organic carbon storage by a factor of 1.5. We suggest that the high-energy tidal dynamics of the North Sea coast lead to high inputs of sediments at the mainland salt marshes, leading to fast vertical soil growth and to dilution of soil organic carbon with deposited minerals. Lastly, we observed that the livestock grazing effect was more consistent within North Sea salt marshes, probably because of changes in the soil biogeochemistry caused by trampling. In contrast, the grazing effect in Baltic Sea salt marshes is more variable and likely influenced by changes in belowground plant productivity under grazing.

2.2 | INTRODUCTION

Salt marshes and other blue carbon ecosystems, such as seagrass meadows and mangroves, are characterized by high rates of organic carbon sequestration in soils and function more effectively as carbon sinks than many other terrestrial and aquatic ecosystems (McLeod et al. 2011, Lovelock and Duarte 2019, Macreadie et al. 2021). Blue carbon ecosystems globally cover less than 0.2 % of the ocean surface but account for 50 % of the marine SOC burial. At the same time, the global area of blue carbon ecosystems declines at a rapid rate, with an estimated annual decline of 1-2 % for salt marshes (Duarte et al. 2013). Soil carbon sequestration is the outcome of organic matter input to the soil and its microbial decomposition as output (Duarte et al. 2005, Lovelock and Reef 2020). The fate of organic matter inputs to the soil depends on various variables influencing carbon persistence. Flooding leads to waterlogged soils that reduce decomposition through shifts in microbial functioning towards anaerobic metabolism (Neubauer and Megonigal 2021). SOC stocks of blue carbon ecosystems are fed by both autochthonous and allochthonous organic inputs. Autochthonous organic matter is derived from in-situ primary productivity, while allochthonous organic matter stems from external sources, such as aquatic primary production, and is deposited in the salt marshes through sedimentation (Needelman et al. 2018).

Salt marshes cover approximately 5.5 million ha globally (McOwen et al. 2017) estimating a global total of ~862 to 1,350 Tg SOC (157-245 Mg/ha) (Macreadie et al. 2021). Studies assessing the global SOC stocks of salt marshes show large variability (Alongi 2020, Macreadie et al. 2021, Maxwell et al. 2023), emphasizing the need of regional studies for estimating national blue carbon stocks. In Europe, national budgets of salt marsh SOC stocks were compiled recently for UK (Mason et al. 2022) and Denmark (Leiva-Dueñas et al. 2024). In Germany, salt marshes are widespread along the North Sea coast and to a lesser extent along the coast of the Baltic Sea. Blue carbon stocks have only been assessed in a handful of case studies (Mueller et al. 2019b, Buczko et al. 2022, Mueller et al. 2023). A comprehensive study describing carbon storage in salt marshes along both German coastlines of North Sea and Baltic Sea is still missing.

Salt marshes of the North Sea and the Baltic Sea coast greatly differ with respect to geomorphology and other abiotic conditions (Dijkema 1990, Elschot et al. 2024). North Sea salt marshes along the mainland coast form in front of dikes and are exposed to strong hydrodynamics and mesotidal conditions. Island salt marshes of the North Sea coast form under less exposed conditions in the lee of back-barrier islands (Elschot et al. 2024). The Baltic salt marshes differ in morphology and hydrodynamic exposure due to the semi-enclosed nature of the Baltic Sea, resulting in microtidal to non-tidal conditions and a salinity of 5-10 PSU which is much lower than at the North Sea coast with 32-34 PSU (Dijkema 1990). The mesotidal conditions at the North Sea coast lead to clearly distinguishable vegetation zones along an elevation gradient, where the highest zone reflects the oldest stages in succession (Olff et al. 1997, Suchrow and Jensen 2010). In contrast to the fast-

accreting minerogenic salt marshes of the North Sea, the microtidal Baltic salt marshes are characterized by low sediment deposition rates and slow-accreting organogenic soils (Dijkema et al. 2010, Nolte et al. 2013a).

Salt marsh SOC stocks can show strong variability in response to sedimentation, vertical accretion rate and succession. Higher SOC stocks are generally connected to progressing influence of vegetation e.g. in later successional stages (Connor et al. 2001, Spohn et al. 2013, Ouyang and Lee 2014, Hansen et al. 2017).

The majority of salt marshes in Germany have been impacted by anthropogenic activity over the past centuries. This is primarily due to land reclamation and agricultural practices. Even today, livestock grazing remains a prevalent activity in many salt marshes (Rupprecht et al. 2023). Livestock grazing can have variable effects on salt marsh SOC stocks due to a variety of mechanisms. First, grazing can increase root:shoot ratios by partially removing the aboveground biomass (Davidson et al. 2017), which can decrease sediment trapping (Schulze et al. 2021). Second, grazing can increase root productivity leading to greater belowground organic matter input to the soil (Elschot et al. 2015). Third, grazers compact the soil via trampling (Nolte et al. 2014) thereby reducing oxygen availability through increased water-logging (Keshta et al. 2020), which ultimately may slow down organic matter decomposition (Schrama et al. 2013, Nolte et al. 2014, Mueller et al. 2017). For salt marshes in the Netherlands and Denmark, an increase in the SOC stock under grazing has been reported (Elschot et al. 2015, Leiva-Dueñas et al. 2024).

The objective of this study is to provide a comprehensive overview of salt marsh SOC stocks along the North Sea and Baltic Sea coasts of Germany. Our study is based on SOC assessments in 14 marsh sites comprising a total of 146 soil cores. We aim to identify geomorphological and land-use factors affecting salt marsh SOC stocks along the German coasts by addressing the following hypotheses: 1) Baltic salt marshes have a greater SOC stock than North Sea salt marshes due to predominantly organogenic soil formation; 2) In North Sea salt marshes, SOC density increases with succession and is greatest in mature high-marsh zones; 3) Livestock grazing increases SOC density via soil biogeochemical changes and 4) decreases the proportion of allochthonous SOC via reduced plant-mediated sediment trapping.

2.3 | MATERIAL AND METHODS

***FIGURE 2.1** | Overview map of study sites in Germany. Three distinct saltmarsh types were sampled. Baltic Sea, North Sea mainland and North Sea island salt marshes indicated by different colors.*

In order to assess the differences in SOC stocks between contrasting geomorphological settings of salt marshes in Germany, three distinct salt marsh types were sampled: Baltic Sea salt marshes, North Sea mainland salt marshes and North Sea island salt marshes. In North Sea salt marshes, sampling plots were arranged along transects on the elevation gradient representing pioneer, low marsh, and high marsh vegetation zones. Effects of livestock grazing on SOC storage were assessed in an additional campaign.

2.3.1 | FIELD SITE DESCRIPTION

Located along the SE North Sea coastline, the Wadden Sea stretches from Denmark, via Germany to the Netherlands. Here, minerogenic salt marshes cover about 42,500 ha from which 25,060 ha are located along the German North Sea coast (Elschot et al. 2024). North Sea mainland salt marshes are developing along the mainland coast, mostly in front of dikes. Most salt marshes of this type developed through land-reclamation activities along the coast over past centuries. Today, these salt marshes are hydrologically disturbed by artificial drainage ditches or their remnants. Furthermore, management practices like livestock grazing and mowing still apply to approximately 50 % of all North Sea salt marshes (Elschot et al. 2024). Typically, grazed North Sea mainland salt marshes are located closer to the dike than non-grazed areas. This consequently entails that these grazed salt-marsh soils tend to be older (Elschot et al. 2024). North Sea island salt marshes cover approximately

25 % of the German North Sea salt marshes and form in lee of barrier islands. This sheltered geomorphic setting leads to lower sediment deposition rates compared to the more exposed mainland salt marshes (Olff et al. 1997, Elschot et al. 2024). North Sea island salt marshes have a larger share of hydrologically undisturbed relief, and they can be described as mostly natural (Elschot et al. 2024). The German North Sea coast as high-energy coast with mesotidal ranges constitutes salt marshes with clearly distinguishable vegetation communities across the elevation gradient (Olff et al. 1997, Suchrow and Jensen 2010). The gradual increase of elevation results in different flooding frequencies which are then reflected by three vegetation zones: pioneer zone, low marsh, and high marsh. The low-energy coasts of the Baltic Sea lead to salt marshes that often lack a clear vegetation zonation as flooding is mostly due to irregular wind-driven water-level changes (Dijkema 1990). In contrast to the extensive North Sea salt marshes, Baltic salt marshes usually do not exhibit a clear elevation gradient but rather show small-scale vegetation heterogeneity representing different abiotic conditions and/or successional stages. In comparison to North Sea salt marshes as prograding systems, Baltic salt marshes are often smaller and most likely older. Today, they cover a total of 8,050 ha in Germany of which about half is grazed by livestock (Wanner 2009). Baltic salt marshes typically develop in the shelter of dunes and lagoons and do not differentiate morphologically between mainland and island coasts. Due to storm floods, marine sediments occasionally deposit on the marsh surface (Dijkema 1990). Under non-grazed conditions, Baltic salt marshes mostly develop into tall-grass communities dominated by Phragmites australis. In contrast, livestock grazing promotes small-stature vegetation and the establishment of halophytes (Dijkema 1990).

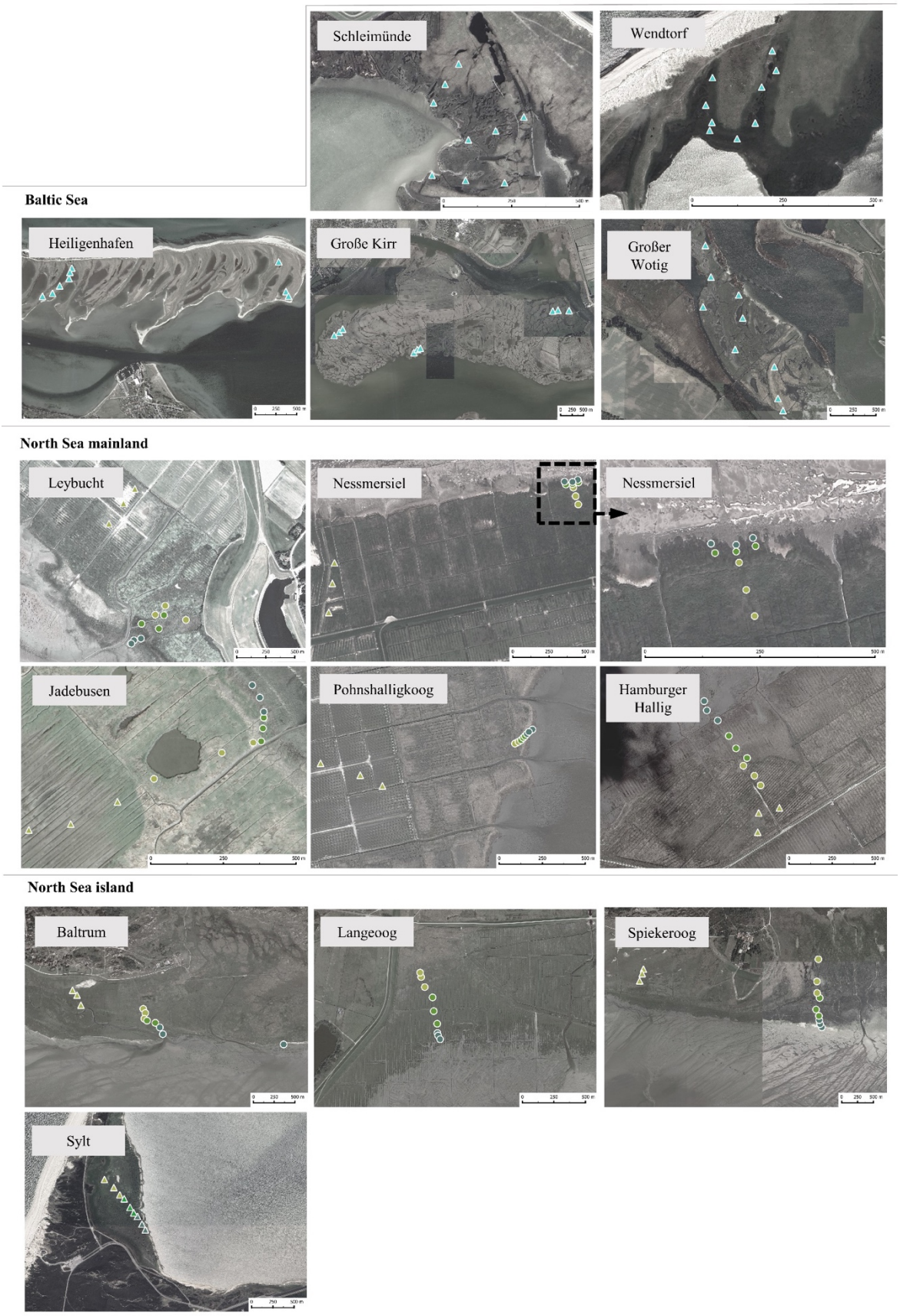

FIGURE 2.2 | *Overview of study sites and sampling positions. Color code of circles depicts zonation within North Sea salt marshes: pioneer zone (blue), low marsh (green) and high marsh (yellow). Baltic salt marshes show no clear zonation (blue points represent "no zone"). Triangles represent non-grazed areas, circles represent grazed areas.*

2.3.2 | STUDY DESIGN FOR ASSESSING SOC STOCKS AND DENSITY OF DIFFERENT SALT MARSH TYPES AND VEGETATION ZONES

By including salt marshes of the North Sea mainland coast, the North Sea islands and the Baltic Sea coast, all three relevant salt marsh types based on extent along the German coastlines are represented in this study (Fig. 2.1.2). The 14 study sites were sampled using a transect design to cover gradients of different plant communities and management types. The sampled transects of the North Sea salt marshes spanned this gradient in elevation and included all three vegetation zones, i.e. high marsh, low marsh and pioneer zone. Based on previous ground truthing, transects at the Baltic coast were laid to capture small-scale vegetation heterogeneity. Soil cores from all 14 study sites were taken between November 2021 and September 2022 (Tab. 2. S. 1.1.a).

2.3.3 | SOIL SAMPLING AND VEGETATION ANALYSIS

In each of the 14 study sites, 8-12 plots (Tab. 2. S 1.1.a) were sampled. For assessing vegetation composition and structure, plant species composition and coverage, as well as the percentage of bare soil and dead plant matter were recorded for each plot within a 100 x 100 cm square. Vegetation height was measured at five points within each plot. To quantify aboveground biomass, plants were cut 2 cm above the soil on a 25 x 25 cm square centered in each plot. Biomass samples were put into paper bags, transported to the laboratory, and weighed after drying at 60°C for a minimum of three days.

For the quantification of SOC content, soil bulk density, SOC δ13C signature, and nitrogen content, a single 1-m soil core was taken from the center of each plot (Fig. 2.2). An Eijkelkamp peat sampler was used for taking soil cores, which allowed compaction-free sampling of a half-cylindrical core with a diameter of 5 cm. The use of the peat sampler for mineral soils required pre-coring with a narrow (3-cm diameter) gouge auger to reduce friction resistance during coring (Mueller et al. 2023). Each core was sliced into 10 cm increments, transferred into plastic bags and transported to the laboratory for further processing.

2.3.4 | ANALYSIS OF SOIL PARAMETERS

Fresh soil samples were homogenized and weighed before and after being air dried at 60°C for at least five days. Dry soil bulk density was calculated from sample dry weight and volume. Gravimetric water content was calculated from the ratio of sample fresh weight to dry weight. Prior to elemental and isotope analysis, macroscopic root residues were removed using tweezers.

Electrical conductivity, pH and sand content were measured in subsamples. For electrical conductivity, 5 g of milled dry soil was dissolved in 25 mL of deionized water and measured with a benchtop conductivity meter (Cond 7310). Soil pH was measured by dissolving 2 g of milled dry soil in 5 mL 0.01 M CaCl2 solution. The samples were shaken regularly for a period of 1 h and

afterwards measured with a benchtop pH meter (Multi 9310 IDS). Mud and sand contents were approximated by passing subsamples of 2-5 g through a 0.06-mm test sieve.

To remove inorganic carbon (carbonate minerals) from soil samples, we applied the following acidification procedure: A fraction of all soil samples was milled and acidified with 10% HCl until no visible effervescence was observed. The acidified samples were weighed before and after acidification and the difference in dry weight was used as a correction factor before elemental (carbon and nitrogen) analysis. For quantifying carbon and nitrogen contents, 2-35 mg of acidified dry soil was weighted into tin capsules and analyzed with an element analyzer (EURO EA 3000, Euro Vector, Italy). The evolved CO_2 was further passed to a coupled isotope ratio mass spectrometer (nu Horizon, Nu Instruments Limited, UK) for assessing the δ13C signature. Obtained nitrogen data were used for calculating the C/N ratio of samples. C/N and δ13C signatures were used to examine SOC origin (i.e. allochthonous vs. autochthonous) (Khan et al. 2015, Mueller et al. 2019a).

SOC data with carbon contents below 0.1% lack precision. Nevertheless, these SOC measurements, which account for 19.1 % of the total dataset, were retained in subsequent statistical analyses rather than being discarded or set to zero. However, carbon contents were occasionally too low for accurate δ13C assessments, leading to the exclusion of these isotopic data from further analysis.

SOC density (g C / cm3) was calculated from soil bulk density (g dry soil / cm^3) and SOC content (g C / g dry soil). SOC stock (Mg C/ha) was calculated in two steps. First, for each 100-cm core, the SOC density values of all 10-cm increments were averaged to determine the mean SOC density per core. Second, the mean SOC stock per site was calculated across all cores and converted to a per-hectare basis. Missing values in individual 100-cm cores (5.2% of the total dataset) were estimated through interpolation. Interpolated values were only used for SOC stock calculation. The upscaled total German salt marsh SOC stock (Tg SOC) was calculated by multiplying the mean, standard error, median and interquartile range (IQR) of type-specific salt marsh SOC stock with the areal extent of the respective salt marsh type. The data regarding the areal extent were taken from (Wanner 2009) for Baltic salt marshes and Elschot et al. (2024) for North Sea salt marshes. In addition to the North Sea island and mainland salt marshes, Elschot et al. (2024) reports on Hallig marshes and summer polders, which collectively account for approximately 12% of the potential total salt-marsh extent of German salt marshes. However, Hallig marshes and summer polders are strongly hydrologically altered due to dikes and revetments that impair natural flooding. They were not sampled in the present study and are excluded from the calculation of the total German salt-marsh SOC stock.

2.3.5 | ADDITIONAL STUDY FOR ASSESSING EFFECTS OF LIVESTOCK GRAZING ON SOC STOCKS

Livestock grazing effects on SOC stocks were additionally assessed in a separate campaign, that followed a parallel design (instead of a transect design) and allowed comparison of grazed vs non-grazed plots in similar successional stages/ marsh ages (Fig. 2.3). The additional campaign was carried out in four of the study sites (North Sea mainland: Pohnshalligkoog, Nessmersiel; Baltic Sea: Schleimünde, Heiligenhafen). These assessments were restricted to the top 30 cm of soil because grazing histories vary across sites, making it difficult to accurately attribute any effects on the deeper soil layers to grazing.

Sampling took place in October to November 2023. Four or five cores each were taken from grazed and non-grazed areas in each of the four selected study sites resulting total in 38 cores (Tab. 2.S. 1.1.b). Samples were processed as described for the SOC stocks. Loss on ignition was used to determine soil organic matter (SOM). Carbon and nitrogen content, δ13C signature, pH and electrical conductivity were measured in samples of 0-10 cm and 20-30 cm depth and interpolated for the 10-20 cm section (text S. 1.2).

Aboveground and belowground biomass was harvested in September 2023. Aboveground plant samples were cut from a 30 x 30 cm square, dried at 60°C for 5 days and weighed. Belowground biomass was retrieved with an Edelman corer (diameter 5 cm; depth 20 cm) centered within the aboveground biomass square. The belowground biomass samples were washed free from soils, dried at 60°C for 5 days, and weighed.

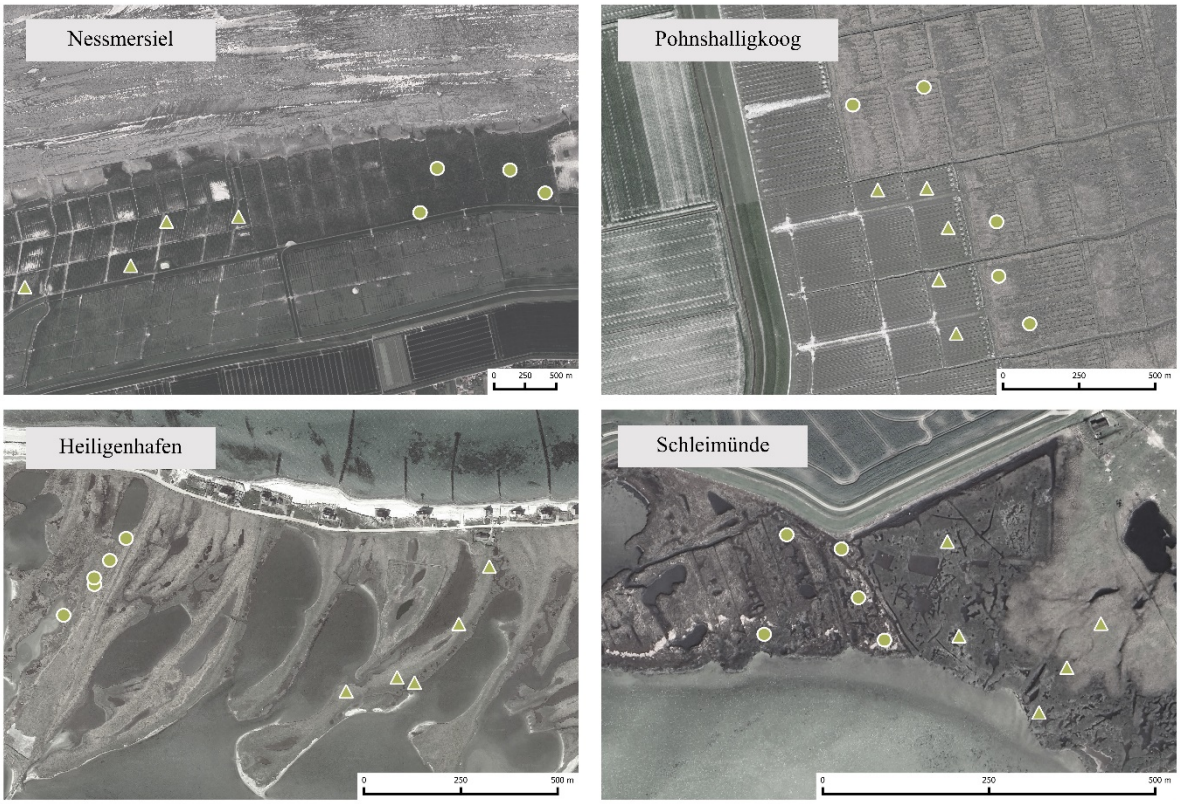

***FIGURE 2.3** | Overview of study sites with additional plots to compare grazed (triangle) and non-grazed (circle) areas.*

2.3.6 | DATA ANALYSIS

This study distinguishes soil properties between topsoil (0-30 cm) and subsoil (30-100 cm) core sections, and calculated average δ13C, SOC, soil bulk density and electrical conductivity, sand content and pH for these soil sections. For analyzing effects of vegetation zone, only data from non-grazed North Sea salt marshes were included, because only for these salt-marsh types vegetation zonation was clearly discernable. In order to investigate livestock grazing effects, the dataset comprised data from the additional livestock grazing campaign, as well as from high marsh grazed and non-grazed plots in Jadebusen, Leybucht, Baltrum and Spiekeroog (Fig. 2.2, yellow points). The analysis of the grazing effect on δ13C was constrained to data from the uppermost 10 cm, as the grazing effect on vegetation is expected to decrease with increasing depth.

As most data was not normally distributed, Kruskal-Wallis tests were used to test for the effect of vegetation zone (pioneer zone, low marsh, high marsh) and grazing (grazed, non-grazed) on SOC, δ13C, soil bulk density, aboveground and belowground biomass, sand content and gravimetric water content. Prior to running the statistical tests and creating the graphs, the mean of these measures was calculated as follows: SOC stock graphs display the mean of top- and subsoils of the respective salt marsh type and site. In order to display and test the zonation effect on non-grazed North Sea salt marshes, mean values for each vegetation zone-site combination were calculated for

both topsoil (0-30 cm) and subsoil (30-100 cm) and used in separate Kruskal-Wallis and Dunn's test for pairwise comparison. When displaying and testing for grazing effects, mean values for each grazing treatment-site combination were calculated for the topsoil and used in Kruskal-Wallis tests. Data has been processed using Rstudio (Version 2024.04.2).

2.4 | RESULTS

2.4.1 | SALT MARSH SOC STOCKS OF THE GERMAN BALTIC AND THE NORTH SEA

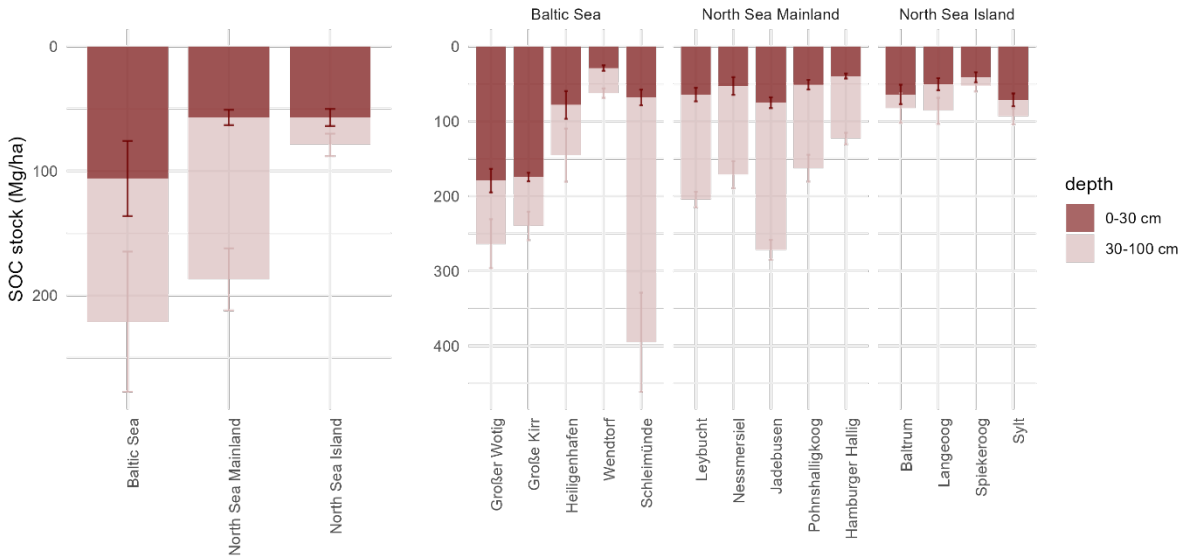

***Figure 2.4** | SOC stocks (Mg/ha) of different salt-marsh types (left) and the individual study sites (right) across the top 30 cm and 100 cm. Shown are means ± standard error.*

In German salt marshes, approximately 5.40 ± 0.928 Tg SOC were stored (Tab. 2.1.b). On average, the German salt marshes stored 168±26.2 Mg SOC/ha within the top 100 cm of soil (Tab. 2.1.b). Based on single cores, the SOC stock ranged from 12 to 695 SOC Mg/ha across the 0–100 cm profile. Baltic salt marshes displayed greatest average SOC stock (Fig. 2.4, Tab. 2.1.b), caused primarily by high SOC contents within the topsoil (Fig. 2.4, Tab. 2.1.a), whereas the high average subsoil SOC content in the Baltic salt marshes was strongly excelled by the high subsoil content of the study site Schleimünde (Fig. 2.4). North Sea mainland and island salt marshes had similar SOC contents in their topsoil (Fig. 2.4, Tab. 2.1.a). However, the North Sea island salt marshes stored the least SOC within the entire one-meter soil profile (Fig. 2.4, Tab. 2.1 b). North Sea mainland sites exhibited the highest SOC stock within the subsoil, with a SOC stock exceeding more than twice that of the topsoil (Fig. 2.4, Tab. 2.1 a). North Sea island salt marshes showed the least variability in SOC stocks, whereas Baltic Sea salt marshes had the highest variability in SOC stocks (Fig. 2.4, Tab. 2.1 b).

Table 2.1 *| Salt marsh-type specific a) mean values of SOC stock, SOC density, SOC content and δ13C in SOC for topsoil (0-30 cm) and subsoil (30-100 cm) b) mean, median and sum values of total area in ha that is covered by salt marshes, SOC in Mg/ ha and SOC in Tg. Note: ± SE, Standard Error. [a](Wanner 2009), [b](Elschot et al. 2024).*

a)

Saltmarsh type	Depth-profile	SOC stock (Mg/ha)	±SE	SOC density (g/cm³)	± SE	SOC content (%)	±SE	$SO^{13}C$ signature (‰)	±SE
Baltic Sea	subsoil	116	53.5	0.016	0.008	2.34	1.44	-24.45	0.97
	topsoil	106	30.2	0.035	0.010	7.86	2.14	-27.34	0.49
North Sea island	subsoil	22	5.1	0.003	0.001	0.21	0.10	-24.31	0.18
	topsoil	57	6.8	0.017	0.002	2.19	0.20	-24.38	0.03
North Sea mainland	subsoil	130	18.9	0.018	0.003	1.53	0.33	-23.73	0.16
	topsoil	57	6.1	0.017	0.002	2.05	0.36	-23.94	0.22

b)

		SOC (Mg/ha)				Tg SOC	
	total area in ha	mean	±SE	median	±IQR	Upscaling based on mean	±SE
Baltic Sea	8050 [a]	221	56.3	240	118	1.78	0.453
North Sea island	5370 [b]	78	9.0	84	13	0.42	0.048
North Sea mainland	17120 [b]	187	24.9	171	41	3.20	0.426
total	**30540**	**168**	**26.2**	**154**	**143**	**5.40**	**0.928**

2.4.2 | VEGETATION ZONE EFFECTS IN NORTH SEA SALT MARSHES

In non-grazed North Sea salt marshes, the SOC density peaked in the low marsh with a mean of 0.019±0.0042 g/cm³ in the topsoil. SOC density was lower in the high marsh and lowest in the pioneer zone (Fig. 2.5 A, Tab. 2.2). Despite a similar trend in SOC density was observed in the subsoil, no significant difference between zones were identified in the subsoil (Fig. 2.5 A, Tab. 2.2). Topsoil δ13C in SOC decreased with succession from pioneer zone, via low marsh to high marsh (Fig. 2.5 E, Tab. 2.2). This effect was less pronounced in the subsoil (Tab. 2.2). Sand content was lowest and gravimetric water content was highest in the topsoil of the low marsh (Fig. 2.5 C, D). Aboveground biomass was lowest in the pioneer zone and did not differ between low marsh and high marsh (Fig. 2.5 F, Tab. 2.2).

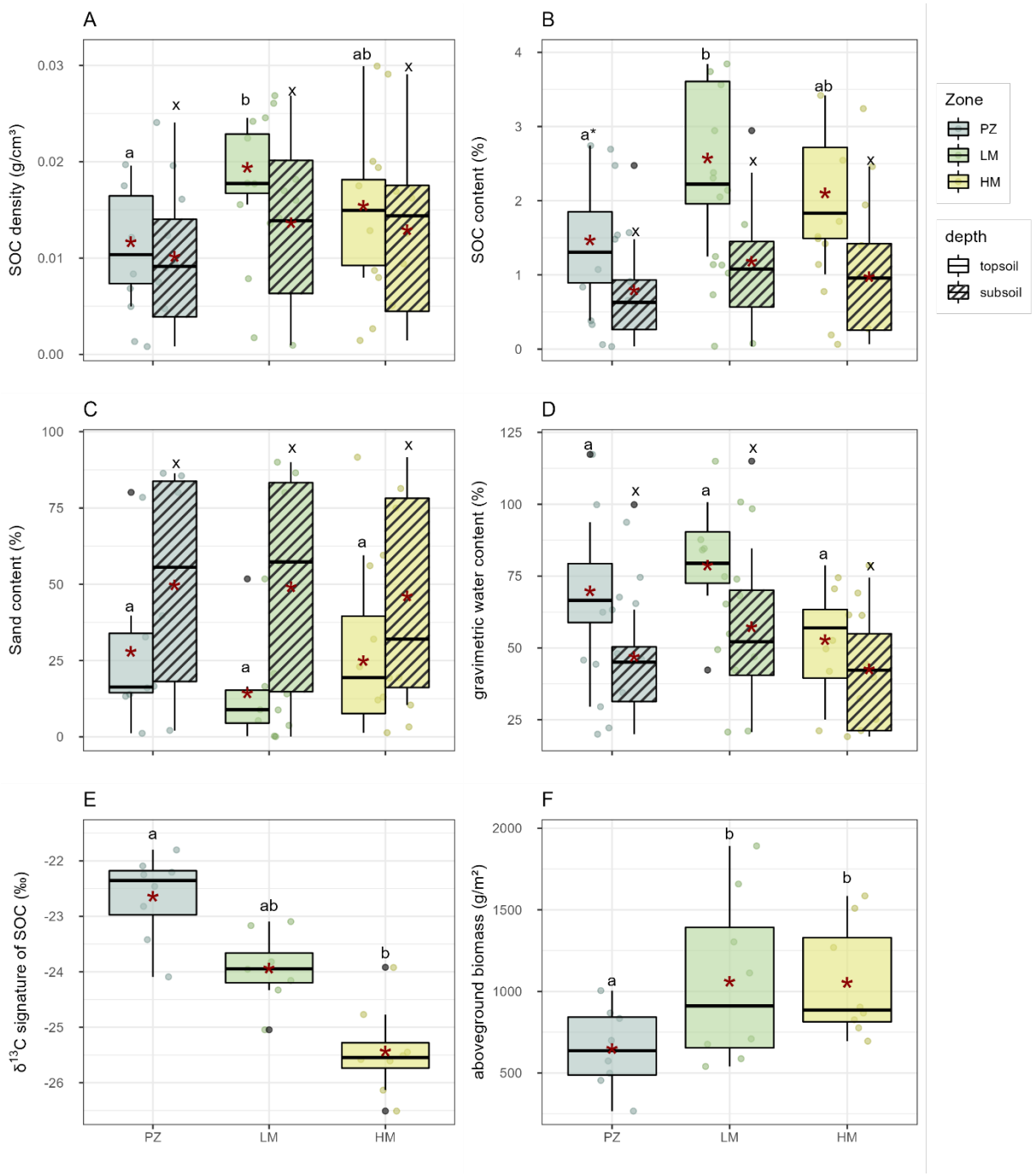

***FIGURE 2.5** | SOC content (%) **A**, SOC density (g/cm^3) **B**, sand content (%) **C**, gravimetric water content (%) **D**, $\delta^{13}C$ signature of SOC (‰ VPDB) **E**, and aboveground biomass AGB (g/m^2) **F** across vegetation zones reflecting progressing succession from pioneer zone (PZ), via low marsh (LM) to high marsh (HM) in North Sea salt marshes. Boxplots display the median (centered line), 25-quatrile and 75-quartile. Red stars display mean values of each site. Shaded boxplots display subsoil, not shaded boxplots display the topsoil. Single data points (means of each site-by-zone combination) are overlaid. Small letters indicate statistical significance (p-value < 0.05; * p-value <0.1) between zones based on Dunn test. Differences between topsoil and subsoil were not tested.*

***Table 2.2** | Mean vegetation height (cm), aboveground biomass (dry weight (DW, g/m²)), δ13C signature of SOC, SOC density (g/cm³) and SOC content (%) in the topsoil and subsoil for non-grazed North Sea salt marshes. Note: ± SE – Standard error.*

Zone	Mean height (cm)	DW AGB (g/m²)	Depth-profile	SOC $\delta^{13}C$ signature (‰)	±SE	SOC density (g/cm³)	±SE	SOC content (%)	±SE
pioneer zone	28.04	649.95	topsoil	-22.64	0.29	0.012	0.0017	1.47	0.26
			subsoil	-23.26	0.19	0.010	0.0014	0.80	0.12
low marsh	29.43	1080.42	topsoil	-23.89	0.38	0.019	0.0042	2.52	0.74
			subsoil	-23.49	0.27	0.014	0.0018	1.23	0.16
high marsh	26.52	1054.11	topsoil	-25.43	0.23	0.015	0.0033	2.10	0.76
			subsoil	-24.70	0.22	0.013	0.0021	0.97	0.14

2.4.3 | LIVESTOCK GRAZING EFFECTS

Livestock grazing increased the topsoil SOC density (Fig. 2.6 A) by approximately 50%. Grazing effects were more pronounced in the top 10 cm compared to deeper soil depths (Fig. 2.S4.1.). Soil bulk density (g/cm²) slightly increased with livestock grazing (Fig. 2.6 C). A slight decrease in the δ13C signatures was observed under grazing (Fig. 2.6 D). Grazing did not increase belowground biomass and significantly decreased aboveground biomass (Fig. 2.6 E, F).

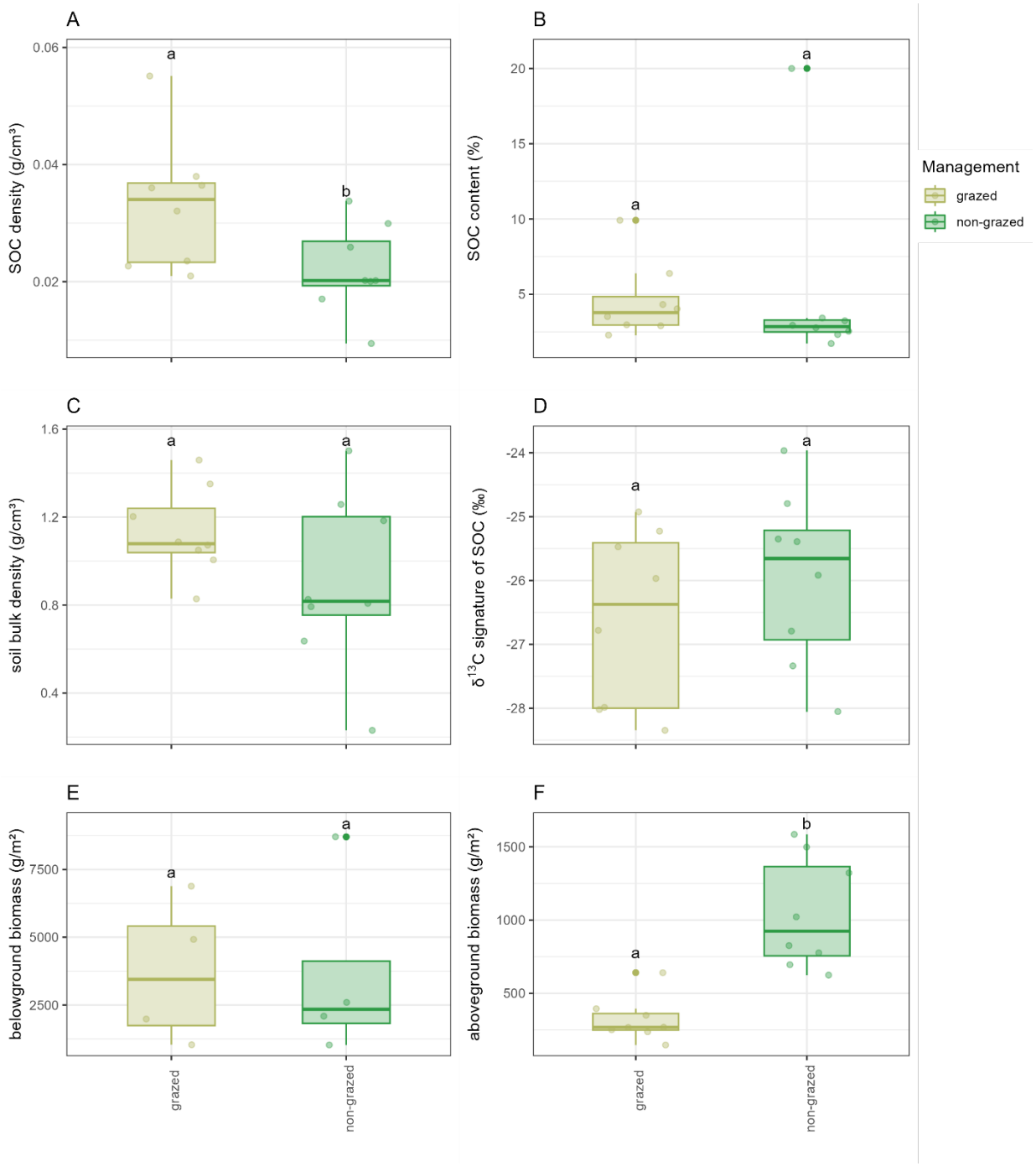

***FIGURE 2.6** | Livestock grazing effects on SOC density (g/cm²) **A**, SOC content (%) **B**, soil bulk density (g/cm²) **C**, the δ¹³C signature of SOC in the topsoil **D**, the belowground biomass (g/m²) **E** and the aboveground biomass (g/m²) **F**. Boxplots display the median (centered line), 25-quatrile and 75-quartile. Single datapoints (site means) are overlaid. Boxes not connected by the same letter are significantly different at p < 0.05 based on Kruskal-Wallis test. Note: Data from North Sea pioneer zones and low marshes are excluded.*

2.5 | DISCUSSION

2.5.1 | SALT MARSH SOC STOCKS OF THE GERMAN BALTIC AND NORTH SEA

We found an average SOC stock of 168±26.2 Mg SOC/ha (mean±SE), which is comparable to global averages of 162±259 Mg/ha for salt marshes reported by Duarte et al. (2013), and

approximately half compared to values reported in more recent meta-studies (Alongi (2020) with 317.2 ± 19.1 Mg SOC/ha (mean±SE); Maxwell et al. (2023) with 231±134 Mg SOC/ha (median ± median absolute deviation); this study with 154±143 (median±IQR)). Previous studies from the North Sea region (Elschot et al. 2015, Mueller et al. 2019b, Mueller et al. 2023, Leiva-Dueñas et al. 2024) and Baltic Sea region (Buczko et al. 2022, Leiva-Dueñas et al. 2024) indicate similar SOC stocks as reported here. SOC stocks of North Sea island salt marshes, which is 78±9 Mg SOC/ha, are below the German average of 168±26.2 Mg/ha whereas salt marshes located on the North Sea mainland coast and at the Baltic Sea, 187±24.9, 221±56.3 respectively, exceed the German average SOC stock.

The topsoil SOC stock of the North Sea salt marshes is approximately half that of the topsoil SOC observed in Baltic Sea salt marshes. The difference in topsoil SOC stock between North Sea mainland and islands salt marshes are rather small. Nonetheless, North Sea island salt marshes exhibit the lowest carbon stock, primarily due to the underlying sandy parent material, that dominated the one-meter profile of this salt marsh type. It can be assumed that this sandy foundation has not been significantly influenced by the salt marsh vegetation (Elschot et al. 2015, Pollmann et al. 2021), resulting in little to no additional carbon input and thus SOC content steeply declines down-core resulting in the lowest SOC stocks in North Sea island (Allen 2000, Elschot et al. 2024) salt marshes. In contrast, the high-energy North Sea mainland salt marshes are characterized by high rates of fine-grained sediment deposition (Allen 2000, Elschot et al. 2024). High rates of sediment deposition lead to a fast rates of minerogenic vertical accretion and enables rapid soil formation in these relatively young systems. The low-energy Baltic Sea salt marshes, on the other hand, form highly organic topsoils due to microtidal conditions that promote peat formation (Dijkema et al. 2010, Nolte et al. 2013a). The topsoil SOC stock of Baltic Sea salt marshes are greater than the one of North Sea mainland salt marshes. Despite the highly organic topsoils, Baltic Sea and North Sea mainland salt marshes SOC stocks are comparable across the whole one-meter depth profile. The high sediment deposition rate in North Sea mainland salt marshes leads to a dilution of the SOC with minerals (Granse et al. 2024) while simultaneously allowing for fast vertical accretion, resulting in the formation of thicker salt marsh soils with less organic-rich topsoil compared to that found in slow-accreting Baltic Sea and North Sea island salt marshes (see also Kirwan and Megonigal 2013). Consequently, 1-m SOC stocks are comparable between low-energy Baltic Sea and high-energy North Sea mainland salt marshes.

This study and previous research on North Sea and Baltic Sea salt marshes (e.g. Buczko et al. 2022, Leiva-Dueñas et al. 2024) reveal considerable spatial variability in SOC stocks both between different types of salt marshes and within the same type, emphasizing the necessity for regional assessments. Variability between sites both in topsoil and one-meter soil profiles was found to be the highest in Baltic Sea salt marshes, where we also found the highest variability in plant community composition (Fig. 2.S2.2). Numerous studies emphasize the strong control of plant

community composition on SOC dynamics (Langley et al. 2009, Langley and Megonigal 2010, Saintilan et al. 2013), therefore it is likely that the high variability in SOC stocks in Baltic Sea salt marshes is driven by larger variability in plant community composition and associated plant traits. Nevertheless, the differences in plant communities also indicate varying environmental settings at the different sites (Hulisz et al. 2016). For instance, sites in the southeastern Baltic (Große Kirr & Großer Wotig) had the highest topsoil SOC. Both sites lay within a lagoon which entails reduced water exchange, riverine inflow and shallow waters which provides protection from storm surge deposits and erosion (Hulisz et al. 2016). Moreover, the resulting lower salinity and flooding increase plant productivity which in turn increases the organic carbon input into the soil (Van de Broek et al. 2016, Hansen et al. 2017).

In contrast, the northern Baltic marsh sites (Schleimünde, Wendtorf, and Heiligenhafen) are less sheltered as they are situated behind beach ridges and dunes. These locations are more prone to storm surges, which can lead to erosion and increased salinity (Hulisz et al. 2016), resulting in low SOC stocks, as observed in Wendtorf. Additionally, storm surges can cause the redeposition of sand over the marshes (Dijkema 1990), which may lead to the burial of marshes, an occurrence suggested for Schleimünde. In this location, we found inconsistent presence of an organic layer in the topsoil, while denser peat layers were identified at greater depths. This phenomenon has been observed previously where reed peat layers were found under beach ridges in Heiligenhafen (Wanner 2009).

In German salt marshes (excluding Hallig and summer polder salt marshes) approximately 5.40 ± 0.928 Tg SOC are stored. This is somewhat higher than the value estimated in the review by Macreadie et al. (2021) (3.41-4.9 Tg SOC in German salt marshes). This is most likely due to the lower areal extent that has been used as the basis by Macreadie et al. (2021). The amount of 5.40 ± 0.928 Tg is proportionate with approximately 20 Tg CO2 equivalents (eCO2).

2.5.2 | ZONATION EFFECTS ON NORTH SEA SALT MARSH SOC

We hypothesized that SOC would increase from pioneer zone, via low marsh to high marsh under proceeding “terrestrial” influence (Connor et al. 2001, Spohn et al. 2013, Ouyang and Lee 2014, Hansen et al. 2017, Mueller et al. 2020a). Indeed, we found the high marsh topsoils to be most depleted in 13C which is to be expected given the persistent influence of C3- dominated plant communities along soil development and proceeding succession (Suchrow and Jensen 2010, Whitaker et al. 2015). However, despite the increasing terrestrial influence with proceeding succession from pioneer zone, via low to high marshes, this study found the SOC peaks in the low marsh, decreasing significantly towards the pioneer zone and slightly towards the high marsh. The high marsh as the oldest successional stage with highest elevation entails reduced tidal influence and thus augmented aeration of the soil enhances oxidation of organic matter (Hemminga and Buth 1991, Mueller et al. 2016). Furthermore, the highest SOC content in the low marsh is associated

with the lowest sand and highest water content. It has previously been shown that water content correlates positively and sand content correlates negatively with SOC content in salt marshes (Kelleway et al. 2016, Stagg et al. 2017, Leiva-Dueñas et al. 2024), through reducing microbial remineralization of SOC by decreasing oxygen availability (Kelleway et al. 2016, Chapman et al. 2019) and higher mineral association of SOC with fine sediments (Baldock and Skjemstad 2000).
Plant community composition and associated plant traits control soil biogeochemistry and SOC dynamics in coastal wetlands (Saintilan et al. 2013, Mueller et al. 2016, Granse et al. 2024, Mittmann-Goetsch et al. 2024, Mueller and Megonigal 2024). In North Sea salt marshes, plant communities clearly differ between vegetation zones (Fig. 2.S3.2.). Non-grazed high marsh and pioneer zone were found to have the lowest plant species richness with mono-dominant plant communities. On the contrary, the low marsh exhibited comparatively high plant species richness. Plant diversity has been shown to increase SOC across different ecosystems (Lange et al. 2015, Chen et al. 2020b). This is primarily driven by the increasing plant trait functionality of the more diverse plant community (De Deyn et al. 2008, Ford et al. 2016), which is associated with increased plant productivity (Duffy et al. 2017). At any rate, in this study the SOC peak in the low marsh cannot be explained by the aboveground biomass. Likewise, plant diversity increases belowground productivity through root space partitioning by functionally different species (Loreau and Hector 2001, Steudel et al. 2011). Thereby it can be assumed, that direct belowground inputs through root productivity and root exudation are highest in the low marsh. This is also emphasized by Redelstein et al. (2018) who found the highest fine root biomass in the low marsh for both island and mainland North Sea salt marshes. Furthermore, Granse et al. (2024) found a greater sediment-trapping capacity in high marsh compared to low marsh plant communities, resulting in greater dilution of SOC with mineral sediments in the high marsh. Conclusively, we suggest that the higher SOC quantity in the low marsh is potentially caused by shifts in plant productivity and SOC decomposition or stabilization processes linked to low oxygen-availability (as a result of fine soil texture and more regular inundation). Furthermore, SOC is likely lost and diluted in the high marsh soil as a consequence of soil aeration and higher sediment trapping, respectively.

2.5.3 | LIVESTOCK GRAZING EFFECTS ON SALT MARSH SOC DENSITY

In line with our third hypothesis, we found an overall increase in SOC density under livestock grazing in the topsoil across Baltic and North Sea salt marshes. This effect is strongest in the top 10 cm and vanishes with soil depth (Fig. 2.S4.1). Similar effects of livestock grazing on SOC density were reported by Elschot et al. (2015) and Leiva-Dueñas et al. (2024) for salt marshes in the Netherlands and Denmark, respectively. Conversely, a global meta-analysis with most observations from European sites revealed no consistent effect of livestock grazing on SOC (Davidson et al. 2017). Livestock grazing affects vegetation and soil processes related to SOC decomposition

(Elschot et al. 2015, Davidson et al. 2017, Mueller et al. 2017). Trampling associated with grazing increases bulk density by compacting soils (Nolte et al. 2013a) and alters pore connectivity (Keshta et al. 2020). These changes increase water saturation in the soil and subsequently decrease soil oxygen availability and microbial activity (Mueller et al. 2017, Keshta et al. 2020). In North Sea salt marshes, we confirm a raise in soil bulk density with livestock grazing, whereas this effect was not found in Baltic Sea salt marshes. Baltic Sea salt marshes have higher sand content than North Sea salt marshes (Fig. 2.S2.1 D) which has been shown to alleviate possible grazing effects on soil compaction (Schrama et al. 2013, Keshta et al. 2020).

Most consistency in the SOC-density response towards grazing is found in North Sea mainland salt marshes, whereas responses in Baltic Sea salt marshes remain variable (Fig. 2.S4.2 A; Fig. 2.S4.3 A). Under grazing, the removal of the aboveground biomass can additionally cause a shift in carbon allocation towards belowground biomass, directly increasing the belowground carbon inputs (Elschot et al. 2015). Belowground biomass responses to grazing varied from positive to negative among sites. In Baltic Sea salt marshes, we observed an increase in SOC under grazing in one site (Heiligenhafen), which could be explained by increased belowground biomass (Fig. 2.S4.3 A, E). The other Baltic site (Schleimünde) did not show a difference in SOC density between grazed and non-grazed areas despite increased soil bulk density in grazed plots. Here we found belowground biomass to be higher in non-grazed plots (Fig. 2.S4.3 E). Therefore, we argue that, within Baltic Sea salt marshes, compaction effects through trampling are mitigated by changes in belowground productivity.

The reduction of aboveground biomass as a result of livestock grazing decreases sediment trapping, which consequently reduces the deposition of marine sediments (Schulze et al. 2021). Here, we propose that the SOC dilution through mineral sediments (Granse et al. 2024) is a direct consequence of non-grazing on plant-sediment interactions. This phenomenon results in a higher dilution of SOC with allochthonous mineral sediment under non-grazed conditions. Indeed, our results show in line with our fourth hypothesis, that grazing leads to a higher share of autochthonous carbon sources in the SOC pool by displaying more depletion of δ13C signatures (Khan et al. 2015). Elschot et al. (2015) argue that grazing increases the belowground biomass which in return could cause an increased autochthonous carbon input. However, we do not find a consistent increase of belowground biomass with grazing and therefore suggest that the increase of δ13C in non-grazed salt marshes is the outcome of less sediment trapping resulting in higher dilution with allochthonous carbon sources (Mueller et al. 2019b, Granse et al. 2024).

2.6 | CONCLUSION AND IMPLICATIONS

Throughout this study we propose sedimentary properties to be a key driver for differences in SOC stock and density between salt marsh types and within zonation. Lower sediment deposition rates

in Baltic salt marshes, North Sea low marsh vegetation and salt marshes under livestock grazing are associated with higher SOC densities. Sedimentation dynamics are controlled by plant community composition and associated traits, whereas plant community composition is controlled by grazing or flooding regime. The higher sediment deposition rates in North Sea mainland salt marshes presumably allow them to keep pace with accelerated rates of sea-level rise (Kirwan et al. 2016, Elschot et al. 2024) bearing higher potential for future climate change mitigation. Baltic Sea salt marshes store considerable amounts of SOC underscoring the necessity to protect these ecosystems to prevent potential carbon emission as a consequence of marsh loss (e.g. marsh edge erosion).

2.7 | ACKNOWLEDGEMENT

We would like to thank Kathryn Nicol and Hannah Hosbach for their insightful field work contributions and for their consistently reliable work. This study was carried out in the framework of the BMBF funded project sea4soCiety (project number 03F0896F). Further, Ella Logemann was funded by Deutsche Forschungsgemeinschaft as associated doctoral researcher of the Research Training Group 2530 ‘‘Biota-mediated effects on Carbon cycling in Estuaries’’ (project number 407270017). Peter Mueller was funded by Deutsche Forschungsgemeinschaft (DFG) in the framework of the Emmy Noether program (502681570).

Open Research

The data sets used in this study are archived at PANGAEA.

Data supporting the comparison of salt marsh types and the analysis of zonation effects on SOC stocks are available at: https://doi.org/10.1594/PANGAEA.982732 (Logemann et al., 2025a).

Data supporting the analysis of management effects on SOC stocks are available at: https://doi.org/10.1594/PANGAEA.982734 (Logemann et al., 2025b).

CHAPTER THREE | REDOX CONTROLS EXUDATE-DERIVED CARBON STABILITY IN COASTAL WETLAND SOILS

REDOX CONTROLS EXUDATE-DERIVED CARBON STABILITY IN COASTAL WETLAND SOILS

To be submitted to *Soil Biology and Biogeochemistry*.

Hao Tang[1, 3†] & **Clarisse Goesele**[2†], Namid Krüger[4], Xiaolin Dou[5], Meng Lu[6], Kai Jensen[2], and Peter Mueller[3, 4*]

[1]The Faculty of Geography Resource Sciences, Sichuan Normal University, Chengdu, 610066, China

[2]Institute of Plant Science and Microbiology, University of Hamburg, Hamburg, 22609, Germany

[3]Department of Natural and Environmental Sciences, University of Kaiserslautern-Landau, Landau, 76829, Germany

[4]Institute of Landscape Ecology, University of Münster, Münster, 48149, Germany

[5]Research Center for Eco-Environmental Sciences, Chinese Academy of Sciences, Beijing, 100085, China

[6]School of Ecology and Environmental Science, Yunnan University, Kunming, 650091, China

[†]Hao Tang and Clarisse Goesele contributed equally to this work

*Corresponding author: hao.tang (hao.tang@rptu.de)

Keywords: Mineral-organic associations, soil organic carbon, $^{13}CO_2$ labeling, blue carbon, salt marsh

3.1 | ABSTRACT

Coastal wetlands are global hotspots of soil carbon (C) sequestration, but the processes and sources contributing to long-term soil C stores of these ecosystems are not yet fully understood. Root exudates, although chemically considered highly labile, can substantially contribute to stable soil C pools in terrestrial upland soils, but their fate under anoxic conditions of wetland soils remains poorly understood. A two-tier $13CO_2$ pulse-labeling approach was applied to investigate the stability and turnover of root exudate-derived C in coastal wetland soils. In a 440-day long-term incubation (Experiment I), 13C signals from Spartina anglica root exudates remained detectable in soils, with greater retention under anoxic than oxic conditions, indicating that root exudate-derived C can persist in wetland soils over extended time periods. A four-week incubation with soils amended with ^{13}C-labeled root exudates from Spartina anglica or Elymus athericus examined CO_2 and CH_4 production and their C isotopic signatures (Experiment II). Initially, oxygen addition markedly enhanced the mineralization of both native soil organic C and exudate-derived C, with negligible isotopic shifts indicating similar oxygen sensitivity of both C sources. Over the four weeks, gradual shifts in the isotopic signatures of produced gases suggested either a slightly higher oxygen sensitivity of native soil C than exudate-derived C, or depletion of the added exudates. Combined results from Experiments I and II demonstrated the strong oxygen sensitivity of exudate-derived C, with oxic conditions enhancing mineralization and anoxic conditions favoring stabilization. Overall, our findings highlight the dual role of root exudates as both readily decomposable C inputs and precursors of persistent soil organic matter, providing new insights into the redox control of root-derived C dynamics in wetland soils.

3.2 | INTRODUCTION

Coastal wetlands, such as salt marshes and mangroves, are ecosystems that store large amounts of carbon (C), often referred to as "blue C". Although their global area is relatively small compared to other ecosystems, coastal wetlands store a disproportionately large fraction of global soil organic carbon (SOC) (McLeod et al. 2011, Nahlik and Fennessy 2016, Maxwell et al. 2023). The remarkable C sequestration capacity of coastal wetlands results from high rates of plant productivity and suppressed microbial decomposition in anoxic soils (Duarte and Prairie 2005). However, shifts in wetland hydrology, such as prolonged wetter or drier conditions, can alter redox regimes and thereby affect the capacity of coastal wetlands to sequester and store C, potentially shifting them from C sinks to C sources (Kirwan and Megonigal 2013).

Organic C in coastal wetlands comes from allochthonous sources (such as inputs from rivers, estuaries, or the ocean) and autochthonous sources (Saintilan et al. 2013). Autochthonous inputs include plant litter, rhizomes/roots, and root exudates, each of which has distinct chemical composition and decomposition dynamics. Root exudates are usually labile and can be quickly used by microbes (Anderson et al. 2024), while lignin-rich plant litter is more resistant and decomposes at a slower rate. Root exudates represent a dynamic C flux that supplies soluble organic compounds directly to microbes in the rhizosphere, acting as a "live-root C pump" (Jones et al. 2009). The composition of root exudates mainly includes organic acids, sugars, amino acids, and various secondary metabolites (Canarini et al. 2019). Some exudates classes, such as phenols, are known to inhibit soil microbial activity (Hamer and Marschner 2005, Sogin et al. 2022) and, under anoxic conditions, even labile exudates such as glucose have been shown to induce negative priming (Krüger et al. 2025), whereas others act as substrates that promote organic matter turnover or support stabilization through binding with minerals (Hamer and Marschner 2002). Although knowledge of root exudate functions in C cycling is growing for upland soils, the role of root exudates in wetland C stabilization remains poorly explored.

Root exudates in upland soils can follow several pathways that influence stability. Low-molecular-weight compounds such as organic acids, sugars, and amino acids are quickly taken up by microbes, and the resulting microbial products can associate with minerals to form mineral-associated organic matter (MAOM), a process central to the Microbial Efficiency-Matrix Stabilization (MEMS) framework (Cotrufo et al. 2013, Lehmann and Kleber 2015) Exudates can also bind directly to reactive mineral surfaces, particularly clays and Fe/Al oxides, thereby reducing microbial access (Keiluweit et al. 2015, Hemingway et al. 2019). In addition, root-derived compounds may promote soil aggregation through interactions with microbial extracellular polymers and fungal hyphae, providing physical protection (Baumert et al. 2018).

Beyond the pathways observed in upland soils, the stabilization of organic matter in wetlands is strongly influenced by redox state. Hydrological dynamics such as periodic flooding, oxygen

limitation, and fluctuating redox conditions create complex microbial and mineral responses (Megonigal et al. 2004, Keiluweit et al. 2017, Mueller and Megonigal 2024). Under oxic conditions, reactive Fe and Al oxides promote the formation of organo–mineral associations that effectively protect organic C, whereas anoxic conditions can liberate mineral-bound organic matter through reductive dissolution or pH-driven desorption (Grybos et al. 2009, Bai et al. 2021, Afsar et al. 2023). Under anoxic condition, Fe and S cycling may either promote stabilization through co-precipitation with iron-containing minerals or enhance C losses through reductive dissolution and fermentation pathways (Lalonde et al. 2012, Hall and Silver 2015). At the same time, the decomposition of chemically more recalcitrant organic C with low nominal oxidation states is more strongly constrained by oxygen availability—or by the availability of electron acceptors in general—than the decomposition of chemically more labile compounds with higher nominal oxidation states (Kristensen et al. 1995, Keiluweit et al. 2016, Lin et al. 2021). Because root exudates are typically considered chemically labile, consisting mainly of organic acids, sugars, and amino acids with relatively high nominal oxidation states, their decomposition is likely less limited by electron acceptor availability (Mueller and Megonigal 2024). Most of these mechanisms, however, have been described under relatively static redox conditions. In natural wetlands, shifts between oxic and anoxic conditions may strongly influence these processes. Oxygen reintroduction may, through coupled microbial–mineral interactions, accelerate the mineralization of exudate-derived C that was previously stabilized. Thus, redox fluctuations likely play a pivotal role in regulating the fate of root exudate C in wetlands, yet the processes governing this fate remain poorly understood.

Our study employed a two-tier experimental approach to investigate the stability of root exudate-derived C under contrasting redox conditions in coastal wetlands, using a $^{13}CO_2$ pulse-labeling technique. In Experiment I, *Spartina anglica* plants were pulse-labeled with $^{13}CO_2$ while growing in wetland soils, thereby introducing ^{13}C-labeled root exudates into the soil. The soils amended with ^{13}C-labeled root exudates were subsequently subjected to long-term incubations to assess the persistence of exudate-derived C under anoxic conditions and its response to a subsequent oxic shift. In Experiment II, soils from microcosms in which *S. anglica* and *Elymus athericus* plants had been pulse-labeled with $^{13}CO_2$, and thus contained ^{13}C-labeled root exudates, were used in short-term incubations to evaluate species-specific effects and the role of oxygen availability in regulating exudate turnover. We hypothesized that: (1) Root exudate-derived organic C can stabilize in anoxic wetland soil. (2) Oxygenation causes rapid mineralization of exudate-derived C stabilized under anoxic conditions. (3) Oxygenation accelerates the decomposition of native SOC more strongly than that of root exudates, reflecting that the decomposition of chemically recalcitrant organic matter is more strongly constrained by electron acceptor availability than that of chemically labile compounds.

3.3 | METHODS

3.3.1 | EXPERIMENT I: LONG-TERM STABILITY OF ROOT EXUDATE-DERIVED CARBON

Plant preparation

S. anglica plants were collected from a salt marsh site at Hamburger Hallig (54°60'21.53'' N, 8°81'66.29'' E) on April 26, 2019. Prior to labeling, plants were cultivated under waterlogged soil conditions for two months in a greenhouse at the Institute of Plant Science and Microbiology, University of Hamburg. Six weeks before labeling, plants were transplanted into microcosms (10 cm diameter × 15.2 cm depth), each containing approximately 1100 g of homogenized tidal-creek sediment collected from the same site at Hamburger Hallig. Microcosms were maintained under continuously waterlogged conditions, with the water level kept just above the soil surface. Salinity and ion availability were controlled by adding synthetic sea salt to achieve a salinity of 15 practical salinity units (PSU).

Labeling procedure and sample collection

Three waterlogged *S. anglica* soil microcosms were pulse-labeled with $^{13}CO_2$ over a period of 10 days. Each day, microcosms were enclosed for 2.5–3.5 h in an airtight acrylic glass chamber (Fig. 3.1A). The $^{13}CO_2$ was generated by acidifying approximately 0.1 g sodium bicarbonate-^{13}C (98 atom %, Sigma-Aldrich, St. Louis, USA) with 8 mL of 10% hydrochloric acid, which elevated the CO_2 concentration inside the chamber from ambient levels (~400 ppm) to 2100–2800 ppm. A labeling pulse was terminated once the CO_2 concentration declined to ~200 ppm, reflecting the balance between photosynthetic uptake and respiratory release. One additional plant–soil microcosm remained unlabeled and served as a control. Bulk soil was sampled on days 0, 3, 7, and 11 and immediately frozen. On day 11, soils containing ^{13}C-labeled root exudates of *S. anglica* were collected and used in the subsequent long-term incubation experiment.

Long-term incubation experiment (0 – 440 days)

A microcosm experiment was conducted using ^{13}C-labeled soil subsamples to evaluate the decomposition and stabilization of root exudates. The experiment included two treatments: labeled and unlabeled soils. In total, twelve microcosms were established under continuously waterlogged conditions. Soil was sampled nine times over a 15-month period (days 1, 5, 8, 46, 52, 58, 89, 220, and 440) to monitor temporal changes in $\delta^{13}C$ signatures (Fig. 3.1B, blue section).

Redox-shift incubation (440–693 days)

Following the 440-day sampling, three of the microcosms containing soils with labeled root exudates were maintained under waterlogged (anoxic) conditions, while three of the previously

anoxic microcosms were switched to oxic conditions. Both the oxic and anoxic sets were resampled 253 days later (i.e., on day 693 of the experiment) for soil $\delta^{13}C$ analysis (Fig. 3.1B, light section).

$\delta^{13}C$ analysis

Soil samples were oven-dried at 60 °C for 48 h. After drying, samples were ground using a mortar, transferred into glass vials, and treated with 0.5 mL of 10% HCl solution to remove carbonates. Samples were dried again at 60 °C for 48 h. For C isotope determination, 0.7–0.8 mg of dried samples were weighed into 4 × 6 mm tin cups (HEKAtech, Germany). Carbon isotope analyses were performed using an isotope-ratio mass spectrometer (Nu Horizon, Nu Instruments Limited, UK) coupled to an elemental analyzer (EURO-EA 3000, Euro Vector, Italy) in a continuous-flow configuration (setup provided by HEKAtech, Germany). Two standards were used for validation: IAEA-600 caffeine ($\delta^{13}C$ = –27.8‰) and BBOT [2,5-bis-(5-tert-butyl-2-benzo-oxazol-2-yl)thiophene] ($\delta^{13}C$ = –25.9‰).

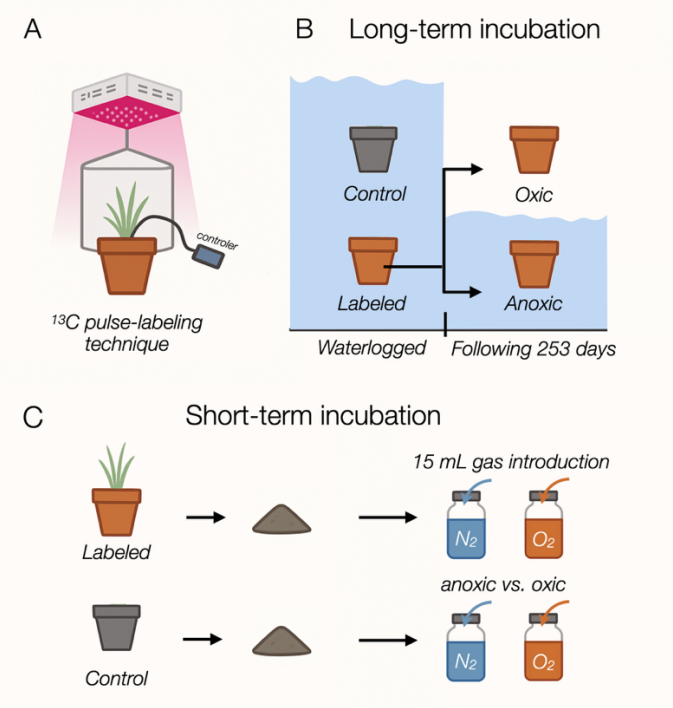

***FIGURE 3.1** | Overview of the experimental design, (A) a ^{13}C pulse labeling scheme, (B) Experiment I: Long-term stability of root exudate-derived carbon, and (C) Experiment II: short-term oxygen effects on root exudate stability.*

3.3.2 | EXPERIMENT II: SPECIES-SPECIFIC AND OXYGEN EFFECTS ON ROOT EXUDATE STABILITY

^{13}C pulse-labeling of plants

In 2022, *S. anglica* and *E. athericus* plants were collected from Hamburger Hallig (54°60’21.53″ N, 8°81’66.29″ E) and cultivated for four months in pots (10 cm diameter × 15.2 cm depth) filled with homogenized tidal-creek sediment from the same site as in Experiment I in a greenhouse at

the Institute of Plant Science and Microbiology, University of Hamburg. Three uniformly growing plants of each species (n = 3 for *S. anglica*, n = 3 for *E. athericus*) were selected for the ^{13}C pulse-labeling experiment. The labeling was performed for five consecutive days, with a duration of 3.5 hours per day. On the sixth day, the labeling was terminated, and the soils containing ^{13}C-labeled root exudates from *S. anglica* and *E. athericus* were separately collected. In addition, non-vegetated control soils (n = 3) from the same sediment were prepared and treated identically to the planted pots. A portion of the samples was used for ^{13}C content analysis, while the remaining soils were stored at -80°C for the subsequent incubation experiment.

Anoxic and oxic incubation experiment

Inside an anaerobic glove box, 50 g of thawed, ^{13}C-labeled soil (all soils were sieved to remove plant material prior to incubation) from *S. anglica* and *E. athericus* were separately weighed into 120 mL gas-tight incubation bottles (n = 12 per species, prepared as 3 natural replicates × 2 technical replicates x 2 treatment). Additionally, non-vegetated soils (unlabeled) served as a control treatment (n = 6, prepared as 3 natural replicates × 2 treatment). Each bottle received 20 mL of anoxic water prepared as a concentration of 0.0282 mol/L K_2SO_4 solution to simulate the ionic strength and sulfate availability of natural seawater. After removal from the glove box, incubation bottles were thoroughly mixed for 2 hours on a shaker and then pre-incubated for two weeks.

Following pre-incubation, all jars were flushed with pure nitrogen to remove residual oxygen and establish anoxic starting conditions. the two treatments were distributed between oxic and anoxic conditions (one in each), yielding 6 oxic and 6 anoxic replicates per species, and 3 oxic and 3 anoxic control replicates (Fig. 3.1C). Oxic conditions were established by adding 20 mL of pure oxygen to the headspace, while anoxic conditions were maintained by adding 20 mL of pure nitrogen. Each week, 20 mL of headspace gas was first collected from every bottle for subsequent analysis of CO_2, CH_4, and $\delta^{13}C$ signatures, following the method of Krüger et al. (2025) using three connected syringes. The bottle pressure was measured before each gas sampling, and gas sampling and replenishment were repeated weekly for a total of four weeks. Gas samples for isotopic measurements ($\delta^{13}C$) were stored in 120 mL gas-tight containers with 10 mL of saturated zinc acetate solution (43 g/ 100 mL) until analysis, whereas CO_2 and CH_4 concentrations were determined directly using gas chromatography.

CO_2, methane and related ^{13}C gas measurements

CO_2 and CH_4 concentrations were quantified using a gas chromatograph (SRI 8610 GC/FID, equipped with a methanizer jet from SRI Instruments Europe, Bad Honnef, Germany). The $\delta^{13}C$ isotopic signatures of the gases were analyzed with a cavity ring-down spectrometer (G2201-i, Picarro, Santa Clara, CA, USA) equipped with a small-sample introduction module (SSIM)

operating with synthetic air. The amounts of CO_2 and methane in the headspace of the incubation jars were calculated by applying the ideal gas law. The respiration was approximated by the difference of the amounts of the gases in the headspace at timepoint t_x and t_{x-1} considering also the missing gas due to the gas samplings. The respiration of CO_2 and methane were combined to a total respiration flux (mg C). The isotopic signature of the total C gases in the headspace was calculated by multiplying the isotopic signature (in atom %) of each gas by its proportion of the total C gases and then summing these values (Krüger et al. 2025).

3.3.3 | STATISTICS AND ANALYSIS

For Experiment I, one-way ANOVA was used to test for differences in $\delta^{13}C$ isotopic signatures of SOC between oxic and anoxic treatments, and between ^{13}C-labeled and unlabeled soils across sampling dates. For Experiment II, two-way ANOVA was performed to evaluate the effects of plant species (*S. anglica* versus *E. athericus*) and redox condition (oxic versus anoxic) on cumulative respiration and $\delta^{13}C$ of gases in the headspace. To account for variability among replicates in Experiment II, we calculated $\Delta\delta^{13}C$ values as the within-replicate difference between oxic and anoxic treatments ($\delta^{13}C_{oxic} - \delta^{13}C_{anoxic}$), and then averaged these values across replicates for statistical evaluation. This metric reflects the isotopic shift in respired C gases induced by oxygenation, with positive values indicating higher $\delta^{13}C$ under oxic conditions and negative values indicating higher $\delta^{13}C$ under anoxic conditions. When significant main or interaction effects were detected ($p < 0.05$), post hoc pairwise comparisons were conducted using Tukey's HSD test. All statistical analyses were carried out in R (Version 4.3.2), and data visualization was performed with Datagraph (Version 5.4).

3.4 | RESULTS

The $\delta^{13}C$ signature of SOC declined rapidly within the first 8 days of the microcosm experiment, whereas soils without ^{13}C labeling maintained stable SOC isotopic signatures throughout the experiment (Fig. 3.2). During the first week (day 0 to day 8), the $\delta^{13}C$ signature of SOC in the ^{13}C-labeled soils decreased sharply from +37.0‰ to +6.6‰. Between day 8 and day 89, the $\delta^{13}C$ signatures of SOC stabilized within the range of +2.0‰ to +8.4‰. At later time points, mean values further decreased to +0.8‰ at day 220 and +0.3‰ at day 440. In contrast, soils without ^{13}C-labeled remained stable between –23.5‰ and –23.1‰ until day 440, after which $\delta^{13}C$ signatures of SOC slightly increased to –15.8‰. Following the 440-day incubation, a subsequent redox-shift experiment was conducted by incubating labeled soils for an additional 253 days under contrasting hydrological conditions. The $\delta^{13}C$ signature of SOC was significantly higher under anoxic (+8.8 ± 5.9‰) than under oxic conditions (–3.1 ± 3.2‰; Fig. 3.2).

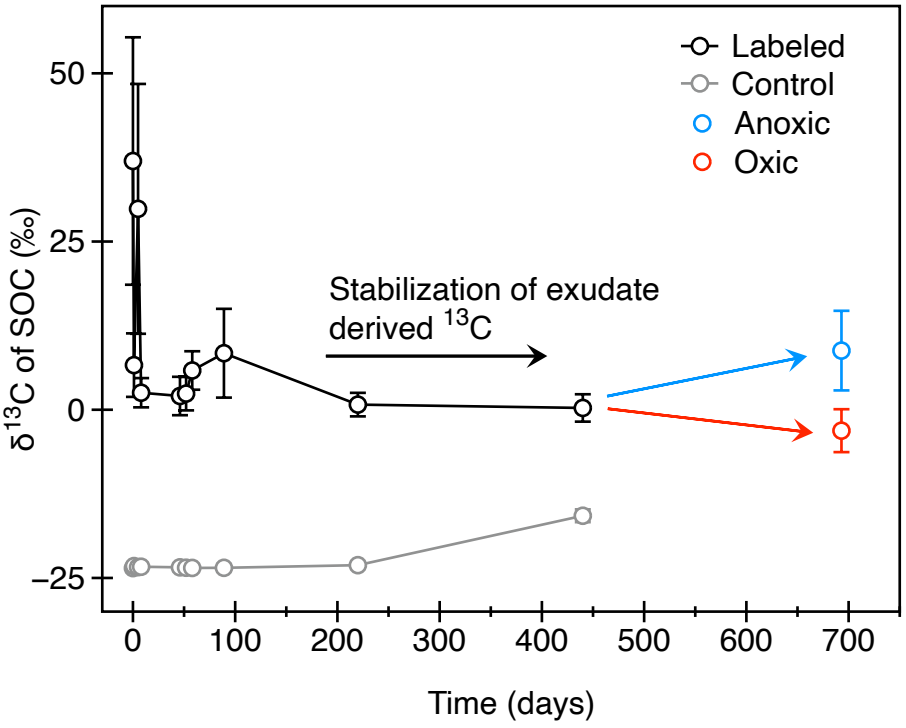

***FIGURE 3.2** | δ^{13}C signatures of soil organic carbon in ^{13}C-labeled and unlabeled soils during the long-term incubation (0–440 days; sampling on days 1, 5, 8, 46, 52, 58, 89, 220, and 440). Following day 440, a redox-shift incubation was conducted in which subsets of the labeled soils were maintained under anoxic (waterlogged) or switched to oxic (drained) conditions and resampled after 253 additional days (day 693). Values represent mean ± SE.*

Experiment II – Species and oxygen effects on root exudate dynamics

Cumulative respiration

The cumulative total soil respiration over four weeks exhibited clear differences between oxic and anoxic conditions. No significant differences were observed in the first two weeks ($p = 0.31$ at week 1; $p = 0.64$ at week 2), whereas from week 3 onward respiration rates under oxic conditions were markedly higher than under anoxic conditions (168% higher at week 3, $p < 0.001$; 250% higher at week 4, $p < 0.001$; Fig. 3.3). In the oxic treatments, cumulative respiration in soils previously planted with S. anglica and E. athericus increased significantly from week 1 to week 4 ($p < 0.01$) and reached 4.0 ± 0.3 and 4.8 ± 0.2 mg C, respectively, compared to 3.9 ± 0.1 mg C in the control after four weeks. E. athericus soils respired significantly more than the control ($p = 0.03$), whereas S. anglica soils did not differ ($p > 0.05$). Under anoxic conditions, cumulative respiration did not change significantly from week 1 to week 4, but soils previously planted with S. anglica and E. athericus showed significantly higher cumulative respiration than the control ($p < 0.05$). In addition, during the incubation, a clear CH_4 flux to the headspace was observed in the anoxic S. anglica soils, whereas in the oxic treatments, CH_4 concentrations in the headspace decreased, indicating net CH_4 consumption.

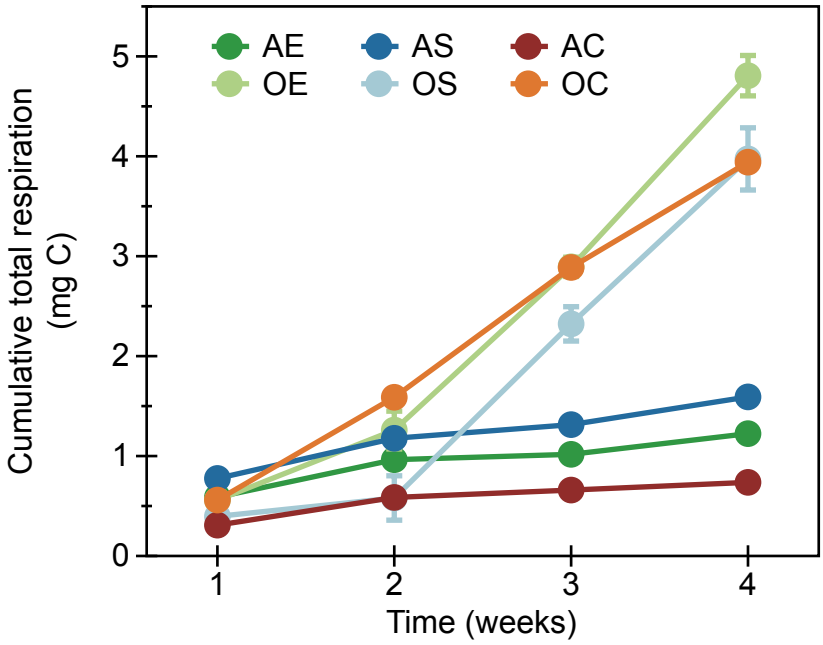

***FIGURE 3.3** | Cumulative total respiration over four weeks of incubation under oxic and anoxic conditions for soils previously planted with Spartina anglica and Elymus athericus (plants removed prior to incubation), as well as control soils (without ^{13}C labeling). All values are mean ± SE. Under both oxic and anoxic conditions, there were six replicates for the soils containing exudates and three replicates for the control. Note: A represents anoxic condition, O represents oxic condition, S represents S. anglica, E represents E. athericus, and C represents control without plant.*

Sources of CO_2 and methane

The $\delta^{13}C$ signature of total headspace C (CH_4 + CO_2) from soil containing exudates was significantly higher than that of control soils (Fig. 3.4). Within each species, $\delta^{13}C$ values remained relatively stable throughout the four-week incubation, with no significant temporal differences detected from week 1 and week 4 under either oxic or anoxic conditions. Across all treatments, $\delta^{13}C$ signatures in the headspace were consistently higher in jars with soils affected by *S. anglica* than in those affected by *E. athericus*.

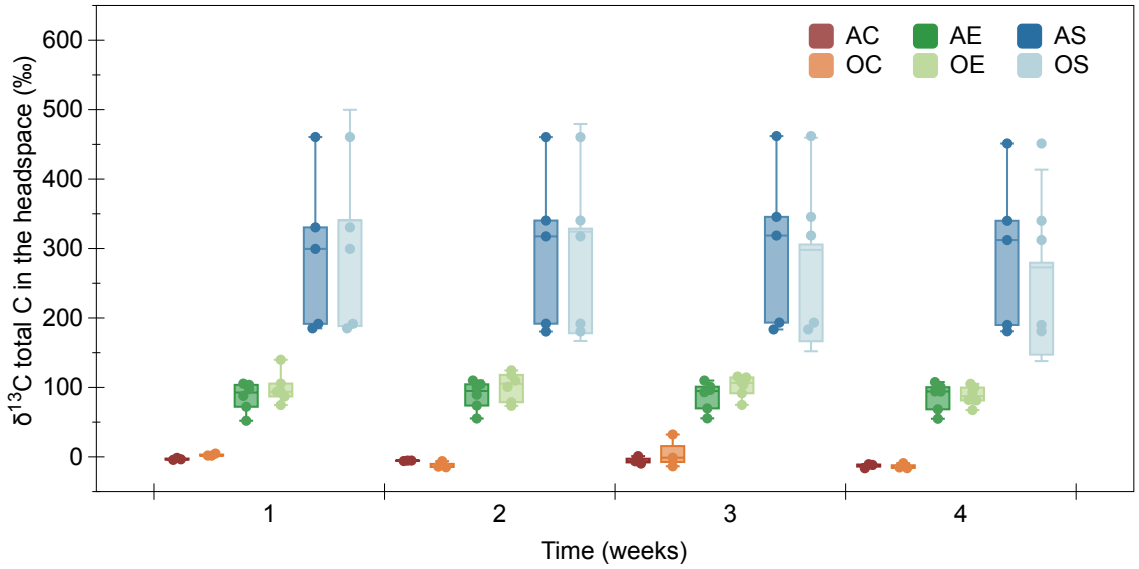

FIGURE 3.4 *| The $\delta^{13}C$ signature of total carbon in the headspace over four weeks of incubation under oxic and anoxic conditions for rhizosphere soils previously planted with ^{13}C-labeled Spartina anglica and Elymus athericus (plants removed prior to incubation), as well as unplanted control soils (without ^{13}C labeling). All values are mean ± SE. Under both oxic and anoxic conditions, there were six replicates for the soils containing exudates and three replicates for the control Note: A represents anoxic condition, O represents oxic condition, S represents S. anglica, E represents E. athericus, C represents control without previous plantings.*

The $\Delta\delta^{13}C$ signatures of C gases in the headspace (oxic – anoxic difference) showed contrasting temporal dynamics between the two species. For *E. athericus*, $\Delta\delta^{13}C_{OE-AE}$ values remained positive from week 1 to week 3 (12.6‰, 12.0‰, and 13.9‰, respectively), with only minor changes relative to week 1 (-5% at week 2 and +10% at week 3), and declined strongly toward zero by week 4, falling from 12.6‰ at week 1 to 1.5‰ (an 88% decrease). However, none of these changes were statistically significant (paired t-tests, $p = 0.89$, 0.92, and 0.32 for weeks 2–4 vs week 1). In contrast, for *S. anglica*, $\Delta\delta^{13}C_{OS-AS}$ shifted from positive values at week 1 (20.8‰) to near zero at week 2, decreasing by 86% to 3.0‰, and further decreased to -13.2‰ at week 3 (a 164% decrease relative to week 1) and -34.8‰ at week 4 (a 268% decrease). The decline in *S. anglica* treatment became statistically significant by week 4 ($p = 0.03$), whereas earlier time points showed strong but non-significant trends (week 2, $p = 0.08$; week 3, $p = 0.10$).

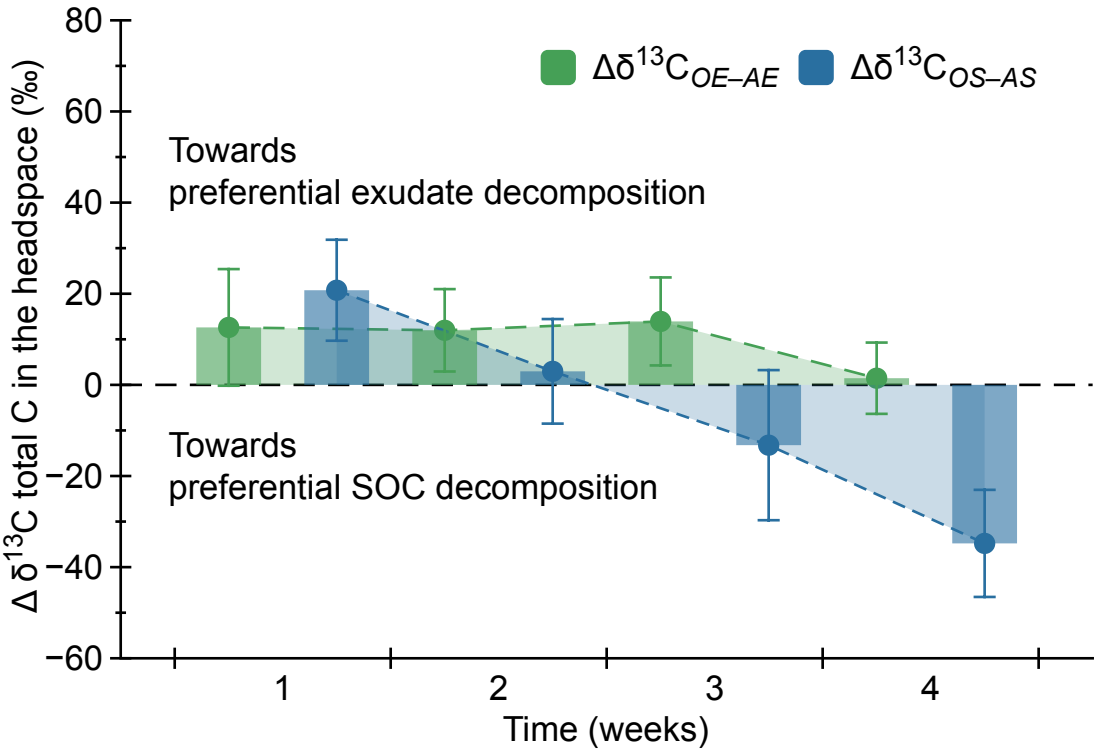

***FIGURE 3.5** | Changes in $\delta^{13}C$ signature of total headspace carbon over four weeks of incubation under oxic (O) and anoxic (A) conditions in rhizosphere soils previously planted with ^{13}C-labeled S. anglica (S) and E. athericus (E) (plants removed prior to incubation). Data are presented as mean ± SE. To reduce variability among replicates, $\Delta\delta^{13}C$ values represent the change in response to O_2 addition, calculated as the within-replicate difference between oxic and anoxic conditions and then averaged across replicates. Specifically, $\Delta\delta^{13}C_{OE-AE}$ denotes the paired difference between $\delta^{13}C$ under anoxic (AE) and oxic (OE) conditions for E. athericus, and $\Delta\delta^{13}C_{OS-AS}$ denotes the paired difference between $\delta^{13}C$ under oxic (OS) and anoxic (AS) conditions for S. anglica, and values are one-to-one paired at each time point.*

3.5 | DISCUSSION

3.5.1 | PERSISTENCE OF ROOT EXUDATE-DERIVED C UNDER ANOXIC CONDITIONS

In the long-term incubation experiment (Experiment I), the $\delta^{13}C$ signature of SOC derived from *S. anglica* root exudates remained detectable after 440 days. Although a sharp decline occurred during the first weeks, the $\delta^{13}C$ signature of SOC stabilized after approximately three months (Fig. 3.2). This pattern supports our first hypothesis that root exudate-derived C can persist in wetland soils over extended periods under anoxic conditions. The initial rapid decline followed by stabilization indicates that some labile exudate compounds triggered a transient pulse of microbial respiration, whereas a fraction of the C inputs became incorporated into more persistent soil pools. Similar long-term residual signals have also been reported in upland ^{13}C tracer studies, where a portion of fresh inputs could still be detected over time scales ranging from several months to years (Jones et al. 2009, Gunina and Kuzyakov 2015). Such stabilization has often been attributed to the incorporation of microbial transformation products into more stable soil organic C pools (Cotrufo et al. 2013, Keiluweit et al. 2015, Lehmann and Kleber 2015, Hemingway et al. 2019). In our study, anoxic conditions likely reduced microbial decomposition rates, thereby enhancing the retention of root

exudate-derived C. The persistent $\delta^{13}C$ signature of SOC observed after more than a year of incubation thus indicates that, despite their typically labile nature, root exudates can contribute to long-term C storage in wetland soils when decomposition is constrained by the absence of oxygen (Fig. 3.6, left panel).

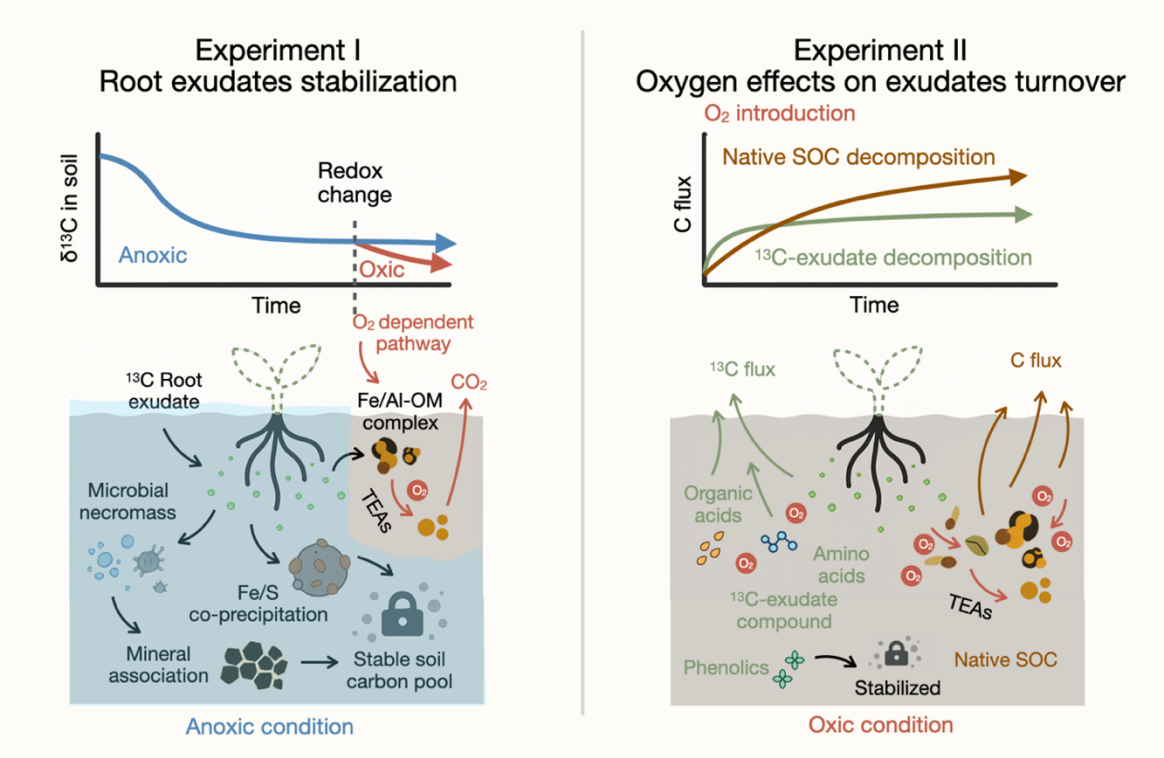

***FIGURE 3.6** | Conceptual summary of the fate of root exudate-derived carbon in coastal wetland soils under contrasting redox conditions. Left: Experiment I (long-term microcosm). Right: Experiment II (short-term microcosm).*

3.5.2 | OXYGEN-INDUCED MINERALIZATION OF ROOT EXUDATE-DERIVED CARBON STABILIZED UNDER ANOXIC CONDITIONS

Results from both the long-term (Experiment I) and short-term (Experiment II) microcosms revealed that oxygen affected the stabilization of root exudate-derived C in a time-dependent manner. In the long-term microcosm experiment (Experiment I), after an initial 440-day anoxic phase, soils underwent a 253-day redox shift in which replicate microcosms were either kept anoxic or switched to oxic conditions (Fig. 3.1B). At day 693, the $\delta^{13}C$ signature of SOC declined substantially under oxic conditions but remained stable under anoxic conditions (Fig. 3.2). Similarly, in the four-week microcosm experiment (Experiment II), soils amended with root exudates exhibited significantly higher cumulative total soil respiration under oxic than anoxic conditions (Fig. 3.3). Because the $\delta^{13}C$ signature of total headspace C showed no shift in response to oxygenation, both native SOC and exudate-C decomposition was clearly stimulated by oxygen (Fig. 3.4). Together, these patterns clearly indicate that exudate-derived C, once stabilized in anoxic

soils, became rapidly mineralized following oxygenation, strongly supporting our second hypothesis.

Although our data do not directly quantify microbial or mineral processes, the rapid mineralization observed after oxygen exposure is consistent with the release from electron-acceptor limitation and the subsequent stimulation of oxic respiration. In anoxic wetland soils, microbial metabolism relies on less efficient terminal electron acceptors (TEAs) (Megonigal et al. 2004), potentially leading to incomplete oxidation of root-derived substrates and the temporary stabilization of exudate-derived C. In addition, the oxidation of ferrous iron (Fe^{2+}) that accumulated under prolonged anoxia may have further contributed to the rapid C loss following oxygenation. Oxygen exposure can promote the oxidation of Fe^{2+} to Fe^{3+} and the formation of reactive oxygen species (ROS) via Fenton-type reactions, which can abiotically oxidize and mobilize organic matter previously associated with reduced Fe minerals (Chen et al., 2020). This abiotic oxidation pathway likely acted in concert with renewed aerobic microbial metabolism to enhance the mineralization of root-exudate-derived C. Thus, while Fe(III) oxides can promote long-term SOC stabilization under persistently oxic conditions (Bai et al. 2021, Afsar et al. 2023, Neiske et al. 2025), oxygen re-introduction after prolonged anoxia can have the opposite effect—enhancing, rather than suppressing, C loss. This mechanistic interpretation supports our second hypothesis, demonstrating that oxygen re-introduction rapidly destabilizes and mineralizes C under anoxic conditions.

3.5.3 | OXYGEN-MEDIATED SHIFTS BETWEEN DECOMPOSITION AND STABILIZATION OF EXUDATE-DERIVED AND NATIVE SOC

Building on the results of Experiment II, we further analyzed how oxygen influenced the stability of exudate-derived C, using isotopic labeling to distinguish it from native SOC. Thus, we calculated paired $\delta^{13}C$ differences between oxic and anoxic treatments from paired replicates of the same soil sample ($\Delta\delta^{13}C_{OE-AE}$ and $\Delta\delta^{13}C_{OS-AS}$). During the first two weeks, $\Delta\delta^{13}C$ values were consistently positive across both plant systems, indicating that oxygen stimulated the mineralization of exudate-derived C stronger than the mineralization of SOC. As incubation progressed, $\Delta\delta^{13}C$ values gradually decreased and approached zero or even became slightly negative in the *S. anglica* treatment. This pattern suggests that the mineralization of SOC was slightly more stimulated by oxygen than the mineralization of exudate-derived C. This change from relatively stronger exudate to SOC mineralization in response to oxygen is either cause by the depletion of exudate-derived substrates over time, or a delay in the response of SOC mineralization by the microbial community slowly adapting to oxygen availability (Fig. 3.6, right panel). Thus, these findings support our third hypothesis and emphasize that oxygen exposure can gradually shift the dominant source of respired C from exudate-derived inputs to native SOC as decomposition proceeds.

In addition to redox conditions, plant species also exerted a strong influence on isotopic dynamics. $\delta^{13}C$ values were consistently higher in soils previously planted with *S. anglica* than in those with *E. athericus*, suggesting differences in either the quantity or the isotopic composition of exudate inputs. Interestingly, although *E. athericus* showed slightly stronger ^{13}C labeling in its plant tissues (roots, stems, and leaves), the corresponding ^{13}C enrichment in soil organic matter was lower than in *S. anglica* (see Supplement, Tab. 3.S1). This pattern may reflect differences in C allocation efficiency or isotopic discrimination associated with their photosynthetic pathways, as *S. anglica* (a C_4-related halophyte) typically exhibits higher $\delta^{13}C$ values than the C_3 species *E. athericus* (O'Leary 1998, Whitaker et al. 2015, Busch et al. 2020). Such species-specific traits are well documented, as plants vary not only in exudation rates but also in chemical profiles, ranging from low-molecular-weight organic acids and amino acids to secondary metabolites such as phenolics that can suppress microbial activity (Canarini et al. 2019). Although exudate chemistry was not directly analyzed in this study, these isotopic differences suggest that plant identity regulates both the magnitude and temporal pattern of exudate-derived C turnover under contrasting redox conditions.

3.6 | IMPLICATIONS

Our findings provide important insights into how redox dynamics regulate C stabilization in coastal wetland soils. The combined short- and long-term experiments demonstrate that oxygen availability not only alters the balance between decomposition and stabilization but also determines the direction and reversibility of these processes under fluctuating redox regimes. In wetlands, where oxygen exposure is intermittent and transient, its influence diverges from mechanisms typically described for upland soils: rather than promoting long-term stabilization through Fe/Al mineral associations alone, oxygen pulses trigger rapid mineralization of stabilized organic C and reshape the timing of C preservation and loss. This highlights the need to reconsider how oxygen-driven processes are represented in conceptual and process-based models of wetland C cycling.

Our isotopic results suggest that may differences in the composition and release rate of exudates between plant species may influence stabilization pathways under contrasting redox conditions. Labile compounds such as organic acids and amino acids are generally decomposed rapidly, but may also contribute to stable organic matter under oxic conditions through microbial transformation or mineral association. In contrast, phenolic and other oxygen-demanding compounds might preferentially persist under anoxic conditions due to inhibited oxidative degradation (Fig. 3.6, right panel). These compound-specific and plant-dependent differences highlight that the chemical diversity of root exudates can alter the partitioning between labile and stabilized C pools. Future studies of wetland C cycling should therefore incorporate the variability in exudate composition and redox dynamics to better understand C stabilization potential in coastal ecosystems.

3.7 | CONCLUSION

Our study demonstrates that root exudate-derived C in coastal wetland soils exhibits both short-term reactivity and long-term persistence under contrasting redox conditions. In the long-term microcosm experiment, the $\delta^{13}C$ signature of SOC from *S. anglica* root exudates remained detectable for more than 440 days under anoxic condition, and oxygen reintroduction subsequently led to rapid mineralization, indicating that exudate-derived C can persist under prolonged anoxic conditions but becomes highly reactive upon re-oxygenation. In the short-term microcosm, oxygen addition markedly enhanced the mineralization of both native SOC and exudate-derived C. Isotopic evidence indicated that both C sources exhibited comparable oxygen sensitivity initially, whereas over time, the isotopic shifts suggested a slightly stronger oxygen response of native SOC or the progressive depletion of added exudates. Together, our findings reveal that oxygen availability is a key control on the balance between C stabilization and decomposition in wetland soils. Root exudates thus play a dual role, as rapidly degradable substrates fueling short-term respiration and as precursors of more persistent soil C that can be stabilized under anoxic conditions. Overall, our results highlight the central role of redox fluctuations in governing the persistence of blue C in dynamic coastal wetlands.

3.8 | ACKNOWLEDGEMENTS

This study was funded by the Emmy Noether Programme of Deutsche Forschungsgemeinschaft (DFG; grant No. 502681570). Hao Tang gratefully acknowledge the financial support of the Alexander von Humboldt Foundation for the project 'International Climate Protection Fellowship' (Ref. 3.5-CHN-1235018-IKS-P), the National Natural Science Foundation of China (42403074), Sichuan Provincial Natural Science Foundation (2025ZNSFSC1166), Key Laboratory of Land Resources Evaluation and Monitoring in Southwest (Sichuan Normal University), Ministry of Education, International Cooperation Fund (TDSYS202313). We thank Hedda Müller and Emilia Reimann for assisting with lab work.

Author contributions

Hao Tang - conceptualization and design, methodology and data collection, investigation, visualization, writing – original draft and review & editing. Clarisse Goesele - conceptualization and design, methodology and data collection, investigation, writing – original draft and review & editing. Namid Krüger - methodology and data collection, formal analysis and interpretation, visualization, writing – original draft and review & editing. Xiaolin Dou - methodology and data collection, writing – original draft and review & editing. Meng Lu - methodology and data collection, writing – original draft and review & editing. Kai Jensen - conceptualization and design, writing – original draft and review & editing. Peter Mueller - conceptualization and design, writing

– original draft and review & editing, project administration and supervision, funding acquisition and resources.

Competing interests

The contact author has declared that none of the authors has any competing interests.

3.9 | SUPPLEMENTS

***TABLE 3.S1** | $\delta^{13}C$ signatures of roots, stems, leaves, and soils of Elymus athericus and Spartina anglica. Values are mean ± SE (n = 3).*

Plant type	$\delta^{13}C$ signature (‰)			
	Leaf	Stem	Root	Soil
Elymus athericus	803.43 ± 224.71	528.80 ± 234.47	805.14 ± 231.45	-21.42 ± 1.08
Spartina anglica	441.10 ± 87.47	144.59 ± 54.75	898.45 ± 190.15	-20.23 ± 1.35

BOX A | SPECIES IDENTITY AND REDOX STATE DETERMINE ROOT EXUDATE EFFECTS ON METHANE PRODUCTION IN COASTAL WETLAND SOILS

Hao Tang & **Clarisse Goesele**, Namid Krüger, Kai Jensen, and Peter Mueller

BA.1 | INTRODUCTION

Coastal marshes are important components of the global carbon cycle, acting as long-term carbon sinks (Temmink et al. 2022) while also emitting methane (Rosentreter et al. 2021a, Rosentreter et al. 2021b). Marsh plants strongly influence methane cycling because their roots modify soil redox conditions through processes such as root exudation and root oxygen loss (ROL) (Haviland and Noyce 2024). Root exudation—the release of recently fixed carbon into the rhizosphere—supplies labile, low-molecular-weight compounds that can stimulate microbial activity (Jones et al. 2009, Oburger and Jones 2018, Canarini et al. 2019).

Although only a few studies have examined root exudation in wetland ecosystems, they consistently show that exudation can enhance methane production and emission (Waldo et al. 2019, Turner et al. 2020, Haviland and Noyce 2024, Girkin et al. 2025). Importantly, exudation rates and chemical profiles differ markedly among plant species, influencing carbon quality (Koyama et al. 2025) and shaping methanogenic microbial communities (Yuan et al. 2019, Kim et al. 2020a). This highlights species-specific root exudation as a potentially important driver of methane cycling in marsh soils. However, most exudate–methane studies have been conducted under static redox conditions, despite the fact that coastal marshes experience strong, hydrology-driven fluctuations in oxygen availability. Such dynamic redox environments likely regulate whether exudates are mineralized aerobically or funneled into anaerobic pathways, including methanogenesis. Understanding the fate of root exudates under fluctuating hydrological–redox conditions is therefore essential for predicting plant-mediated methane dynamics in coastal marshes.

In the following, we addressed two research questions:

(1) Do root exudates from *Elymus athericus* and *Spartina anglica* differently/similarly fuel methane production?

(2) Do background soil redox conditions modulate methane production from these species-specific root exudates?

To address these research questions, soils from microcosms in which *S. anglica* and *E. athericus* plants that were pulse-labeled with $^{13}CO_2$ in a previous experiment and thus contained ^{13}C-labeled root exudates, were used in a short-term incubation experiment, to evaluate species-specific effects on methane production and the regulating role of oxygen availability.

BA.2 | MATERIAL & METHODS

A ^{13}C pulse-labeling experiment to generate soils enriched with species-specific root exudates from *S. anglica* and *E. athericus* was conducted. Plants were collected from the Hamburger Hallig at the North Sea coast (54°60'21.53'' N, 8°81'66.29'' E) and cultivated in homogenized mudflat sediment from this site prior to labeling. Following a five-day $^{13}CO_2$ pulse labeling campaign, bulk soil from each species and non-vegetated controls were harvested for incubation.

To test how exudate origin and background redox conditions influence carbon mineralization and methane production, ^{13}C-labeled soils were incubated for four weeks under repeated O_2-pulse or strictly anoxic conditions. Headspace gases were sampled weekly to quantify CO_2, methane. Gas concentrations were determined by gas chromatography. Total respiration followed the calculations described in Chapter 3.

BA.3 | RESULTS & DISCUSSION

Methane production occurred only in anoxic treatments containing *S. anglica* derived root exudates, whereas neither oxygen-pulse treatments nor soils enriched with E. *athericus* exudates produced detectable methane emissions (Fig. BA.1). This clearly demonstrates that (i) species-specific exudate composition fuels methanogenesis differentially. The exclusivity of methane production in *S. anglica* treatments aligns with previous findings that *Spartina* species release methylated compounds that stimulate methylotrophic activity, thereby increasing methane production and emission (Yuan et al. 2019, Kim et al. 2020a). Moreover, that methane was produced only under persistently anoxic conditions highlights that (ii) background soil-redox state is a key prerequisite for methanogenesis from root-derived carbon.

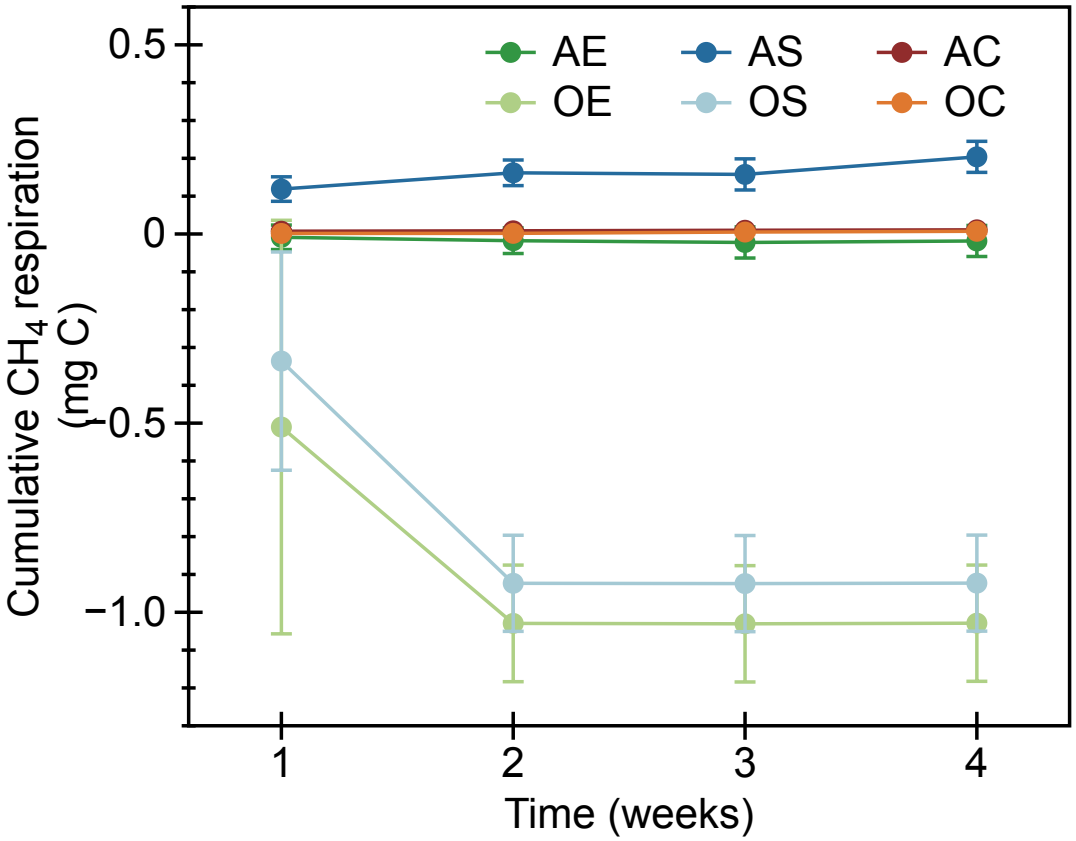

FIGURE BA.1 | *Cumulative methane respiration over four weeks of incubation under oxic and anoxic conditions for soils previously planted with S. anglica and E. athericus (plants removed prior to incubation), as well as control soils (without 13C labeling). All values are mean ± SE. Under both oxic and anoxic conditions, there were six replicates for the soils containing exudates and three replicates for the control. Note: A represents anoxic condition, O represents oxic condition, S represents S. anglica, E represents E. athericus, and C represents control without plant.*

In contrast, oxygen-pulse treatments did not support methane production. Because the incubation jars were not flushed prior to the initial sampling (t_0), small amounts of residual CH_4 were present in all treatments (see Fig. BA.1 for starting concentrations not at 0). This unintended initial condition nevertheless revealed an additional pattern: in the oxygen-pulse treatments methane concentrations dropped rapidly following the first O_2 pulse in both *S. anglica* and *E. athericus*, indicating aerobic methane consumption by methanotrophs (Philippot et al. 2008). Thus, oxic pulses promoted methane oxidation rather than production.

Together, our findings show that both plant species identity and fluctuating background redox conditions are critical determinants of methane cycling in coastal marsh soils. Future work should elucidate the mechanisms driving species-specific exudate transformations and how dynamic redox fluctuations shape the balance between methane production and oxidation.

CHAPTER FOUR | VEGETATION CONTROL ON SOIL REDOX DETERMINES GRAZING EFFECTS ON METHANE EMISSIONS FROM COASTAL MARSHES

VEGETATION CONTROL ON SOIL REDOX DETERMINES GRAZING EFFECTS ON METHANE EMISSIONS FROM COASTAL MARSHES

To be submitted to *Journal of Applied Ecology*.

Clarisse Goesele*[1], Ella Logemann[1], Cheng (Caroline) Chen[1], Lars Kutzbach[2], Kai Jensen[1], and Peter Mueller[1,3]

[1] Institute of Plant Science and Microbiology, University of Hamburg, 22609 Hamburg, Germany

[2] Institute of Soil Science, University of Hamburg, 20146 Hamburg, Germany

[3] Institute of Environmental Sciences, RPTU Kaiserslautern-Landau, 76829 Landau, Germany

*clarisse.goesele@uni-hamburg.de

Keywords: blue carbon, carbon sequestration, livestock grazing, methane emissions, salt marsh, top-down control, wetlands

4.1 | ABSTRACT

The reducing soils of coastal marshes store carbon effectively, but the same conditions can promote methane emissions, lowering the ecosystem's climate change mitigation potential. Given the widespread use of coastal marshes for livestock grazing, it is crucial to assess how this land use affects methane emissions and may influence the overall greenhouse-gas balance of these ecosystems. We compared methane emissions between grazed and ungrazed coastal marshes along the German North and Baltic Sea coastlines, with the aim to identify ecological and biogeochemical drivers that control potential grazing effects on methane emissions. On average, livestock grazing tended to reduce methane emissions, but the overall effect was not significant, since the direction and magnitude of grazing effects were highly variable across sites. These variable methane emission responses across sites could be attributed to site-specific grazing responses in belowground biomass, soil organic carbon and soil redox potentials. Significant correlations among belowground biomass, soil redox and methane emissions suggest that grazing effects on belowground biomass controlled methane emissions via plant-mediated soil redox changes. Furthermore, grazing led to lower methane emissions by reducing the abundance of indicator plant species associated with high methane emissions, such as *Phragmites australis, Tripolium pannonicum* and *Juncus maritimus*. Our study provides novel insights into the plant control of methane emissions from coastal marshes and yields important implications for predicting global change and land-use effects on coastal carbon and greenhouse gas cycling.

4.2 | INTRODUCTION

Wetlands are the largest natural source of methane (CH_4) to the atmosphere. They account for 4-6% of global land area while contributing up to 53% of global methane emissions (Rosentreter et al. 2021b). Methane is produced in waterlogged soils during the terminal step of organic matter decomposition when oxygen and all other alternative electron acceptors have been depleted (Segers 1998). Hence, methane emissions are highly dependent on the soil redox state, which is in turn is highly sensitive to both abiotic and biotic factors (Sutton-Grier et al. 2011, Mueller et al. 2020b, Sulman et al. 2022).

Methane emissions from coastal marshes are often lower compared to other wetland types, because in addition to the soil redox state, salinity, – or more precisely, sulfate availability – is a primary factor determining wetland methane dynamics (Bridgham 2006, Rosentreter et al. 2021b). Regular flooding with sulfate-rich seawater enables sulfate-reducing bacteria to outcompete methane producers (i.e., methanogenic archaea) (King and Wiebe 1980, Davidson et al. 2021). Consequently, coastal wetlands, including marshes, typically show a clear negative relationship between salinity and CH_4 emissions (Poffenbarger et al. 2011, Arias-Ortiz et al. 2024).

Wetland plants exert important control on CH_4 emissions by functioning as sources of both electron donors and electron acceptors to the rhizosphere (Turner et al. 2020, Koop-Jakobsen et al. 2021, Mittmann-Goetsch et al. 2024). Through their aerenchyma tissues, they facilitate a bi-directional gas exchange, releasing oxygen (O_2) into the rhizosphere and transporting CH_4 from the soil to the atmosphere (Dacey and Klug 1979, Armstrong et al. 2000, Vroom et al. 2022). By releasing organic matter via root turnover and root exudates to the soil, plants increase the availability of electron donors for microbial methanogenesis (Mueller et al. 2020b, Turner et al. 2020, Määttä and Malhotra 2024, Girkin et al. 2025). Certain plant species, such as *Phragmites australis* and *Spartina alterniflora*, have been shown to enhance methane emissions (Van der Nat and Middelburg 2000, Brix et al. 2001, Comer-Warner et al. 2022), likely due to their extensive belowground biomass and efficient internal gas transport mechanisms (Cheng et al. 2007, Fuchs et al. 2024).

Land use such as livestock grazing, other agricultural practices, drainage or damming can impact both biotic and abiotic ecosystem processes in coastal marshes with potentially important consequences for methane cycling (Kirwan and Megonigal 2013, Kroeger et al. 2017). Livestock grazing is a globally relevant land-use in coastal marshes, and it is particularly common in large parts of Europe (Tessier et al. 2003, Nolte et al. 2014, Barr and Bell 2017), South America (Di Bella et al. 2015, Sica et al. 2016) and East Asia (Suzuki and Suzuki 2011, He et al. 2015, Ning et al. 2019). It is established that livestock grazing alters soil redox and vegetation properties, often with important consequences for soil organic carbon (SOC) cycling in coastal marshes (Davidson et al. 2017, Mueller et al. 2017, Ford et al. 2019, Harvey et al. 2019, Leiva-Dueñas et al. 2024, Logemann et al. 2025). By contrast, potential effects of livestock grazing on methane emissions in coastal

marshes remain poorly understood (Ford et al. 2012). Based on the established mechanistic insight into grazing effects on coastal marsh redox and SOC dynamics, it is however possible to identify at least two redox-dependent pathways by which grazing may increase methane emissions from coastal marshes (Fig. 4.1).

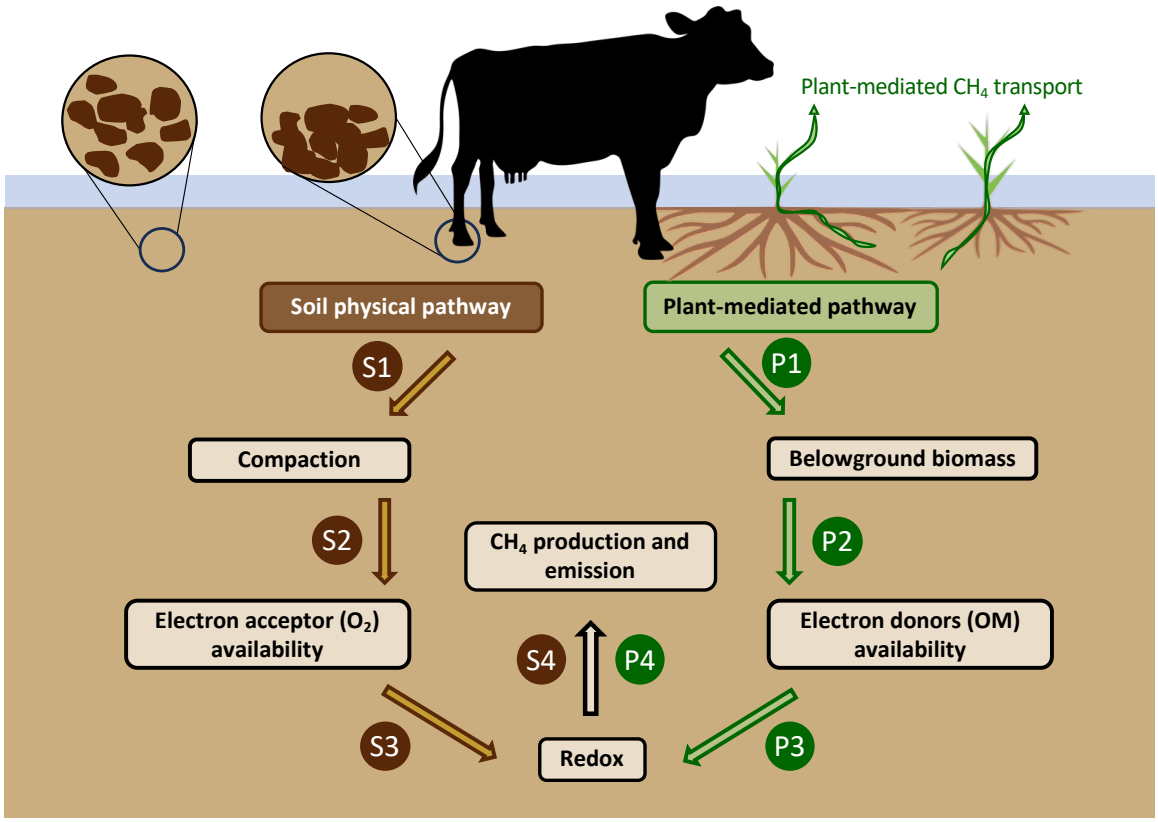

***FIGURE 4.1** | Conceptual framework of livestock-grazing effects on methane emissions from coastal marshes via the soil physical pathway (left) and the plant-mediated pathway (right). Arrows and the described mechanisms depict specific expected correlations between parameters. The soil physical pathway predicts that (S1) trampling-driven soil compaction, which (S2) increases soil bulk density, leading to (S3) reducing soil conditions and (S4) methane production and emission. The plant-mediated pathway predicts that (P1) grazing increases belowground biomass allocation and thus (P2) organic matter input to the soil, leading to (P3) reducing soil conditions and (P4) methane production and emission. In addition, the potential for a redox-independent plant-mediated transport of methane from soil to the atmosphere is illustrated. Cow symbol from Pixabay: https://pixabay.com/de/vectors/kuh-symbol-kuh-bos-stier-bauernhof-1653039/*

The soil-physical pathway predicts that trampling by livestock grazing increases soil compaction and drainage (Nolte et al. 2013b) leading to lower soil oxygen availability and redox (Elschot et al. 2015, Mueller et al. 2017, Bakker et al. 2019), enhancing methane production and consequently emissions. The plant-mediated pathway predicts that livestock grazing increases belowground biomass allocation (Elschot et al. 2015, Graversen et al. 2022), enhancing organic-matter input to the soil and thereby promoting reducing conditions that favor methane production (Turner et al. 2020, Määttä and Malhotra 2024, Girkin et al. 2025). Both pathways therefore predict increased methane emissions in response to livestock grazing in coastal marshes.

In this study, we aimed to determine whether livestock grazing indeed increases methane emissions across multiple sites along two coastal regions in Northern Germany, namely the North Sea and the Baltic Sea coast. Along both coastlines, livestock grazing has been carried out on large areas of coastal marshes for centuries (Elschot et al. 2024). Due to the semi-enclosed feature of the Baltic Sea with little exchange of seawater with the Atlantic, salinity levels are much lower in coastal marshes at the Baltic Sea (5–10 PSU) compared to those along the North Sea coast (32–34 PSU; Dijkema (1990)). By comparing grazing effects between these coastal regions, we aimed to acquire a more general mechanistic insight into the effects of livestock grazing on methane emissions in coastal marshes. We hypothesized (1) that methane emissions will be higher in grazed compared to ungrazed coastal marshes due to trampling-driven soil compaction and increased soil reduction (soil-physical-pathway hypothesis). We further hypothesized (2) that this grazing effect is more pronounced in Baltic Sea than in North Sea coastal marshes, due to the higher methane production potential of the sulfate-poor Baltic Sea coastal marshes. Finally, we hypothesized (3) that additional site-specific variation in the methane emission response to grazing is explained by plant species-specific positive grazing effects on belowground biomass allocation (Plant-mediated-pathway hypothesis).

4.3 | MATERIAL AND METHODS

4.3.1 | STUDY SITES AND SAMPLING DESIGN

Study sites were identified along the North Sea and Baltic Sea coastlines of Germany based on clear grazed-ungrazed contrasts within sites (Fig. 4.2). The study design included two marsh sites on the North Sea coast, Nessmersiel (N1) and Pohnshalligkoog (N2), and two on the Baltic Sea coast, Heiligenhafen (B1) and Schleimünde (B2) (Fig. 4.2 b-e). At each site, grazed and ungrazed areas were selected based on similar elevation ranges and distances to the shoreline to keep environmental factors other than grazing as constant as possible. Five plots were distributed randomly in both grazed and ungrazed treatment areas resulting in a total of N = 40 plots across the four sites (Fig. 4.2).

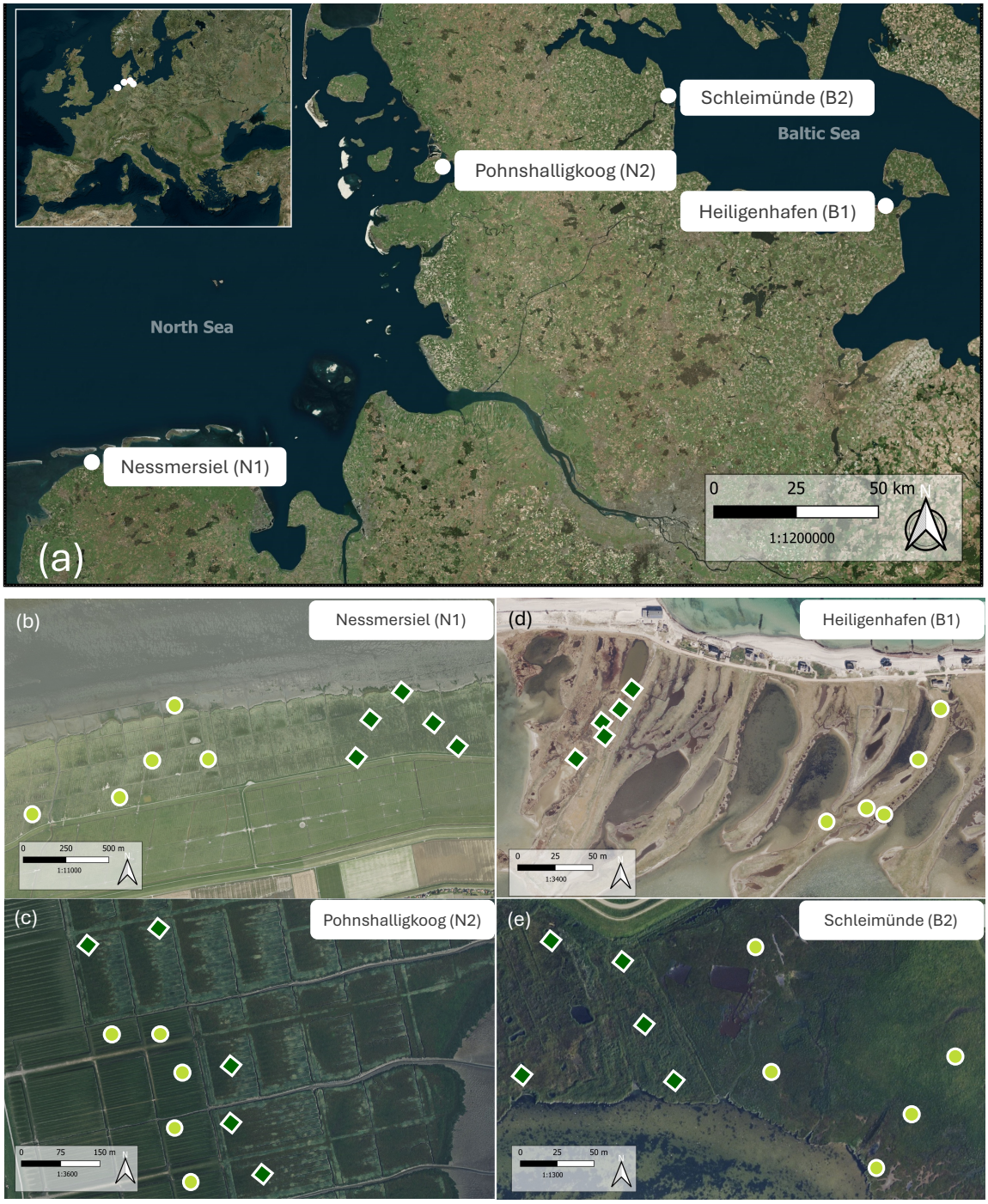

***FIGURE 4.2** | [a] Overview of the four study sites across Northern Germany. [b-e] Plot locations within the study sites Nessmersiel (N1) and Pohnshalligkoog (N2) at the North Sea coast, and within the study sites Heiligenhafen (B1) and Schleimünde (B2) at the Baltic Sea coast. Circles indicate grazed and squares indicate ungrazed plots.*

4.3.2 | METHANE FLUX MEASUREMENTS

Flux measurements, applying a closed chamber method, were conducted in regular intervals of six weeks from February 2023 to December 2023. In total, eight campaigns were carried out. Flux measurements were conducted around low tide, i.e. when soil surfaces were not flooded.

We used flexible (i.e. height-adjustable) portable closed chambers and permanently installed collars as described by Yang et al. (2024). One of two chamber types (50 cm and 100 cm in height) were chosen depending on vegetation height. Chambers were equipped with fans on the inside for air circulation. During each flux measurement, air temperature and relative humidity inside the chamber were measured. Photosynthetically active radiation (PAR) was measured outside with a sensor installed on top of the chamber.

Two types of portable laser-based trace-gas analyzers – a Micro Portable Greenhouse Gas Analyzer (ABB GLA131 Series Microportable Analyzers, ABB Inc. Measurement & Analytics, Quebec, Canada) or a portable $CH_4/CO_2/H_2O$ Trace Gas Analyzer (LI-7810, LI-COR Environmental, Lincoln, NE, US)) – were used to quantify methane concentration changes inside the chamber headspaces during 6-min flux measurements. The methane fluxes were calculated based on linear regression slopes of methane concentration change over time. After visual inspection of each individual flux measurement, 5.6% of all methane fluxes were excluded from the dataset due to analyzer errors or chamber leakage. For further flux evaluation, a combination of the root mean square error (RMSE; threshold at 5 ppb) and coefficient of determination (R^2; threshold at 0.85) of the linear regressions was used (adapted from Kutzbach et al. (2007)). This method ensured the inclusion of high-quality flux measurements close to zero, which would have been excluded if considering the R^2 threshold alone. Methane flux measurements were considered acceptable if either the RMSE of the linear regression of the concentration-over-time-data was below the threshold of 5 ppb or the R^2 of this linear regression was above 0.85. A satisfactory RMSE could therefore offset a sub-threshold R^2, and conversely, a strong R^2 could justify accepting a flux despite an elevated RMSE (see Fig. 4.S1). Flux-calculation statistics were conducted in R (version 4.5.0 (2025-04-11)).

4.3.3 | VEGETATION PROPERTIES

Vegetation composition and structure were assessed in September 2023 by recording plant community composition and percent cover of species, along with percent cover of bare soil and standing dead plant matter, within each plot inside the flux collar. During the field campaign, it was not possible to reliably distinguish between *Festuca rubra* and *Juncus gerardii* in grazed plots, therefore, these species were combined and treated as a single functional group for analysis. Vegetation height was measured for five random individuals, along with the tallest and shortest plant within each flux collar. To quantify aboveground biomass, plants were cut 2 cm above the soil surface in 30 cm x 30 cm squares approx. 50 cm adjacent to the flux collars. Biomass samples were transported to the laboratory in plastic bags and weighed after drying at 60 °C for five days. Belowground biomass was sampled using an Edelmann corer (diameter 5 cm; depth 20 cm) within

the aboveground biomass sampling square. The belowground biomass samples were washed free from soils, dried at 60 °C for five days and then weighed.

4.3.4 | SOIL PROPERTIES

Soil bulk density was quantified as a proxy to assess trampling-driven soil compaction. Single 50-cm deep soil cores were taken from each of the aboveground biomass sampling squares in September 2023, using an Eijkelkamp peat sampler (5 cm diameter). Bulk density was calculated based on sample dry weight and soil volume from the upper 20 cm of the soil core. To assess grazing effects on substrate (organic matter) availability for soil microbial communities, SOC content was quantified in the same soil samples following protocols outlined in Logemann et al. (2025).

To understand grazing effects on soil redox conditions, two complementary assessments were carried out. Redox potential measurements [mV] at 5-10 cm soil depth adjacent to the flux collar were carried out every six weeks during each flux measurement using a handheld Pt-tipped redox electrode and an Ag/AgCl reference electrode (3 M KCl solution) connected to a portable, high impedance redox potential meter (Model No.: 4612; ecoTech, Germany). The readings were corrected to the redox potential of the standard hydrogen electrode (+207 mV) (Mansfeldt 2003). Redox measurements were complemented by the Indicator-of-Reduction-In-Soils (IRIS) technique (Rabenhorst and Burch 2006, Rabenhorst 2013), which allowed us to calculate a Reduction Index [RI; %] integrated over the 6-week periods between single campaigns. The IRIS technique is based on the reduction of Fe (III) to Fe (II) under anoxic soil conditions by Fe-reducing microorganisms. Since Fe (II) is soluble, the area of removed paint indicates the oxygen concentrations in the soil, where lower oxygen concentrations result in more paint removal. Hence a more positive RI indicates more reducing soil conditions. IRIS protocols followed Mittmann-Goetsch et al. (2024). Each flux collar was equipped with two IRIS sticks reaching to 60 cm soil depth each 10 cm adjacent to the flux collar.

Soil temperature and volumetric water content were measured 10 cm adjacent to the flux collar during each CH_4 flux measurement. To account for salinity as an influencing factor across sites, a water sample was collected from the adjacent seawater body during each campaign, assuming that soil salinity within the marsh often reflects that of the adjacent water body (Mitsch 2009). Seawater salinity was then determined using a handheld refractometer (Model No.: 282030, Sybon, Germany).

4.3.5 | STATISTICAL ANALYSIS

As the first step of data analysis, data distributions were visually assessed. Methane flux data were not normally distributed and therefore log-transformed. Since the dataset included negative values, log-transformation required adding a constant of +10 to each value.

To assess the overall grazing effect on CH_4 emissions, soil bulk density, and other environmental variables (hypothesis 1), repeated measurements were first averaged per plot, then aggregated by

site and treatment. Site-level means for grazed and ungrazed plots were compared using paired t-tests (n = 4 sites).

To test whether grazing effects on methane emissions differed between coasts and sites (hypothesis 2), site-specific linear mixed models were calculated assessing the effects of livestock grazing, sampling campaign as well as their interaction. Plot-id was included as a random factor. For pairwise comparison, Tukey-tests were applied for each campaign.

To test if grazing affected methane emissions through changes in belowground biomass allocation and soil organic carbon (hypothesis 3), grazing effects on belowground biomass and soil organic carbon were evaluated with t-tests at the site level (n = 5 plots per treatment). Subsequently, correlations among belowground biomass, soil organic carbon, redox potentials and methane emissions were calculated.

To assess the relationship between plant community composition and methane emissions, plant species were categorized based on their association with methane flux categories (high or low fluxes). First, the dataset was split into one high and one low methane flux category using the average of 2.31 methane [mg CH_4 m^{-2} day^{-1}] methane flux of the total dataset as threshold value (low flux < mean, n = 217; high flux > mean, n = 42). Next, plant species that served as indicators for one of the two flux categories were identified. Finally, non-metric multidimensional scaling (NMDS) was used to further explore potential grazing effects operating via changes in plant species composition. Specifically, NMDS was used to assess compositional variation among plots and to examine relationships between plant species composition and plant relevant parameters, including methane emissions, belowground biomass, aboveground biomass, and soil redox potential. Species were visually distinguished in the ordination plot according to their association with high or low methane flux categories, as identified in the indicator species analysis.

Statistics were conducted in R (version 4.5.0 (2025-04-11)). All LMMs were performed using the *lmer* function from the *lme4* R package (Douglas Bates 2018). Correlations were calculated using the *rcorr* function from the *Hmsic* R package (Tab. 4.2) or the cor.test function from the *stats* R package (Fig. 4.S2 a-c). The *indicspecies* R package was used to categorize plant species in methane categories. This method identified indicator species based on a permutation test of the point-biserial correlation coefficient (De Cáceres and Legendre 2009). Environmental variables were fitted post hoc to the ordination using the *envfit* function from the *vegan* R package.

4.4 | RESULTS

On average, methane emissions tended to be higher from grazed than ungrazed areas across the four sites; however, this difference was not significant based on paired t-tests (Fig. 4.3a, Tab. 4.1), because direction and magnitude of grazing effects was highly variable across sites (Fig. 4.4 a-d).

Likewise, none of the other soil and plant parameters assessed differed consistently between grazed and ungrazed areas across the four sites (Tab. 4.1).

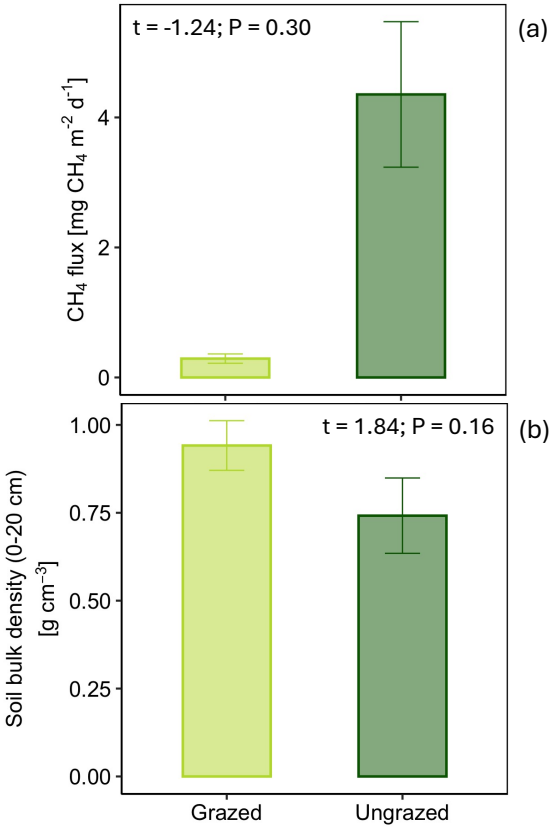

***FIGURE 4.3** | Average annual methane emissions and soil bulk density in grazed and ungrazed treatments across all sites [a, b]. Error bars represent standard errors. For statistical comparison of grazed and ungrazed treatments, paired t-tests were conducted using site-level means, with site as the pairing factor (n = 4). Values indicate t-statistics. For CH_4 emissions, means are shown on the original scale, while statistical testing was performed on log-transformed values.*

***TABLE 4.1** | Results overview of paired t-tests using site-level means, with site as paring factor (n =4) testing for overall grazing effects on soil and plant variables.*

	Grazed	Ungrazed		
	mean ± se	mean ± se	t-value	P-value
CH_4 flux [mg CH_4 m^{-2} d^{-1}]	0.29 ± 0.07	4.35 ± 1.12	-1.24	0.30
Redox potential [mV]	286 ± 13	290 ± 16	-0.01	0.99
Reduction Index [%]	28 ± 2	32 ± 3	-1.11	0.35
Belowground biomass [kg m^{-2}]	3.76 ± 0.67	3.68 ± 0.74	-2.12	0.12
Soil organic carbon [%]	8.04 ± 1.59	10.91 ± 3.08	-0.53	0.63
Soil bulk density [g cm^{-3}]	0.94 ± 0.07	0.74 ± 0.11	1.84	0.16
Volumetric water content [%]	54 ± 2	55 ± 3	-0.55	0.62
Aboveground biomass [kg m^{-2}]	0.38 ± 0.06	1.1 ± 0.16	-1.12	0.34
Soil Temperature [°C]	12.06 ± 0.53	11.65 ± 0.45	1.44	0.24

Direction and magnitude of grazing effects on methane emissions differed strongly between sites, while within each site the direction of the effect was consistent across all sampling campaigns (Fig. 4.4 a-d). At site B2, CH_4 emissions were significantly lower under grazed (0.22 ± 0.1 mg CH_4 m^{-2} day^{-1}) than ungrazed (13.37 ± 3.70 mg CH_4 m^{-2} day^{-1}) conditions (Estimate = -0.59; P = 0.001; Fig. 4.4d), with significant differences based on pairwise comparisons observed for three out of eight campaigns (May, June, August). Similarly, at site N2, CH_4 emissions tended to be lower under grazed (0.11 ± 0.14 mg CH_4 m^{-2} day^{-1}) than ungrazed conditions (3.45 ± 1.54 mg CH_4 m^{-2} day^{-1}; Estimate = -0.14; P = 0.39; Fig. 4.4b), while a significant difference based on pairwise comparisons occurred during only one out of eight campaigns (March). By contrast, at site B1 and site N1, no significant differences in CH_4 emissions were observed between treatments during any of the campaigns. At site B1, average CH_4 emissions even tended to be higher under grazed (0.65 ± 0.24 mg CH_4 m^{-2} day^{-1}) than ungrazed conditions (0.07 ± 0.05 mg CH_4 m^{-2} day^{-1}; Estimate = 0.05; P = 0.33; Fig. 4.4c). N1 showed consistently no differences between grazed (0.23 ± 0.06 mg CH_4 m^{-2} day^{-1}) and ungrazed areas (0.23 ± 0.13 mg CH_4 m^{-2} day^{-1}; Estimate = 0; P = 0.99; Fig. 4.4a).

In line with the grazing effects on methane emissions, direction and magnitude of grazing responses in belowground biomass and SOC content varied between sites. In two sites (N2 and B2) grazing tended to reduce belowground biomass (Fig. 4.4 f,h) and significantly reduced SOC content (Fig. 4.4j,l), while the other two sites exhibited opposite patterns (N1: Fig. 4.4e,i; B1: Fig. 4.4g,k).

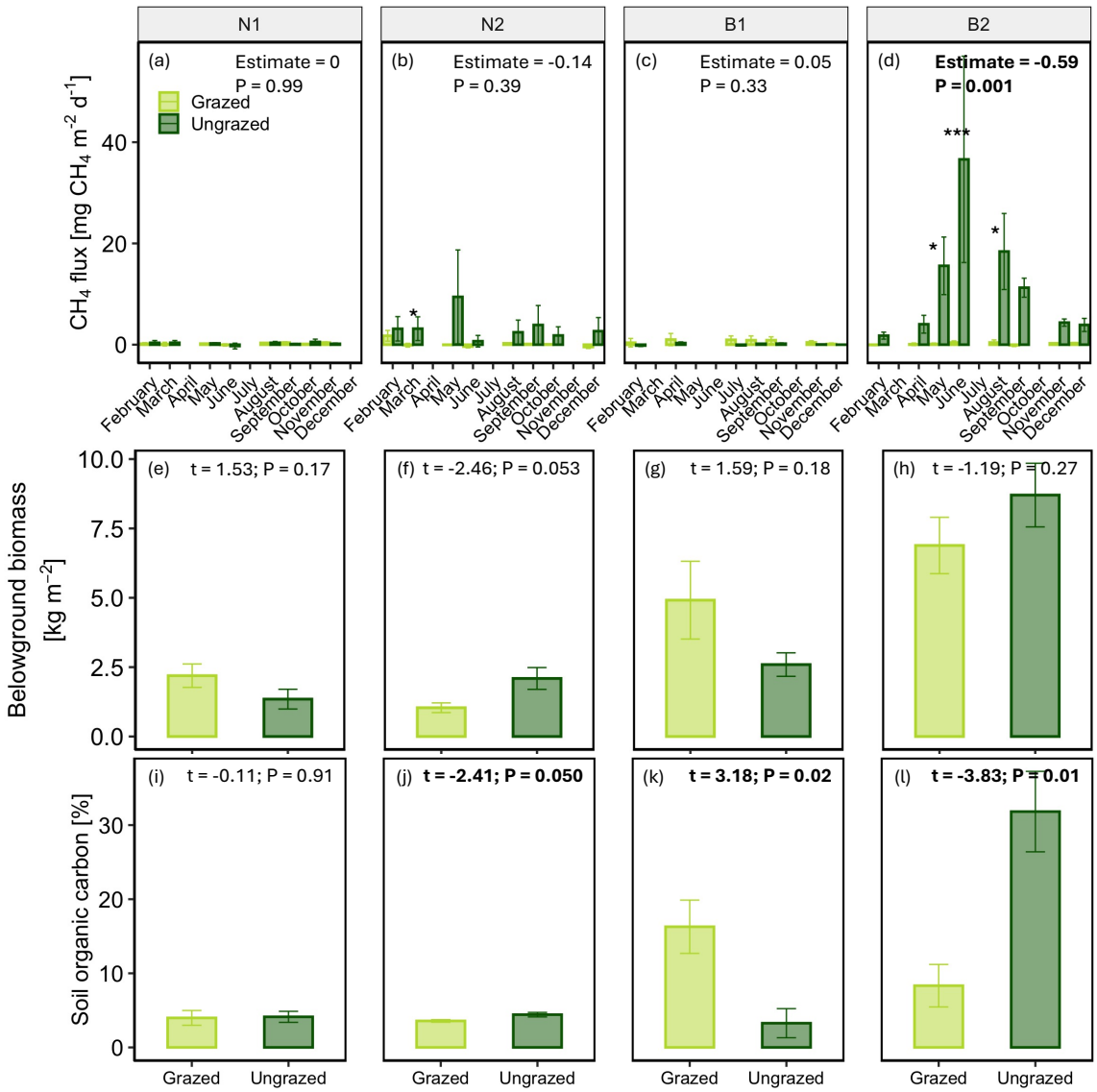

FIGURE 4.4 *| Seasonal pattern of methane emissions [a-d] in grazed (light green bars) and ungrazed treatment areas (dark green bars) in the four study sites (N1 and N2 at the North Sea, B1 and B2 at the Baltic Sea). Bars represent mean CH_4 fluxes per sampling campaign based on measurements from five plots per grazing treatment and site; error bars represent SE. Values above bars indicate model estimates (β) from linear mixed-effects models with grazing treatment and its interaction with month as fixed effects and plot ID as random effect. Stars denote significance differences based on Tukey pairwise comparisons during individual campaigns (P < 0.05 *, P < 0.01 **, P < 0.001 ***. Belowground biomass [e–f] and SOC [i-l] in grazed and ungrazed treatments of the four study sites. Bars represent site-level treatment means ± SE, and values indicate t-statistics from independent t-tests.*

Belowground biomass and SOC content were positively correlated and emerged as the two strongest predictors of soil redox conditions (both redox potential and reduction index), which in turn were the main controls on methane emissions (Tab. 4.2). Furthermore, methane emissions correlated negatively with soil bulk density and positively with soil water content (Tab. 4.2). No significant correlations were found between methane emissions and aboveground biomass, salinity, air and soil temperature, relative humidity of air, and radiation (Tab. 4.2).

TABLE 4.2 | *Pearson correlations, based on plot-level means, between methane emissions and potential environmental predictor variables. Values represent Pearson correlation coefficients (r) and corresponding significance levels (P < 0.05 *, P < 0.01 **, P < 0.001 ***).*

	log CH_4 flux	Redox potential	Reduction Index	Belowground biomass	Soil organic carbon	Dry bulk density	Volumetric water content	Aboveground biomass	Salinity	Air Temperature	Soil Temperature	Relative Humidity
Redox measurements	**-0,59** ***											
Reduction Index	**0,52** ***	**-0,72** ***										
Belowground biomass	**0,59** ***	**-0,67** ***	**0,62** ***									
Soil organic carbon	**0,58** ***	**-0,62** ***	**0,55** ***	**0,67** ***								
Dry bulk density	**-0,59** ***	**0,45** **	**-0,53** ***	**-0,50** ***	**-0,78** ***							
Volumetric water content	**0,42** **	**-0,36** *	**0,49** **	**0,33** *	**0,35** *	-0,25						
Aboveground biomass	0,19	0,07	-0,07	-0,05	-0,06	0,03	-0,08					
Salinity	-0,22	**0,52** ***	-0,27	**-0,60** ***	**-0,43** **	0,07	0,03	-0,03				
Air Temperature	-0,16	**0,31** *	-0,16	**-0,40** *	**-0,31** *	0,03	-0,15	0,16	**0,59** ***			
Soil Temperature	-0,14	0,07	-0,12	-0,19	-0,15	0,03	**-0,32** *	-0,11	**0,39** *	**0,75** ***		
Relative Humidity	-0,14	-0,17	0,06	0,19	0,10	0,14	0,08	**-0,43** **	-0,24	**-0,59** ***	-0,22	
Radiation	-0,07	-0,05	-0,01	-0,11	-0,13	0,00	-0,10	-0,13	0,20	**0,68** ***	**0,56** ***	**-0,39** ***

Vegetation of grazed areas was mostly dominated (single species cover > 60%) by *Puccinellia maritima* in N1, N2 and B1, while *Juncus geradii* and *Puccinellia maritima* dominated B2. Vegetation of the ungrazed areas on the North Sea coast was predominantly a mix of non-dominant species (all single species covers < 60%), often with *Elymus athericus* and either *Atriplex prostrata* or *Suaeda maritima* reaching higher cover values (see Fig. 4.S3 for detailed plant distribution).

Based on the categorization of plant species into "high" and "low" methane-flux groups, three plant species were significantly associated with the "high-flux" category ($P < 0.05$): *Phragmites australis*, *Tripolium pannonicum*, and *Juncus maritimus*. *Plantago maritima* tended toward the "high-flux" category, although not significantly ($P = 0.08$). Six plant species were (not significantly) associated with the "low-flux" category: *Elymus athericus*, *Artemisia maritima*, *Limonium vulgare*, *Glaux maritima*, *Atriplex portulacoides*, and *Argentina anserina* ($P > 0.05$). All remaining species could not be assigned to either flux category. The NMDS ordination (revealed clear grouping patterns based on grazing treatment and coastal location, with distinct environmental gradients (Fig. 4.5). The three high-flux species were aligned with vectors representing CH_4 emissions and below- and aboveground biomass and were generally associated with the ungrazed treatment. *Tripolium pannonicum* and *Juncus maritimus* occurred in sites on both coasts, whereas *Phragmites australis* was only present in the Baltic Sea sites. In contrast, *Elymus athericus*, was restricted to the North Sea sites and similarly occurred exclusively within the ungrazed ellipse. Belowground biomass and soil redox potential pointed in the opposite directions, reflecting strong negative correlation. The grazed treatment ellipse was mostly entirely nested within both coastal ellipses, whereas the ungrazed ellipse extended beyond both coastal ellipses and encompassed almost the full range of environmental vectors and species categories. This pattern was driven particularly by *Phragmites australis* and *Elymus athericus*.

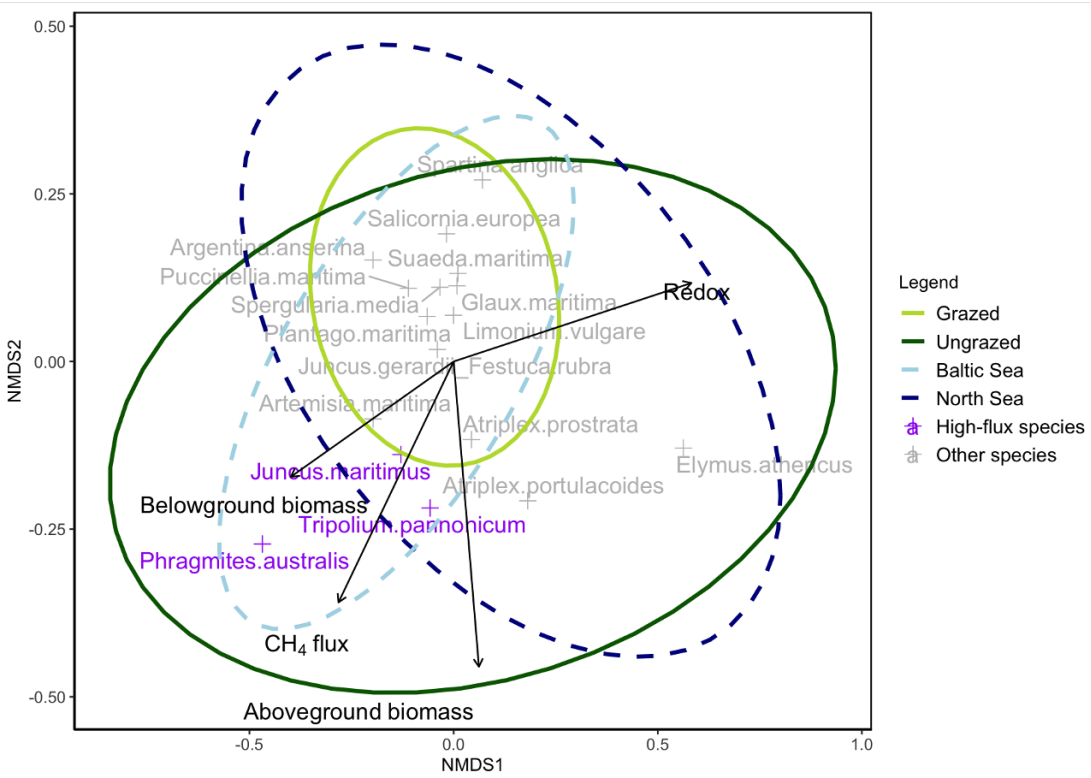

***Figure 4.5** | Non-metric multidimensional scaling (NMDS) ordination (Euclidean distance, stress = 0.15) of plant species composition in relation to grazing treatment, coast, and vegetation relevant parameters. High-flux species are indicated in purple and other species in grey. Grazing treatments and coasts are represented by ellipses: grazed (light green), ungrazed (dark green), Baltic Sea (light blue dashed) and North Sea (dark blue dashed). Environmental vectors ($P < 0.05$) represent correlations with key variables: CH_4 emissions and belowground biomass align positively with high-flux species, the Baltic Sea and the ungrazed treatment, while redox diverges in the opposite direction of belowground biomass, indicating a strong negative correlation. The ungrazed ellipse extends beyond coastal ellipses, driven by species such as Phragmites australis that is dominant in ungrazed marshes of Baltic Sea and Elymus athericus that is dominant in ungrazed marshes of the North Sea coast.*

4.5 | Discussion

Contrary to our first hypothesis, methane emissions were on average not higher but tended to be lower in grazed than in ungrazed treatments (Fig. 4.3a). As expected, grazing tended to increase soil bulk density (Fig. 4.3b), aligning with the proposed soil physical pathway by which trampling (i.e. soil compaction) could decrease drainage and soil redox and consequently stimulate methane emissions (Fig. 4.1). However, soil bulk density was significantly positively correlated with soil redox and significantly negatively with methane emissions (Tab. 4.2). In sites N2 and B2, grazing increased bulk density (Fig. 4.S4b,d) but decreased methane emissions (Fig. 4.4b,d), while in site B1, grazing decreased bulk density (Fig. 4.S4c) but increased methane emissions (Fig. 4.4c), contradicting the proposed mechanistic links of the soil physical pathway (Fig. 4.1). Additionally, grazing effects on soil water content varied across sites (Fig. 4.S4e-h), and we did not find expected links between soil water content and methane emissions. That is, in site B1, grazing decreased water content on average but increased methane emissions, while in site N1, grazing increased water

content on average but showed no effect on methane emissions. Taken together, these results suggest that grazing effects on methane emissions cannot be explained by the proposed soil physical pathway.

We further hypothesized that grazing effects on methane emissions would be more pronounced in Baltic Sea than North Sea marshes (hypothesis 2), due to the greater methane production potential in the less saline Baltic Sea marshes. While methane emissions were indeed greatest in one of the Baltic Sea sites (Fig. 4.4d) and sea water salinity was lower compared to the North Sea (Fig. 4.S5), there was no evidence that grazing changed methane emissions in Baltic Sea marshes more strongly or consistently compared to the North Sea marshes. Instead, the methane response to grazing varied qualitatively across all sites, independent of the coastline, with either higher, lower, or similar emissions observed in grazed relative to ungrazed treatments (Fig. 4.4a-d). These multidirectional responses suggest more complex grazing effects on soil biogeochemistry and methane emissions than those predicted by the soil-physical pathway hypothesis or by salinity differences alone.

Our third hypothesis proposed that site-specific variation in methane responses to grazing would be explained by the plant-mediated pathway, predicting that grazing effects on belowground biomass determines soil redox conditions and ultimately methane emissions. Indeed, belowground biomass was a key driver influencing SOC and redox conditions and, in turn, methane emissions across all sites (Tab. 4.2). Belowground biomass was significantly positively correlated with SOC (Fig. 4.S2a), while SOC was significantly negatively correlated with redox potential (Fig. 4.S2b). Redox potential in turn was the strongest predictor of methane (Tab. 4.2, Fig. 4.S2c), supporting the hypothesis that belowground biomass stimulates methane production by reducing the soil via electron donor (i.e. organic matter) input. Grazing effects on belowground biomass and SOC content were mixed across sites but consistently reflected the direction of the methane response to grazing (Fig. 4.4). That is, at site B1, grazing was associated with higher belowground biomass and SOC content (Fig. 4.4g, k) and increased methane emissions compared to the ungrazed areas (Fig. 4.4c), while at sites N2 and B2 grazing was associated with lower belowground biomass and SOC content (N2: Fig. 4.4f,j; B2: Fig. 4.4h,l) and decreased methane emissions compared to the ungrazed areas (Fig. 4.4b,d). These findings suggest a plant-mediated mechanism through which grazing influences methane emissions in coastal marshes, with grazing-induced changes in belowground biomass controlling redox conditions and ultimately methane emissions.

While our data provide evidence that plant roots shape methane emissions by determining organic matter input to the soils, either via root turnover or root exudation (Mittmann-Goetsch et al. 2024), there are additional mechanisms by which wetland roots affect methane emissions (Määttä and Malhotra 2024). This might be reflected in the high variability in methane emissions under low soil redox potentials (Fig. 4.S2c). Wetland plant species can facilitate methane transport to the atmosphere via aerenchyma, bypassing the oxic soil layer where methane would otherwise be oxidized to CO_2 (Vroom et al. 2022). This process is closely linked to root architecture, as lateral

roots and root tips have been identified as key features in mediating methane transport (Henneberg et al. 2012). Furthermore, wetland plants can reduce methane emissions by oxidizing the rhizosphere and stimulating aerobic methanotrophy (Segers 1998, Wang et al. 2018, Capooci et al. 2024). Plant species can differ strongly in their effects on soil redox and consequently methane emissions (Sutton-Grier and Megonigal 2011, Mueller et al. 2020b). Therefore, it is possible that several community- or species-specific differences in belowground functional traits contributed to the observed grazing effects on methane emissions.

This plant-mediated and species-dependent interpretation aligns with findings by Ford et al. (2012), the only other study to date that directly examined the effect of livestock grazing on methane emissions in coastal marshes. They compared grazed and ungrazed plots within a single marsh site and proposed that plant species identity had a stronger influence on methane emissions than the impacts of grazing on soil conditions. We argue that grazing-induced shifts in plant community composition likely contribute to differences in methane emissions, because species differ in their functional traits. In our study, all species significantly associated to the "high-flux" category occurred exclusively in ungrazed marsh areas, independent of coast (Fig. 4.5, Fig. 4.S3). While studies have shown that *Phragmites australis* (as one of the identified "high-flux "species) can stimulate methane emissions (Mueller et al. 2016, van den Berg et al. 2020, Vroom et al. 2022), plant trait-based methane emission predictions remain limited. For example, Ge et al. (2025) reported large regional variation in methane emissions from *Phragmites australis* and *Spartina* species, suggesting that focusing on species identity alone without considering the environmental context is insufficient to predict methane emissions. Our study applied a multi-site, broad-scale approach across diverse marsh ecosystems to capturing a wide range of environmental conditions and plant communities. This broader spatial scope allowed us to acquire some generalizable insight into plant-community controls on methane emissions. However, understanding how species-specific traits influence methane cycling remains an important knowledge gap and was beyond the scope of our non-manipulative study design.

4.6 | CONCLUSION

While a consistent overall grazing effects on methane emissions from coastal marshes could not be identified, our study provides novel mechanistic insight into grazing effects on methane cycling. We show that plant-mediated soil redox conditions, driven by belowground biomass, are the primary control on grazing effects on methane emissions from coastal marshes. Moreover, we found that this plant-mediated effect may be further reinforced by grazing-induced plant community shifts that lead to an exclusion of species that enhance methane emissions. Understanding these plant-mediated mechanisms is essential for improving predictions of methane emissions under different

land-use types and for augment coastal marsh management strategies that aim at maximizing climate change mitigation benefits.

4.7 | ACKNOWLEDGMENTS

We would like to thank everyone involved in this project: Claudia Mählmann for her organizational support, Simon Thomsen, Volker Kleinschmidt, Merle Steinhagen, and Monica Salazar Otiz for technical work, David Holl for providing the LICOR-Analyser, and the student assistants and bachelor candidates Daniel Rohmarker, Robin Assmann, Lia Ruhrus, Linnea Lehnen, Hannah Hosbach, Arthur Haas, and Luka Hansen for their help with field- and lab work. This study was carried out in the framework of the BMBF funded project sea4soCiety (project number 03F0896F) and the Stifterverband project GREENTRIALS. Clarisse Goesele was funded by Deutsche Forschungsgemeinschaft as associated doctoral researcher of the Research Training Group 2530 "Biotapmediated effects on Carbon cycling in Estuaries" (project number 407270017). Peter Mueller was funded by Deutsche Forschungsgemeinschaft (DFG) in the framework of the Emmy Noether Program (502681570). Open Access funding enabled and organized by Projekt DEAL.

Author Contributions

Clarisse Goesele and Peter Mueller and Kai Jensen conceived the ideas and designed the field experiment; Clarisse Goesele and Caroline Chen collected the data; Clarisse Goesele, Ella Logemann and Lars Kutzbach analysed the data; Clarisse Goesele and Peter Mueller led the writing of the manuscript; Clarisse Goesele created the tables and figures. All authors contributed critically to the drafts by reviewing and editing and gave final approval for publication.

Data availability

All data and scripts are available on GitHub [https://github.com/clarissegoesele/repo_grazing_ghg.git].

The repository includes:

(i) L0 ghg data: pre-processed flux data together with flux evaluation script

(ii) L1 data: pre-processed ghg, reduction index, vegetation, carbon stock, elevation data, along with the data-pasting script

(iii) L2 data: the completed data frame, with the script on statistical analysis and figure-generation

Conflict of interest

The authors declare no conflict of interest.

4.8 | SUPPLEMENT

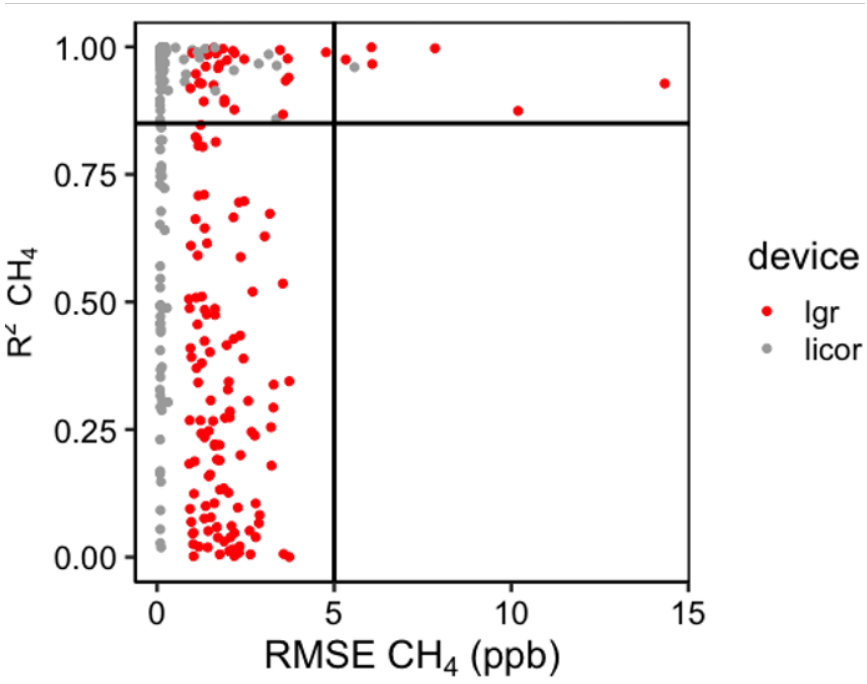

FIGURE 4.S1 *| Combination of R^2 and RMSE as criteria for flux quality control of linear regression results. Methane flux measurements were considered acceptable if either the RMSE of the linear regression of the concentration-over-time-data was below the threshold of 5 ppb or the R^2 of this linear regression was above 0.85.*

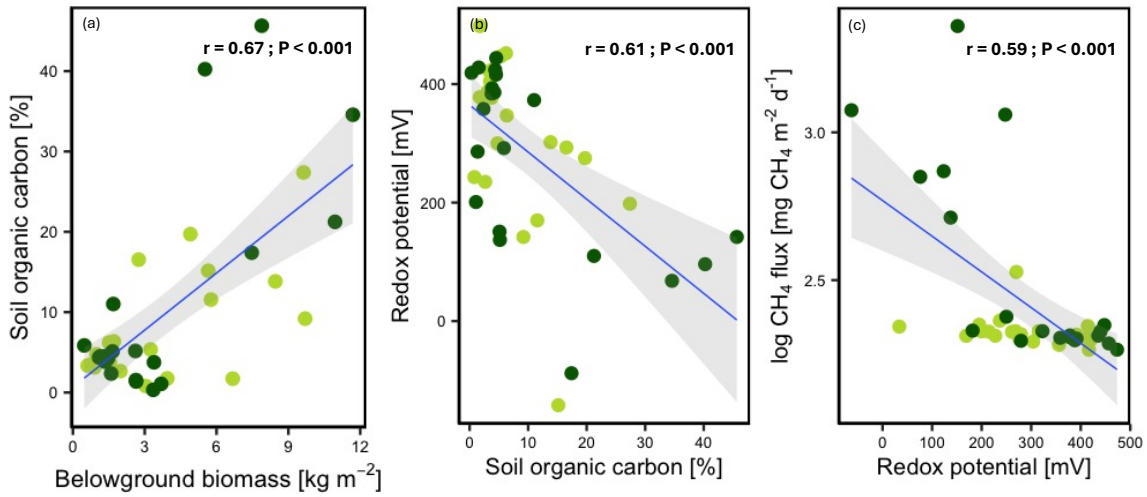

FIGURE 4.S2 *| Panel [a] shows SOC versus belowground biomass, panel [b] redox potential versus SOC and panel [c] shows redox potential versus methane emissions. Panels [a-c] include Pearson correlation coefficients (r) with corresponding p-values, linear fit, and 95% confidence intervals.*

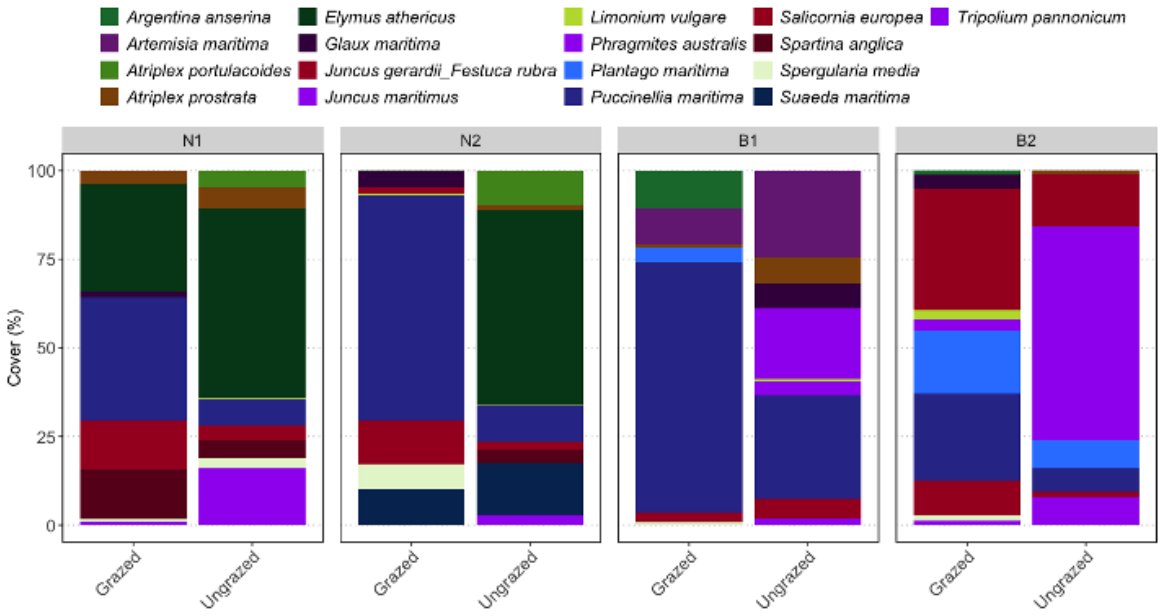

Figure 4.S3 *| Species distribution in grazed and ungrazed marshes at each site. Panels show plant species cover standardized to 100% per treatment within each site. "High-flux" species are indicated in purple*

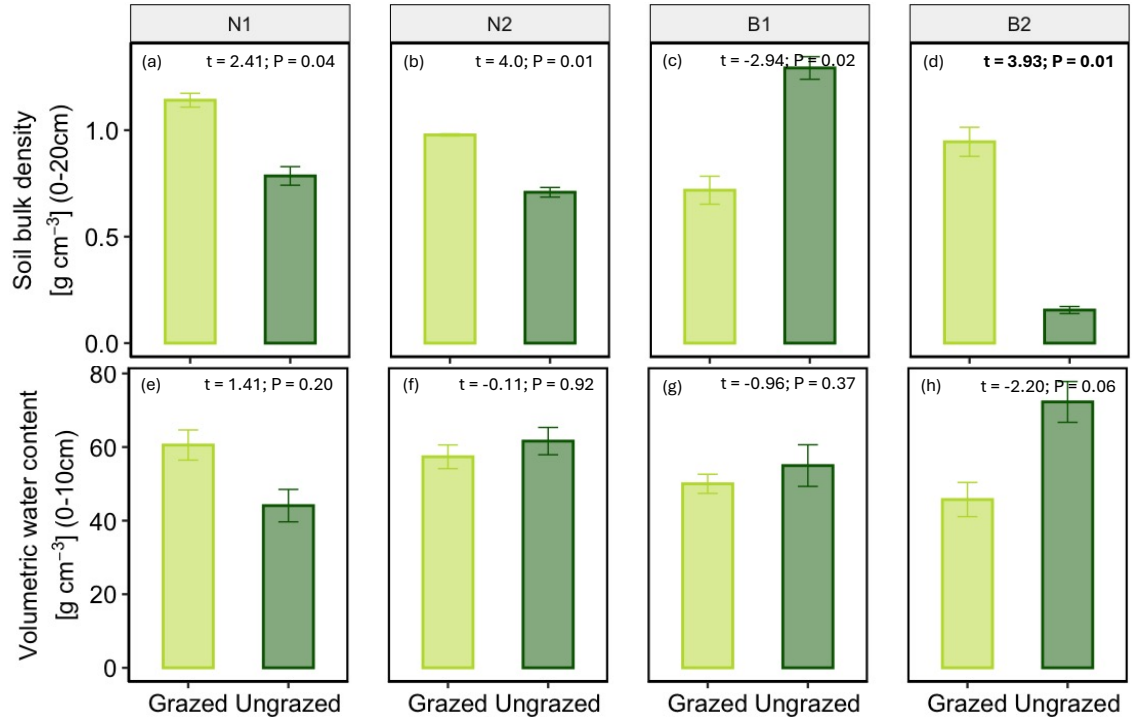

Figure 4.S4 *| Soil bulk density [a-d] and volumetric water content [e-h] in grazed and ungrazed treatments within each site. Bars represent site-level treatment means ± SE, and values indicate t-statistics from independent t-tests.*

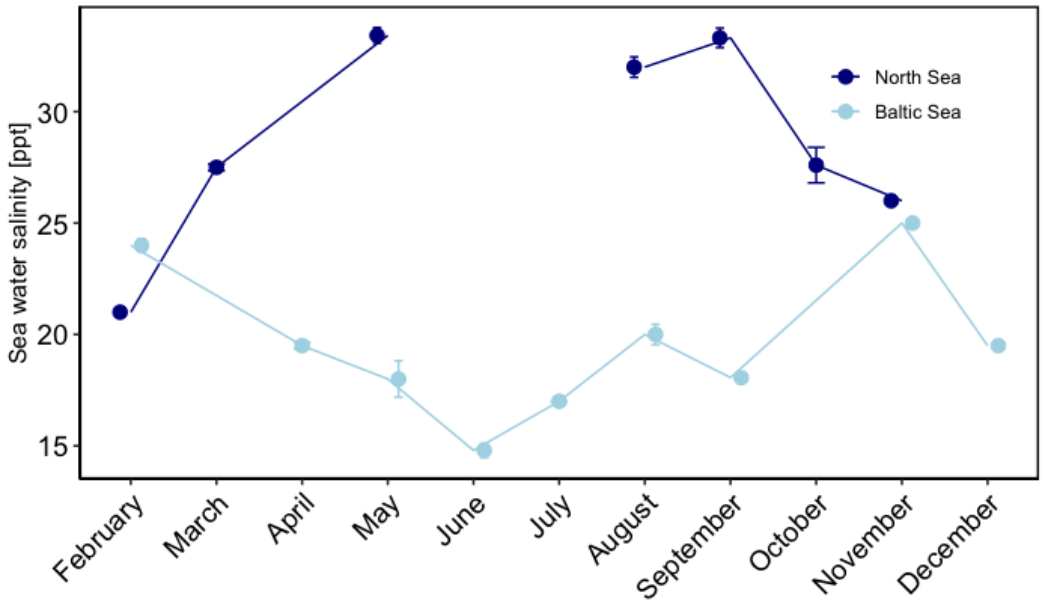

Figure 4.S5 **|** *Seawater salinity measured in the North and Baltic Sea across sampling campaigns. Values represent measurements from water samples collected from the adjoining seawater body during each campaign, as marsh soil salinity often reflects the adjacent water body.*

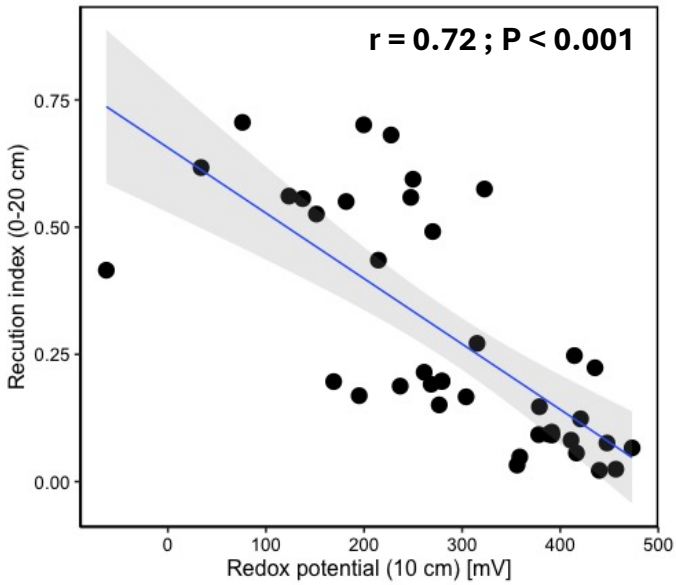

Figure 4.S6 **|** *The redox measurements (mV) using the Pt-tipped electrode are backed up by the reduction index (%) from the root zone (0-20cm). With a decreasing redox potential, the reduction index increases, which reflects an increase in reduced areas on the IRIS stick (r^2= 0.72, P <0.001).*

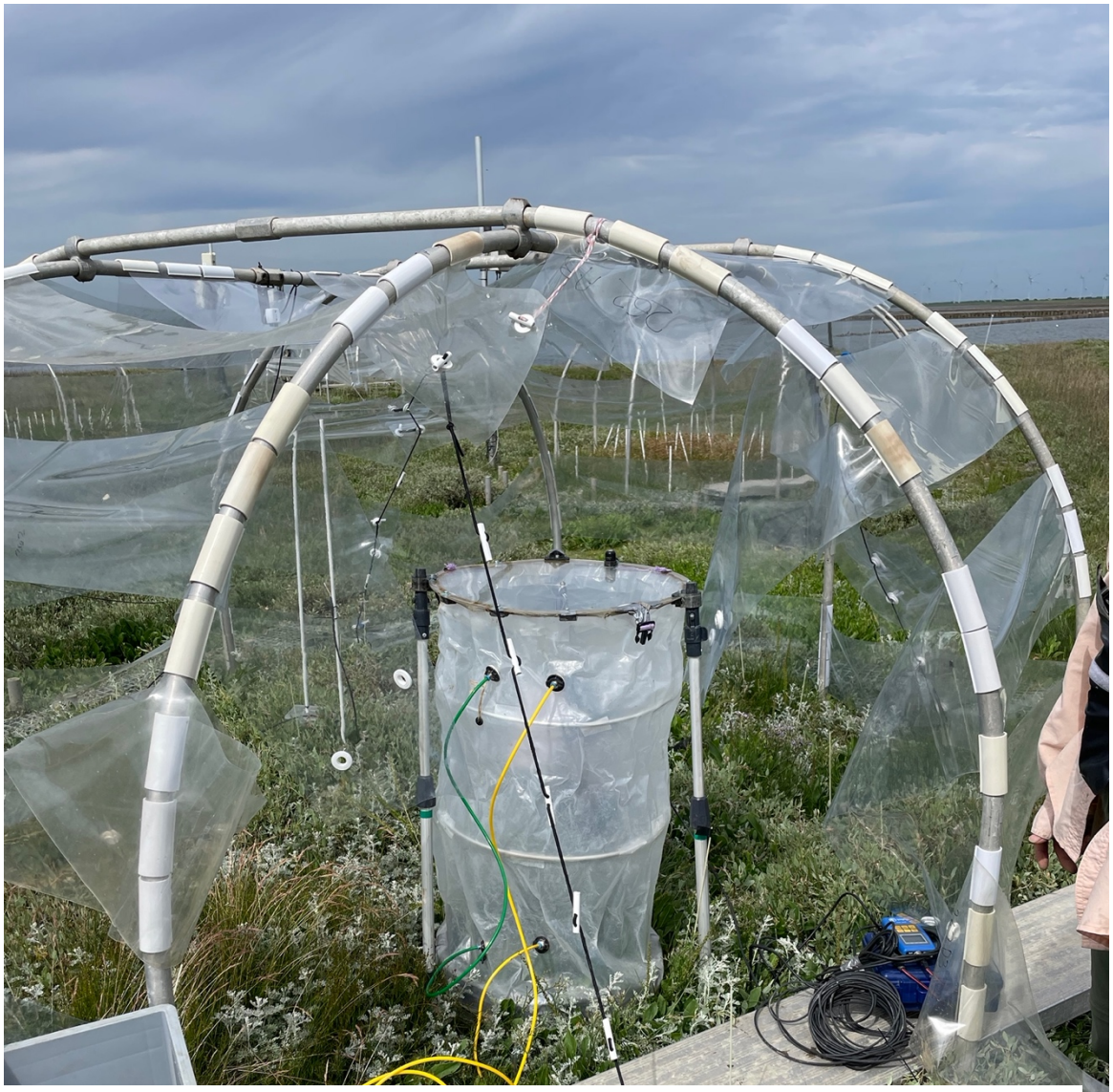

CHAPTER FIVE | WARMING STIMULATES SOIL REDUCTION AND METHANE PRODUCTION IN SALT MARSHES

WARMING STIMULATES SOIL REDUCTION AND METHANE PRODUCTION IN SALT MARSHES

To be submitted to *Global Change Biology*.

Clarisse Goesele[1†] & Julian Mittmann-Goetsch[1†], Viktoria Unger[1], Kai Jensen[1], Susanne Liebner[2,3], Simon Thomsen[1], Roy Rich[4], Lars Kutzbach[5], Cheng (Caroline) Chen[1], Alexander Bartholomäus[2], and Peter Mueller[6]

[1] Institute of Plant Science and Microbiology, Universität Hamburg, Hamburg, Germany

[2] GFZ Helmholtz Centre for Geosciences, Geomicrobiology, Potsdam, Germany

[3] Institute for Biochemistry and Biology, Universität Potsdam, Potsdam, Germany

[4] Smithsonian Environmental Research Center, Edgewater, MD, USA

[5] Institute of Soil Science, Center for Earth Research and Sustainability (CEN), Universität Hamburg, Hamburg, Germany

[6] Institute for Environmental Sciences, Rheinland-Pfälzische Technische Universität, Kaiserslautern Landau, Germany

[†] Clarisse Goesele and Julian Mittmann-Goetsch contributed equally to this work

Corresponding author: clarisse.goesele@uni-hamburg.de

Keywords: redox potential, climate change, coastal wetlands, methanogenesis, methanotrophy

5.1 | ABSTRACT

Coastal wetlands are globally significant carbon sinks, but their oxygen-depleted soils also facilitate the production of methane, a greenhouse gas with a 45 times higher sustained-flux global warming potential than CO_2. Carbon storage and methane fluxes are governed by the redox potential, which reflects the balance between electron acceptors and electron donors. Climate warming is expected to shift these processes since reductive pathways are generally more temperature-sensitive than oxidative ones. Hydrology-driven redox constraints are expected to reduce warming effects in frequently flooded zones and soil layers. We therefore hypothesized that warming will decrease soil redox potentials, with most pronounced effects in the high-elevation zones and topsoil layers. We further hypothesize that decreasing soil redox potentials, caused by warming effects, will lead to higher methane production and emission. To address this knowledge gap, we investigated soil redox dynamics by continuous redox potential measurements and by the indicator-of-reduction-in-soils method, assessing Fe-reduction, as well as methane fluxes and the composition of the active microbial community through 16S amplicon sequencing (on rRNA transcripts) in a whole-ecosystem warming experiment (MERIT) in a salt marsh of the European Wadden Sea. In line with our hypothesis, warming decreased soil redox potentials, with the most pronounced effects in the high marsh and in topsoils. However, warming effects on the reduction index were most pronounced in the pioneer zone and in subsoils, where methane fluxes also increased in line with our second hypothesis. Stronger warming responses at the marine end of the marine–terrestrial gradient—are further corroborated by methanogenic microbes responding to warming primarily in the pioneer zone. We find an increased abundance in methylotrophic genera (*Methanosarcina*, *Methanococcoides*) in warmed plots, which aligns with increasing methane fluxes. We suggest that the higher temperature sensitivity of methanogenesis relative to methanotrophy underlies these dynamics. Overall, our findings contrast previous findings, by showing direct warming effects on methane production in anoxic soils of salt marshes.

5.2 | INTRODUCTION

Coastal wetlands rank among the most effective natural systems for long-term carbon storage (McLeod et al. 2011, Temmink et al. 2022), simultaneously they act as sources of methane (CH_4) (Rosentreter et al. 2018), a greenhouse gas with 45 times the sustained-flux global warming potential of CO_2 (Neubauer and Megonigal 2015). This balance between carbon storage and methane release arises from waterlogged soil conditions, which create low-oxygen (i.e. low redox potential) environments: while oxygen limitation slows decomposition and enhances carbon burial, it also supports microbial pathways that generate methane (Rosentreter et al. 2018, Temmink et al. 2022, Eyre et al. 2023). Therefore, soil redox potential has emerged as an important variable for evaluating and predicting the climate change mitigation potential of coastal wetlands under future warming (Lee et al. 2025, Zhu et al. 2025).

Soil redox potentials reflect the availability of electron acceptors and donors, which strongly influence microbial-driven decomposition processes (Sutton-Grier et al. 2011, Zhang and Furman 2021). Climate warming exerts a strong control on redox-sensitive microbial processes, with reductive processes generally showing greater increases with warming than oxidative processes (Bullock et al. 2013, Lee et al. 2025). This differential sensitivity extends to methane metabolism, where methanogenesis (reductive process) is expected to be favored over methanotrophy (oxidative process) under warmed conditions (Segers 1998, Noyce and Megonigal 2021). Incubation studies support this prediction, consistently showing that microbial methanogenesis is strongly stimulated by elevated temperature (Inglett et al. 2011, Yvon-Durocher et al. 2014, Chen et al. 2020a). However, robust field experimental insight remains scarce.

Results from a peatland whole-ecosystem warming experiment suggest that methanogenic processes are indeed favored under warming (Hopple et al. 2020, Wilson et al. 2021). These findings are partly supported by findings from a brackish coastal wetland whole-ecosystem warming experiment, where warming led to higher methane emissions (Noyce et al. 2023). However, we currently lack the understanding of how coastal marshes with higher salinities respond to global warming. Here, enhanced sulfate concentrations can allow sulfate-reducing microbes to outcompete methanogenic microbes (Kristjansson and Schönheit 1983), and strong increases in methane emissions have been associated with decreases in salinity and thereby sulfate concentrations (Bartlett et al. 1987).

Several wetland studies have shown that the effects of warming are largely confined to zones and soil layers where redox constraints are minimal (Wilson et al. 2016, Tang et al. 2023). In salt marshes, frequent tidal inundation limits temperature-induced changes in water table, thereby buffering and outweighing the direct effects of warming. As a results, hydrology remains the dominant control (Rich et al. 2023, Cui et al. 2024, Guan et al. 2025), and the influence of warming is expected to become more pronounced along the marine–terrestrial gradient (Rich et al. 2023).

This study was carried out in the in-situ whole-ecosystem warming experiment (MERIT: Marsh Ecosystem Response to Increased Temperatures) in a salt marsh on the European Wadden Sea coast of Schleswig-Holstein, Germany. A recent MERIT study found that soil redox potential is strongly shaped by flooding frequency and soil depth (Tang et al. 2023), while it is expected to decrease with warming under which reductive processes are favored (Bullock et al. 2013, Lee et al. 2025). Along the marine-terrestrial gradient hydrology has been observed to supress warming effects for plant belowground biomass (Menzel et al. 2025) and microbial communities (Mittmann-Goetsch et al. 2025), where warming effects were most evident in the high marsh. We therefore hypothesize [1] that warming will decrease soil redox potentials, with most pronounced effects in the high-elevation zones and topsoil layers. We further hypothesize that [2] decreasing soil redox potentials, caused by warming effects, will lead to higher methane production and emission.

5.3 | MATERIAL & METHODS

5.3.1 | SITE DESCRIPTION

The MERIT (Marsh Ecosystem Response to Increased Temperature) experiment, initiated in 2018, is located in a salt marsh on Hamburger Hallig in the German Wadden Sea (54°36′06.7″N, 8°48′57.4″E). This whole-ecosystem warming study combines passive aboveground and active belowground heating, with soil warming to 100 cm soil depth. Aboveground warming is achieved using open-top chambers that trap heat and solar radiation, while belowground warming is delivered via a system of horizontal (GX-088L3106 GX, 9.8 Ω/m, 240 V) and vertical (GX 088L3100, 9.8 Ω/m, Danfoss, Denmark) heating cables. The experiment comprises three replicate plots of 8 m² within each of three distinct marsh zones along the marine–terrestrial gradient: the pioneer zone, low marsh, and high marsh. Each zone includes three temperature treatments (ambient, +1.5 °C, and +3.0 °C) resulting in a total of 27 plots. Soil temperatures are continuously measured at 5 cm, 25 cm, 75 cm depth. A detailed description of the experimental setup and its operation can be found in Rich et al. (2023).

5.3.2 | SOIL REDOX

Soil redox potentials were constantly measured in a subset of the plots (N = 9), using an automated redox system, consisting of 96 sensors, with two measurement depths respectively (15 cm, 75 cm). A combination of 36 sensors (Sander Smits, Netherlands) and 60 sensors (built using in-house protocol) were installed in spring 2023 and 2024, respectively. Redox potentials were measured against 3 M KCl (Ag/AgCl) reference electrodes. Values were recorded using a combination of CR1000X Data loggers (Campbell Scientific, USA), and AM 16/32 Multiplexer (Campbell

Scientific, USA). Redox data were corrected to the standard hydrogen electrode by adding +207 mV to the values (Mansfeldt 2003).

IRIS (Indicator of Reduction in Soils) sticks were used to determine a soil reduction index. Sticks were installed in six consecutive campaigns, each spanning a six-week period during 2023. The method followed standard protocols (Rabenhorst and Burch 2006). Iron (Fe) oxides were applied to white PVC sticks and deployed. The capacity of solid-phase Fe (III) oxides to be reduced, by microbial Fe reducers, to soluble Fe (II) under anoxic conditions is used to assess soil-reduction in soils. After retrieval, sticks were carefully rinsed with tap water. After drying, sticks were scanned using an overhead scanner (Viisan, China). White pixels on the images were determined using a supervised classification tool (Mittmann-Goetsch et al. 2024). Reduction index was calculated as the share of white pixels from total pixels, where high amounts of paint removal are reflected in high reduction indices. The resulting reduction index thus not only provides an integrated measure of soil anoxia over the deployment period, but also quantitatively reflects the potential for microbial Fe reduction, a key redox process that indicates strongly reducing conditions while still operating at a higher energetic yield than sulfate reduction.

5.3.3 | METHANE FLUXES

Three plots per zone and temperature treatment (N = 27) were investigated for methane fluxes. Flux measurements, by a closed chamber method, were conducted in regular intervals of six weeks from March 2023 to October 2023. In total, six campaigns were carried out. Flux measurements were conducted around low tide, i.e. when soil surfaces were not flooded.

For methane flux measurements, a flexible (i.e. height-adjustable) portable closed chamber (100 cm in height) as described by Yang et al. (2024), and permanently installed flux collars were used. The chamber was equipped with fans on the inside for air circulation. During each flux measurement, air temperature and relative humidity inside the chamber were measured. Photosynthetically active radiation (PAR) was measured outside with a sensor installed on top of the chamber.

Two types of portable laser-based trace-gas analyzers – a Micro Portable Greenhouse Gas Analyzer (ABB GLA131 Series Microportable Analyzers, ABB Inc. Measurement & Analytics, Quebec, Canada) or a portable $CH_4/CO_2/H_2O$ Trace Gas Analyzer (LI-7810, LI-COR Environmental, Lincoln, NE, US) – were used to quantify methane concentration changes inside the chamber headspaces during 6-min flux measurements. The methane fluxes were calculated based on linear regression slopes of methane concentration change over time. After visual inspection of each individual flux measurement, 5% of all methane fluxes were excluded from the dataset due to analyzer errors or chamber leakage. For further flux evaluation, a combination of the root mean square error (RMSE; threshold at 5 ppb) and coefficient of determination (R^2; threshold at 0.85) of

the linear regressions was used (adapted from Kutzbach et al. 2007). This method ensured the inclusion of high-quality flux measurements close to zero, which would have been excluded if considering the R^2threshold alone. Methane flux measurements were considered acceptable if either the RMSE of the linear regression of the concentration-over-time-data was below the threshold of 5 ppb or the $R^2$of this linear regression was above 0.85. A satisfactory RMSE could therefore offset a sub-threshold R^2, and conversely, a strong R^2 could justify accepting a flux despite an elevated RMSE (see Fig. 5.S1). Flux-calculation statistics were conducted in R (version 4.5.0 (2025-04-11)).

5.3.4 | SOIL MICROBES

Soil sampling was carried out in September 2022. From each of the 27 plots, a single soil core (100 cm deep) was collected using a 2.5-cm-diameter gauge auger. To prevent microbial cross-contamination, the auger was thoroughly rinsed with ethanol and deionized water after each sampling. Each core was sectioned into four depth intervals (5–10 cm, 20–30 cm, 40–50 cm, and 80–100 cm), resulting in four samples per core. Immediately after collection, samples were placed on dry ice in the field and during transport, and subsequently stored at –80 °C in the laboratory until RNA extraction.

Total RNA was extracted from soil samples using the GeneMATRIX Environmental DNA & RNA Purification Kit (Roboklon, Germany) following the manufacturer's instructions. The RNA was further purified with the Turbo DNA-free kit (Thermo Fisher, Germany). For cDNA synthesis, reverse transcription PCR was performed to convert single-stranded RNA into complementary DNA (cDNA). In a PCR tube on ice, 10 µl sterile distilled water, 1 µl 10 mM dNTP mix (Invitrogen, USA), 1 µl pd(N)6 random hexamer primers (GE Healthcare, USA), and 1 µl RNA sample were combined (total volume 13 µl). This mixture was heated at 65 °C for 5 minutes in a PCR machine (Bio-Rad, USA) to denature secondary structures, then immediately cooled on ice. After brief centrifugation, 1 µl sterile distilled water, 1 µl 0.1 M DTT, 1 µl SuperScript III Reverse Transcriptase (Thermo Fisher, Germany), and 4 µl 5× First-Strand Buffer were added. The reaction was gently mixed by pipetting. Primer annealing was performed at 25°C for 5 minutes, followed by reverse transcription at 50°C for 60 minutes. The reaction was terminated by heating at 70°C for 15 minutes to inactivate the enzyme. cDNA concentrations were measured using a Qubit 2.0 Fluorometer (Invitrogen, USA) with dsDNA HS and BR assay kits (Thermo Fisher, Germany).

Amplicon libraries were prepared using in-house barcoded primer pairs targeting the V3–V4 hypervariable regions of the 16S rRNA gene (Uni515-F: GTGTGYCAGCMGCCGCGGTAA; Uni806-R: CCGGACTACNVGGGTWTCTAAT). PCR reactions (25 µl) contained 10× Pol Buffer C (Roboklon, Germany), 0.5 µM of each primer, 0.2 mM dNTP mix (Thermo Fisher, Germany), 2 mM $MgCl_2$, 1.25 U Optitaq Polymerase (Roboklon, Germany), PCR-grade water, and 1 µl template cDNA. Negative controls included PCR water and RNA extract. The PCR program was:

initial denaturation (5 min, 95°C); 32 cycles of denaturation (30 sec, 95°C), annealing (30 sec, 56°C), elongation (1 min, 72°C); and a final elongation (7 min, 72°C). PCR products were purified using HighPrep™ PCR clean-up reagents (Magbio Genomics, USA) per manufacturer's protocol. PCR product concentrations were normalized and pooled with controls. The pool was sent for sequencing to Eurofins Genomics (Ebersberg, Germany). The library preparation was done by PCR-free adapter ligation. Sequencing was done on the Illumina MiSeq platform using 2 x 300 bp paired end mode using the V3 chemistry. Sequencing data were demultiplexed using cutadapt v3.4 with parameters -e 0.2 -q 15,15 -m 150 --discard-untrimmed. Amplicon sequence variants (ASVs) were generated using DADA2 v1.20 in R v4.1 with pooled approach and filtering parameters maxN=10, truncQ=20, rm.phix=TRUE, and minLen=150. Read pair merging was done using function "mergePairs" provided by the DADA2 package. Taxonomic assignment used DADA2 and the SILVA database v138.1. Further data processing was performed in R (v4.4.2) with RStudio (v2024.09.1+394) and the packages ggplot2, phyloseq, and vegan. ASVs assigned to chloroplasts or mitochondria and singletons were removed before rarefaction to 5000 reads.

Functional annotation of prokaryotic taxa was performed using the Tax4Fun2 R package. Genes involved in methane oxidation (https://www.kegg.jp/module/M00174), and methylotrophic- (https://www.kegg.jp/kegg-bin/show_module?M00356), acetoclastic- (https://www.kegg.jp/kegg-bin/show_module?M00357), and hydrogenotrophic- (https://www.kegg.jp/kegg-bin/show_module?M00567) methanogenesis respectively, were included using the KEGG (Kyoto Encyclopedia of Genes and Genomes) database. The balance between methanogenic and methanotrophic processes was analyzed using rRNA-based functional predictions (Tax4Fun2) across three salt marsh zones (pioneer zone, low marsh, high marsh) and three temperature treatments (ambient, +1.5°C, +3.0°C). Methylotrophic, acetoclastic and hydrogenotrophic methanogenesis were pooled together, to represent all methanogenic processes. This approach characterized the putatively active methane-cycling microbial community along the marine-terrestrial gradient of the marsh. A ratio of the methanogenic predicted functional potential to methanotrophic predicted functional potential was calculated, based on normalized counts per copy number of Tax4Fun2 prediction on the 16S rRNA transcripts. Hereafter this ratio is referred to as methanogenesis to methanotrophy ratio.

Rooting depth patterns at our sites were used to define two soil intervals. For microbial analyses, samples were pooled into a topsoil layer (10–30 cm), strongly influenced by live roots, and a subsoil layer (40–100 cm), where live root influence was minimal. For redox characterization, reduction indices from IRIS sticks were pooled over the same topsoil layer (10–30 cm), but only down to 60–80 cm in the subsoil, reflecting the installation depth of the sticks.

5.3.5 | STATISTICAL ANALYSIS

The automated soil redox potential data was summarized on hourly mean values and plotted for the entire warming period. Due to insufficient replication of the respective warming treatments (eight sensors in one plot per treatment and zone; N = 9), we refrained from calculating statistics (i.e. GLMMs, ANOVA) with the redox potential data. We therefore included reduction index data, assessed using IRIS sticks, with duplicate IRIS sticks per plot in each campaign.

For the reduction index, distributions for both topsoil and subsoil were first assessed visually. Since both reduction index datasets followed a beta distribution, we fitted generalized linear mixed models (GLMMs) using the beta_family (link = "logit"), to assess the effects of temperature treatment, marsh zone and soil depth on the reduction index. Reduction index values were aggregated per plot (n = 27) and campaign (n = 10) within each depth increment (topsoil: 10 cm, 20 cm, 30 cm; subsoil: 60 cm, 70 cm, 80 cm). Fixed effects included zone, temperature treatment, and season, while depth nested within plot ID was specified as a random effect to account for repeated measurements across campaigns and depth. In addition, reduction index (0-80 cm) and temperature data (5 cm, 25 cm, 75 cm) were averaged at the plot level, and then linear regressions were calculated to assess the relationships between reduction index and soil temperature.

For methane emissions, data were normally distributed and therefore analyzed using a GLMM with Gaussian error distribution. Methane fluxes were measured once per plot in each campaign, resulting in five values per plot (March, May, June, August, September). The model included zone, temperature treatment, and season as fixed effects and plot ID as a random effect to account for repeated measurements. In addition, methane fluxes, reduction index (10-30 cm) and temperature data (5 cm) were averaged at the plot level and then linear regression were calculated to assess the relationship between methane fluxes and both reduction index and soil temperature.

To test how warming affected methanogenic activity relative to methanotrophic activity, we calculated the ratio between methanogenic and methanotrophic potential processes. Microbial ratio data were separated into topsoil (5-10 cm, 20-30 cm) and subsoil (40-50 cm, 80-100 cm). After visual inspection, abundances were found to be non-normally distributed and were therefore log-transformed. Data were aggregated by plot ID and depth. GLMMs were then fitted with zone and temperature treatment as fixed effects and plot ID as a random effect, accounting for repeated measurements across depths. In addition, reduction index (0-30 cm) and the ratio between methanogenic and methanotrophic potential processes (0-100 cm) were averaged at the plot level and then linear regression were calculated to assess the relationship between reduction index and the ratio between methanogenic and methanotrophic potential processes.

For all models, the significance of main effects (zone, temperature treatment, and season, where applicable) and their interactions was tested using Type-III Wald χ^2 tests (car:Anova). Pairwise comparisons were performed using Tukey's HSD tests.

Bubble plots were created to visually assess changes in the structure of the microbial communities involved in methane cycling. Microbes were assigned at genera level, where possible, to one of the following groups: acetoclastic methanogenesis, hydrogenotrophic methanogenesis, methylotrophic methanogenesis, Type I methanotrophy, Type II methanotrophy, verrucomicrobia methanotrophs and sulfate reducers.

All statistical analyses were conducted with the software R Studio version 4.4.1 (R Core Team, 2024). Data was prepared using R packages dplyr broom and lubridate. All plots were created using R package ggplot2 with extensions ggpubr and ggpmiscs. GlmmTMB Tukey´s pairwise comparisons were performed using the R package emmeans.

5.4 | RESULTS

5.4.1 | SOIL REDOX

Across all temperature treatments, the strongest differences in soil redox potentials were observed among the marsh flooding frequency zones (Fig. 5.1a). Average redox potentials over the entire vegetation period (temporal) and both soil layers (spatial) increased along the marine-terrestrial gradient, from the pioneer zone (–112.1 ± 0.8 mV, mean ± se) to the low marsh (–43 ± 3 mV, mean ± se) and the high marsh (192.2 ± 4 mV, mean ± se). Both temporal and spatial variation was generally lowest in the pioneer zone, moderate in the low marsh, and highest in the high marsh topsoil (Fig. 5.1a). Redox potentials were lower in the subsoil compared to the topsoil, with differences between the marsh zones (Fig. 5.1a). In the low marsh and pioneer zone, depth-related differences were smaller and less consistent, than in the high marsh. Differences in soil redox potentials with warming treatments differed among zones and depths. In the high marsh topsoil, both temperature treatments (+1.5 °C, +3.0 °C) lowered redox potentials relative to ambient conditions, while in the subsoil +3.0°C plots were lower than ambient but the +1.5 °C plots showed slightly higher values. In the low marsh topsoil, +3.0 °C plots showed slightly higher redox potentials compared to ambient, while +1.5 °C plots were lower. In the low marsh subsoil, both warming levels generally resulted in higher redox potentials than ambient. In the pioneer zone, soil redox potentials showed little variability overall, and no consistent warming response was detected (Fig. 5.1a).

Reduction index (assessed using IRIS sticks) increased significantly with soil temperature across the entire soil profile from 0–80 cm ($R^2 = 0.26$, $p < 0.01$; Fig. 5.1b, Tab. 5.1). In topsoil (0–30 cm) and subsoil layers (60–80 cm), values were significantly higher in summer than in spring ($p < 0.001$, Fig. 5.1c, Tab. 5.1). In the topsoil, neither zone nor temperature treatment had a significant effect on reduction index, whereas in the subsoil, reduction index was significantly affected by zone ($p < 0.05$), temperature treatment ($p < 0.001$), and season ($p < 0.001$). Because zone interacted significantly with temperature treatment ($p < 0.01$), season ($p < 0.001$), and their interaction effect

($p < 0.01$), main effects must be interpreted with caution. Interaction patterns showed that in the pioneer zone subsoil, reduction index increased significantly in spring under +1.5°C warming ($p < 0.05$; Fig. 5.1c). In the low marsh subsoil, reduction index increased significantly under both +1.5°C ($p < 0.05$) and +3.0°C ($p < 0.01$) temperature treatments (Fig. 5.1c). In the pioneer zone topsoil, reduction index also tended to increase with warming in both spring and summer ($p > 0.05$, Fig. 5.1c).

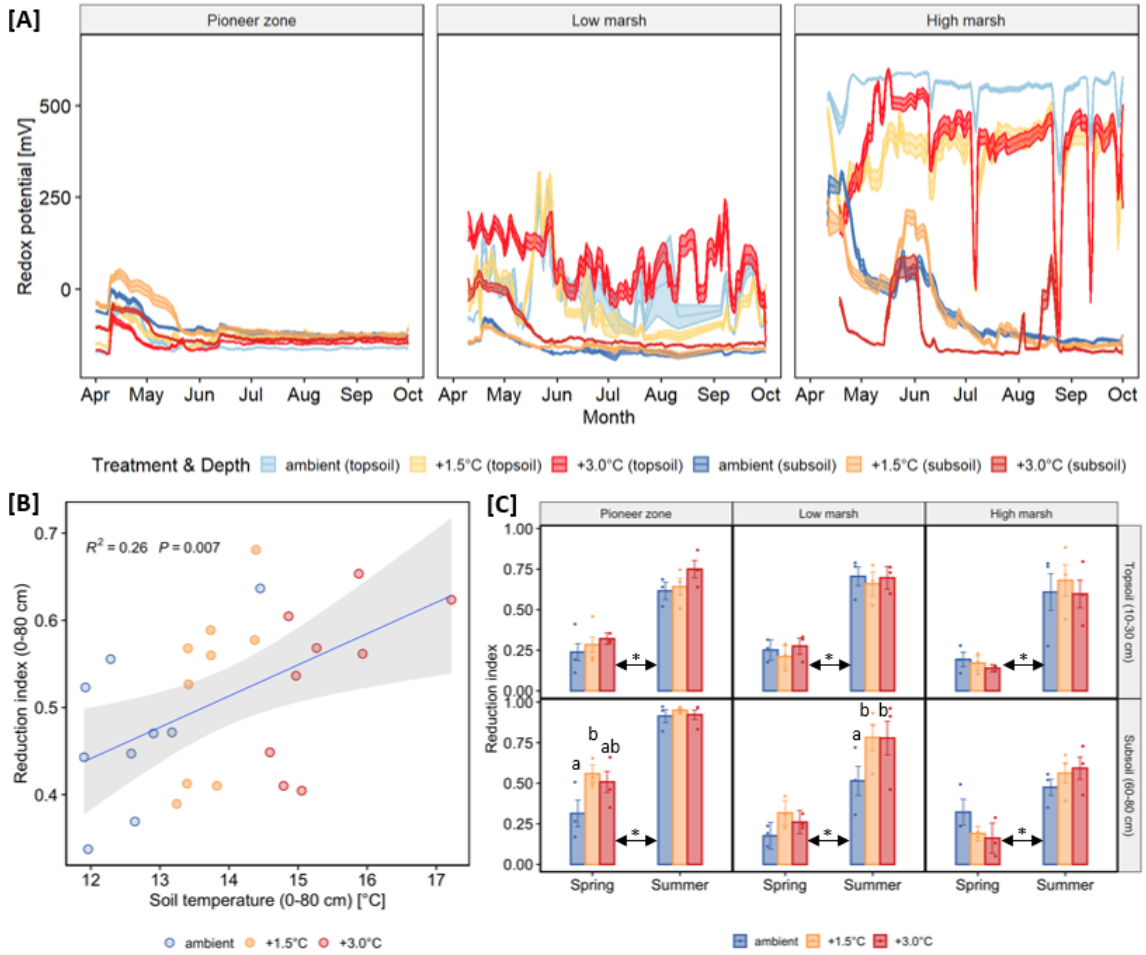

***FIGURE 5.1** | [A] Soil redox potentials (mV) from automated redox system (Apr 2024 – Oct 2024). [B] Linear regression between plot mean soil temperature and mean reduction index for vegetation period of 2023. Soil temperatures were averaged for the entire vegetation period (Mar-Oct 2023), at plot level across continuous temperature measurements at 5 cm, 25 cm and 75 cm soil depth. Reduction index (Mar-Oct 2023) was averaged at plot level across 0-80 cm depth. Shown are linear regression coefficient R^2 with corresponding p-values, linear fit, and 95% confidence intervals. [C] Reduction index data from vegetation periods (Mar-Sep 2023) in topsoil (10-30 cm) and subsoil (60-80 cm) layers across the marsh zones (pioneer zone, low marsh, high marsh) and the temperature treatments (ambient, +1.5 °C, +3.0 °C). Differences between zones are indicated as follows: * p < 0.05. Significant differences between temperature treatments within each zone and season are indicated with letters based on Tukey HSD pairwise comparison (p < 0.05).*

5.4.2 | METHANE FLUXES

Methane fluxes were generally low (mean -1.34 ± 4.51 µmol m^{-2} d^{-1}) and ranged from -288.4 µmol m^{-2} d^{-1} to 172.09 µmol m^{-2} d^{-1}. Methane fluxes increased significantly with increasing reduction index ($R^2 = 0.19$; $p < 0.05$; Fig. 5.2a, Tab. 5.1) and with increasing soil temperature at 5 cm depth

($R^2 = 0.17$; $p < 0.05$; Fig. 5.2b, Tab. 5.1). Both temperature treatment and season had a significant effect on methane fluxes (both $p < 0.001$). As revealed by the two significant interaction effects between temperature treatment and zone ($p < 0.05$) and zone and season ($p < 0.01$), the effect of warming on methane fluxes depends on the context. During spring, methane fluxes in the pioneer zone were significantly higher in the +1.5°C temperature treatment compared to the ambient controls ($p < 0.05$; Fig. 5.2c, Tab. 5.1). In summer, temperature treatments did not differ with respect to methane fluxes (Fig. 5.2c).

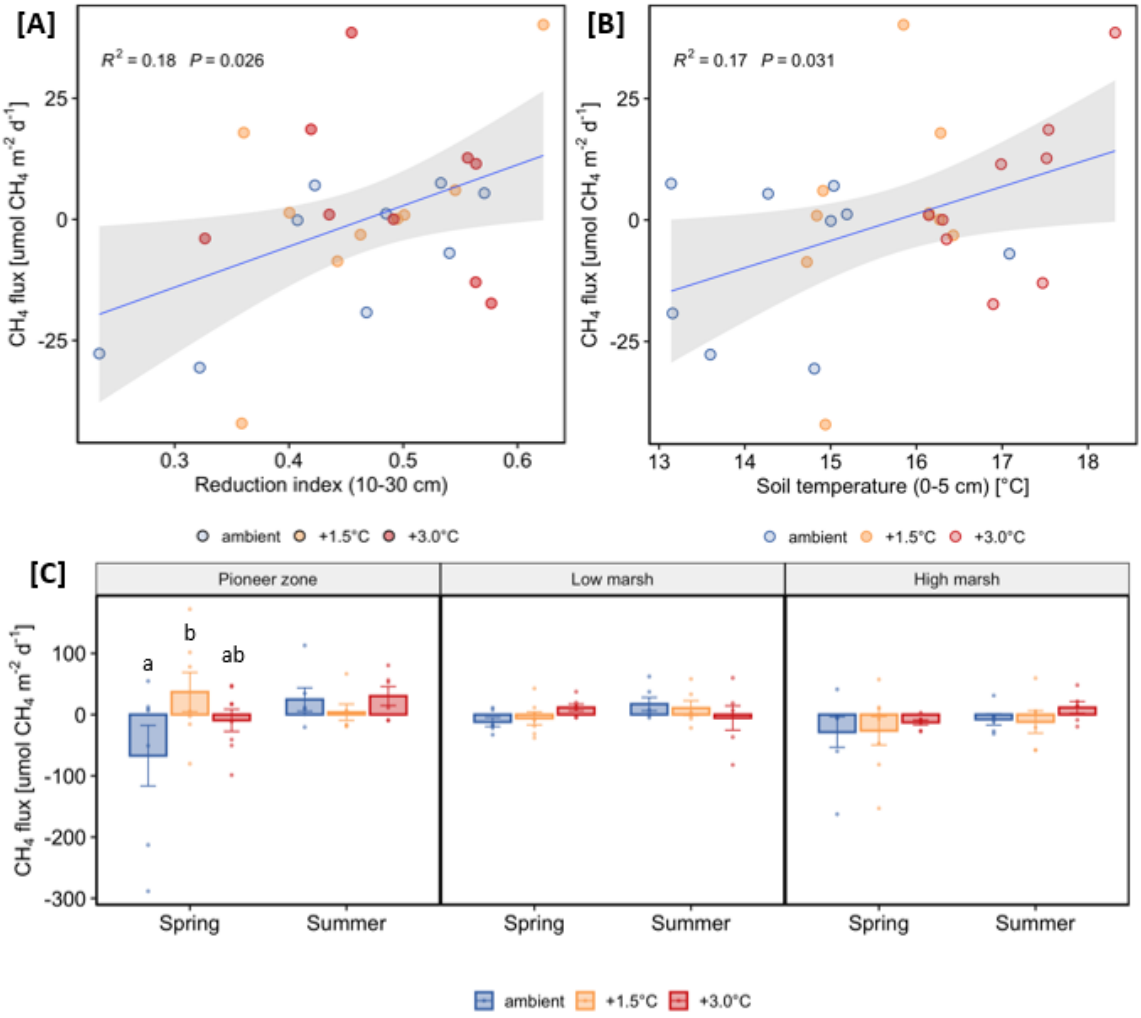

***FIGURE 5.2** | Methane flux data: [A] Linear regression between reduction index (Mar-Oct 2023) and methane fluxes (Mar-Oct 2023) shown are linear regression coefficient R^2 with corresponding p-value, linear fit, and 95% confidence intervals. [B] Linear regression between plot surface temperature (Mar-Oct 2023) and methane fluxes (Mar-Oct 2023). Shown are linear regression coefficient R^2 with corresponding p-value, linear fit, and 95% confidence intervals. [C] Differences in methane fluxes (µmol m^{-2} d^{-1}) between the three temperature treatments (ambient, +1.5 °C, 3.0 °C), in two seasons (spring, summer), in the three marsh zones (pioneer zone; low marsh, high marsh). Significant differences between temperature treatments within each zone and season are indicated with letters based on Tukey HSD pairwise comparison ($p < 0.05$).*

5.4.3 | SOIL MICROBES

The methanogenesis to methanotrophy ratio increased significantly with increasing reduction index ($R^2 = 0.30$; $p < 0.01$; Fig. 5.3a, Tab. 5.1). Zone had a significant main effect on the methanogenesis

to methanotrophy ratio. In the topsoil (10-30 cm), the ratio was significantly higher in the pioneer zone compared to both low marsh ($p < 0.01$) and high marsh ($p < 0.01$). In the subsoil (50-100 cm), the ratio differed significantly between all zones (Fig. 5.3b). In the subsoil, the methanogenic to methanotrophic ratio tended to decrease in response to warming ($p = 0.13$). The +1.5 °C temperature treatment shows higher ratios compared to ambient plots, while the ratio is lower in the +3.0 °C temperature treatments (Fig. 5.3b).

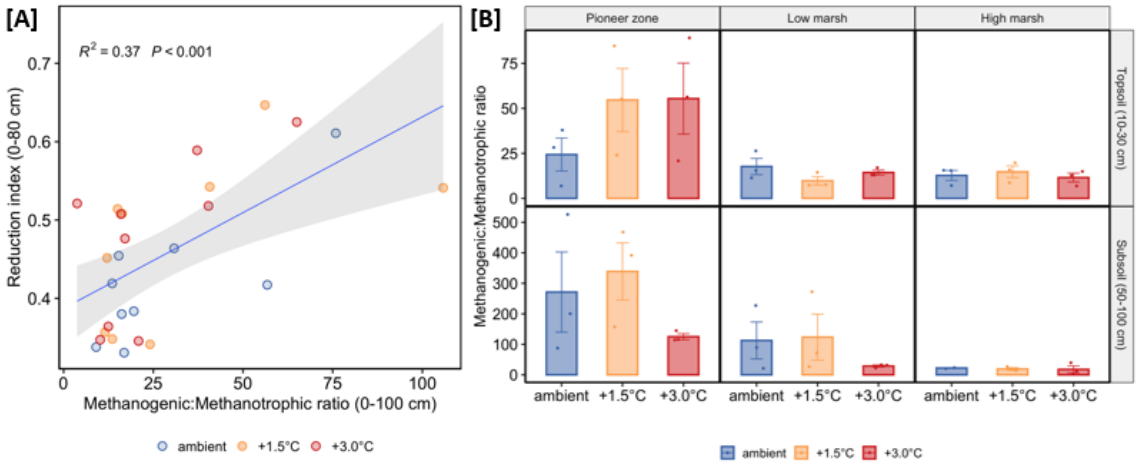

FIGURE 5.3 | *[A] Linear regression between reduction index (Mar-Oct 2023) across the entire measurement depth (0-80 cm) and the methanogenesis to methanotrophy ratio, across the entire soil depth (0-100 cm). Shown are linear regression coefficient R^2 with corresponding p-value, linear fit, and 95% confidence intervals. [B] Differences in the methanogenesis to methanotrophy ratio between the three temperature treatments (ambient, +1.5 °C, 3.0 °C) in the three marsh zones (pioneer zone, low marsh, high marsh), within the topsoil layer at 10-30 cm soil-depth and subsoil layer at 50-100 cm. Shown are barplots with errorbars (mean ± se). Functional groups were assigned from 16S rRNA transcript data using Tax4Fun2.*

TABLE 5.1 | *Results of the generalized linear mixed models (GLMMs) testing for differences between marsh zones (pioneer zone, low marsh, high marsh), temperature treatment (ambient, +1.5 °C, +3.0 °C), seasons (spring, summer) conducted for both topsoil samples (0-30 cm depth) and subsoil samples (40-100 cm depth). Methane fluxes were tested on plot level (N = 27). Significant effects are indicated in bold (p < 0.05).*

Factor / Parameter	Reduction index		Methane fluxes	Methanogenesis to methanotrophy ratio	
	Topsoil (10-30 cm)	Subsoil (60-80 cm)	Plot	Topsoil (10-30 cm)	Subsoil (40-100 cm)
Zone	χ^2 = 1.55, p = 0.46	χ^2 = 6.57, p < 0.05	χ^2 = 4.34, p = 0.11	χ^2 = 18.46, p < 0.001	χ^2 = 42.39, p < 0.001
Treatment	χ^2 = 1.96, p = 0.38	χ^2 = 16.27, p < 0.001	χ^2 = 15.63, p < 0.001	χ^2 = 0.45, p = 0.8	χ^2 = 4.16, p = 0.13
Season	χ^2 = 24.16, p < 0.001	χ^2 = 85.09, p < 0.001	χ^2 = 11.18, p < 0.001		
Zone x Treatment	χ^2 = 2.92, p = 0.57	χ^2 = 15.99, p < 0.01	χ^2 = 9.83, p < 0.05	χ^2 = 5.6, p = 0.23	χ^2 = 0.91, p = 0.92
Zone x Season	χ^2 = 0.22, p = 0.89	χ^2 = 22.78, p < 0.001	χ^2 = 3.96, p = 0.14		
Treatment x Season	χ^2 = 0.47, p = 0.79	χ^2 = 4.81, p = 0.09	χ^2 = 10.44, p < 0.01		
Zone x Treatment x Season	χ^2 = 1.23, p = 0.89	χ^2 = 16.27, p < 0.01	χ^2 = 7.33, p = 0.12		

The analysis of methane-cycling microbial communities revealed distinct spatial patterns and differential responses to experimental warming across the three marsh zones and two soil layers. Among methanogenic archaea, hydrogenotrophic methanogens showed a restricted distribution, being present in the pioneer zone with *Methanolacinia* (family Methanomicrobiaceae) detected in 3.0°C plots in topsoil layer (0-30 cm). This functional group was absent from the low and high marsh zones. Methylotrophic methanogens displayed a broader spatial distribution across pioneer zone plots, than hydrogenotrophic forms. The family Methanosarcinaceae, particularly the genus *Methanococcoides*, showed notable presence in the pioneer zone topsoil, with substantially increased detection under moderate temperature treatment (+1.5 °C). *Methanosarcina*, also belonging to Methanosarcinaceae, appeared in the pioneer zone, under both moderate (+1.5 °C) and high (+3.0 °C) temperature treatments. The methylotrophic order Methanofastidiosales occurred twice in subsoils, both in +3.0 °C in the pioneer zone and in ambient treatments in the low marsh. Type II methanotrophs dominated the methane-oxidizing community and showed the most widespread distribution across all marsh zones. Within the Type II methanotrophs, several genera were consistently detected across zones and soil layers, with the highest presence observed in the high marsh topsoil under both moderate (+1.5 °C) and high (+3.0°C) temperature treatments. Type II genera, belonged to Methyloligellaceae and Beijerinckiaceae families (Fig. 5.4). Type I

methanotrophs were most abundant in the pioneer zone (Fig. 5.4). Here Methylomonadaceae and Cycloclasticaceae were the two detected families. Methylomonadaceae showed increasing abundance in the subsoil (40-100 cm) with both temperature treatments (+1.5 °C, +3.0 °C), while they were absent in this soil layer under ambient conditions.

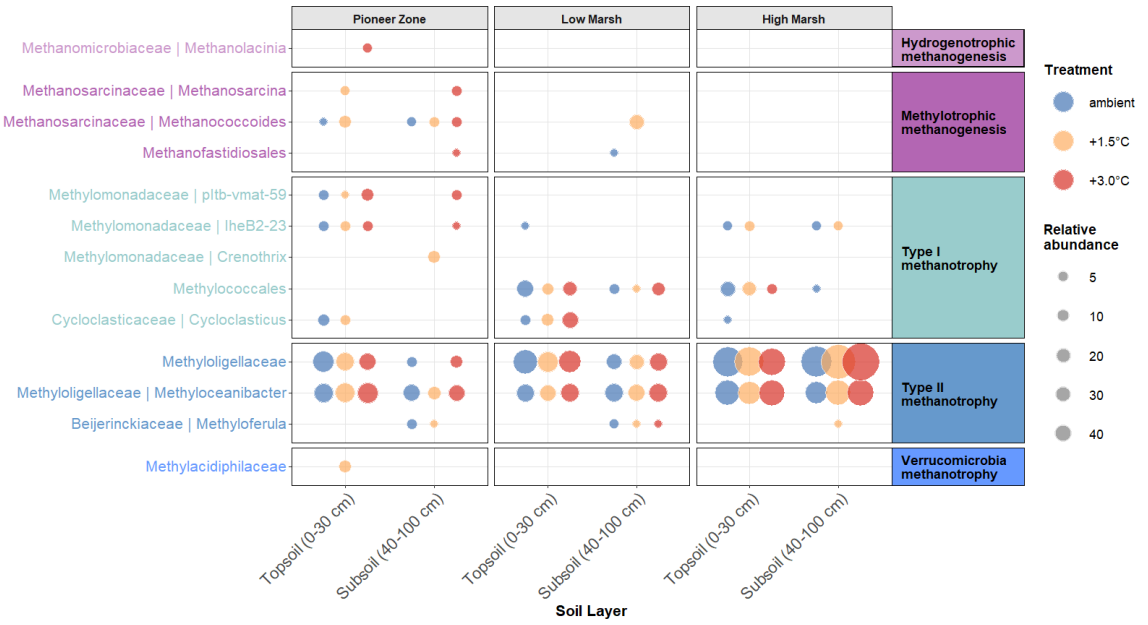

***FIGURE 5.4** | Microbial community composition of methane cycling microbes, both bacteria and archaea based on rRNA transcript sequencing. Shown are bubble plots with relative abundance of hydrogenotrophic methanogens, methylotrophic methanogens, Type I and Type II methanotrophs and Verrucomicrobia methanotrophs. Bubbles are shown for topsoil (0-30 cm) and subsoil (40-100 cm) samples and across the marine-terrestrial gradient (pioneer zone, low marsh, high marsh) and between the three temperature treatments (ambient, +1.5 °C, +3.0 °C). Sequencing data are shown on genus level, while families are indicated at the y-axis. Orders are shown, where they can be assigned to respective groups in their entirety (i.e. Type II methanorophy: Methylococcales, methylotrophic methanogens: Methanofastidiosales).*

5.5 | DISCUSSION

The automated redox potential measurements data is supportive of our first hypothesis, in which we predicted that warming would decrease soil redox potentials, with most pronounced effects in higher elevated zones and topsoils. We observed warming effects on redox potentials primarily in the topsoil high marsh and topsoil low marsh zones, while the pioneer zone showed no clear trends (Fig. 5.1a). This result aligns with previous findings that warming can negatively influence redox-sensitive processes in wetland soils (Noyce et al. 2023, Lee et al. 2025). This pattern further supports our hypothesis that high-elevation zones would be most responsive to warming, as these areas experience the greatest baseline redox variability and are less poised by constant tidal inundation. This is in line with other studies from a peatland warming experiment, where warming effects on decomposition processes were restricted to top-soil layers (Wilson et al. 2016, Hopple et al. 2020). Previously reported results from the MERIT experiment demonstrated that these hydrology-driven limitations of warming effects are also present in salt marshes, here both

microbial functioning (Mittmann-Goetsch et al. 2025) and belowground biomass (Menzel et al. 2025) were only responsive to warming in the high marsh.

Reduction index and redox potential were negatively correlated (Fig. 5.S1), but warming effects differed between methods (Fig. 5.1a & 5.1c). IRIS sticks may register brief reducing events in frequently flooded zones that are missed or averaged out by electrode data due to rapid re-oxidation during drainage (Evans et al. 2021). Thus, IRIS films could be more sensitive to changes in microbially mediated reduction in wet zones, while electrodes better capture warming responses in drier zones with higher mean redox values (Gotoh and Patrick Jr. 1974). In the high marsh, mean redox potentials were at 264.6 ± 6.6 mV across the entire soil profile, which is not within the range of iron reduction measured with the IRIS method (Zhang and Furman 2021). However, redox potential measurements at 75 cm depth in the high marsh were at −77.8 ± 2.8 mV; in subsoils, warming also led to more reduction on IRIS sticks, though not statistically significant (Fig. 5.1c). Importantly, IRIS is only responsive under strongly reducing conditions where Fe(III) reduction actively dissolves the coating (Jenkinson and Franzmeier 2006, Rabenhorst et al. 2008). Such conditions are largely absent from high marsh topsoils, which typically remain well-aerated (Tang et al. 2023), meaning that IRIS and electrode data partly reflect different ranges of the redox spectrum. Taken together, the here presented IRIS sticks and automated redox potential measurements yield very strong evidence for warming effects on soil redox conditions.

The IRIS reduction index data revealed a more complex picture. That is, the data clearly showed that temperature (both season and temperature treatment) is a strong driver of soil reduction (Fig. 5.1b). However, against our first hypothesis warming effects were most pronounced in the top- and subsoil layers in the pioneer zone (Fig. 5.1c). Our second hypothesis stated that increases in reduction index (i.e. decreases in redox potential) would increase methanogenesis and methane emissions. Indeed, we found a significant increase of reduction index with warming in the pioneer zone subsoil, along with strong trends in topsoil in spring, while we simultaneously find a significant increase of methane emissions with warming in the pioneer zone in spring. The second hypothesis is further supported by the significant positive relationship between reduction index and methane fluxes (Fig. 5.2a), which demonstrates the fundamental coupling between redox conditions and methane dynamics in salt marshes. This relationship aligns with the established biogeochemical theory that low redox potentials favor methanogenic over methanotrophic processes (Hirano et al. 2013).

This interpretation is supported by the functional prediction analysis using Tax4Fun2, which revealed that the methanogenesis to methanotrophy ratio increased in moderate warming treatments (+1.5 °C) in the pioneer zone (Fig. 5.3b) and limited to the topsoil also in the strong warming treatment (+3.0 °C). Although these effects were not statistically significant, the trend mirrors the observed increase in methane fluxes (Fig. 5.2c) and aligns with evidence that even relatively small methanogenic populations can exert disproportionate functional activity (Cai et al. 2022).

Increasing methanogenic activity over methanotrophy can also be explained by the higher Q_{10} of methanogenesis (4.1) compared to methanotrophy (1.9) and sulfate reduction (1.6) (Segers 1998, Bodegom and Stams 1999). Mean ambient surface soil temperatures at our site range between 13.6 °C and 15.3 °C (Rich et al., 2023), which is below the temperature optima for methanogenesis of approximately 25-30 °C (Metje and Frenzel 2005, Conrad 2023). However, rapid increases of methanogenesis with warming have previously been reported for temperatures below the temperature optima (Arnosti et al. 1998, Yvon-Durocher et al. 2014). At our site, the stimulating effects of warming on methane fluxes were limited to the moderate temperature treatment of +1.5 °C (Fig. 5.2c), while the higher temperature increase of +3.0 °C did not lead to further increases compared to ambient conditions. Studies in other wetland ecosystems, including peatlands, have reported warming-driven increases in methanogenic potential and methane emissions (Hopple et al. 2020, Wilson et al. 2021). In contrast, research from low-salinity coastal wetlands has documented strong methane stimulation only at larger temperature increments (e.g. +5.1 °C; Noyce and Megonigal 2021, Noyce et al. 2023, Lee et al. 2025) highlighting that temperature responses of methane emissions vary across wetland types and salinity regimes.

This moderate warming effect in a salt marsh on methane cycling is surprising, since methanogenesis in salt marshes is expected to be suppressed due to competition from sulfate-reducing bacteria (SRB), which preferentially use hydrogen or acetate under high-sulfate conditions (Oremland and Polcin 1982, Poffenbarger et al. 2011). In fact, sequencing of putatively active microbes (rRNA transcripts) revealed a high abundance of sulfate reducing microbes (Fig. 5.S2). This makes the observed increase in methane fluxes in the pioneer zone especially interesting, since the pioneer zone is the most frequently flooded zone with high sulfate input (Rich et al. 2023). Some studies, however, suggest that methanogenesis can become more pronounced when sulfate is depleted more rapidly under elevated temperatures (Weston and Joye 2005, Noyce and Megonigal 2021). In this case, methanogenesis does not outcompete sulfate reduction directly, but rather becomes thermodynamically favorable once sulfate, the preferred electron acceptor, is exhausted. This temperature-driven shift has been described by Van Hulzen et al. (1999), who reported enhanced methanogenic activity following sulfate depletion under warmer conditions.

More recent studies show that the suppression of methanogenesis by sulfate reducers is not always of importance. Yuan et al. (2019) showed that the salt marsh plant *Spartina alterniflora* can increase methane production potential by providing non-competitive substrates (e.g., Trimethylamine), beneficial for methylotrophic methanogens. We argue, that *Spartina anglica,* the dominant species in the pioneer zone at our site, may provide similar substrates, that enable methanogenesis to respond to warming in the pioneer zone (Fig. 5.2c). This view is supported by a study from Kim et al. (2020b), who showed that *Spartina anglica* introduction stimulates methylotrophic methanogenesis. Additionally, this argument finds strong support in the abundance of methylotrophic methanogens (Methanosarcinaceae), in the soils of the pioneer zone (Fig. 5.4).

Methanosarcinaceae have been found to benefit strongly from the presence of *Spartina* (Yuan et al. 2019). Both genera (*Methanosarcina and Methanococcoides*) found in our soils show an increase in abundance with the temperature treatments which aligns with the higher methane fluxes under elevated temperature treatments (Fig. 5.2c). Incubation studies have previously associated *Methanococcoides* with methane emissions from coastal sediments (Dong et al. 2024). Interestingly, some methylotrophic methanogens were found exclusively in the +3.0°C warmed plots of the pioneer zone (Fig. 5.4).

While the significant positive relationship between root ingrowth biomass and soil reduction index (Fig. 5.S3) supports this mechanistic link, it cannot fully explain the warming-induced increase in methane fluxes. This is consistent with previous findings from this site showing that belowground biomass does not respond strongly to warming (Menzel et al. 2025). Nevertheless, the dominance of *Spartina* in the pioneer zone and its capacity to release methylated compounds aligns with the observed increase in methylotrophic methanogens and methane fluxes under warming, suggesting that plant-mediated substrate supply plays an important role in regulating methane emissions in this zone.

However, we find a strong positive relationship between the ratio of methanogenic to methanotrophic microbial processes and reduction index (Fig. 5.3a). Although not statistically significant, the observed differences in this ratio (Fig. 5.3b) between temperature treatments suggest that warming effects on soil redox conditions and methane fluxes are predominantly microbially driven, likely because reductive processes show greater temperature sensitivity than oxidative processes (Bullock et al. 2013, Lee et al. 2025). Finally, we stress that this study did not measure rates of methanogenesis or methanotrophy, and therefore does not provide direct links between microbial activity and methane fluxes. To get a deeper understanding on warming effects on these rates and their interactions with microbial activity and methane fluxes, these processes should be addressed simultaneously in future studies.

5.6 | CONCLUSION

Taken together, our findings highlight that salt marsh methane dynamics are responsive to warming. The results provide evidence that microbe–soil redox interactions, rather than plant-mediated effects, are the dominant drivers of warming responses of land-atmosphere methane fluxes in minerogenic marshes. Importantly, the results underscore that even under sulfate-rich, tidally influenced conditions, methanogenesis can be stimulated by moderate warming.

Our study shows that warming alters redox dynamics and methane cycling in salt marsh soils, with effects varying across seasons, zones and soil depths. While high marsh soils confirmed our first hypothesis of reduced soil redox potentials under warming, the reduction index revealed the strongest warming effects in the pioneer zone, where moderate warming (+1.5 °C) also significantly

increased methane fluxes. These responses suggest that methanogenesis can be stimulated even under high salinity and sulfate availability, likely due to the higher temperature sensitivity of reductive processes compared to oxidative ones and the activity of methylotrophic methanogens able to co-exist with sulfate-reducing bacteria.

5.7 | ACKNOWLEDGEMENTS

CrediT authorship contribution statement

Clarisse Goesele: Writing – original draft, formal analysis, data curation, investigation, conceptualization, visualization, methodology

Julian Mittmann-Goetsch: Writing – original draft, formal analysis, data curation, investigation, conceptualization, visualization, methodology

Viktoria Unger: Writing – review & editing, supervision, investigation, conceptualization, project administration

Kai Jensen: Funding acquisition, supervision, conceptualization, writing – review & editing, project administration

Susanne Liebner: Conceptualization, writing – review & editing, resources

Simon Thomsen: Methodology, writing – review & editing, project administration, methodology

Roy Rich: Methodology, writing – review & editing, project administration

Lars Kutzbach: Writing – review & editing, supervision, validation, conceptualization, methodology

Chen (Caroline) Cheng: Writing – review & editing, investigation

Alexander Bartholomäus: Formal analysis, writing – review & editing

Peter Mueller: Funding acquisition, supervision, conceptualization, writing – review & editing, project administration

Acknowledgments

We are grateful to Claudia Mählmann for her assistance with organizational matters. We also thank the Nationalpark Schleswig-Holsteinisches Wattenmeer for granting permission to conduct the MERIT research experiment at their site. Special thanks go to Anke Saborowski and Oliver Burckhardt for their laboratory support at GFZ Potsdam. We further thank Alexander Brodehl, Lia Ruhrus, Luka Hansen, Marvin Gothmann and Daniel Rohmaker for their help with field and laboratory work, as well as Dirk Granse, Tom Kamin, Jörn Ehlers, and Monica Salazar Ortiz for their contributions to the MERIT experiment. We acknowledge David Holl for the provision and technical support for the $CH_4/CO_2/H_2O$ Trace Gas Analyzer. We acknowledge Miriam Fuß and Norman Rüggen for their preparations of the automated redox system. We thank Mathis Drieu for

his support with redox data monitoring pipelines. We acknowledge financial support from the Open Access Publication Fund of Universität Hamburg.

Competing interests

The authors declare no conflict of interest.

Data availability

Data and code are available at https://github.com/JulianMiGoe/merit_response_repo. The raw sequencing data is publicly available on the European Nucleotide Archive (ENA) under project accession number PRJEB91652 (https://www.ebi.ac.uk/ena/browser/view/PRJEB91652)

Financial support

Clarisse Goesele was funded in the framework of the BMBF funded project sea4soCiety (project number 03F0896F). Julian Mittmann-Goetsch was funded by Fischer Stiftung (Stifterverband für die Deutsche Wissenschaft) within the SEAL-C junior research group. Clarisse Goesele and Julian Mittmann-Goetsch were funded by the Deutsche Forschungsgemeinschaft (DFG, German Research Foundation) within the Research Training Group (RTG) 2530 Biota-mediated effects on carbon cycling in estuaries (grant no. 407270017). Peter Mueller was funded by DFG via the Emmy Noether Program (502681570).

5.8 | SUPPLEMENT

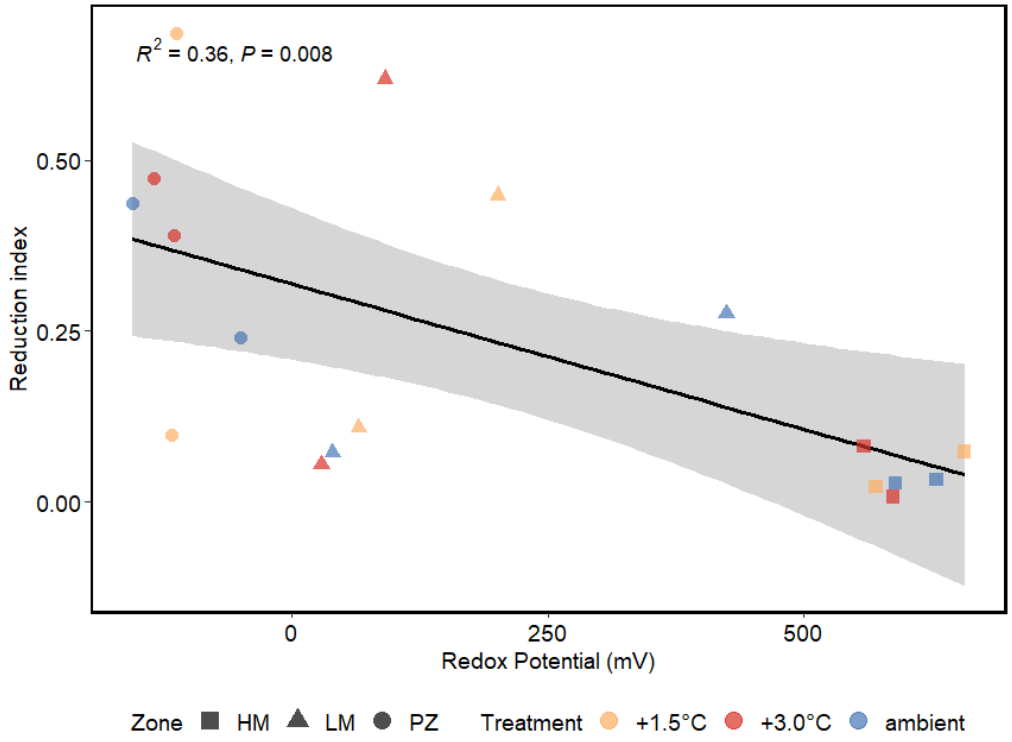

FIGURE 5.S1 | *Redox potential measurements from automated redox system and reduction index measurements from IRIS sticks campaigns in 2024.*

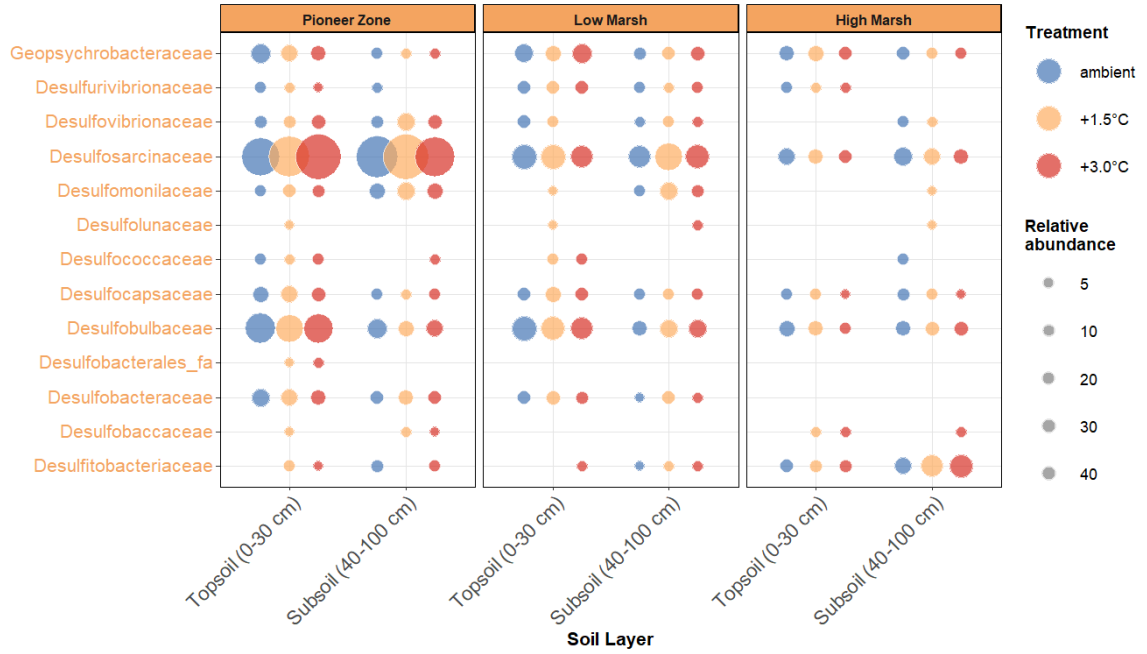

FIGURE 5.S2 | *Microbial community composition of sulfate reducing microbes, based on rRNA transcript sequencing. Shown are bubble plots with relative abundance of sulfate reducing microbes (Family level). Bubbles are shown for topsoil (0-30 cm) and subsoil (40-100 cm) samples and across the marine-terrestrial gradient (pioneer zone, low marsh, high marsh) and between the three temperature treatments (ambient, +1.5°C, +3.0°C). Sequencing data are shown on family level.*

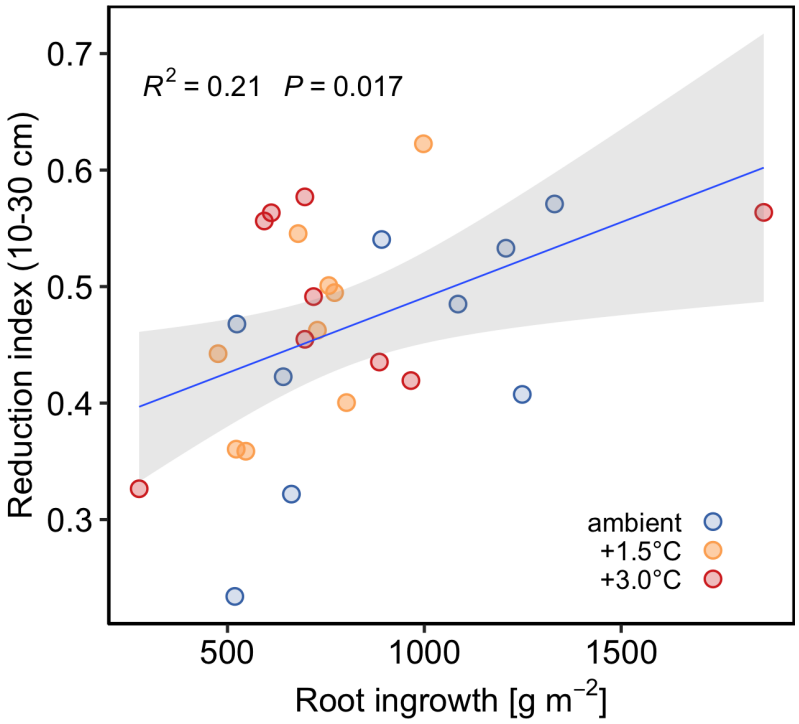

FIGURE 5.S3 | *Regression analysis with reduction index data from 2023 and ratio of methanogenic to methanotrophic microbial processes, as assessed via 16S Sequencing of rRNA transcripts in 2022.*

BOX B | HIDDEN METHANE OXIDATION WITHIN WETLAND PLANT TISSUES

Clarisse Goesele & Julian Mittmann-Goetsch, Lena Hessler, Cheng (Caroline) Chen, Viktoria Unger, Kai Jensen, Susanne Liebner, Peter Mueller, and Jana Träumer – *In preperation*

BB.1 | INTRODUCTION

Coastal marshes are important components of the global carbon cycle, acting as long-term carbon sinks (Temmink et al. 2022) while also emitting methane (Rosentreter et al. 2021a, Rosentreter et al. 2021b). Net methane fluxes are ultimately an equilibrium product of methanogenesis (acetoclastic, hydrogenotrophic and methylotrophic) and methanotrophy (Segers 1998, Parmentier et al. 2011, Capooci et al. 2024). Methane oxidation (methanotrophy) in soils is globally widespread, contributing about 5–10% to the atmospheric methane sink (Saunois et al. 2020, Davidson et al. 2024). Aerobic methanotrophy is also well documented in terrestrial and freshwater ecosystems, including strong plant-associated methane oxidation in *Sphagnum* and brown-mosses where endophytic methanotrophs can reduce emissions by up to 35% (Raghoebarsing et al. 2005, Liebner et al. 2011, Parmentier et al. 2011). Methanotrophic microbes have also been found in tree-barks, where they effectively reduce methane emissions (Jeffrey et al. 2021). Other studies report that tree stems can also be the source of methane emissions, providing habitats for methanogenic archaea (Covey and Megonigal 2019, Barba et al. 2024). While soil methane production and consumption pathways in coastal wetlands have been widely examined (Keshta et al. 2023, Chen et al. 2024), endophytic methane cycling has received far less attention. *Spartina* roots have been found to be inhabited by endophytic sulfate reducing microbes (Rolando et al. 2022), however there is no evidence of methanotrophic or methanogenic bacteria and archaea in salt marsh plant tissues. Improving our understanding of methane-cycling microbes in coastal marsh plants is therefore essential for accurately assessing their contribution to greenhouse gas dynamics and predicting ecosystem responses to future environmental change.

Notably, coastal marsh methane dynamics are also governed by tidal water fluctuations that impose rapidly shifting redox conditions. These alternating oxic–anoxic phases influence methane cycling in soils (Cui et al. 2024), raising the question if endopyhtic methane-cycling microbes respond with changes in abundance under such fluctuating conditions.

To investigate the potential role of plant biomass as a location for methane cycling under fluctuating redox regimes, we conducted a three-tier tidal-mesocosm experiment using two characteristic marsh species, *Spartina anglica* and *Elymus athericus* grown under tidally controlled oxic, semi-anoxic, and anoxic conditions. Specifically, we (1) measured methane fluxes using two chambers applied sequentially: the first enclosing the entire plant-soil system, and the second enclosing only

the aboveground biomass to isolate plant methane fluxes, (2) assessed methane oxidation potential of plant tissues in laboratory incubations, and (3) quantified methanotrophic and methanogenic gene abundance in bulk soil, roots, stems, and leaves.

BB.2 | MATERIAL & METHODS

S. anglica and *E. athericus* plants were collected from a salt marsh site at Hamburger Hallig (54°60'21.53" N, 8°81'66.29" E) in September, 2024. Plants were planted in homogenized soil from this salt marsh mudflats. Plants were cultivated in a full-factorial mesocosm setup including plots planted with either *S. anglica*, *E. athericus*, or left as bare soil as unplanted controls, each exposed to three redox treatments (oxic, semi-anoxic, anoxic; Fig. BB.1). Each species and redox combination was replicated three times (18 mesocosms total). Plants were grown under oxic, semi-anoxic, or anoxic (i.e. waterlogged, semi-waterlogged, or dry) soil conditions for two months in a greenhouse at the Institute of Plant Science and Microbiology, University of Hamburg. Three weeks before the greenhouse gas measurement campaigns, plants were transplanted into microcosms (16 cm diameter × 20 cm depth). Tidally fluctuating water levels were activated two weeks before the start of the measurement campaign. Microcosms were maintained under their assigned redox treatment, which were confirmed with continuous soil-redox potentials measurements, prior to the experiment (Fig. BB.S1). Pt-tipped electrodes and a 3M KCl reference electrode, connected to a combination of CR1000X Data loggers (Campbell Scientific, USA), and AM 16/32 Multiplexer (Campbell Scientific, USA) were used. Redox potentials were averaged across the three measurement depths (5, 10, 20 cm). Redox potentials were corrected for the standard hydrogen electrode by adding +207 mV (Mansfeldt 2003). Salinity was controlled by adding synthetic sea salt to reach a salinity of ~10 PSU.

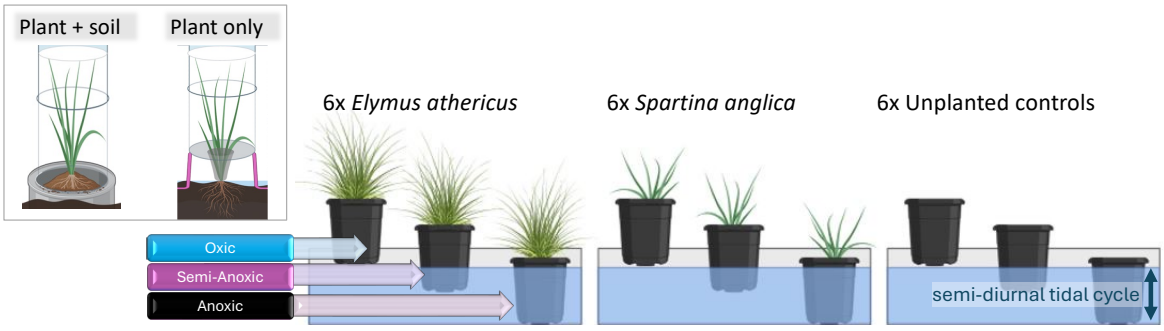

***FIGURE BB.1** | Schematic overview of the full-factorial mesocosm setup and chamber designs. The experiment comprised three planting treatments (Spartina anglica, Elymus athericus, unplanted controls), randomly assigned across three basins (100 cm × 60 cm × 40 cm). Each basin contained three elevational steps that created distinct redox environments (oxic, semi-anoxic, anoxic). Each planting treatment was duplicated at each elevation, resulting in N = 18 pots. A semi-diurnal tidal cycle was generated using pumps controlled by an automated unit. Two chamber designs were used: one enclosing the entire plant–soil system ("plant + soil") and one enclosing only the aboveground biomass ("plant only") to isolate plant-mediated methane fluxes.*

Methane fluxes were measured in November and December 2024. Two closed chamber types were used and applied sequentially on each mesocosm:

(1) plant and soil measurements: a 20 or 40 cm (height depending on vegetation) transparent acrylic glass chamber was placed over both plant and soil, followed immediately by
(2) plant only measurements: a 30cm transparent acrylic glass chamber positioned to enclose only the aboveground biomass of the same mesocosm (Fig. BB.1).

Methane concentration changes over time inside each chamber headspace were recorded over 3 minutes using a portable laser-based trace-gas analyzer (ABB GLA131 Series Microportable Analyzer, ABB Inc., Canada). Fluxes were derived from the linear change in headspace concentration over time (see Box A for detailed flux analysis).

Finally, plant and soil material was destructively harvested after flux measurements were done. Fresh plant stems and leaves (≥2.5 g) were harvested for headspace incubation experiment where methane uptake from aboveground plant tissues was quantified. Plant materials were immediately sealed in headspace bottles and then injected with 1.0 mL CH_4; on day 4 bottles were vented and reinjected with 1.5 mL CH_4. Methane concentrations were measured over 11 days by extracting 350 µL headspace gas per sample and analyzing 250 µL aliquots by gas chromatography (Agilent 7890A GC System). Mesocosm plant samples from roots, stems and leaves were carefully separated using a sterile blade. All compartments were washed, to sterilize surfaces following (Zhang et al. 2019).

Genomic DNA was extracted from soil and plant samples using the NucleoSpin® Soil Kit (Macherey-Nagel, Germany) following manufacturer instructions, with adaptations for plant tissues and modified centrifugation and elution steps. Eluates were stored at -20 °C. Plasmid DNA containing target genes (*pmoA, mcrA*) was isolated from transformed E. coli DH5α strains using the Presto™ Mini Plasmid Kit (Geneaid, Taiwan), with similar modifications applied, and stored at -20 °C. Quantitative PCR (qPCR) was performed to quantify methanotrophic (*pmoA*) and methanogenic (*mcrA*) microbes using specific primers A189f/mb661 (Auman et al. 2000) and mlas-F/mcrA-rev (Steinberg and Regan 2008). Plasmids carrying 16S rRNA gene sequences were cloned and serially diluted to provide standards for absolute quantification. DNA concentrations were measured with a NanoDrop spectrophotometer (Thermo Scientific, USA). qPCR reactions were conducted in 10 µL volumes using SYBR Green master mix (5 µL SYBR Green Master Mix, 0.25 µL forward primer, 0.25 µL reverse primer, 3.5 µL distilled water, 1 µL DNA template) on a CFX96 Touch Real-Time PCR Detection System (Bio-Rad, USA). The qPCR program consisted of an initial denaturation (98 °C, 180 s), followed by 40 cycles of 95 °C (15 s), 60 °C (30 s), and 72 °C (30 s), and a final melt curve from 65 °C to 94 °C at 0.56 °C s^{-1}.

BB.3 | STATISTICAL ANALYSIS

To directly quantify the contribution of plant emissions to methane exchange, ΔCH_4 fluxes for each mesocosm as the difference between plant-only and whole plant–soil flux measurements (CH_{4plant} – $CH_{4plant+soil}$) were calculated. These Δ values were then used to test whether plant-only fluxes differed from whole-system fluxes, and whether this effect varied between species. Non-parametric tests were used, since the flux data were not normally distributed. Pairwise Wilcoxon rank-sum tests with Benjamini–Hochberg (FDR) correction were used to compare ΔCH_4 fluxes among redox treatments.

Linear regressions were calculated to test for the effect of incubation time on the methane concentration in the incubation experiment.

Two-way ANOVAs were calculated to test for differences in gene abundance of target genes (*pmoA*, *mcrA*) between planting treatments (*S. anglica*, *E. athericus*, unplanted control) and location (soil, root, stem, leaf). Tukeys HSD test was used for pairwise comparison following significant ANOVA tests. Homogeneity of variance was confirmed using Levene test ($p > 0.05$) prior to the ANOVA calculations.

BB.4 | RESULTS & DISCUSSION

The ΔCH_4 fluxes showed that enclosing only the plant generally reduced methane emissions relative to plant–soil measurements (Table BB.1). *S. anglica*, exhibited significant negative ΔCH_4 values across all redox treatments, indicating consistent plant-associated methane oxidation. In *E. athericus*, ΔCH_4 values were significantly negative under anoxic conditions, while oxic mesocosms showed a clear but non-significant negative trend and semi-anoxic conditions showed little effect (Fig. BB.1).

***TABLE BB.1** | One-sample Wilcoxon tests for ΔCH_4 (H_0: $\Delta = 0$) within the two species Elymus athericus and Spartina anglica and the three redox treatments (oxic, semi-oxic, anoxic).*

Species	Redox treatment	n	*p*-value
Elymus athericus	oxic	10	0.064
Elymus athericus	semi-anoxic	10	0.375
Elymus athericus	**anoxic**	**10**	**0.005**
Spartina anglica	**oxic**	**10**	**0.002**
Spartina anglica	**semi-anoxic**	**10**	**0.002**
Spartina anglica	**anoxic**	**10**	**0.004**

The magnitude of ΔCH_4 differed between species: *S. anglica* indicated significantly higher plant driven methane consumption than *E. athericus* (Wilcoxon rank-sum test, W = 820, $p < 0.001$). In contrast, ΔCH_4 did not differ significantly between redox treatments (all FDR-corrected $p > 0.05$),

indicating that species identity, rather than background soil redox conditions, were the primary driver of variation in ΔCH_4. Although treatment differences were not statistically significant, the oxic mesocosms showed the smallest plant-driven reduction in methane flux - a pattern consistent with lower methane production under oxic conditions, which inherently limits the methane available for microbial oxidation.

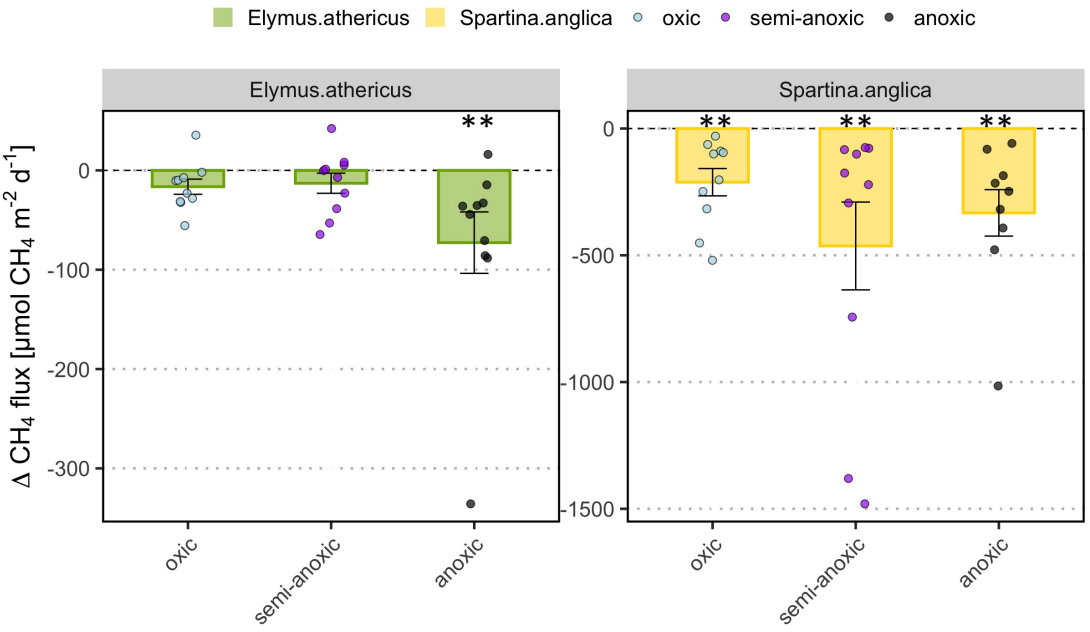

FIGURE BB.2 *| ΔCH_4 for E. athericus and S. anglica under oxic, semi-anoxic, and anoxic conditions. Jittered points represent individual mesocosm measurements (n = 10 per species × treatment). Bars indicate median values with interquartile ranges. Asterisks mark significant differences from zero within species and treatments (one-sample Wilcoxon tests; Table BB.1) and significant species-level differences (Wilcoxon rank-sum test). Significance levels: p < 0.05 *; p < 0.01 **; p < 0.001 ***.*

The incubation experiment supported the flux-based findings. With initial methane levels standardized to 100 %, methane decreased by ~10 % in both *S. anglica* and *E. athericus* over 11 days. Linear regressions per species and treatment confirmed significant methane decreases in both species, at similar rates between the oxic and semi-anoxic treatment while the anoxic treatment showed the steepest slope (Fig. BB.3). These results demonstrate that plant tissues harbor active methane-oxidizing microbes.

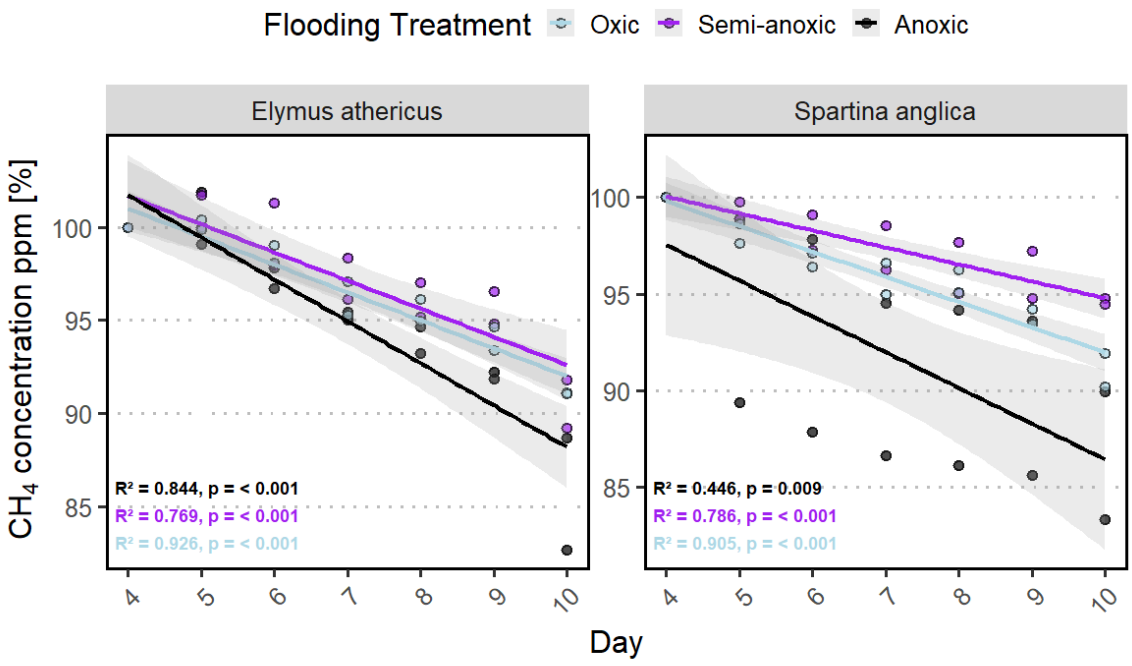

***FIGURE BB.3** | Incubation experiment results are shown as simple linear regressions for both species S. anglica and E. athericus x treatments. Shown are days since equilibrium on the x-axis and methane concentration in parts per million on the y-axis. Initial methane concentration was calibrated to 100%.*

This functional activity was supported by the detection of methanotrophic (*pmoA*) and methanogenic (*mcrA*) genes in all plant compartments from both species, roots, stems, and leaves - as well as in bulk soil for both species (Fig. BB.4). These patterns confirm that methanotrophic and methanogenic microbes in salt marshes are not limited to soils but also occur within plant tissues.

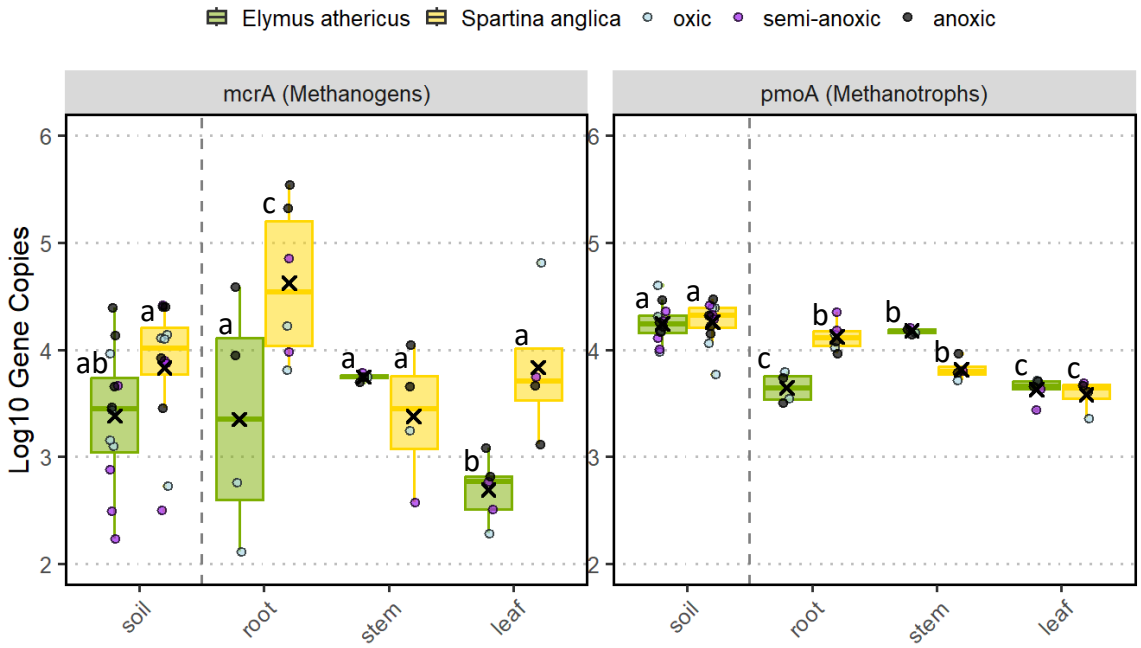

***FIGURE BB.4** | Results from qPCR are shown as Log_{10} gene copies per g fresh weight for methanogens (mcrA) and methanotrops (pmoA) in soil samples and three compartments (root, stem, leaf) of two planting treatments (S. anglica, E. athericus). Gene copies are shown as boxplots, with colored lines indicating median values and black "x" mean values. Significant differences in gene abundance between species and soil and plant compartments are indicated with letters based on Tukey HSD pairwise comparison ($p < 0.05$).*

Importantly, because methanotrophic microbes were detected in both soils and plants, while methane reductions occurred predominantly in plant-only chamber measurements (Fig. BB.S2), this provides strong evidence that methane uptake is primarily driven by microbes residing within the plant tissues. This conclusion is consistent with findings from terrestrial and freshwater systems, that showed methane oxidation capacities related to plant-associated methanotrophic microbes (Liebner et al. 2011, Jeffrey et al. 2021).

Interestingly, the abundance of methanogenic microbes appears to be higher in plants grown under anoxic conditions, compared to the other treatments, while methanotrophic communities showed no such differences (Fig. BB.4). Still, methane oxidation seems to be accelerated in plants grown under anoxic conditions, as indicated by their higher methane uptake relative to oxic treatments (Fig. BB.2, Fig. BB.3). This suggests that methanotrophic microbes may increase methane oxidation rates in response to increased methanogenesis, since methanotrophy is mainly methane limited (Megonigal and Schlesinger 2002). Therefore, plant-associated methane oxidation capacity appears to adapt to soil redox conditions, suggesting that methanotrophic activity within plant tissues may buffer methane emissions even under fluctuating tidal and oxygen regimes typical of coastal marsh ecosystems.

Taken together, this study identifies a previously undocumented plant-associated methane sink in salt marsh vegetation. This novel insight not only advances our understanding of methane cycling in coastal wetlands but may also have broader relevance for other ecosystems with fluctuating water tables, such as peatlands (Evans et al. 2021).

BB.5 | SUPPLEMENT

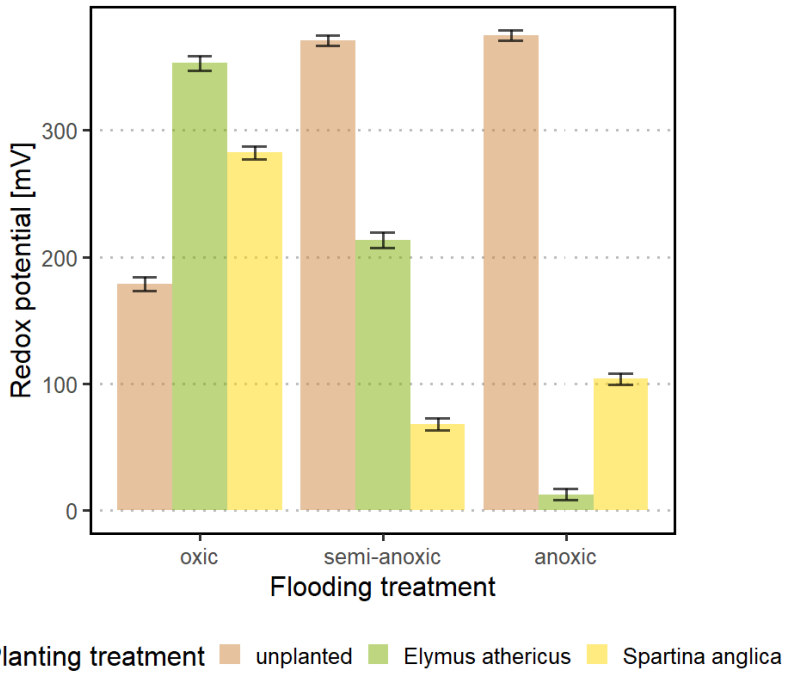

FIGURE BB.S1 | *Mean soil-redox potentials [mV] measured prior to the start of the mesocosm experiment to confirm the assigned redox treatments. Shown are mean redox potentials as bar plots by flooding x planting treatment. Error bars indicate standard error.*

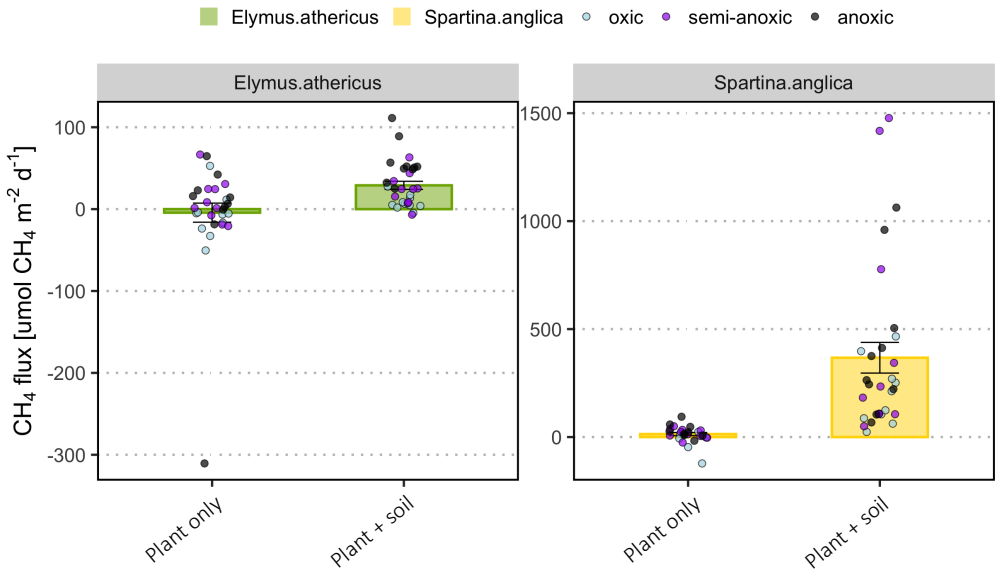

FIGURE BB.S3 | *All methane fluxes from E. athericus and S. anglica from both chambers ("plant only" and "plant + soil").*

BOX C | BALANCING R^2 AND RMSE AS FILTER CRITERION FOR QUALITY CONTROL OF METHANE FLUX ACROSS MAGNITUDES

Clarisse Goesele & Lars Kutzbach, *in preparation*

BC.1 | INTRODUCTION

Coastal marshes are increasingly recognized as important components of the global carbon cycle, functioning both as long-term carbon sinks (McLeod et al. 2011, Temmink et al. 2022) and as sources of greenhouse gases such as methane (CH_4) (Rosentreter et al. 2021a, Rosentreter et al. 2021b). Wetlands are the largest natural source of atmospheric methane, accounting for 4-6% of global land area while contributing up to 53% of global methane emissions (Rosentreter et al. 2021a, Rosentreter et al. 2021b). Methane is a greenhouse gas approximately 28 times more potent than carbon dioxide in a 100-year time frame (Neubauer and Megonigal 2015, Saunois et al. 2020). Thus, even small changes in methane emission rates may be climate relevant. Reported methane fluxes from coastal marshes span a wide range, from net uptake to substantial emissions (–94 to 94,200 μmol CH_4 m^{-2} day^{-1}; Rosentreter et al. (2021a)), reflecting high spatiotemporal variability. This variability however is not only derived from site specific biogeochemical variations (Rosentreter et al. 2021a), but also from a large variety of regression models, methane flux quality control (QC), and filtering methods implemented by researchers (Jentzsch et al. 2025). Methane fluxes from chamber measurements are typically estimated as the slope of the change in gas concentration over the chamber-closure period, with corrections based on the ideal gas law to account for e.g. temperature, and chamber pressure. To minimize measurement artefacts and capture methane fluxes that most closely represent true, undisturbed conditions, several best-practice guidelines for non-steady-state chamber measurements have been published (e.g. Pavelka et al. (2018), Fiedler et al. (2022), Maier et al. (2022), Jentzsch et al. (2025)). These guidelines emphasize key aspects of chamber design and operational setup, flux calculation, as well as recommendations for flux model selection. Jentzsch et al. (2025) found that the recommended chamber equipment and methane flux calculation are widely adopted and researchers modify the flux evaluation procedure mainly by selecting different fitting functions to describe the concentration-time relationship (see examples in Maier et al. (2022)). Many flux estimation packages for R or MATLAB including model selection exist (Maier et al. 2022, Wilson et al. 2024), however, as flux QC filtering criteria, most scripts and studies rely primarily on the coefficient of determination (R^2) as the dominant quality criterion (Jentzsch et al. 2025).

Reliance on any single metric, however, can be problematic: Using R^2 as a filter criterion discriminates against low fluxes, which have a lower signal-to-noise ratio. On the other hand, using

RMSE as filter criterion might discriminate against high fluxes, since the unexplained variance around the concentration-over-time trends often scales positively with the flux magnitude. As a result, inconsistencies in flux QC and filtering affect comparability across studies and contribute to persistent uncertainty regarding methane emissions from coastal marshes (Fiedler et al. 2022).

To address this methodological challenge, we propose a simple and transferable flux QC approach that uses a combination of R^2 and RMSE as filter criterion. We test this method using methane flux data from two contrasting coastal marsh types: polyhaline North Sea marshes, expected to exhibit low methane emissions, and mesohaline Baltic Sea marshes, where higher methane emissions are anticipated (Poffenbarger et al. 2011, Bridgham et al. 2013, Al-Haj and Fulweiler 2020).

BC.2 | MATERIAL & METHODS

Flux measurements & calculation

Flux measurements, by a closed chamber method, were conducted from March 2023 to October 2023 (N = 388). A flexible (i.e. height-adjustable) portable closed chamber (50 cm and 100 cm in height, depending on vegetation) as described by Yang et al. (2024), and permanently installed flux collars were used. Two types of portable laser-based trace-gas analyzers – a Micro Portable Greenhouse Gas Analyzer (ABB GLA131 Series Microportable Analyzers, ABB Inc. Measurement & Analytics, Quebec, Canada) (LGR) and a portable $CH_4/CO_2/H_2O$ Trace Gas Analyzer (LI-7810, LI-COR Environmental, Lincoln, NE, US) (LiCOR) – were used to quantify CH_4 concentration changes inside the chamber headspaces during 6-min flux measurements. The LiCOR measures at a precision of 0.6 ppb at 2 ppm with 1-second averaging (LI-COR-Environmental 2023) and the LGR measures at a precision of 0.9 ppb at 1-second averaging (Envicontrol 2023). The measurement ranges for methane were 0–100 ppm for both analyzers (Envicontrol 2023, LI-COR-Environmental 2023).

Methane fluxes were derived from the linear change in chamber headspace gas concentration over time. Methane concentrations were recorded at 1-second intervals and regressed against time using ordinary least squares. Molar fluxes (μmol CH_4 m^{-2} d^{-1}) were calculated from the slope of the regression, accounting for chamber volume (m^3), footprint area (m^2), air temperature (K), and atmospheric pressure (Pa).

Flux QC and filtering

Flux quality was evaluated using the combined criterion based on the coefficient of determination (R^2) and the root mean square error (RMSE) of the concentration-time regression, adapted from Kutzbach et al. (2007) (Fig. BC.1). Fluxes were accepted if either:

1. RMSE <= 5 ppb, and/or
2. R^2 >= 0.85.

The 0.85 R^2 threshold was selected in accordance with (Jentzsch et al. 2025). The RMSE threshold was not set to factory-specified accuracy values since these reflect bench-top performance and were not achievable under in situ field conditions. Instead, the RMSE threshold at 5 ppb was visually selected by plotting the RMSE against the methane flux (Fig. BC.S1).

The complete flux calculation and flux quality control workflow will be made available on GitHub upon request.

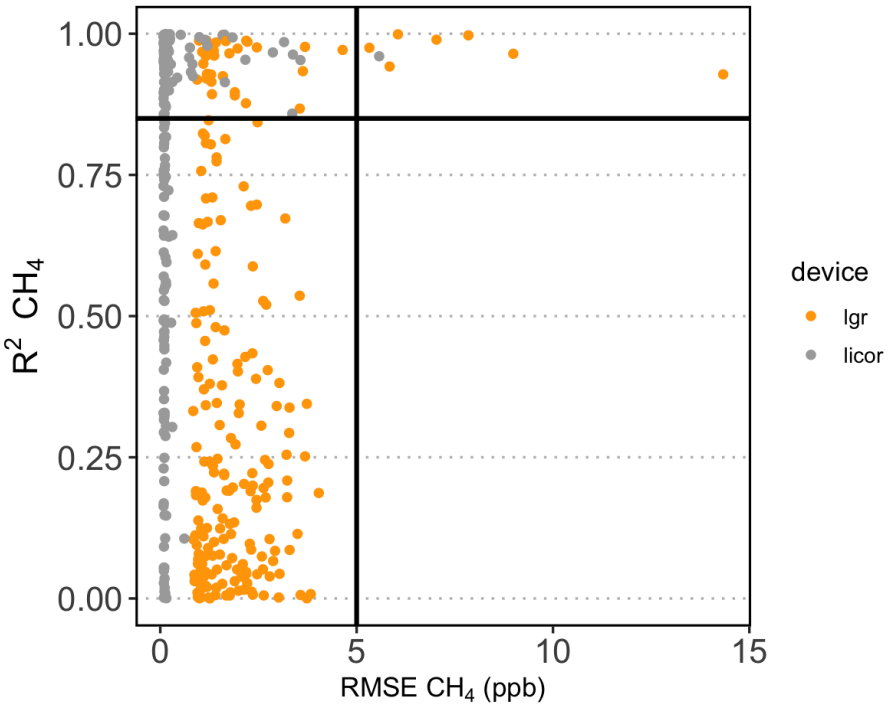

***FIGURE BC.1** | Combination of R^2 and RMSE as criteria for flux quality control of linear regression results. Methane flux measurements were considered acceptable if either the RMSE of the linear regression of the concentration-over-time-data was below the threshold of 5 ppb or the R^2 was above 0.85. Figure was adapted from Kutzbach et al. (2007).*

BC.3 | STATISTICAL ANALYSIS

For each device, differences in mean methane fluxes among the three filtering methods (R^2 filter, RMSE filter, combined filter) were calculated and tested using one-way ANOVA, followed by Tukey pairwise comparisons where applicable. All data analyses were conducted in R (version 4.5.0 (2025-04-11)).

BC.4 | RESULTS & DISCUSSION

Mean methane fluxes across all measurements were (mean ± SE) 69.85 ± 13.10 µmol CH_4 m^{-2} d^{-1} (SD: 256.43), ranging from −289.12 to 2908.02 µmol CH_4 m^{-2} d^{-1}. Using the combined RMSE–R^2 filter approach retained 100% of the fluxes for both devices, resulting in mean fluxes of 88.17 µmol

CH_4 m^{-2} d^{-1} for the LGR and 47.98 µmol CH_4 m^{-2} d^{-1} for the LiCOR (Tab. BC.1). In contrast, using the R^2 threshold alone would have retained only 18% of the LGR dataset and 55% of the LiCOR dataset, both yielding the highest mean methane fluxes (446.57 µmol CH_4 m^{-2} d^{-1} for the LGR and 86.70 µmol CH_4 m^{-2} d^{-1} for the LiCOR; Tab. BC.1). Applying only the RMSE filter would have retained 97 % of LGR fluxes and 99 % of LiCOR fluxes, with corresponding mean fluxes of 44.06 and 44.47 µmol CH_4 m^{-2} d^{-1}, respectively (Tab. BC.1).

***TABLE BC.1** | Numbers of the total amount of methane fluxes (total N), retained methane fluxes (retained N), retained amount in %, and the resulting mean methane fluxes (mean methane flux in µmol CH_4 m^{-2} d^{-1}) for each filtering method (R^2 filter, RMSE filter, combined filter) applied to the LGR and LiCOR dataset respectively. Filtering thresholds are R^2 >= 0.85 and RMSE <= 5ppb.*

Device	Filter method	Total N	Retained N	Retained %	mean CH_4 flux
LGR	R^2 filter	208	37	18	446.57
LGR	RMSE filter	208	202	97	44.06
LGR	combined filter	208	208	100	88.17
LiCOR	R^2 filter	175	96	55	86.70
LiCOR	RMSE filter	175	174	99	44.47
LiCOR	combined filter	175	175	100	47.98

For the LGR dataset, ANOVA pairwise contrasts showed significant differences in mean methane fluxes (µmol CH_4 m^{-2} d^{-1}) between the combined filter and the R^2 filter ($p < 0.001$), and between the R^2 and RMSE filter ($p < 0.001$), while no significant difference was found between the combined and RMSE filter (p = 0.33; Fig. BC.2). For the LiCOR dataset, significant differences were detected only between the R^2 and RMSE filter ($p = 0.04$), whereas all other contrasts were non-significant (Fig. BC.2).

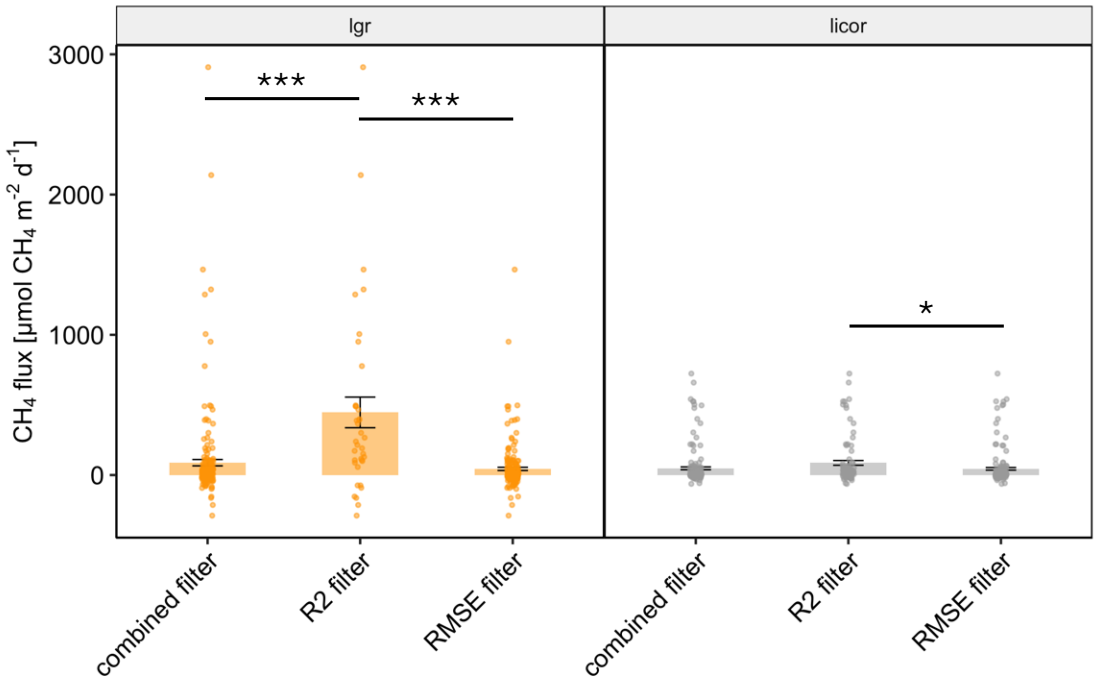

FIGURE BC.2 | *Differences in methane fluxes (µmol CH_4 m^{-2} d^{-1}) between the three filtering methods (R^2 filter, RMSE filter, combined filter), for the LGR and the LiCOR respectively. Significant differences between filtering methods within each device are indicated with stars based on Tukey HSD pairwise comparison. Significance levels: p < 0.05 *; p < 0.01 **; p < 0.001 ***.*

These differences in mean methane fluxes (Fig. BC.2) highlight that using either R^2 or RMSE alone as a filter criterion in methane flux quality control introduces strong differences in mean methane fluxes. R^2 filters out low fluxes, while RMSE discriminates against higher fluxes (Tab. BC.1). The combined filtering criterion reduces these systematic biases and provides a more balanced assessment across the full range of observed methane flux magnitudes.

While establishing standardized R^2 and RMSE threshold combinations could improve comparability, such thresholds must be set for analyzer models individually, as indicated by the differences between LGR and LiCOR used for this present study (Fig. BC.2). In line with this, Waldo et al. (2019) applied a combination of a substantially higher RMSE threshold of 500 ppb and a higher R^2 threshold of 0.9 for mesocosm methane fluxes. These fluxes were measured with both, a Los Gatos Research Ultraportable Greenhouse Gas Analyzer and a Picarro G2201-I CRDS, further highlighting the need for instrument-specific and context-dependent, i.e. dataset-specific R^2 and RMSE limits.

Further, the applied combination of filter criterions in flux QC ensures that the usage of different devices in generating a single dataset becomes more comparable because thresholds can be set to devices specifically.

Although linear regressions were used in the present methane flux analysis, the proposed filtering approach is not restricted to linear models. The combined filter criterion can be applied to non-linear fits and extended to other trace gases, such as CO_2 or N_2O, making it widely transferable.

Overall, the combined RMSE-R^2 filtering method reduces bias toward high fluxes and ensures that low or near-zero fluxes are not arbitrarily discarded or replaced with minimum detectable flux values (Fiedler et al. 2022). Preserving this information from close to zero, low fluxes is essential for accurately capturing ecosystem methane fluxes, both methane emissions and methane uptake. However, open questions remain, e.g. whether only fluxes with high R^2 values should be considered "accurate," or whether more nuanced, multi-metric approaches, such as the one presented here, are better suited for ecosystem-scale methane flux evaluation.

BC.5 | SUPPLEMENT

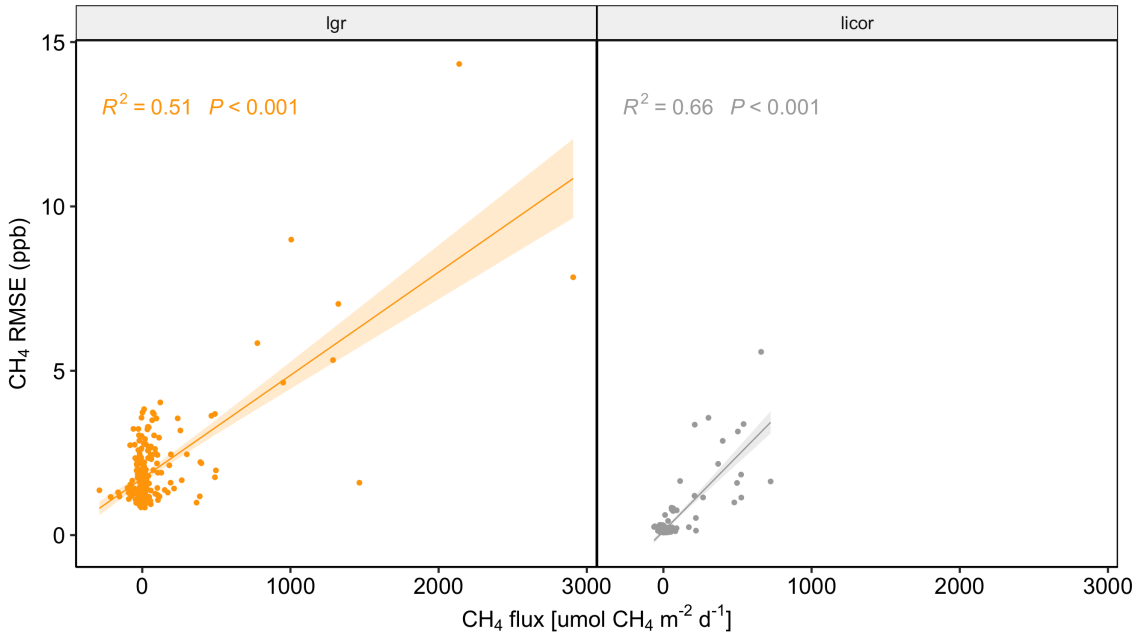

FIGURE BC.S1 | *Linear regression between methane flux RMSE (ppb) and methane fluxes (µmol CH_4 m^{-2} d^{-1}). With increasing methane fluxes, the RMSE increases for both devices (LGR: R^2 = 0.51, p < 0.001; LiCOR: R^2 = 0.66, p<0.001) and a threshold of 5ppb was chosen as filter criterion.*

CHAPTER SIX | SYNTHESIS

SYNTHESIS INTRODUCTION

Coastal marshes are vital ecosystems that play a role in climate regulation by sequestering and storing large amounts of carbon (McLeod et al. 2011, Lovelock and Duarte 2019, Macreadie et al. 2021). However, they have also been increasingly recognized as significant sources of greenhouse gases (Rosentreter et al. 2021a, Rosentreter et al. 2021b). The soils of coastal wetlands are typically reducing, as any oxygen entering the soil is rapidly depleted by aerobic microbial respiration during the degradation of SOM (Kristensen et al. 1995, Bailey-Serres and Voesenek 2008). These anoxic and reducing environments slow down SOM decomposition and promote carbon stabilization and long-term sequestration (Chmura et al. 2003, Keiluweit et al. 2017), but also favor the production and emission of methane (Segers 1998).

Wetland plants are central regulators of carbon processes in coastal marshes. Particularly their belowground activity through root litter inputs, root exudation, ROL and internal gas transport, has been identified as a key driver of soil biogeochemical processes (Hinsinger et al. 2006, Haviland and Noyce 2024, Määttä and Malhotra 2024, Mittmann-Goetsch et al. 2024). Contrary to the long-standing assumption that methane production in coastal wetlands primarily occurs in deeper, persistently anoxic soil layers, recent research demonstrates that methane can also be generated in anoxic microsites within the root zone, which are formed by plant-mediated root exudation of labile carbon compounds (LaCroix et al. 2019, Waldo et al. 2019, Haviland and Noyce 2024). However, species identity exerts a strong influence on plant-soil interactions, since wetland plants differ in their root traits, exudation rates, and the composition and relative abundance of compounds actively secreted or leaked by roots into the rhizosphere (Canarini et al. 2019, Ritter et al. 2025). These differences can lead to possibly contrasting effects on rhizosphere redox dynamics and microbial activity (Seitz et al. 2022). Despite growing evidence for such species-level differentiation, knowledge on the species-specific effects on methane emissions, and how these processes are soil-redox controlled, remains limited.

The species-specific nature of plant-soil interactions underscores that belowground processes are inherently context-dependent. In coastal wetlands, environmental gradients such as salinity, hydrology, and SOC content determine which plant species and therefore which root traits dominate a given site (Qiu et al. 2023, Li et al. 2025a). These patterns of plant community composition, in turn, define how soil-redox conditions and carbon turnover respond to global change pressures such as warming (Noyce and Megonigal 2021, Tang et al. 2023, Li et al. 2025b) and land use change (Tessier et al. 2003, Tang et al. 2020).

How plants mediate methane fluxes via soil-redox regulation is only scarcely represented broad-scale, i.e across environmental gradients (Määttä and Malhotra 2024). Furthermore, it remains unclear how plant communities and their functional traits respond to global change pressures, and how such responses may alter soil biogeochemical functioning and the overall carbon balance of

coastal marshes. Addressing these knowledge gaps is essential for predicting whether coastal marshes will maintain their role as carbon sinks or shift toward becoming net greenhouse gas sources under future environmental change.

To address these gaps, I established a conceptual framework built on the assumption that wetland plants regulate soil-redox conditions and thus processes of carbon turnover, specifically methane production, oxidation, and ultimately emission and uptake. In the following section, I (6.1) establish this conceptual framework – hereafter referred to as the root-redox-methane framework. The validity of this framework is then (6.2) assessed under current environmental conditions and (6.3) the global change pressures land-use change and (6.4) global warming. Finally, I close this synthesis with (6.5) an integrated synthesis of the root-redox-methane framework and (6.6) a discussion of its limitations and future research perspectives.

KEY FINDINGS

Chapter 2 Soil Organic Carbon Stocks of German Salt Marshes: A Comparative Study Along Low-and High-Energy Coastlines

I found that, both marshes store comparable amounts of SOC to a depth of one meter. However, their contrasting environmental settings – microtidal Baltic Sea marshes versus mesotidal North Sea marshes – resulted in higher SOC accumulation in Baltic topsoils (30 cm), likely due to sediment dynamics causing SOC dilution in the North Sea marshes. I found positive effects of livestock grazing on topsoil SOC in North Sea marshes, most likely driven by trampling-induced changes in soil biogeochemistry. In contrast, grazing effects were more variable in Baltic Sea marshes, with belowground plant productivity emerging as the primary driver of SOC dynamics. This highlights the important role of plant-soil interactions, mediated through plant productivity, in shaping carbon storage along these coasts.

Chapter 3 Redox controls exudate-derived carbon stability in coastal wetland soils

In Chapter 3, I demonstrated that root exudates, from both species, can persist under continuously anoxic and therefore reducing soil-redox states, while fluctuations between oxic and anoxic conditions promoted their mineralization. These findings provide novel insights into how background soil-redox states govern plant-soil carbon dynamics and contribute to organic carbon stabilization in coastal wetlands.

Box A Species identity and redox state determine root exudate effects on methane production in coastal wetland soils

Box A provides brief insights into methane production from root exudates. I found that the persistence of root exudates under continuously reducing soil redox conditions fueled methane production, yet this effect was species-specific: only *S. anglica* exudates stimulated methane production, while *E. athericus* exudates did not. Importantly, neither species' exudates fueled methane production under fluctuating soil-redox conditions. These results demonstrate that both plant species identity and background soil-redox state critically influence methane cycling in coastal marsh soils.

Chapter 4 Vegetation control on soil redox determines grazing effects on methane emissions from coastal marshes

I found that plant-mediated changes in soil-redox conditions played a central role in regulating methane emissions in grazed and ungrazed areas of coastal marshes. While livestock grazing tended to reduce methane emissions on average, the overall effect was not significant due to high variability among sites. This variation was linked to site-specific and species-specific responses in

belowground biomass, SOC, and soil redox potential. Correlations between belowground biomass, SOC, soil redox potential, and methane fluxes indicated that grazing altered methane emissions primarily by influencing plant-mediated soil redox processes through changes in root biomass.

Chapter 5 Warming stimulates soil reduction and methane production in salt marshes

Warming effects on redox potential were most pronounced in the high marsh, while the reduction index responded most in the pioneer zone, where warming increased methane emissions; simultaneously, methane uptake decreased in the high marsh. Therefore, warming led to increased methane emissions despite only minor effects on belowground biomass previously reported at this site (Menzel et al. 2025). I found that this increase was attributed to methanogenic archaea becoming more abundant in the lower elevation pioneer zone, while methanotrophic microbes declined in higher elevation zones. These findings suggest a higher temperature sensitivity of methanogenesis relative to methanotrophy, suggesting direct warming effects on methane production in anoxic salt marsh soils.

Box B Hidden methane oxidation within wetland plant tissues

I found that *S. anglica* and *E. athericus*, host both methanogenic and methanotrophic microbes within their plant tissues (leaves, stems and roots). Despite their coexistence, I found net methane uptake associated with plant tissues. Notably, this methane uptake capacity adjusts to soil-redox conditions, suggesting that methanotrophic activity within plant tissues helps buffer emissions under fluctuating tidal and oxygen regimes.

Box C Balancing R^2 and RMSE as filter criterion for quality control of methane flux across magnitudes

I found that using either R^2 or RMSE alone as a as a filter criterion in methane flux quality control introduces strong differences in mean methane fluxes. Each metric alone excludes different subsets of fluxes, whereas the combined criterion reduces these systematic biases to filtering out low (R^2) or high (RMSE) fluxes and provides a more balanced assessment across the full range of observed methane flux magnitudes.

6.1 | ESTABLISHING A ROOT-REDOX-METHANE FRAMEWORK FOR COASTAL MARSHES

Coastal marshes play a central role in the global carbon cycle, simultaneously acting as major carbon sinks (McLeod et al. 2011, Lovelock and Duarte 2019, Macreadie et al. 2021) but also as methane sources (Rosentreter et al. 2021a, Rosentreter et al. 2021b). However, methane emissions are highly variable across space and time, due to environmental characteristics such as salinity, hydrology, and SOC content (Poffenbarger et al. 2011, Arias-Ortiz et al. 2024, Cui et al. 2024) that independently and interactively shape microbial communities and soil-redox conditions. Plants further contribute to this variability because their overall performance and functional traits are strongly influenced by these same environmental conditions (Cui et al. 2024, Li et al. 2025a). Wetland plants have been shown to influence methane emissions from coastal marshes through their root traits, which include root litter inputs, root exudation, ROL, and internal gas transport (Määttä and Malhotra 2024, Girkin et al. 2025). These traits regulate soil-redox conditions in the root zone through alterations to microbial community dynamics. Through these root-redox interactions, plants shape the balance between methane production, oxidation, and ultimately emission (Waldo et al. 2019, Haviland and Noyce 2024).

Previous studies and meta-analyses have shown that methane emissions vary substantially with hydrology and salinity (Poffenbarger et al. 2011, Arias-Ortiz et al. 2024, Cui et al. 2024) but also with vegetation composition and patch structure (Bhullar et al. 2014, Stewart et al. 2024), indicating that both root-redox interactions and environmental controls on soil redox likely drive much of this spatial variability (Ge et al. 2025). However, no study has explicitly tested how root-redox interactions translate into methane production and emissions across contrasting environmental settings or global change pressures such as land-use change and global warming.

To advance the understanding of these uncertainties, the following synthesis tests the central assumption of the conceptual framework, that coastal marsh plants control soil-redox conditions and thereby regulate methane emissions across contrasting background redox conditions and under different global change pressures (land-use, warming). In the following subsections 6.1.1-6.1.5, I examine how species-specific plant functional traits, represented by belowground biomass and root exudation, relate to soil-redox conditions and eventually control carbon transformations and methane emissions from coastal marshes.

Using an extended dataset that combines the full methane flux dataset from Chapter 4, the ambient (non-warmed) data from Chapter 5, and measurements from an additional site (Fig. 6.1; Tab. 6.1), I assessed relationships between root traits, soil-redox conditions, and methane emissions. Details on methane flux measurements, plant trait and soil-redox parameter assessments (including the usage of soil redox potential and soil reduction index measurements) are provided in Chapters 4 and 5. Box C provides an overview of how I evaluated the wide range of fluxes, by balancing R^2 and RMSE, to ensure comparability across sites. This consolidated dataset forms the empirical basis

for evaluating the root-redox-methane framework and for examining its mechanisms under contrasting background conditions and global change pressures.

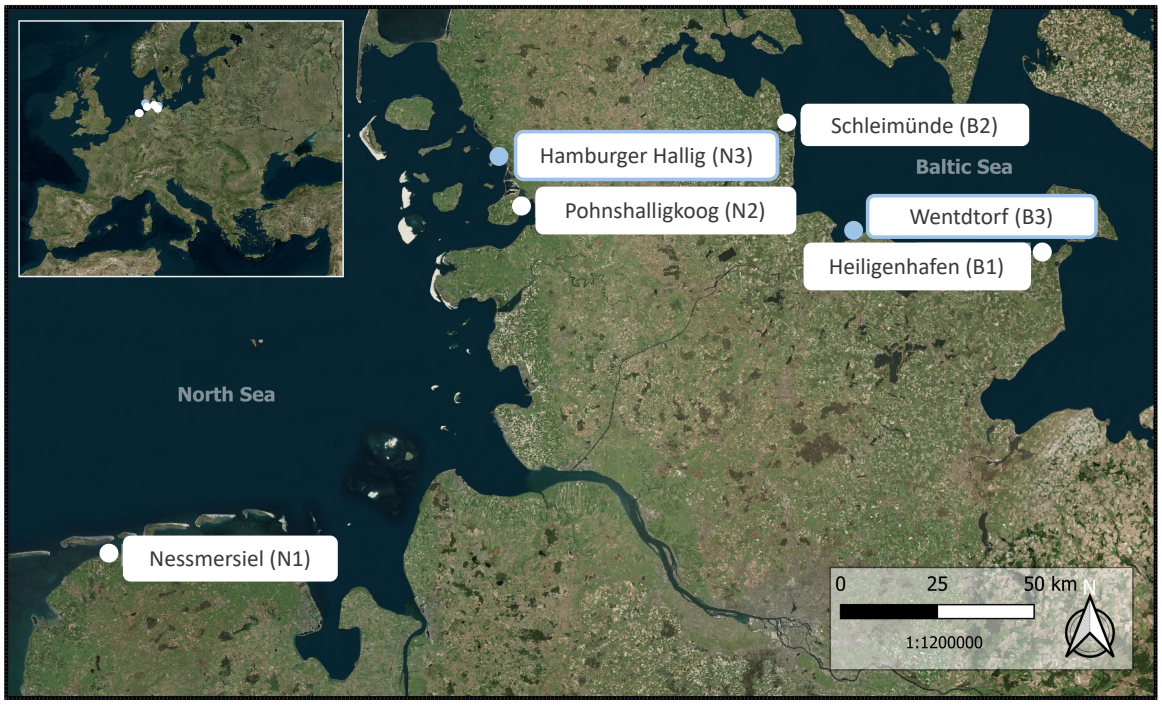

***FIGURE 6.1** | Overview of the six study sites across Northern Germany. Sites that were not included in Chapter 4 are highlighted in blue.*

***TABLE 6.1** | Site overview including their coastal region, management regime and number of plots sampled at each site.*

Coast	Site	Management	Number of plots
North Sea	Nessmersiel (N1)	grazed, ungrazed	10
North Sea	Pohnshalligkoog (N2)	grazed, ungrazed	10
North Sea	Hamburger Hallig (N3)	ungrazed	9
Baltic Sea	Heiligenhafen (B1)	grazed, ungrazed	10
Baltic Sea	Schleimünde (B2)	grazed, ungrazed	10
Baltic Sea	Wentdorf (B3)	ungrazed	3

6.1.1 | BACKGROUND SOIL-REDOX CONDITIONS CANNOT EXPLAIN METHANE FLUXES ALONE

To test whether environmental controls on soil redox alone can account for methane flux patterns I examined how key environmental variables relate to soil redox potential and methane fluxes. Soil redox potential was strongly correlated with salinity, soil moisture (measured as VWC (%)), and background SOC ($r = –0.56$, –0.56, and –0.47; all $p < 0.001$; Tab. 6.2) suggesting that all three parameters jointly influence soil-redox conditions.

***TABLE 6.2** | Pearson correlations coefficients (r), based on plot-level means, between methane fluxes and predictor variables: soil redox potential (mV), belowground biomass (kg m^{-2}), aboveground biomass (kg m^{-2}), SOC (%), salinity (PSU), and VWC (%). Significance levels: p < 0.05 *; p < 0.01 **; p < 0.001 ***.*

	CH_4 flux		Soil redox potential		Belowground biomass		Aboveground biomass	Soil organic carbon (SOC)		Salinity
Soil redox potential	**-0.48**	***								
Belowground biomass	**0.52**	***	**-0.59**	***						
Aboveground biomass	0.09		0.20		-0.16					
Soil organic carbon (SOC)	**0.42**	***	**-0.56**	***	**0.66**	***	-0.20			
Salinity	-0.24		**0.47**	*	**-0.58**	***	0.15	**-0.58**	***	
Volumetric water content	0.26		**-0.45**	*	**0.34**	*	-0.24	**0.30**	*	0.01

Sulfate concentration in seawater scales linearly with salinity and because sulfate is the thermodynamically favorable terminal electron acceptor under anaerobic conditions, methane emissions are generally expected to decrease with increasing salinity (King and Wiebe 1980, Poffenbarger et al. 2011, Bridgham et al. 2013, Davidson et al. 2021). However, neither salinity nor soil moisture were significantly correlated with methane fluxes (salinity: r = –0.24, p = 0.082; VWC: r = 0.26, p = 0.525). SOC, in contrast, was positively correlated with methane fluxes (r = 0.42, p < 0.001). This is not surprising because SOC is the substrate which is the precursor for methane production (Sha et al. 2011, Schlesinger and Bernhardt 2020).

In contrast to salinity and soil moisture, soil redox potential itself was significantly correlated with methane fluxes (r = –0.48, p < 0.001; Tab. 6.2). This indicates that while salinity, soil moisture, and SOC jointly define the background environmental controls on soil redox, they alone cannot account for the observed variation in methane fluxes (Al-Haj and Fulweiler 2020, Rosentreter et al. 2021b). Instead, root-redox interactions appear to locally modify soil-redox conditions within the broader environmental context (Fig. 6.3), implying that, plant roots can further modulate methane dynamics through their root-redox activity.

6.1.2 | ROOT-REDOX INTERACTIONS AS KEY REGULATORS OF METHANE FLUXES

The dual role of SOC becomes clearer when considering root controls on soil redox. The strong positive correlation between belowground biomass and SOC (r = 0.66, p < 0.001), together with the strong negative correlation between belowground biomass and soil redox potential (r = –0.59, p < 0.001), indicate a tight coupling between root-driven carbon turnover. In fact, belowground biomass was the strongest predictor for both soil redox potential (r = 0.59, p < 0.001) and methane fluxes (r = 0.52, p < 0.001), making root-derived carbon inputs a key driver of soil redox potentials and methane fluxes.

Mechanistically, higher belowground biomass, i.e. higher organic carbon inputs, reduce the soil redox potential by enhancing substrate availability for reduction reactions. This plant-derived organic carbon primarily takes the form of root litter and root exudates (Pan et al. 2024), which are known to stimulate microbial decomposition of SOM (Yarwood 2018). During decomposition, electrons released from organic carbon oxidation are transferred to terminal electron acceptors, linking oxidative and reductive processes within the rhizosphere. As soil conditions become increasingly reducing, the thermodynamic potential for redox reactions declines, slowing down aerobic microbial decomposition and thereby promoting the accumulation of soil organic carbon (Sutton-Grier et al. 2011, Keiluweit et al. 2017). Once terminal electron acceptors are exhausted, methanogenesis can become a dominant pathway, producing methane through acetoclastic, hydrogenotrophic, and/or methylotrophic pathways (Oremland et al. 1982). Methane can then diffuse or be transported through aerenchymatous tissues, which most wetland plants exhibit or develop under anoxic conditions, and be emitted via stems and leaves into the atmosphere (Dacey and Klug 1979, Armstrong et al. 2000, Vroom et al. 2022). In line with these mechanisms, previous studies have shown that higher belowground biomass increases SOC storage (Elsey-Quirk and Unger 2018) but also enhances microbial activity and methane production in wetland soils (Liu et al. 2019).

The strong correlations between belowground biomass and soil redox, and soil redox and methane flux thus demonstrate that root-driven shifts toward more reducing soil conditions promote methane emission, which form the conceptual basis of the framework presented here: plants regulate soil-redox conditions via root-redox interactions and thereby affect carbon transformations and methane emissions. Yet, the observed variability in the strength of the redox-methane correlation (Fig. 6.3a) implies that this root-redox control is not uniform, but contingent on plant species characteristics.

6.1.3 | SPECIES-SPECIFIC ROOT-REDOX INTERACTIONS AS A CONTROL OF METHANE FLUX

In Chapter 4 I identified plant species associated with either high methane emissions (“high-flux” species) or low methane emissions and methane uptake (“low-flux” species), based on a permutation test of the point-biserial correlation coefficient (De Cáceres and Legendre 2009) and the same classification was confirmed by reanalyzing the consolidated dataset (Tab. 6.3). A small group of “high-flux” plant species– *Phragmites australis*, *Tripolium pannonicum* (syn. *Aster tripolium*), and *Juncus maritimus* – were associated with generally high methane emissions. “Low-flux” species, defined as those not significantly assigned to the “high-flux” group, showed substantially lower methane emissions or methane uptake; species not clearly affiliated with either group were considered indifferent but were included within the “low-flux” category for the purposes of statistical analysis, though the indifferent category is recognized in the text. While several studies have documented increasing methane emissions associated with *P. australis* and *S.*

anglica (Mueller et al. 2016, van den Berg et al. 2020, Vroom et al. 2022, Fuchs et al. 2024), comparable research on other coastal marsh species remains limited.

***TABLE 6.3** | Plant species classification based on associated methane fluxes, derived from point-biserial correlation analyses using the consolidated dataset. Species significantly associated with high methane emissions are listed as "high-flux", while species not significantly associated with the "high-flux" group are treated as "low-flux" for the purposes of statistical analysis, though the indifferent category is recognized in the text.*

„High-flux" species	p-value	„Low-flux" species	p-value	Indifferent species ($p > 0.05$)
Phragmites australis	**0.005**	*Elymus athericus*	0.14	*Atriplex laciniata*
Tripolium pannonicum	**0.005**	*Atriplex portulacoides*	0.12	*Atriplex prostrata*
Juncus maritimus	**0.020**	*Limonium vulgare*	0.19	*Juncus geradii*
Plantago maritima	0.14	*Artemisia maritima*	0.31	*Puccinellia maritima*
Festuca rubra	0.14	*Glaux maritima*	0.36	*Salicornia europea*
Suaeda maritima	0.34			*Spartina anglica*
				Spergularia media
				Argentina anserina

Correlations between belowground biomass and soil redox potential demonstrate that, the root-redox relationship held true for both "high-flux" and "low-flux" species alike, since soil redox potential decreased significantly with increasing belowground biomass ("high-flux": r = -0.64, p = 0.019; "low-flux": r = -0.49, p = 0.0012; Fig. 6.2b). Notably, the correlation between belowground biomass and soil redox potential can act bidirectionally, reflecting both the influence of plant roots on soil redox potential and the environmental controls on soil redox, root traits and plant function. Generally, methane emissions increased as soil redox potential decreased ("high-flux": R^2 = 0.29, p = 0.059, "low-flux": R^2 = 0.12, p = 0.024; Fig. 6.2a), however, a root-redox controlled increase in methane fluxes showed predominantly, though not consistently, across sites where "high-flux" or indifferent species were dominant. This pattern indicates that these species can modulate the soil-redox conditions through their root-redox influence, at times overriding environmental controls on soil redox. In other words, plants growing under the same background soil-redox conditions can still create distinct soil-redox microenvironments through differences in their root-redox activity, resulting in contrasting methane emission patterns between species (Lacroix et al. 2025).

While the soil-redox metrics (soil redox potential and soil reduction index), discussed in this dissertation, alone could not disentangle whether soil-redox was primarily controlled by plant-driven or other environmental processes, the methane flux data provide indirect evidence for plant control: if environmental controls on soil redox were dominant, methane fluxes would not vary strongly between species within the same site. The observed variability in methane fluxes (Fig. 6.2a) therefore supports that species-specific root-redox interactions, can locally override environmental controls, reinforcing the importance of species-specific functional traits in mediating the root-redox-methane interactions. Consequently, the strength and direction of methane responses

within the root-redox-methane framework depend strongly on species-specific functional traits such as root exudation.

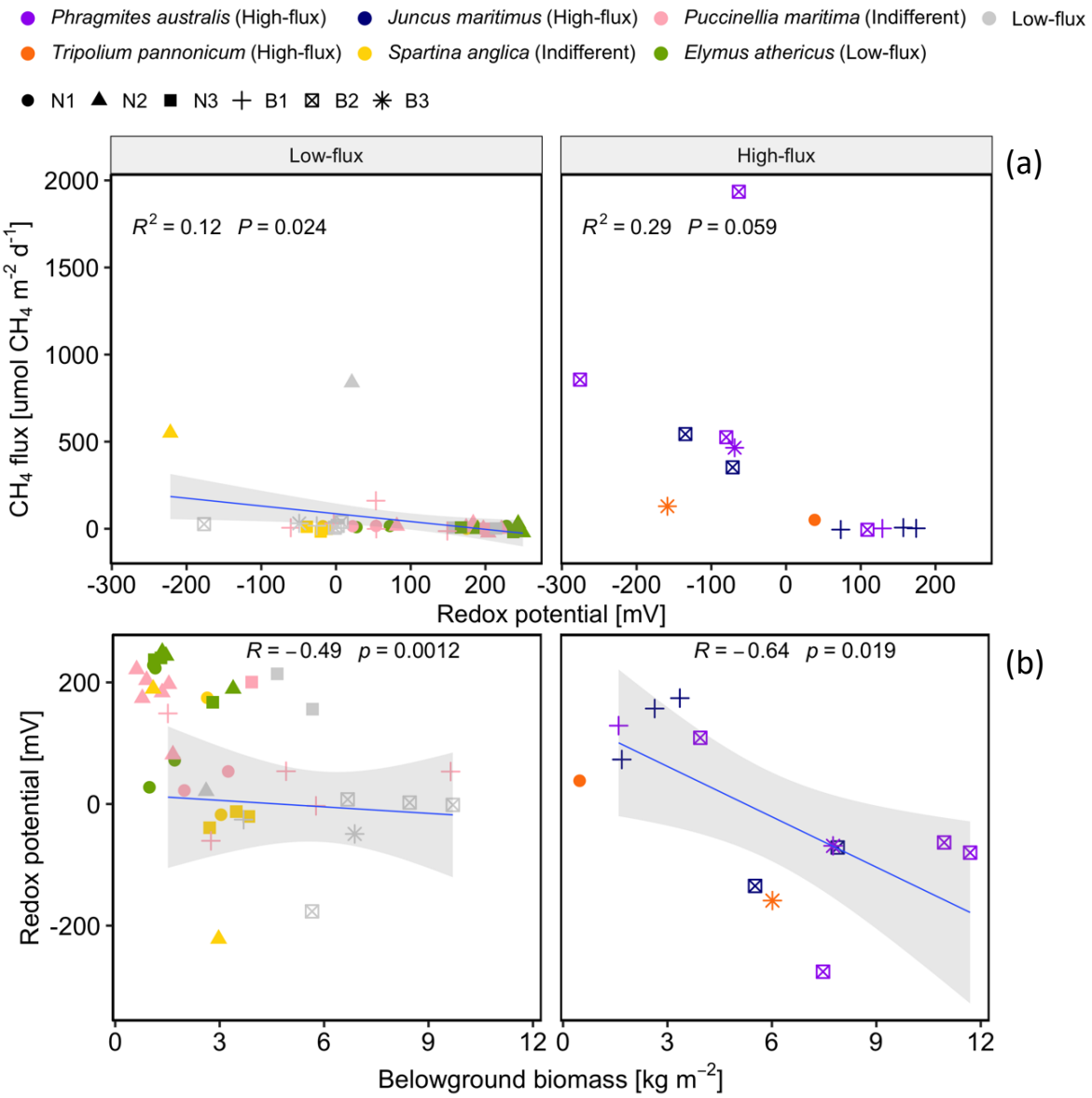

FIGURE 6.2 | *(a) Relationship between methane flux and soil redox potential for "low-flux" and "high-flux" species. In both groups, methane fluxes increase as soil redox potential decreases. (b) Correlation between soil redox potential and belowground biomass for "low-flux" and "high-flux" species, including Pearson correlation coefficients (r) with corresponding p-values, linear fits, and 95 % confidence intervals. Colors indicate the dominant species per plot, and symbol shapes denote the study sites (applies to all panels).*

6.1.4 | ROOT EXUDATION AS KEY PLANT TRAIT IN THE ROOT-REDOX-METHANE FRAMEWORK

Root exudation has been identified as a key plant functional trait influencing methane cycling in wetland ecosystems (Waldo et al. 2019, Haviland and Noyce 2024). Despite growing recognition of its importance, relatively few studies have examined root exudation in coastal wetlands due to methodological challenges of tracing rhizosphere processes under natural conditions, including

rapid microbial turnover of root exudates, high temporal variability in the composition and amount of root exudation, methodological limitations in compound identification, and low ecological relevance of existing extraction approaches (Oburger and Jones 2018, Ritter et al. 2025). Previous studies have reported various pathways that root exudates may undergo depending on prevailing soil-redox state (Keiluweit et al. 2017, Haviland and Noyce 2024, Mueller and Megonigal 2024). However, most of these mechanisms have been described under relatively static soil-redox environments, overlooking the dynamic background conditions characteristic of coastal marshes.

In coastal marshes, periodic flooding causes strong spatial and temporal fluctuations in oxygen availability which has been shown to influence methane emissions (Cui et al. 2024). Consequently, understanding the fate of root exudates under such fluctuating hydrological conditions is essential, as redox fluctuations likely regulate the balance between aerobic exudate mineralization and anaerobic respiration pathways, including methanogenesis (Chapter 3 and Box A).

6.1.4.1 | BACKGROUND SOIL-REDOX STATE CONTROLS FATE OF ROOT EXUDATES

Addressing this gap, I analyzed the fate of root exudates derived from two plants species which are widespread in North Sea salt marshes, the indifferent *S. anglica* and the "low-flux" species *E. athericus*, under conditions with repeated oxygen inputs ("oxic") and under persistently anoxic conditions (Fig. 3.1). Under conditions with recurring oxygen inputs, root exudates from both species were rapidly mineralized (Fig. 3.3). In contrast, under persistently anoxic conditions, mineralization rates were strongly reduced for both species allowing exudates to persist (Fig. 3.3). Prolonged anoxia (440 days) further promoted their persistence (Fig. 3.2) and likely the incorporation of root-derived exudates into a more stable SOC pool (Cotrufo et al. 2013, Keiluweit et al. 2015). Thus, whether exudates were decomposed or stabilized depended on background environmental controls on soil-redox state rather than species identity.

Even under short-term anoxic conditions, mineralization rates were substantially reduced, allowing exudates to persist (Fig. 4.3; also see Sogin et al. 2022). Therefore, topsoil SOC content can, serve as an indicator for plant-derived organic carbon inputs through root exudation. This interpretation is supported by significant positive correlations between belowground biomass and SOC for both plant species groups classified by methane flux ("low-flux": $R^2 = 0.36$, $p < 0.001$; "high-flux": $R^2 = 0.44$, $p = 0.013$; Fig. 6.3).

Together, these relationships between SOC, belowground biomass, and other environmental controls on soil-redox reflect how plant-derived carbon inputs are processed in the soil. In this context, after oxygen input (such as ebbing and low tide) root exudation primarily fuels aerobic microbial processes, leading to rapid carbon turnover (Fig. 3.3). Under anoxic conditions (such as flooding and high tide), however, oxygen depletion and the exhaustion of alternative electron acceptors slow down microbial mineralization (Fig. 3.3) (Keiluweit et al. 2017), allowing labile

root-derived carbon to persist and subsequently fuel methanogenesis (Fig. BA.1) (Whiting and Chanton 1993, Sha et al. 2011). Collectively, these results demonstrate that hydrological conditions govern the balance between exudate mineralization and stabilization, but also methanogenesis, positioning root exudation as a key control on both carbon transformation and methane cycling in coastal marshes.

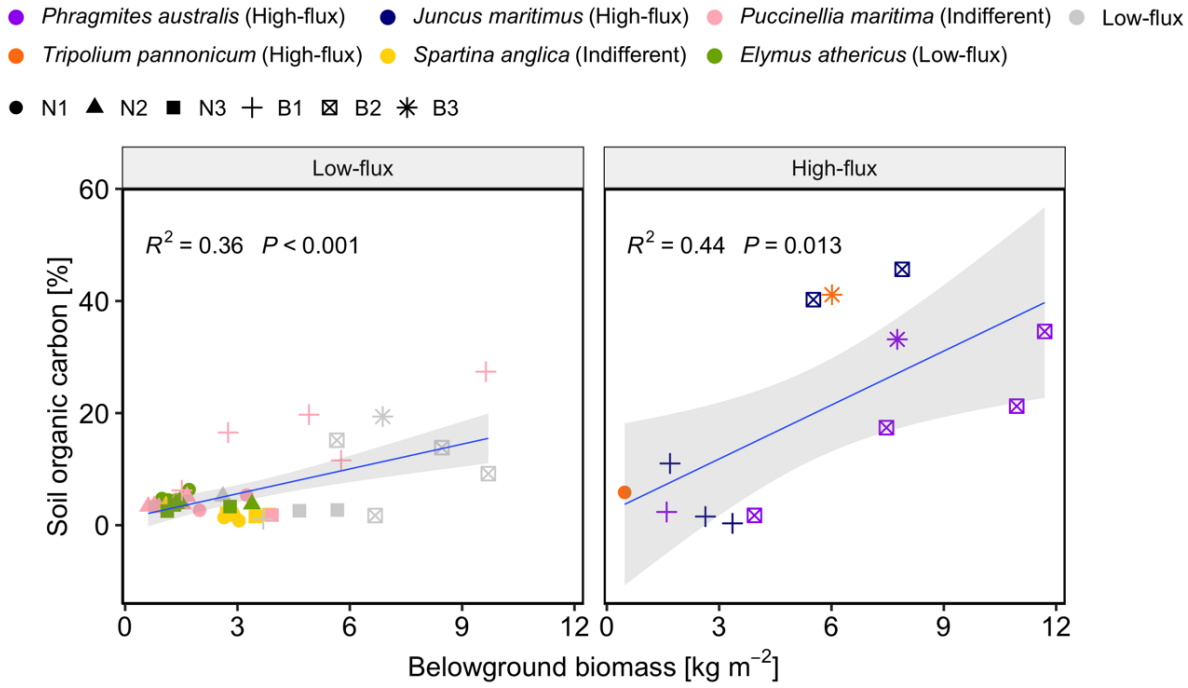

***FIGURE 6.3** | Relationship between SOC and belowground biomass for "low-flux" and "high-flux" species. In both groups, SOC increased significantly with increasing belowground biomass. Colors indicate the dominant species per plot, and symbol shapes denote the study sites (applies to all panels).*

6.1.4.2 | SPECIES-SPECIFIC ROOT EXUDATE COMPOSITION DRIVES VARIABILITY IN METHANE RESPONSE

Species-specific differences in exudate effects on methane production underpin the observed variability in methane fluxes (Fig. 6.2a). Root exudates from *S. anglica* fueled methanogenesis, whereas those from *E. athericus* did not (Fig. BA.1), supporting the idea that root-redox controls on methane fluxes depend on compositional differences in exudates (Haviland and Noyce 2024). "High-flux" species as well as indifferent species such as *S. anglica* could release more labile or microbially available compounds (e.g. methylated-compounds conducive to methylotrophic methanogenesis), thereby amplifying methane production (Yuan et al. 2019, Kim et al. 2020b). This pattern is consistent with soil microbial community differences described in Chapter 5, where *S. anglica* dominated marsh areas exhibited higher abundances of methylotrophic methanogens (Fig. 5.4).

In contrast, "low-flux" species may contribute more recalcitrant forms of exudates or simply invest more in oxidative processes such as ROL, in order to maintain aerobic conditions necessary for root

respiration (Philippot et al. 2008, Pezeshki and DeLaune 2012). Accordingly, Chapter 5 showed higher abundances of aerobic methanotrophs associated with *E. athericus* (Fig. 5.4), and consistent with its low methane emissions. As discussed in Chapter 3, *E. athericus* retained a larger share of recently assimilated carbon in its plant tissues, whereas *S. anglica* released more of this carbon into the soil (Tab. 3.S1), reflecting differing exudation patterns. Similar functional contrasts were reported by Haviland and Noyce (2024) in other wetland species: *Spartina patens* exhibited high exudation rates and methane emissions, whereas *Schoenoplectus americanus* showed greater ROL and correspondingly lower emissions. Together, these findings suggest that species differ in their major root effects on soil redox to either reduce the rhizosphere through root exudation or oxidize it through ROL (Fig. 6.4), with corresponding responses in methane fluxes.

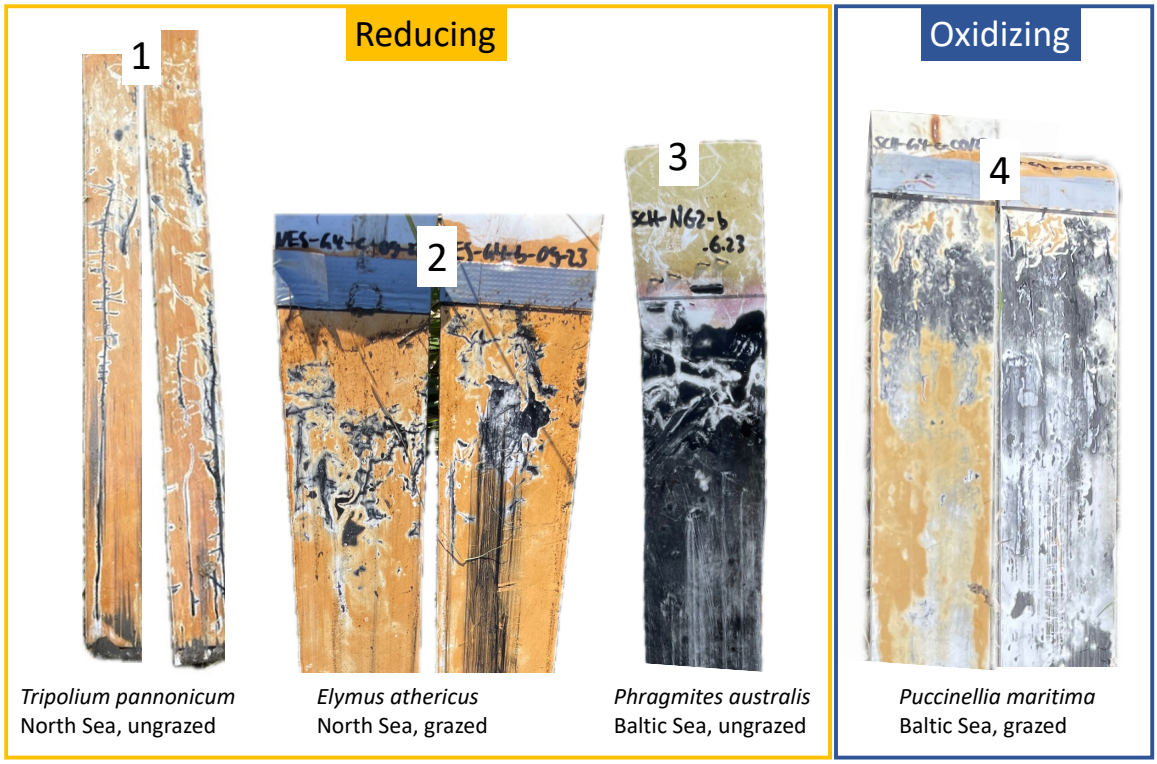

***FIGURE 6.4** | Examples of reducing and oxidizing effects of roots on soil-redox conditions visualized by root patterns on IRIS sticks. Reducing patterns: [1] Tripolium pannonicum (North Sea, ungrazed), [2] Elymus athericus (North Sea, grazed), [3] Phragmites australis (Baltic Sea, ungrazed). Oxidizing pattern: [4] Puccinellia maritima (Baltic Sea, grazed).*

6.1.4.3 | PLASTICITY OF ROOT-REDOX INTERACTIONS AS ANOTHER MODULATING FACTOR INFLUENCING METHANE FLUXES

S. anglica inhabits tidally influenced pioneer zones of salt marshes, where environmental conditions create a constantly reduced soil redox state (Fig 5.1a). *S. anglica* was classified as an indifferent flux species (Tab. 6.3), as it exhibited a high variability in methane fluxes (see Fig. 6.2a, yellow points). This suggests that *S. anglica* is not a fixed "net oxidizer" or "net reducer". Instead, it likely alters the expression of root-redox processes in response to the fluctuating hydrological

conditions, as *S. anglica* is capable of both ROL (Koop-Jakobsen et al. 2017) and the release of root exudates (Chapter 4), even though these processes have only been demonstrated separately. Although the method used for measuring the soil redox state (automated redox sensors) indicated constantly reducing conditions (Fig. 5.1a), it is not suitable for capturing transient fluctuations in soil redox states (Chapter 5). However, short term redox fluctuations occur with tide (Cui et al. 2024), to which plants likely react by changes in their exudation vs. ROL patterns.

Such plasticity has been shown in other wetland plants, which can adjust exudation and oxygen release under changing environmental conditions (Pezeshki and DeLaune 2012), and in other ecosystems (Gao et al. 2024, Shahzad and Gul 2025). In coastal marshes, rapid shifts in root-redox interactions could be triggered by short-term hydrological fluctuations caused by periodic flooding, precipitation, or geomorphological features such as ditches. Under these conditions, plants may increase oxygen transport to the roots to sustain root respiration during transient anoxia (Pezeshki and DeLaune 2012) or enhance exudation to acquire nutrients and maintain microbial activity under reduced or re-oxidizing conditions (Kuzyakov and Gavrichkova 2010, Wen et al. 2022). Thus, the plasticity in root-redox activity may induce a high variability in methane fluxes.

6.1.5 | SPECIES-SPECIFIC ENDOPHYTIC METHANOGENIC AND METHANOTROPHIC MICROBIAL COMMUNITIES CAN DRIVE VARIABILITY IN METHANE RESPONSE

Endophytic methanogenic and methanotrophic microbes have been reported in several wetland plants (Parmentier et al. 2011, Stepniewska et al. 2018, Szubryt et al. 2020, preprint), but evidence remains limited whether coastal marsh plant species host similar microbial communities and whether these microbes influence methane emission under fluctuating soil-redox conditions. In Box B I reported on the novel finding that wetland plant tissues from *S. anglica* and *E. athericus* harbor methanogenic and methanotropic communities (Fig. BB.4). Further I showed that plant tissues have a net uptake effect of methane (Fig. BB.2; Fig. BB.3), adapting to fluctuating redox conditions. Szubryt et al. (2020) similarly reported higher relative abundance of endophytic methanotrophs in *P. australis* and other wetland species, suggesting that plant tissues can generally function as methane sinks.

However, while *E athericus* exhibited a higher abundance of methanotrophic genes, consistent with its lower methane emissions, *S. anglica* showed a higher methanogenic gene abundance in roots and leaves, aligning with its higher methane emissions (Fig. BB.4). Together, these findings suggest that species-specific ratios of endophytic methanogenic to methanotrophic microbial communities contribute to the variability in methane emissions among wetland plant species.

6.1.6 | SYNTHESIS OF THE KEY PLANT-MEDIATED CONTROLS UNDERLYING THE ROOT-REDOX-METHANE FRAMEWORK

Together, the results of Chapter 3, Chapter 5, Box A, and Box B indicate that root exudation, ROL, as well as soil and within-plant microbial activity represent central plant-mediated processes influencing methane emissions from coastal marshes. The balance between root exudation and ROL together with the soil and endophytic microbiomes vary across species, while within species, plasticity in root-redox interactions governs their dynamic adjustment to environmentally driven redox changes. Consequently, I conclude that the species-specific exudation patterns and exudate compound composition, the environmentally driven fate of exudates, together with soil microbial processes influence soil-redox conditions and thereby determine methane production and oxidation, and ultimately methane emissions and uptake from coastal marshes.

The findings from section (6.1) build the empirical foundation of the conceptual root-redox-methane framework developed in this dissertation (Fig. 6.5). Yet, the contrasting hydrological, sedimentary, and geochemical regimes of the two investigated coasts shape distinct soil-redox conditions, in which root-redox interactions likely play different roles (Bhullar et al. 2014, Lacroix et al. 2025). These environmental contrasts provide the foundation for (6.2) examining how root-redox interactions that control methane fluxes are expressed under different coastal settings, and (6.3) how it responds to livestock grazing within each coast. Finally, I explore (6.4) the sensitivity of the root-redox-methane linkage to global warming.

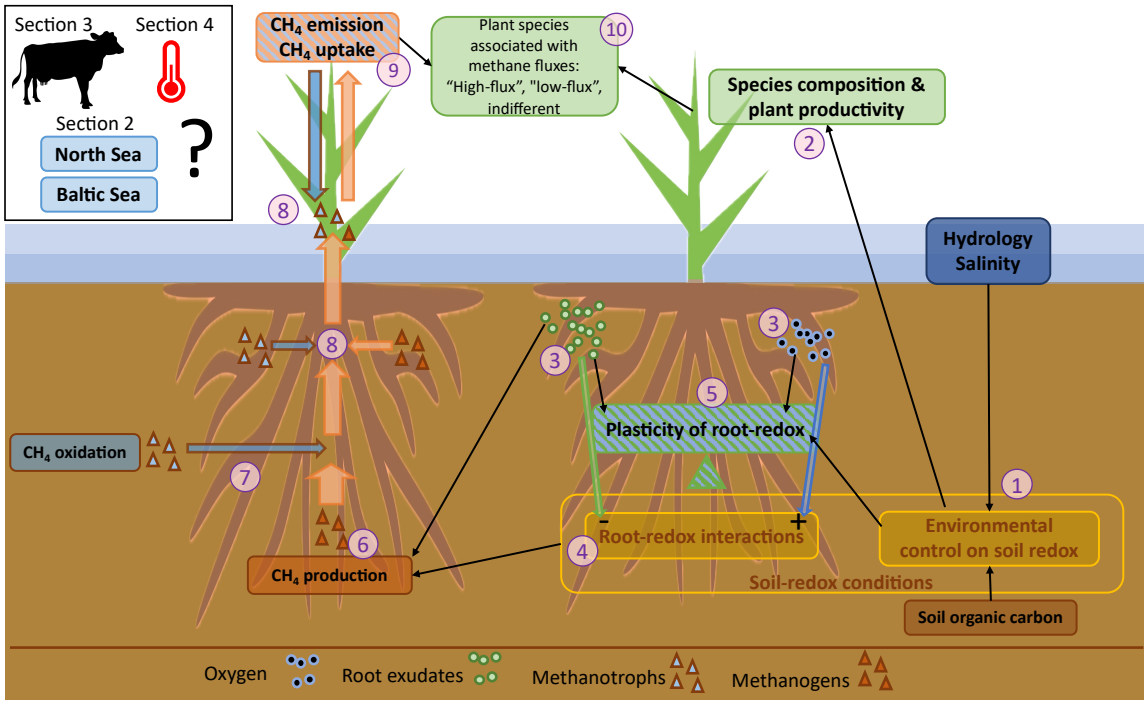

***FIGURE 6.5** | Conceptual framework on the environmentally driven expression of the species-specific root-redox controls on methane fluxes, based on the findings from Section 1 of this synthesis. (1) Soil-redox conditions are shaped by site specific tidal regimes, seawater salinity and soil organic carbon content, which jointly determine (2) plant species composition and productivity. Depending on prevailing (1) environmental controls on soil-redox state, (3) root exudates can contribute to SOC stabilization and (6) the production of methane. (3) Species-specific ROL and root exudation patterns regulate (4) the root-redox effects on soil-redox conditions, which can (5) be flexibly adapted to fluctuating environmentally driven soil-redox changes through plasticity of root-redox interactions. The composition of (3) root exudates plays a key role in fueling methanogenesis, by supplying substrate favorable for methanogenic soil microbes thereby enhancing (6) methane production. Methane can subsequently be oxidized by (7) methanotrophic soil microbes, as well as produced and oxidized by (8) endophytic methanogenic and methanotrophic microbes within plant root, stem and leaf tissues. Together, these processes determine (9) species-specific methane emission and uptake, which form the basis for classifying (10) plant species regarding their respective methane fluxes. This conceptual root-redox-methane framework is examined in Section 6.2 under contrasting environmental settings, in Section 6.3 in response to livestock grazing within each coast, and in Section 6.4 in response to global warming.*

6.2 | TESTING THE ROOT-REDOX-METHANE FRAMEWORK IN TWO CONTRASTING COASTAL SETTINGS

Across the two studied coasts, salinity, hydrology, and SOC, differ markedly (North Sea vs. Baltic Sea; mesotidal, semi-diurnal tides up to 4 m (high-energy) vs. micro- to non-tidal, wind-driven, prolonged inundation (low-energy) (Dijkema 1990); minerogenic (2.05 %) vs. organogenic (7.86 %) topsoils (Tab 3.1; Fig. 1.2); 25-35 PSU vs. 15-25 PSU (Fig. 6.6), controlling the coastal and site-specific plant species composition (Fig. 6.S1). Mean soil redox potential and methane fluxes reflect these contrasting environmental settings. In the low-energy Baltic marshes, soil redox potential averaged –8.6 ± 163.1 mV (n = 204) and methane emissions 230 ± 722.2 µmol CH_4 m^{-2} day^{-1} (n = 144), whereas in the high-energy North Sea marshes, redox averaged 123.6 ± 160 mV (n = 236) and methane emissions 57.6 ± 261.5 µmol CH_4 m^{-2} day^{-1} (n = 195). Globally, these values fall within the lower range of reported coastal marsh methane fluxes (–94 to 94,200 µmol CH_4 m^{-}

^{2} day^{-1}; Rosentreter et al. (2021a)). However, despite similar environmental conditions expected within each respective coastline, methane emissions differ within and between sites of the same coastline, which I attribute to species-specific the root-redox control on methane fluxes.

6.2.1 | ROOT-REDOX INTERACTIONS CONTROL METHANE FLUXES AT THE LOW-ENERGY BALTIC SEA COAST

The low-energy Baltic Sea marshes have low rates of sediment deposition and slow-accreting organogenic soils (Dijkema 1990, Nolte et al. 2013a) that shape both plant community composition and soil biogeochemistry. These organic-rich soils, together with lower salinity and prolonged saturation, create inherently reducing soil environments conducive to methanogenesis (Poffenbarger et al. 2011, Sha et al. 2011).

The correlation matrix for the Baltic Sea indicated that methane fluxes were driven by belowground biomass (r = 0.55, p = 0.006) and soil redox potential (r = -0.44, p = 0.035). Soil-redox itself was jointly influenced by belowground biomass, soil moisture, and SOC (Tab. 6.4), highlighting a tightly interconnected system where belowground biomass, soil redox, and environmental parameters interact through multiple feedbacks rather than acting independently.

TABLE 6.4 *| Pearson correlations coefficients (r), based on plot-level means from Baltic Sea marshes, between methane fluxes and predictor variables: soil redox potential (mV), belowground biomass (kg m^{-2}), aboveground biomass (kg m^{-2}), SOC (%), salinity (PSU), and VWC (%). Significance levels: p < 0.05 *, p < 0.01 **, p < 0.001 ***.*

	CH_4 flux	Soil redox potential	Belowground biomass	Aboveground biomass	Soil organic carbon (SOC)	Salinity
Soil redox potential	**-0.44** *					
Belowground biomass	**0.55** **	**-0.49** *				
Aboveground biomass	0.14	0.18	-0.18			
Soil organic carbon	0.38	**-0.61** **	**0.53** *	-0.20		
Salinity	0.40	-0.40	**0.53** *	0.06	0.14	
Volumetric water content	0.41	**-0.59** **	**0.49** *	-0.22	**0.63** *	0.22

A gradual influence of soil moisture on soil-redox is observed across the Baltic sites: soil redox potential decreases with increasing soil moisture across all sites (B1, B2, B3) and for all plant species (R^2 = 0.35; p = 0.004; Fig. 6.6c). This pattern forms a baseline, demonstrating that hydrological conditions create site specific soil-redox conditions upon which species-specific root-redox interactions control methane fluxes. To resolve these interactions in the Baltic Sea coast, in the following two sections (6.2.1.1 and 6.2.1.2) I analyze the root-redox control of methane emissions within-site between-species and between-site within-species.

6.2.1.1 | WITHIN SITE: "HIGH-FLUX" SPECIES ARE THE PRIMARY DRIVER OF HIGH METHANE EMISSIONS

Within sites, the species-specific differences in root-redox interactions become evident in the correlation between belowground biomass and soil redox potential, since soil redox potential decreased with increasing belowground biomass ($r = –0.49$; $p = 0.017$; Fig. 6.6b). Particularly at B2, while "low-flux" species show a trend towards lower soil redox potentials with increasing belowground biomass (see gray B2 squares in Fig. 6.6b), here redox potentials do not decline as strongly as for "high-flux" species (see violet B2 squares in Fig. 6.6b), indicating clear differences between these methane-flux species groups.

Crucially, the linear regression between soil redox potential and methane fluxes ($R^2 = 0.19$; $p = 0.035$; Fig. 6.6a) shows a clear redox-methane response primarily for "high-flux" species at sites B2 and B3 (see violet B2 and B3 symbols in Fig. 6.6a), where more reducing soil-redox conditions coincide with elevated methane emissions. In contrast, no "low-flux" species at either of the two sites displayed significant methane increases (see gray or pink symbols in Fig. 6.6a), despite similar belowground biomass and the same environmental controls. This observation is crucial for understanding the nuanced role of species-specific root-redox interactions: only the root-redox coupling of "high-flux" species translates into increased methane emissions, even under comparable environmental background settings and similar belowground biomass.

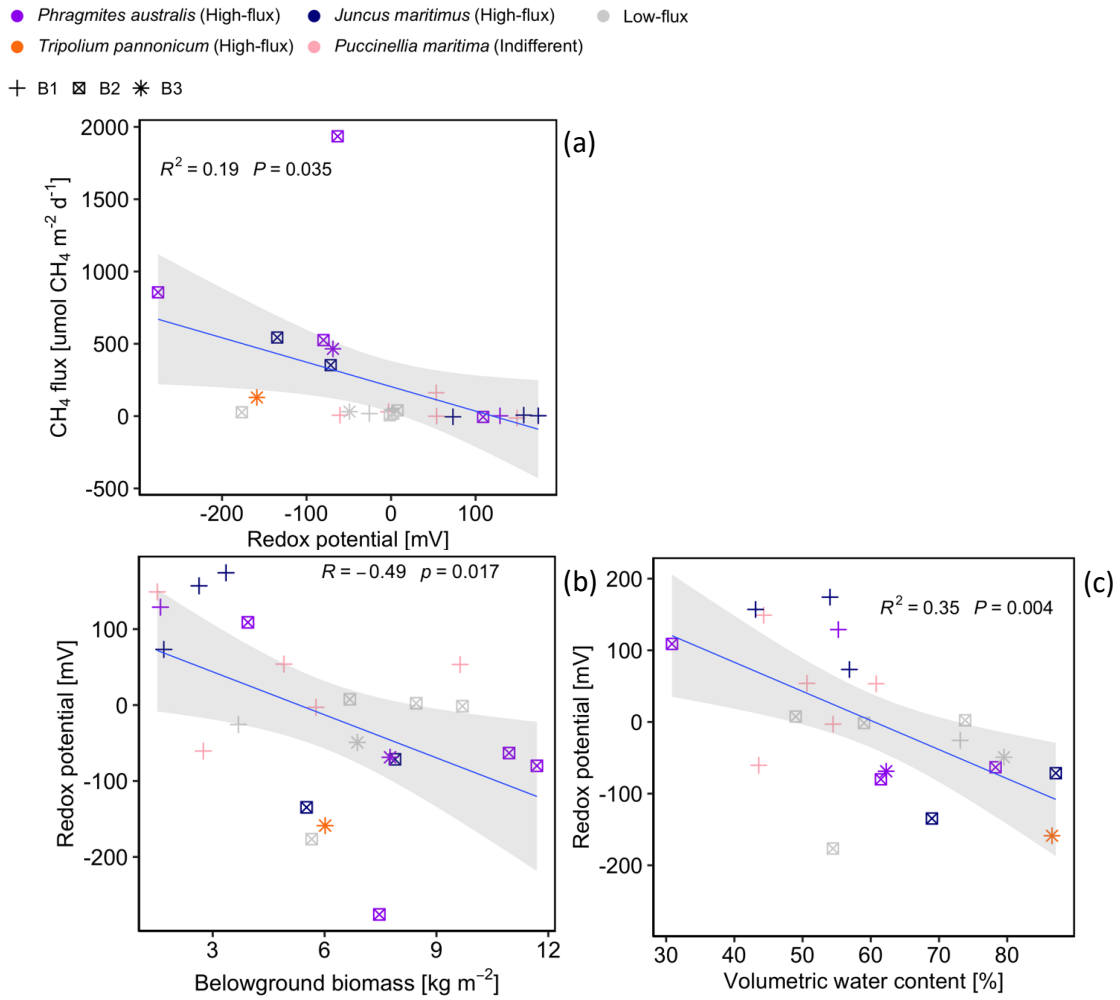

FIGURE 6.6 *| (a) Relationship between methane flux and soil redox potential in Baltic Sea marsh plots. Methane emissions significantly increase as soil redox potential decreases. (b) Correlation between soil redox potential and belowground biomass in Baltic Sea marsh plots, including Pearson correlation coefficients (r) with corresponding p-values, linear fits, and 95 % confidence intervals. (c) Relationship between soil redox potential and VWC in Baltic Sea marsh plots. Soil redox potential significantly decreased with increasing VWC. Colors indicate the dominant species per plot, and symbol shapes denote the study sites (applies to all panels).*

A reason for this strong plant mediated methane response could be species-specific exudation rates (Tab. 3.S1) and exudate composition (see also Canarini et al. 2019) fueling methane emissions (Fig. BA.1). In physiological adaptation to longer term inundated and reducing soils, "high-flux" species such as *P. australis* and *J. maritimus* develop deep, extensive root systems (Mueller et al. 2020b, Mozdzer et al. 2023), with *J. maritimus* additionally forming fibrous, laterally branching roots (Chen et al. 2019). Consequently, both species likely fueled microbial reduction pathways that lowered soil redox potential and enhanced methanogenesis compared to co-occurring "low-flux" species at this site (Fig. BA.1). Further, the extensive and deep reaching aerenchyma from e.g. *P. australis* may have facilitated a direct methane transport from deeper soil layers to the atmosphere, bypassing oxidative soil layers where methane would otherwise be oxidized to CO_2 (Brix et al. 2001, Henneberg et al. 2012, Vroom et al. 2022).

Although ROL was not directly measured, it is plausible, that the more extensive root system of these species also facilitates higher ROL rates to alleviate anoxic stress, creating localized oxidative microsites (Lai et al. 2012, LaCroix et al. 2019). However, wetland species can also develop barriers preventing oxygen loss under waterlogged conditions (Visser et al. 2008). Thus, whether ROL is facilitated or limited, any oxygen leakage into the rhizosphere likely remains too small to counteract methane production under strongly reducing soil conditions (Zhou et al. 2024). This is consistent with the findings I discuss in Box B, where oxidative microbial potential is given within plants and soil, but likely outweighed by methane production given the resulting net methane emission.

Along the Baltic Sea marsh coasts, seawater salinity fluctuated seasonally (15–25 PSU; Fig. 6.7a), yet only "high-flux" species showed pronounced methane responses, displaying an inverse pattern to the salinity cycle (Fig. 6.7b). Earlier studies already reported on species-specific root physological adaptations being the reason for pronounced emissions under similar salinities (Poffenbarger et al. 2011, Seyfferth et al. 2020). In addition, high exudation rates and unique compound composition of "high-flux" species can promote rhizosphere sulfate depletion, thereby weakening the competitive inhibition of methanogens which further enhances methane emissions (Liu et al. 2019, Kim et al. 2020a, Kim et al. 2020b). However, spatial heterogeneity in hydrological influence may further modulate this response. Stewart et al. (2024) show that a high variability of methane emission between different vegetation patches. "High-flux" species could have occupied marsh areas that remain waterlogged for longer periods and therefore experience lower porewater salinity, whereas drier marsh areas could have been more saline, thereby enhancing differences in methane production potential (Seyfferth et al. 2020).

In *T. pannonicum* root-redox interactions that increase methane emissions appear less inherently pronounced. While *T. pannonicum* is a salt tolerant species (Wiszniewska et al. 2019), methane emissions only increased when seawater salinity fell below ~15 PSU (Fig, 6.7c), a common threshold for increased methane emissions described by previous studies (Liu et al. 2019, Arias-Ortiz et al. 2024). Further, unlike *P. australis* and *J. maritimus*, *T. pannonicum* develops only shallow, laterally spreading fibrous root networks (Ludwiczak et al. 2024), providing fewer and shallower vertical transport pathways for methane produced in deeper soil layers (Vroom et al. 2022). This indicates that *T. pannonicum* represents a more environmentally redox-driven "high-flux" case.

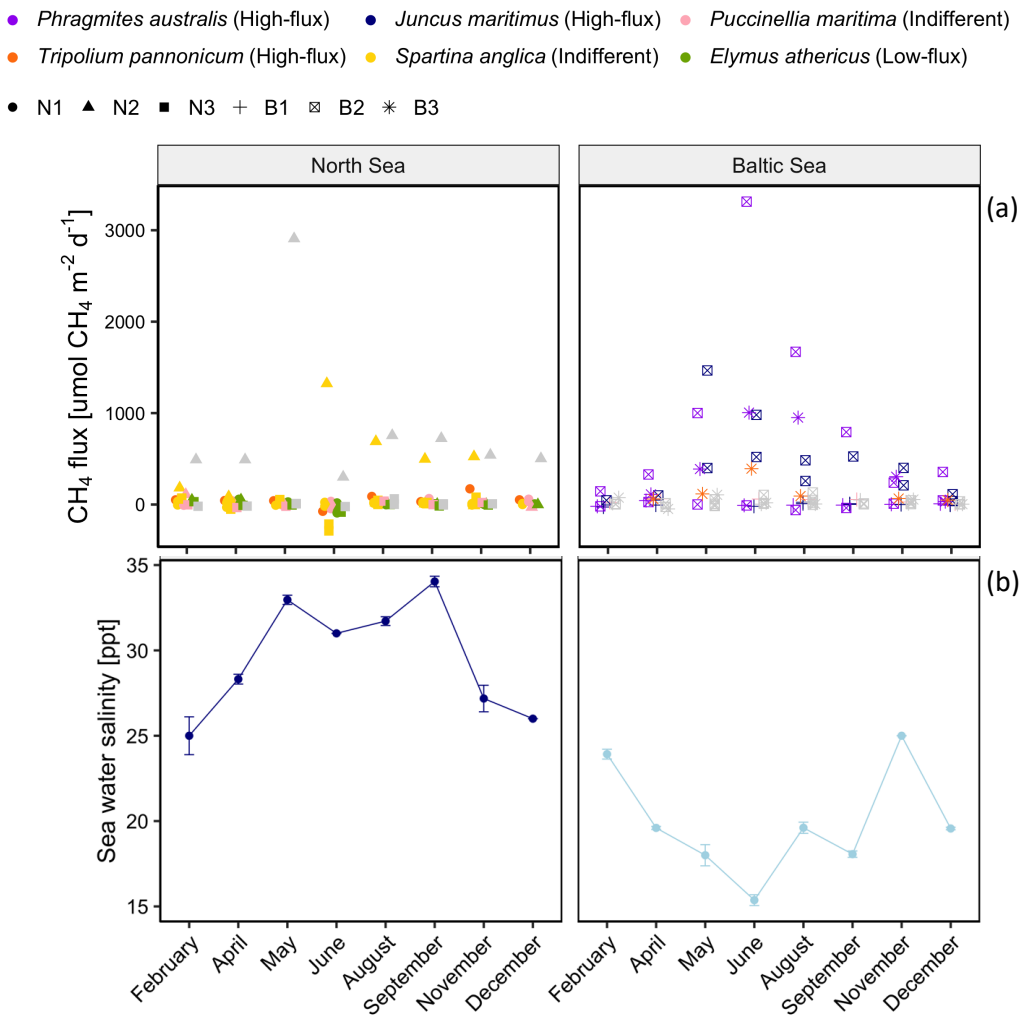

FIGURE 6.7 *| (a) Methane emissions from study sites along the North Sea and Baltic Sea coasts, shown for each sampling campaign. Colors indicate the dominant species per plot, and symbol shapes denote the study sites. (b) Site-level salinity (PSU) measured during each campaign.*

6.2.1.2 | BETWEEN SITES: "HIGH-FLUX" SPECIES RESPONSE IN METHANE FLUXES IS DEPENDEND ON BACKGROUND SOIL-REDOX STATE

The bidirectionality between belowground biomass and soil redox potential becomes evident when comparing "high-flux" species across sites: plots with "high-flux" species present at sites B2 and B3 of the Baltic coast exhibit markedly lower soil redox potentials than conspecific plots at site B1 (Fig. 6.5b), indicating site-specific environmental factors control soil-redox conditions. At the more waterlogged, reducing sites B2 and B3, root-redox interactions of high-flux species were more reducing, resulting in higher methane emissions. This effect was likely further amplified by the high topsoil SOC contents (~20 % and ~30 %; extended dataset), which provide abundant substrate for microbial metabolism (Sha et al. 2011, Bridgham et al. 2013) fueling methanogenic activity by locally relaxing competition between sulfate reducers and methanogens (Kim et al. 2020a, Kim et al. 2020b). In contrast, B1 exhibited lower soil moisture (see purple squares, stars and plus signs in Fig. 6.5c) and lower SOC levels (~9 %; extended dataset), and thus less reducing soil-redox

conditions, thereby representing a relatively dry and less organic-rich subsite within the otherwise organic-rich and reducing Baltic Sea coastline. The “high-flux” species growing at this site did not develop the extensive root structures observed at B2 and B3 (see purple squares, stars and plus signs in Fig. 6.5b), consistent with findings by Li et al. (2014) showing that aquatic *P. australis* ecotypes develop more extensive roots than terrestrial types. A recent study be Ge et al. (2025) reports on varying methane emissions from *P. australis* across different environmental conditions. Consequently, the higher methane emissions from “high-flux” species observed at B2 and B3 compared to B1 likely resulted from the synergistic effects of root physiological adaptations to the prevailing SOC and soil moisture conditions.

Together, the results from sections 6.2.1.1 and 6.2.1.2 indicate that species-specific root-redox interactions amplify methane emissions within strongly reducing soil-redox environments shaped by the low-energy hydrological conditions and biochemical regime of the Baltic Sea, while this amplification is dependent on the background soil-redox state.

6.2.2 | ROOT-REDOX INTERACTIONS CONTROL METHANE FLUXES AT THE HIGH-ENERGY NORTH SEA COAST

In the high-energy North Sea marshes, distinct vegetation zones – from the pioneer zone to the low marsh and the high marsh – reflect pronounced hydrological and sedimentary gradients that shape both plant community composition and soil biogeochemistry (Dijkema 1990, Suchrow and Jensen 2010). Across the North Sea marsh platform, hydrological and biochemical conditions supress methanogenesis in both the sulfate-rich pioneer zone (see Fig. 5.S2 for microbial community composition of SRB) and the well-aerated high marsh (Oremland and Polcin 1982, Poffenbarger et al. 2011, Witte and Giani 2016).

Methane emissions were significantly negatively correlated with soil redox potential across all three sites N1, N2, N3 ($r = -0.48$, $p = 0.006$; Tab. 6.5), demonstrating that soil redox potential was the main driver of methane emissions. Soil redox potential, in turn, was controlled by hydrology, decreasing with increasing soil moisture, consistently across sites ($r = -0.54$, $p = 0.002$; Tab. 6.5).

TABLE 6.5 | *Pearson correlations coefficients (r), based on plot-level means from North Sea marshes, between methane emissions and predictor variables: soil redox potential (mV), belowground biomass (kg m^{-2}), aboveground biomass (kg m^{-2}), SOC (%), salinity (PSU), and VWC (%). Significance levels: p < 0.05 *, p < 0.01 **, p < 0.001 ***.*

	CH_4 flux	Soil redox potential	Belowground biomass	Aboveground biomass	Soil organic carbon (SOC)	Salinity
Soil redox potential	**-0.48** **					
Belowground biomass	0.11	-0.29				
Aboveground biomass	0.14	0.13	0.12			
Soil organic carbon	0.09	0.21	**-0.48** **	0.10		
Salinity	-0.31	-0.10	**0.44** *	0.04	-0.28	
Volumetric water content	0.12	**-0.54** **	**0.49** **	-0.27	-0.28	-0.04

The corresponding linear regression confirmed that this hydrology driven redox gradient aligns with the characteristic North Sea vegetation zonation, with soil redox potential systematically decreasing from the oxidizing high marsh ("low-flux" species *E. athericus*), to the low marsh ("high-flux" *T. pannonicum*), and into the most reducing pioneer zones (indifferent species *S. anglica*) (R^2 = 0.29, p = 0.002; Fig. 6.7c). Importantly, belowground biomass showed no significant correlation with soil redox potential, as all plants present at the North Sea exhibited similarly low belowground biomass ranges (see Fig. 6.7b for within- and between-site differences), compared to belowground biomass ranges at the Baltic Sea coast (Tab. 6.S1).

Overall, these results show a stronger variability of soil-redox conditions and methane fluxes between zones than between sites. Because the hydrological contrast is strongest between then high marsh and the pioneer zone, the following section (6.2.2.1), examines the root-redox controls on methane emissions separately in those two zones.

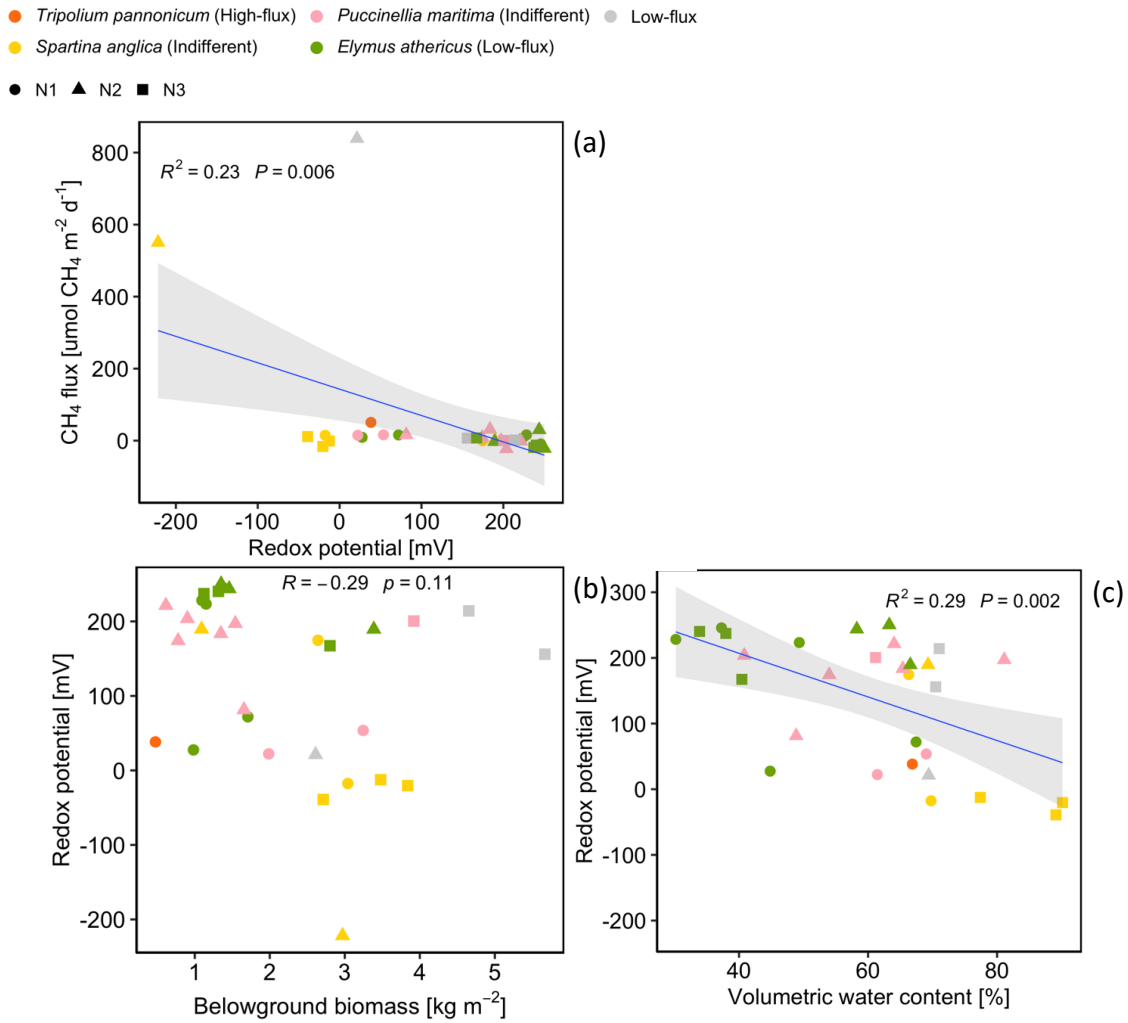

FIGURE 6.8 | *(a) Relationship between methane flux and soil redox potential in North Sea marsh plots. Methane emissions significantly increase as redox potential decreases. (b) Correlation between soil redox potential and belowground biomass in North Sea marsh plots, including Pearson correlation coefficients (r) with corresponding p-values, linear fits, and 95% confidence intervals. (c) Relationship between soil redox potential and VWC in North Sea marsh plots. Soil redox potential significantly decreased with increasing VWC. Colors indicate the dominant species per plot, and symbol shapes denote the study sites (applies to all panels).*

6.2.2.1 | ZONE-SPECIFIC BACKGROUND SOIL-REDOX MODULATES ROOT-REDOX INTERACTIONS AND METHANE FLUXES

High-energy North Sea marsh pioneer zones exhibit consistently hydrologically driven reducing soil-redox conditions (Fig. 5.1a), a pattern measured at site N3 and given the low between-site variability along the North Sea coast, likely representative of pioneer zones at N1 and N2 as well. Nevertheless, root-redox interactions did not lead to increased methane emissions across all pioneer zones. Linear regression showed that an increase in methane emissions with decreasing soil redox potential occurred only at site N2, and only in a single *S. anglica*-dominated plot (yellow triangle in Fig. 6.7a; $R^2 = 0.23$, $p = 0.006$), which also showed consistently higher methane emissions throughout the year than at sites N1 and N3 (yellow bars in Fig. 6.9). This could be due to the fact that N2 represents a relatively low-energy subsite within the otherwise high-energy North Sea

coastline (54°30′12.5″N, 8°57′44.3″E). Under these specific hydrogeomorphic conditions, reduced sediment inputs enable greater autochthonous SOC accumulation. This greater substrate availability could fuel methanogenesis, similar to patterns observed in the mesohaline low-energy Baltic Sea marshes. Finding comparably high methane fluxes in the sulfate-rich pioneer zone of the North Sea was unexpected. However, recent studies show that *Spartina* species (*S. anglica* and *S. alterniflora*) can exude methylated compounds (Yuan et al. 2019, Kim et al. 2020b), which can persist under these waterlogged conditions (Fig. 3.3), leading to the observed high methane emissions from site N2.

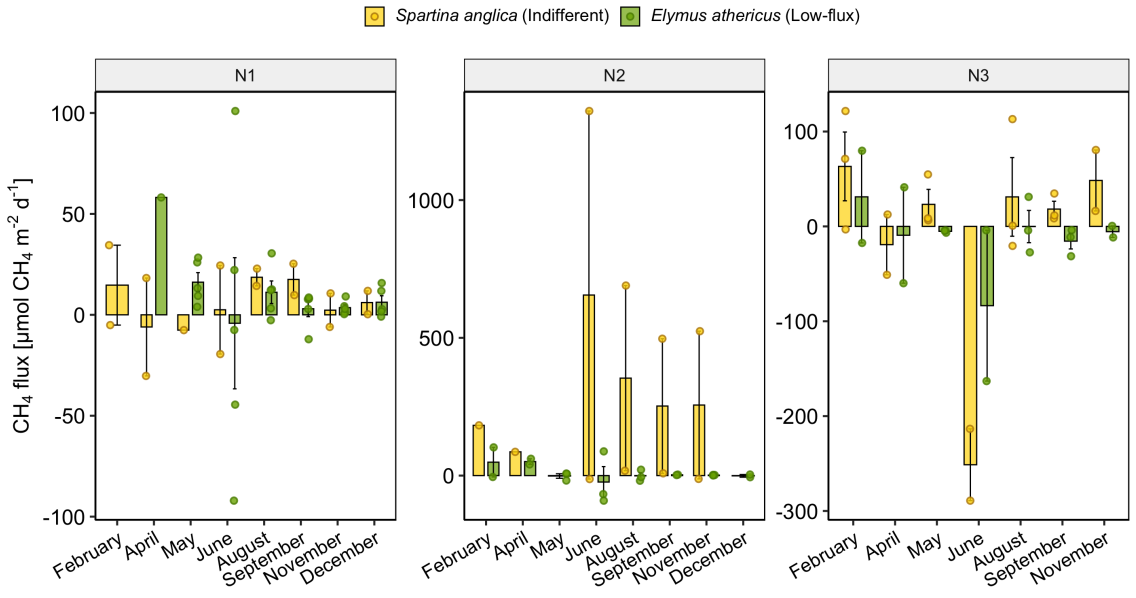

***FIGURE 6.9** | Monthly methane fluxes from North Sea marsh sites N1, N2, and N3. Panels display sites separately, each with its own y-axis scaling to capture site-level variability in methane fluxes. Bars represent monthly mean methane fluxes, while jittered points show individual plot measurements; both are colored by dominant species.*

At the more exposed high-energy sites N1 and N3, hydrological fluctuations impose an additional layer of regulation on the root-redox interactions. Under such conditions, *S. anglica* likely had to adjust its root-redox interactions through physiological plasticity, resulting in temporally variable methane fluxes across *S. ,anglica* plots at N1 and N3 (Fig. 6.9), as plastic root-redox interactions operate on top of an already reducing baseline and enable rapid shifts between rhizosphere methane production and oxidation. Comparable plastic root-redox alterations have been documented in trees responding to seasonal redox fluctuations (Gao et al. 2024), in permafrost systems (Turner et al. 2020), and in tidally driven wetlands (Cui et al. 2024). To resolve such short-term dynamics in detail, continuous (e.g. automated) methane flux measurements would be required; nonetheless, unpublished data from site N3 indicate that methane emissions increase with flooding during summer, but in spring, methane uptake increases during flooding (Fig. 6.S2; from Hauschild et al.,

in preparation). This seasonal divergence in methane response further demonstrates plastic root–redox interactions.

Overall, methane emissions along the North Sea coast where generally low (Fig. 4.4a,b). In line with this, all three North Sea sites were largely dominated by the "low-flux" species *E. athericus* in their high marsh zones, which has been previously shown to oxygenate the rhizosphere (Koop-Jakobsen et al. 2021). While there are currently no studies directly assessing methane emissions from *E. athericus*, these marsh areas likely behave similarly to upland grasslands, which are well researched in terms of methane uptake (Rafalska et al. 2023, Koyama et al. 2024).

In the well-aerated high marsh soils, however, a recent study showed that *E. athericus* is predominantly "net" reducing (Mittmann-Goetsch et al. 2024). Still, the composition of root exudates of *E. athericus* does not appear to promote methanogenesis, even under more reducing or anoxic conditions (Fig. BA.1). Moreover, in the minerogenic North Sea soils, the limited root-derived carbon is likely rapidly consumed as substrate for microbial respiration – predominantly by sulfate-reducing (Fig. 5.4) and aerobic bacteria in soils (Fig. 5.4) – leaving little labile carbon available for methanogenesis. Any methane produced in rhizosphere or within plant tissues is likely rapidly oxidized by soil (Fig. 5.4) and endophytic (Fig. BB.4) methanotrophs. Although methane is likely still produced in deeper, persistently anoxic soil layers, as suggested by porewater data from site N3 (extended dataset), most of it is subsequently oxidized through anerobic methane oxidation via syntrophic sulfate reducing bacteria (SRB) (Knittel and Boetius 2009). This is consistent with the net methane uptake measured in *E. athericus*-dominated marsh areas at site N3 (Fig. 5.2c), indicating that methane oxidation can exceed methane production. Together, this suggests that *E. athericus* represents a functional contrast to "high-flux" species, in which its root-redox activity, combined with background redox states, creates conditions under which methane emissions are suppressed.

Together, the outcomes from Section 6.2 illustrate that the central idea of the proposed root-redox-methane framework is broadly applicable across coastal marshes, while its manifestation is modulated by species-specific root-redox interactions, hydrology, salinity, and SOC, which together govern methane production, oxidation, and ultimately methane emissions and uptake.

6.3 | GRAZING EFFECTS ON THE ROOT-REDOX-METHANE FRAMEWORK WITHIN EACH COAST

Large areas of both the North Sea and Baltic Sea coast are subject to livestock grazing, a common management practice likely to exert substantial impacts on root-redox interactions thereby controlling methane cycling (Ford et al. 2012, Kirwan and Megonigal 2013, Kroeger et al. 2017). In Chapter 4, I tested the assumptions that grazing increases methane emissions through soil-

physical and root-mediated changes in soil-redox conditions by comparing grazed and ungrazed coastal marshes along both coastlines. I identified plant species groups associated with methane fluxes, and speculated how grazing might shift these groups, thereby affecting methane emissions through alterations in belowground biomass and soil-redox conditions. However, I did not demonstrate these relationships at the species level. In the following section, I therefore present correlation and regression analyses that explicitly incorporate "high-flux", "low-flux," and indifferent species to apply and assess how root-redox interactions control methane fluxes under grazed and ungrazed conditions across both coasts.

6.3.1 | GRAZING EXCLUDES "HIGH-FLUX" SPECIES, BALANCING METHANE FLUXES ACROSS GRAZED COASTAL MARSHES

In ungrazed marshes, methane emissions were tightly linked to soil redox potential and increased with decreasing soil redox potential (Baltic Sea: $R^2 = 0.32$; $p = 0.089$; North Sea: $R^2 = 0.51$; $p = 0.009$; Fig. 6.10a), primarily driven by "high-flux" and indifferent species. This pattern mirrors the relationships described above (Baltic Sea: Fig. 6.6a; North Sea: Fig. 6.8a), identifying ungrazed marshes as the primary source of methane emissions (Fig. 4.3a). The correlations between belowground biomass and soil reduction index (Baltic Sea: $r = 0.75$; $p = 0.012$; North Sea: $r = 0.15$; $p = 0.64$; Fig. 6.10b) reinforce this, indicating the same underlying controls are applicable here as well.

Despite the contrasting environmental factors controlling background redox conditions along the two coastlines, grazing led to a consistent outcome. Across all grazed sites, methane emissions remained consistently low throughout the season (Fig. 4.4a-d). This unified response in methane emissions coincided with an exclusion of the main methane emitting species *P. australis* in the Baltic Sea and *S. anglica* in the North Sea marshes (Fig. 6.7a). Previous studies similarly report that the reduction in *S. alterniflora* and *P. australis* reduced methane emissions by 19-75 % (Cheng et al. 2007, Yin et al. 2015). Instead of these species, grazing promoted the wide distribution of grazing-tolerant species such as *P. maritima* (Fig. 6.S1). Grazing-driven changes in species composition, along with the associated shifts in species-specific traits (Smith et al. 2014), have been linked to altered methane fluxes in previous studies (Ford et al. 2012).

However Ford et al. (2012) reported increases in methane emissions under grazing, a pattern also observed at B1, compared to the corresponding ungrazed site (Fig. 4.4c). This likely resulted from plants allocating proportionally more carbon belowground than under ungrazed conditions (Fig. 4.4g), consistent with previous findings of enhanced belowground carbon allocation in response to grazing (Elschot et al. 2015, Graversen et al. 2022). Notably, site B1 is drier and less organic-rich relative to B2 and B3, which resulted in very low methane fluxes including ungrazed areas in the first place (Fig. 4.4c).

6.3.2 | GRAZING INDUCES OXIDIZING ROOT-REDOX INTERACTIONS THEREBY DECREASING METHANE EMISSIONS

Still, overall methane emissions were low from grazed areas. While the root-redox interactions were generally reducing and the soil reduction index increased (i.e soil redox potential decreased) significantly with increasing belowground biomass (North Sea: $r = 0.69$; $p = 0.026$, Baltic Sea: $r = 0.72$; $p = 0.018$; Fig. 6.10b), there was no significant relationship between soil redox potential and methane emissions (North Sea: $R^2 = 0.20$; $p = 0.197$; Baltic Sea: $R^2 < 0.01$; $p = 0.869$; Fig. 6.10a). Additionally, soil reduction index decreased with increasing soil density across both coasts ($r = -0.53$; $p < 0.001$; Tab. 4.2), initially contradicting to the assumption that trampling decreases soil-redox conditions (Nolte et al. 2013b, Elschot et al. 2015, Mueller et al. 2017, Bakker et al. 2019). Together this indicates net oxidizing root-redox responses to the trampling-induced reducing soil conditions. In grazed North Sea marshes, the more oxidizing soils and lower methane emission could reflect hydrological alterations such as drainage (Elschot et al. 2024), which can enhance methanotrophic communities (Ma and Lu 2011). However, such management practices are absent along the Baltic Sea coast (personal observation during study site assessment), indicating that the consistent suppression of methane emissions across both coastlines is unlikely to be driven by drainage. Instead, net oxidizing plant-driven redox regulations likely overrode the trampling-induced reductions in soil-redox conditions, as evidenced by IRIS stick patterns (Fig. 6.4), resulting in the persistently low methane emissions from grazed marsh areas.

The results from Chapter 4 and this synthesis demonstrate that grazing largely lowers methane emissions from coastal marshes. Combined with the increase in SOC density reported in Chapter 2, this management practice can enhance the carbon sink function of these systems. Nonetheless, the locally increased methane emissions at site B1 highlight the importance of site-specific environmental conditions.

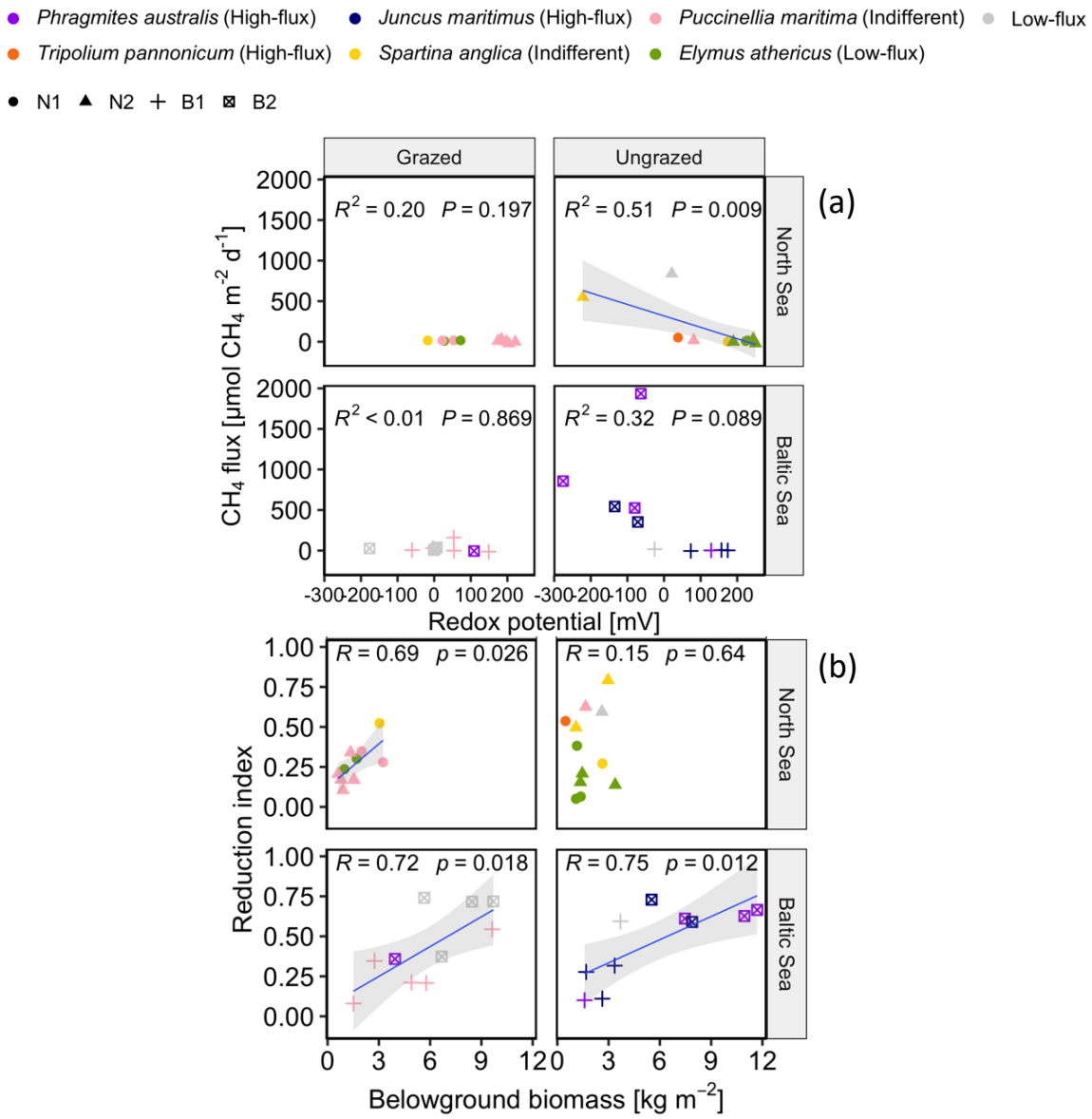

FIGURE 6.10 *| (a) Relationship between methane flux and soil redox potential in grazed and ungrazed plots in North Sea and Baltic Sea marshes. In ungrazed marshes, methane emissions increased as redox potential decreased, which is not the case for grazed marshes. (b) Correlation between soil reduction index and belowground biomass in grazed and ungrazed plots in North Sea and Baltic Sea marshes, including Pearson correlation coefficients (r) with corresponding p-values, linear fits, and 95 % confidence intervals. Colors indicate the dominant species per plot, and symbol shapes denote the study sites (applies to all panels).*

6.4 | WARMING SENSITIVITY OF ROOT-REDOX INTERACTIONS CONTROL METHANE EMISSIONS FROM SALT MARSHES

Warming effects on methane emissions were analyzed at site N3. Frequent tidal inundation usually buffers direct effects of warming (Rich et al. 2023, Cui et al. 2024, Guan et al. 2025, Mittmann-Goetsch et al. 2025), wherefore the influence of warming is expected to become more pronounced in less frequently flooded, higher elevated zones (Rich et al. 2023). Therefore, in Chapter 5 I initially assumed (1) that warming will decrease soil redox potential, with most pronounced effects

in the high-elevation zones and topsoil layers and (2) that decreasing soil redox potential, caused by warming effects, will lead to higher methane production and emission.

Contrary to the expectations, warming effects on the soil reduction index were stronger in the pioneer zone, than in the high marsh (Fig. 5.1a), which resulted in significantly higher methane emissions with moderate (+1.5 °C) warming in this zone (Fig. 5.3.b). Accordingly, the abundance of methylotrophic microbes increased with moderate warming (Fig. 5.4). Interestingly, this pattern cannot directly be explained by root-redox interactions, since biomass showed no sensitivity to warming in the analyzed system (Fig. 5.S3) (Menzel et al. 2025). However, I argue that this effect is still plant driven, likely through increases in root exudation fueling methanogenesis with warming (Zhai et al. 2013, Noyce and Megonigal 2021, Wang et al. 2021). *S. anglica* is know to provide methylated substrates that sustain methylotrophic methanogenesis (Yuan et al. 2019, Kim et al. 2020b). In Box B, I showed that *S. anglica* exudates enhance methane production under anoxic redox conditions (Fig. BA.1). Since the reduction index increased with warming (i.e. redox potential decreased) (Fig. 5.1c), it is likely that these increases can be attributed to higher root exudation rates in response to warming.

The previously reported high variability in methane fluxes from *S. anglica*-dominated zones (see Fig. 6.9 N3 (ambient)), persisted under both seasonal progression and artificial warming (Fig. 5.2c). Although warming and seasonality shifted the redox-methane balance toward more methane uptake in spring and more methane emission in summer, the large methane flux variability remained, suggesting that short-term, tidally driven plasticity in root–redox interactions persist independently of broader seasonal or temporal shifts (Cui et al. 2024).

In contrast, *E. athericus*-dominated high marsh zones showed no warming-induced increases in methane emissions, but strong warming (+3 °C) reduced methane uptake in spring and led to net methane emissions in summer (Fig. 5.2c). This pattern aligns with a warming-induced decrease in topsoil abundance of methanotrophs (Fig. 5.4). This may reflect increases in root exudation from *E. athericus* (Mittmann-Goetsch et al. 2024) with warming, which can suppress methane oxidation by stimulating aerobic respiration by other aerobic microbes than methanotrophs. The data does not indicate that methanogenesis is stimulated in the high marsh. This can be seen in the absence of methanogenic archaea in the high marsh (Fig. 5.4) and redox potentials indicating oxic soils even with warming in the high marsh. Additionally in Box B I showed that *E. athericus* exudates are not linked to methane production.

Together, warming-driven species-specific root-redox interactions ultimately increased methane emissions or decreased methane uptake depending on environmental context. Such interactions, are sensitive to global warming, because rising temperatures alter redox-sensitive processes such as plant productivity (Noyce and Megonigal 2021), root exudation (Zhai et al. 2013) and ROL (Li et al. 2024) and microbial activity (Tang et al. 2023), shifting the balance between methane production

and oxidation and ultimately between methane emission and uptake. The results from Chapter 5 indicate that the net methane-uptake function of minerogenic salt marshes may shift toward net emissions under warming. However, these emissions remain low relative to global averages (Rosentreter et al. 2021a) and are unlikely to offset the substantial carbon-storage capacity of these marshes (Chapter 3). Whether warming will ultimately diminish this storage capacity remains currently unknown.

6.5 | ROOT-REDOX-METHANE FRAMEWORK SYNTHESIS

The root-redox-methane framework represents the central conceptual outcome of this dissertation. It captures how root-redox interactions control carbon transformation and methane emissions from coastal marshes across environmental gradients and in response to global change pressures. Soil-redox conditions, shaped by site-specific hydrology, salinity, and SOC (Chapter 2), but also altered by livestock grazing (Chapter 4) and global warming (Chapter 5) are key determinants of plant species composition, plant productivity and biogeochemical functioning in coastal wetlands. Consequently, root-redox controls vary not only between species, but also within, because plants alter physiological processes in response to their local environmental conditions, and these alterations determine carbon transformation processes, specifically methane cycling.

A key dimension of these adaptations lies in species-specific root exudation and ROL rates, which wetland plants likely flexibly adjust in response to fluctuating soil-redox states. Moreover, not only the rate but particularly the composition of exuded compounds (Box A), influences methane-cycling soil microbial communities and soil-redox states (Chapter 5). Together with, endophytic methanogenic and methanotrophic microbes (Box B) these plant-mediated controls play a decisive role in modulating carbon transformations and methane cycling.

At the low-energy Baltic Sea coast, I found the environmental factors largely conducive to methanogenesis. “High-flux” species amplified the inherently methane-favorable soil-redox conditions through strongly reducing root-redox interactions that lower soil redox potential and increase methane emissions, in comparison to “low-flux” species. However, the magnitude of this regulation differed within species and between sites, indicating that these root-redox controls are context dependent (Fig. 6.11).

In contrast, at the high-energy North Sea coast, hydrology creates distinctive vegetative zones with characteristic soil-redox states – reducing in the pioneer zone, dominated by *S. anglica* and oxidizing in the high marsh, dominated by *E. athericus*. Still in both zones, environmental factors were generally suppressive for methanogenesis, creating a baseline of low methane emissions. The pioneer zones are subject to strong hydrodynamic forces and methanogenesis was largely suppressed, through the effect of high seawater salinities (i.e. soil with high sulfate concentrations). However, plastic root-redox interactions from *S. anglica* in response to fluctuating hydrology were

able to at times override these sulfate-driven constraints, resulting in variably methane emissions within and between sites. While root-redox effects of the "low-flux" species *E. athericus* in the well-aerated high marshes were likely reducing, all methane produced was quickly oxidized, resulting in low methane emissions and methane uptake (Fig. 6.11).

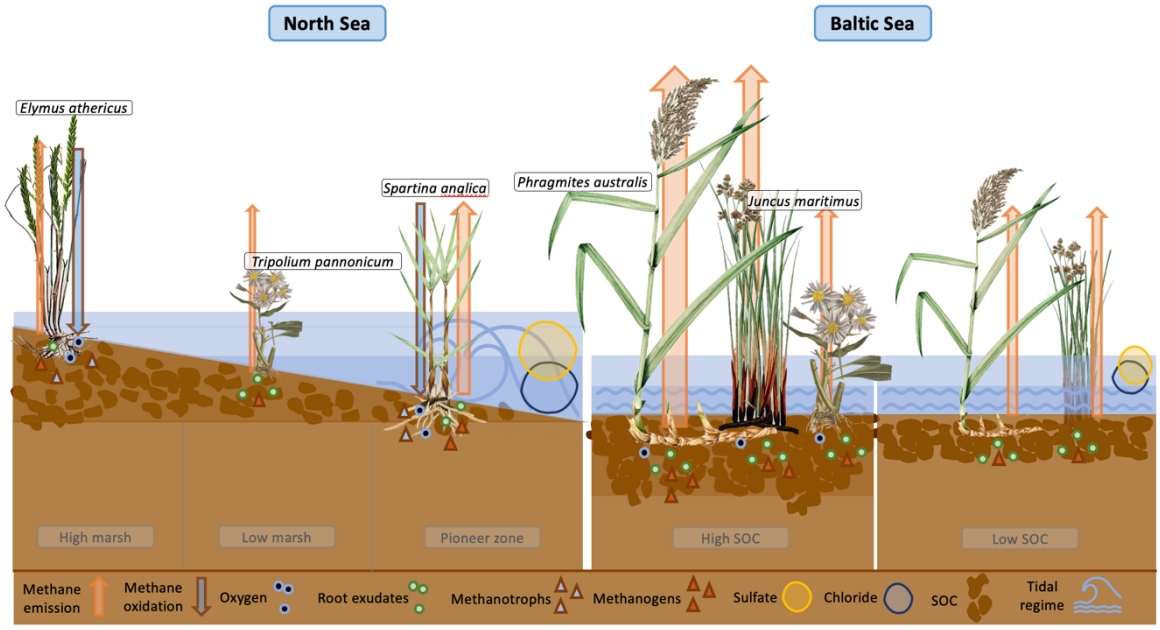

***FIGURE 6.11** | Schematic overview of root-redox interactions controlling methane fluxes from the high-energy North Sea marshes (left) and low-energy Baltic Sea marshes (right). North Sea marshes show hydrology-driven vegetation zonation and generally low methane emissions, resulting from strongly oxidizing soil-redox conditions in the well-aerated E. athericus high marsh and sulfate-rich, methanogenesis suppressing conditions in the S. anglica pioneer zone. Consequently, methane fluxes are low or negative in the high marsh and variable in the pioneer zones. In contrast, Baltic Sea marshes exhibit environmental conditions more conducive to methanogenesis, with SOC content shaping site-to-site differences. Species-specific root–redox interactions further enhance methane production, leading to higher emissions overall. The plant images are from Wikipedia (Elymus athericus, Tripolium pannonicum, Juncus maritimus), Lizzie Harper (Phragmites australis), or self-drawn (Spartina anglica).*

Grazing largely shifted plant species composition from "high-flux" species toward the grazing-tolerant indifferent species *P. maritima*. While trampling-driven soil compaction increased the soil density, soil-redox conditions were high. I attribute this to largely oxidizing root-redox interaction from *P. marimita*. Although this interaction largely decreased methane emission in grazed marshes, they locally exceeded the emissions from corresponding ungrazed areas, highlighting the importance of environmental context (Fig. 6.12).

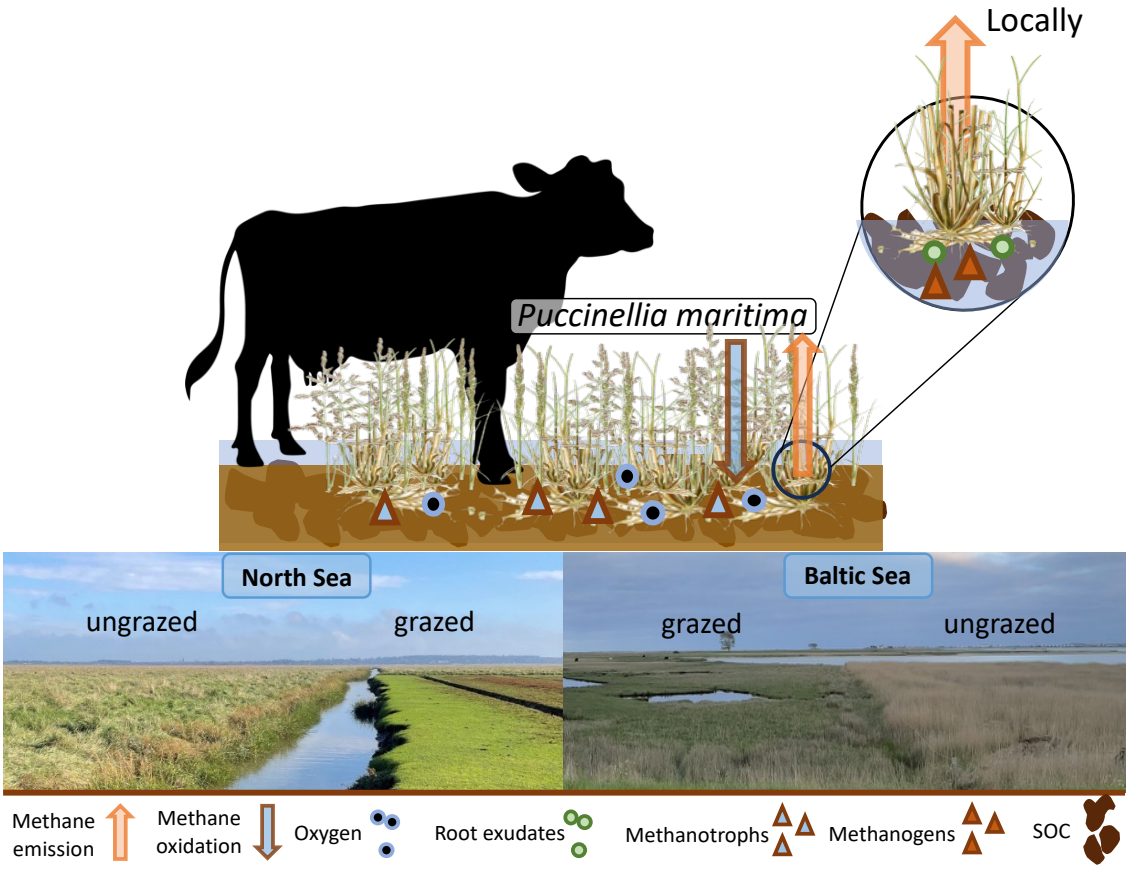

FIGURE 6.12 *| Schematic overview of oxidizing root–redox interactions of Puccinellia maritima in grazed coastal marshes. Grazing shifts vegetation composition toward P. maritima, whose oxidizing root-redox effects generally suppress methane emissions despite trampling-induced soil compaction. Locally, however, environmental conditions can interact with these dynamics to enhance methane fluxes beyond those of adjacent ungrazed areas. Photographs show representative grazed and ungrazed marshes at the North Sea coast (left) and the Baltic Sea coast (right) coasts. The plant image of Puccinellia maritima is from Wikipedia.*

Warming-induced, species-specific increases in methane emissions were most pronounced in the pioneer zone, but also evident in the high marsh through reduced methane uptake. These increases in methane emissions were most likely driven by enhanced root exudation, which fueled methanogenic communities in the pioneer zone, while weakening methanotrophic communities in the high marsh. This demonstrates that warming-driven root–redox responses can override environmentally driven constraints on methanogenesis, ultimately increasing methane emissions with warming (Fig. 6.13).

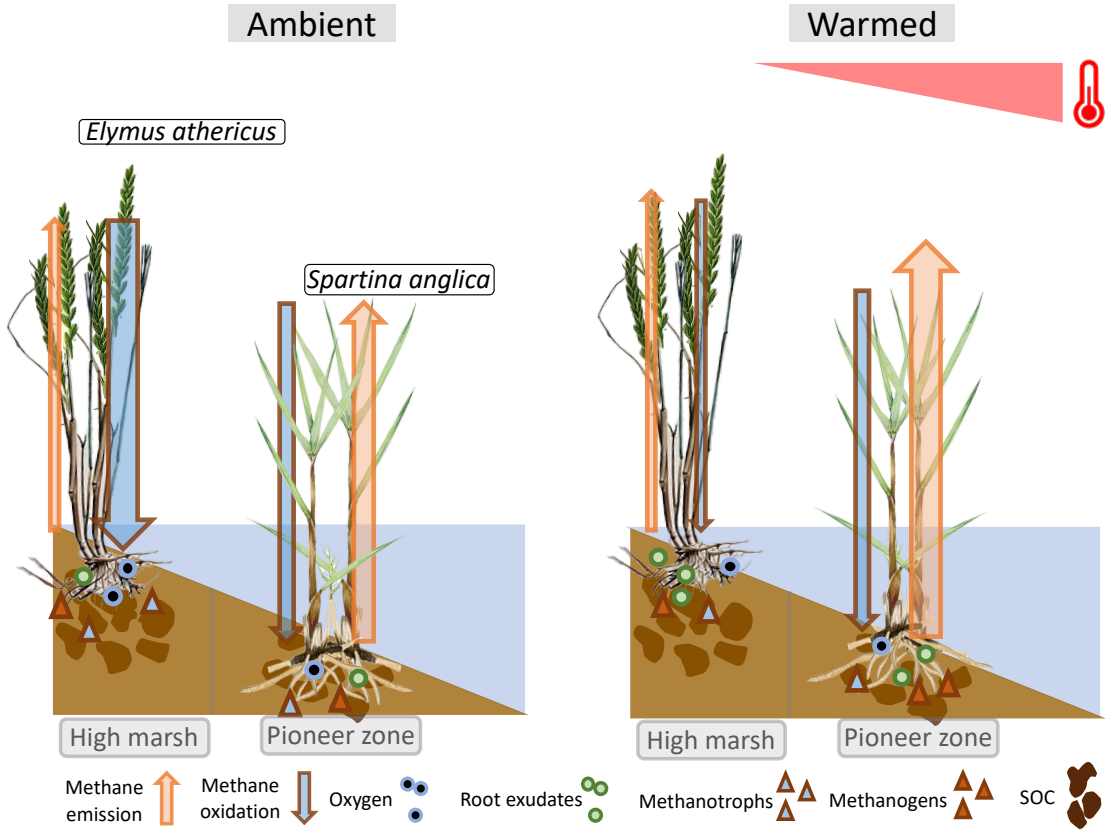

***FIGURE 6.13** | Schematic overview of warming-driven root-redox effects on methane emissions in North Sea salt marshes including the characteristic vegetation zonation under ambient (left) and warmed (right) conditions. Warming likely enhanced species-specific root exudation, stimulating methanogenesis in the pioneer zone and weakening methanotrophy in the high marsh, leading to overall increases in methane emissions. The warming impact on methane emissions was stronger in the pioneer zone than in the high marsh, as indicated by the red triangle in the upper left corner. The plant images are from Wikipedia (Elymus athericus) or self-drawn (Spartina anglica).*

Together, these observations demonstrate that the root–redox–methane framework is broadly applicable across coastal systems, but its strength and expression emerge from a context-dependent feedback loop between species-specific root-redox activities and environmental site conditions. Consequently, this dissertation underscores the need to move beyond fixed methane-flux plant functional groups toward a trait-based continuum.

6.6 | LIMITATIONS AND FUTURE RESEARCH PERSPECTIVES

The main limitation of this dissertation lies in its focus on in situ community-level observations under naturally varying environmental setting, rather than controlled single-species or species-interaction experiments. While this approach was able to capture the realistic ecosystem complexity, the soil redox measurements were unable to fully disentangle the relative contributions of plant-driven vs. environmentally-driven processes, and to separate the effects of individual vs. interacting plant species. In addition, the study did not incorporate seasonal variation in belowground biomass or distinguish between different belowground plant organs (e.g., rhizomes versus fine roots),

limiting the ability to attribute redox dynamics to specific root structures and their functional roles, which previous research has shown to vary seasonally (Liu et al. 2019) and among belowground plant organs (Määttä and Malhotra 2024). Finally, the soil-moisture measurements should be interpreted with caution, due to methodological challenges: volumetric water content measurements may be unreliable in saline soils due to sensor interference. Therefore, the soil moisture data generated for this dissertation is only used relatively. Future studies should rely on alternative approaches, such as determining gravimetric water content with each flux measurement campaign, to obtain more accurate soil moisture estimates under saline conditions. Similarly, Chapter 4 did not account for factors such as grazing duration (seasonal vs. year-round), management intensity (moderate vs. high-density), or grazer type (cattle breed vs. sheep), all of which may influence plant species composition and associated root traits, since these factors have been shown to alter SOC dynamics (Nolte et al. 2014, Davidson et al. 2017). Consequently, the results of this dissertation are predominantly correlational, reflecting associations rather than definitive causal mechanisms.

To achieve this and further advance this framework, future research should integrate controlled mesocosm experiments that systematically vary environmental factors through controlled changes in hydrology, salinity and possibly SOC. Much of the existing literature focuses on dominant species, particularly *Spartina* species and *P. australis* (e.g. Koop-Jakobsen et al. 2017, Kim et al. 2020b, Fuchs et al. 2024, Ge et al. 2025), leaving many other individual species (e.g. *E. athericus*) insufficiently studied despite their important influence on carbon transformation and methane cycling. In addition, how multiple co-occurring species (common in North Sea low marshes) and their associated traits interact and jointly modulate carbon transformation processes remains poorly understood. Therefore, such experiments should include both single-species and mixed-species communities.

Critically, current knowledge of coastal marsh species-specific root exudation and ROL remains extremely limited, and virtually no studies have examined how these traits shift across short term and seasonal timescales. Such phenological plasticity is likely central to root-redox interactions and thus represents a major research gap that must be addressed.

Importantly, mesocosm designs should also evaluate how root-traits, including changes in root morphology, root exudation, and ROL, respond to grazing, warming and possibly other global change pressures such as elevated atmospheric CO_2 concentrations, and assess how these shifts feed back into soil-redox dynamics and carbon transformation processes regarding methane cycling. Linking these root-trait responses with controlled background redox conditions will be essential for mechanistically testing and refining the root-redox-methane framework.

The soil reduction index (IRIS method; Rabenhorst and Burch 2006, Rabenhorst 2013) used in Chapters 4 and 5 provided an integrated measure of soil-redox conditions over the six-week intervals between flux campaigns and was thus particularly useful for explaining belowground processes. It complemented the momentary soil redox potential measurements, which captured

short-term redox states comparable to methane fluxes and soil moisture. Although these two metrics operate at different temporal scales, they were significantly correlated (Fig. 4.S1; Fig. 5.S1) demonstrating that both effectively track soil-redox dynamics. IRIS sticks can indicate whether plants act as soil oxidizers or reducers (Fig. 6.4); however, their interpretation becomes difficult when soils are already strongly reducing due to environmental factors, which can obscure root-driven patterns. To disentangle short-term plant-mediated redox effects from background redox conditions, future work should integrate in situ planar optode measurements (Schmidt et al. 2010). Further, incorporating sulfate-precipitation assessment with IRIS sticks (Fig. 6.S3) would offer a cost-effective means of identifying whether plant activity or elevated SOC drives sulfate depletion; manganese-oxide IRIS sticks could further illuminate the broader redox ladder (Sapkota et al. 2022).

A key strength of this dissertation is the use of consistent chamber-based flux measurements and a standardized flux quality control workflow, improving comparability across sites – an issue that can limit reviews and meta-studies, where methodological differences lead to flux under- or overestimation (Fiedler et al. 2022). Here, the flux evaluation was based on a combined RMSE (5 ppb) and R^2 (0.85) criterion in which either metric could meet its threshold, allowing the inclusion of near-zero and high positive and negative fluxes (Box C). However, this evaluation relied solely on linear models, and future work should incorporate non-linear flux functions, such as exponential or polynomial fits (Kutzbach et al. 2007, Wilson et al. 2024). While the flexible chamber design used for this dissertation enabled large-scale field measurements through its practicality, it introduced uncertainty in chamber volume estimation, which affected the flux accuracy. Future studies should therefore consider more static chamber designs, though capturing full methane-flux variability will ultimately require automated chamber systems (Koskinen et al. 2014, Savage et al. 2014).

Integrating automated chambers with continuous redox-potential measurements, IRIS sticks, and in situ planar optode imaging (Schmidt et al. 2010) could substantially improve temporal resolution and mechanistic understanding of the root-controlled methane fluxes.

The assessment of how two intertwined global-change pressures – warming and elevated atmospheric CO_2 – jointly influence methane cycling is essential to elucidate coastal marsh functioning under climate change. Elevated CO_2 in combination with increased temperatures has been shown to substantially decrease methane emissions from a C_3 plant dominated organic-rich brackish marsh (Noyce et al. 2023). These systems are broadly comparable to Baltic marshes, however, it remains unknown whether minerogenic salt marshes respond similarly particularly given the contrasting photosynthetic pathways of dominant species (C_4 *S. anglica* vs. C_3 *E. athericus*). Indeed, both species already exhibited altered methane fluxes under warming alone, with *S. anglica* showing increased emissions and *E. athericus* showing reduced methane uptake (Fig. 5.2c), consistent with studies that have shown methane production to be enhanced over

methanotrophy with warming. Warming in combination with elevated CO_2 could further enhance productivity in the C_3 species, increasing methane uptake through increases in ROL, as shown in *S. americanus* (Noyce et al. 2023). In contrast, *S. anglica*, as a C_4 species less sensitive to elevated CO_2, potentially increase methane production through increases in root exudation (Zhai et al. 2013, Wang et al. 2021). Understanding these divergent plant-specific responses is critical, as they may shift minerogenic salt marshes from functioning as carbon sinks toward becoming net carbon sources.

6.7 | SUPPLEMENT

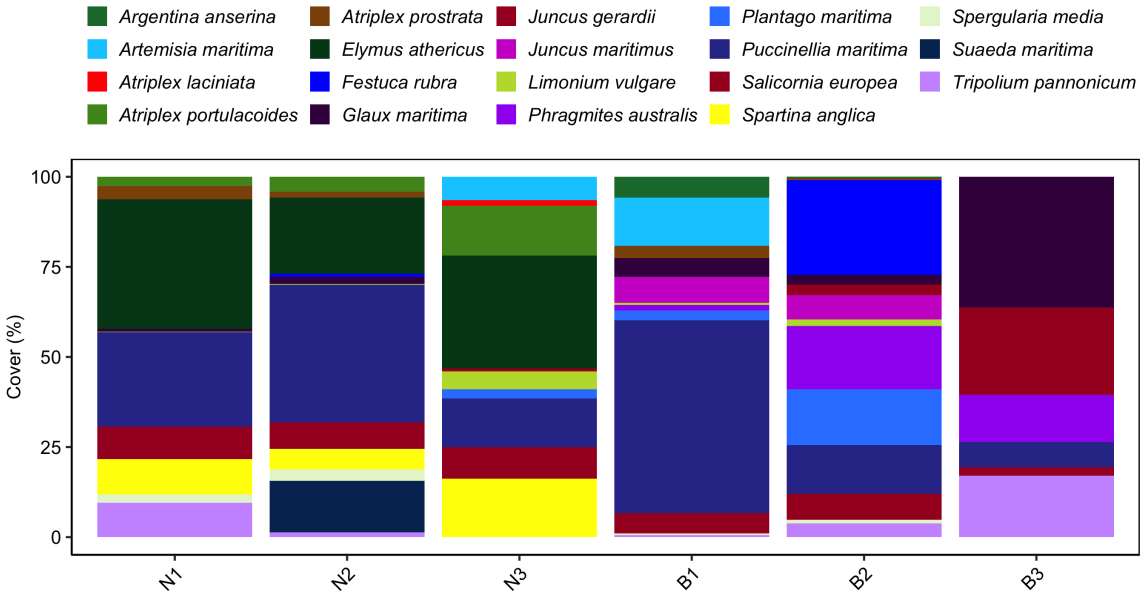

***FIGURE 6.S1** | Distribution of plant species cover at each study site. Species cover values are standardized to a sum of 100%. "High-flux" species are indicated in purple.*

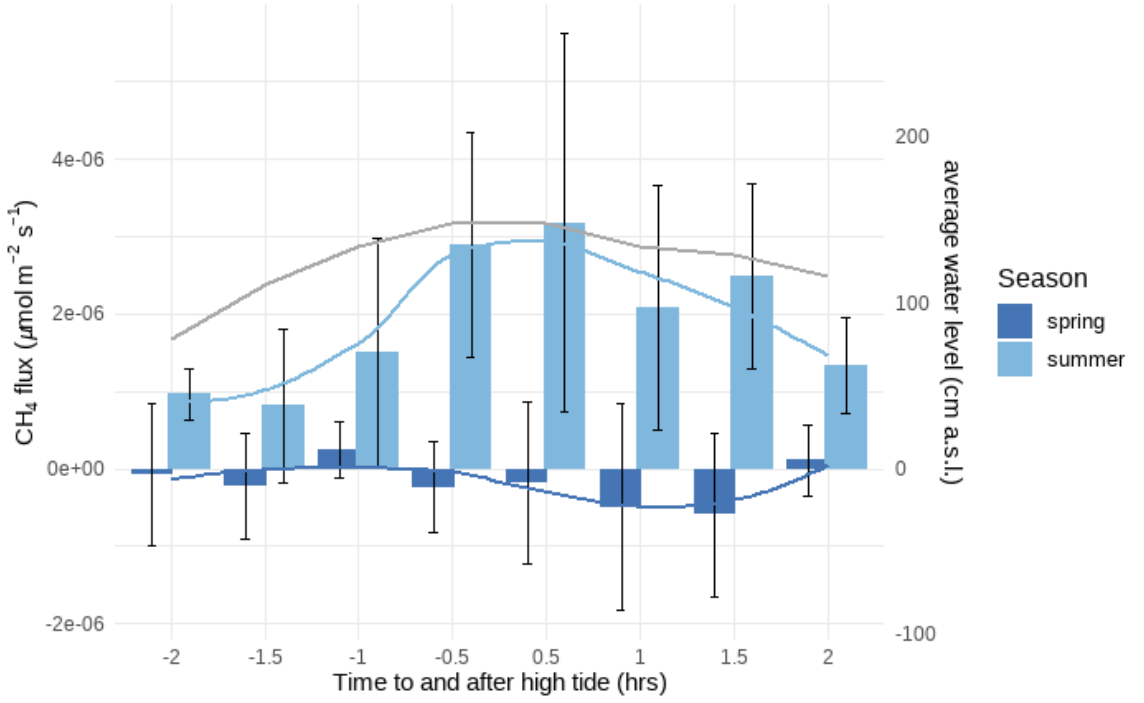

***FIGURE 6.S2** | Combined comparison of methane fluxes over a high tide. Measurements were combined for every half hour despite of the warming treatment. The fluxes were divided into spring (measurements taken between April and early June) and summer (measurements taken from July to September). The grey line shows an average water level height. Values over ~ 155 cm a.s.l. indicate that the tide was flooding the marsh zone. Spring fluxes are overall lower and even show methane uptake during ebbing. Summer methane fluxes are higher especially during high tide and ebbing.*

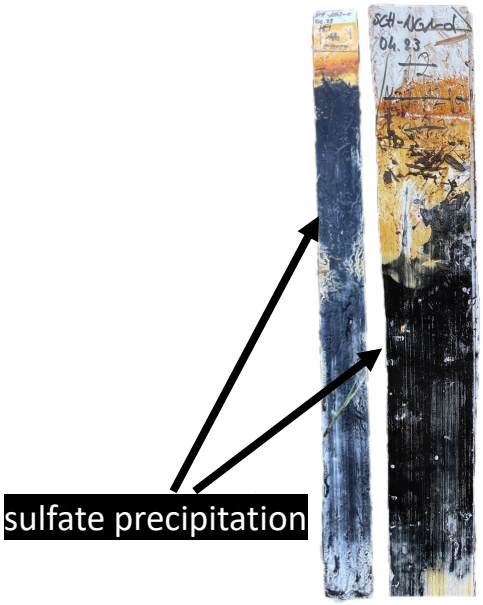

***FIGURE 6.S3** | Examples of sulfate precipitation on IRIS stick.*

***TABLE 6.S1** | Summary of plot-level belowground biomass (kg m $^{-2}$) across North Sea and Baltic Sea marsh plots, grouped by coast and dominant species. Shown are the number of plots, mean, standard deviation (SD), minimum, and maximum biomass values.*

Coast	Dominant species	Number of plots	Mean	SD	Min	Max
Baltic Sea	*Phragmites australis*	6	7.23	3.91	1.60	11.69
North Sea	*Tripolium pannonicum*	1	0.48			
Baltic Sea	*Tripolium pannonicum*	1	6.01			
Baltic Sea	*Juncus maritimus*	5	4.22	2.49	1.69	7.89
North Sea	*Spartina anglica*	7	2.82	0.87	1.09	3.84
North Sea	*Puccinellia maritima*	9	1.78	1.13	0.61	3.92
Baltic Sea	*Puccinellia maritima*	5	4.91	3.13	1.51	9.63
North Sea	*Elymus athericus*	11	1.61	0.77	0.98	3.39
North Sea	Other	3	4.31	1.56	2.61	5.67
Baltic Sea	Other	6	6.84	2.10	3.69	9.70

REFERENCES

<Dissertation_Druck_Mittmann-Götsch_signature.pdf>.

Afsar, M. Z., B. Vasilas, and Y. Jin. 2023. Organo-mineral associations and size-fractionated colloidal organic carbon dynamics in a redox-controlled wetland. Geoderma **439**.

Al-Haj, A. N., and R. W. Fulweiler. 2020. A synthesis of methane emissions from shallow vegetated coastal ecosystems. Glob Chang Biol **26**:2988–3005.

Allen, J. R. L. 2000. Morphodynamics of Holocene salt marshes: a review sketch from the Atlantic and Southern North Sea coasts of Europe. Quaternary Science Reviews **19**:1155–1231.

Alongi, D. M. 2020. Carbon Balance in Salt Marsh and Mangrove Ecosystems: A Global Synthesis. Journal of Marine Science and Engineering **8**.

Anderson, H. M., G. A. Cagle, E. L. W. Majumder, E. Silva, J. Dawson, P. Simon, and Z. B. Freedman. 2024. Root exudation and rhizosphere microbial assembly are influenced by novel plant trait diversity in carrot genotypes. Soil Biology and Biochemistry **197**.

Arias-Ortiz, A., J. Wolfe, S. D. Bridgham, S. Knox, G. McNicol, B. A. Needelman, J. Shahan, E. J. Stuart-Haentjens, L. Windham-Myers, P. Y. Oikawa, D. D. Baldocchi, J. S. Caplan, M. Capooci, K. M. Czapla, R. K. Derby, H. L. Diefenderfer, I. Forbrich, G. Groseclose, J. K. Keller, C. Kelley, A. E. Keshta, H. S. Kleiner, K. W. Krauss, R. R. Lane, S. Mack, S. Moseman-Valtierra, T. J. Mozdzer, P. Mueller, S. C. Neubauer, G. Noyce, K. V. R. Schafer, R. Sanders-DeMott, C. A. Schutte, R. Vargas, N. B. Weston, B. Wilson, J. P. Megonigal, and J. R. Holmquist. 2024. Methane fluxes in tidal marshes of the conterminous United States. Glob Chang Biol **30**:e17462.

Armstrong, W., D. Cousins, J. Armstrong, D. W. Turner, and P. M. Beckett. 2000. Oxygen distribution in wetland plant roots and permeability barriers to gas-exchange with the rhizosphere:: a microelectrode and modelling study with. Annals of Botany **86**:687–703.

Arnosti, C., B. B. Jorgensen, J. Sagemann, and B. Thamdrup. 1998. Temperature dependence of microbial degradation of organic matter in marine sediments: polysaccharide hydrolysis, oxygen consumption, and sulfate reduction. Marine Ecology Progress Series **165**:59–70.

Auman, A. J., S. Stolyar, A. M. Costello, and M. E. Lidstrom. 2000. Molecular characterization of methanotrophic isolates from freshwater lake sediment. Applied and Environmental Microbiology **67**:5253–5261.

Badri, D. V., and J. M. Vivanco. 2009. Regulation and function of root exudates. Plant, Cell & Environment **32**:666–681.

Bai, J., M. Luo, Y. Yang, S. Xiao, Z. Zhai, and J. Huang. 2021. Iron-bound carbon increases along a freshwater–oligohaline gradient in a subtropical tidal wetland. Soil Biology and Biochemistry **154**.

Bailey-Serres, J., and L. A. Voesenek. 2008. Flooding stress: acclimations and genetic diversity. Annu Rev Plant Biol **59**:313–339.

Bakker, J. P., M. Schrama, P. Esselink, P. Daniels, N. Bhola, S. Nolte, Y. de Vries, R. M. Veeneklaas, and M. Stock. 2019. Long-Term Effects of Sheep Grazing in Various Densities on Marsh Properties and Vegetation Dynamics in Two Different Salt-Marsh Zones. Estuaries and Coasts **43**:298–315.

Baldock, J. A., and J. O. Skjemstad. 2000. Role of the soil matrix and minerals in protecting natural organic materials against biological attack. Organic Geochemistry **31**:697–710.

Barba, J., P. E. Brewer, S. R. Pangala, and K. Machacova. 2024. Methane emissions from tree stems - current knowledge and challenges: an introduction to a Virtual Issue. New Phytol **241**:1377–1380.

Barbier, E. B. 2013. Valuing Ecosystem Services for Coastal Wetland Protection and Restoration: Progress and Challenges. Resources-Basel **2**:213–230.

Barr, K., and M. Bell. 2017. Neolithic and Bronze Age ungulate footprint-tracks of the Severn Estuary: Species, age, identification and the interpretation of husbandry practices. Environmental Archaeology **22**:1–14.

Bartlett, K. B., D. S. Bartlett, R. C. Harriss, and D. I. Sebacher. 1987. Methane emissions along a salt marsh salinity gradient. Biogeochemistry **4**:183–202.

Baumert, V. L., N. A. Vasilyeva, A. A. Vladimirov, I. C. Meier, I. Kögel-Knabner, and C. W. Mueller. 2018. Root Exudates Induce Soil Macroaggregation Facilitated by Fungi in Subsoil. Frontiers in Environmental Science **6**.

Bezbaruah, A. N., and T. C. Zhang. 2005. Quantification of oxygen release by bulrush (Scirpus validus) roots in a constructed treatment wetland. Biotechnol Bioeng **89**:308–318.

Bhullar, G. S., P. J. Edwards, and H. O. Venterink. 2014. Influence of Different Plant Species on Methane Emissions from Soil in a Restored Swiss Wetland. PLoS One **9**.

Bodegom, P. M. V., and A. J. M. Stams. 1999. Effects of Alternative Electron Acceptors and Temperature on Methanogenesis in Rice Paddy Soils. Chemosphere **39**:167–182.

Böttcher, M. E., H. J. Brumsack, and C. D. Dürselen. 2007. The isotopic composition of modern seawater sulfate: I. Coastal waters with special regard to the North Sea. Journal of Marine Systems **67**:73–82.

Bradley, P. M., and J. T. Morris. 1990. Influence of Oxygen and Sulfide Concentration on Nitrogen Uptake Kinetics in Spartina Alterniflora. Ecology **71**:282–287.

Bridgham, S. D., H. Cadillo-Quiroz, J. K. Keller, and Q. Zhuang. 2013. Methane emissions from wetlands: biogeochemical, microbial, and modeling perspectives from local to global scales. Glob Chang Biol **19**:1325–1346.

Bridgham, S. D. P. M., J; Keller, Jason K; Bliss, Norman B; Trettin, Carl. 2006. The carbon balance of North American wetlands.

Brix, H., B. K. Sorrell, and B. Lorenzen. 2001. Are Phragmites-dominated wetlands a net source or net sink of greenhouse gases? Aquatic Botany **69**:313–324.

Buczko, U., G. Jurasinski, S. Glatzel, and S. Karstens. 2022. Blue Carbon in Coastal Phragmites Wetlands Along the Southern Baltic Sea. Estuaries and Coasts **45**:2274–2282.

Bullock, A. L., A. E. Sutton-Grier, and J. P. Megonigal. 2013. Anaerobic Metabolism in Tidal Freshwater Wetlands: III. Temperature Regulation of Iron Cycling. Estuaries and Coasts **36**:482–490.

Busch, F. A., M. Holloway-Phillips, H. Stuart-Williams, and G. D. Farquhar. 2020. Revisiting carbon isotope discrimination in C3 plants shows respiration rules when photosynthesis is low. Nature Plants **6**:245–258.

Cai, M., X. Yin, X. Tang, C. Zhang, Q. Zheng, and M. Li. 2022. Metatranscriptomics reveals different features of methanogenic archaea among global vegetated coastal ecosystems. Sci Total Environ **802**:149848.

Canarini, A., C. Kaiser, A. Merchant, A. Richter, and W. Wanek. 2019. Root Exudation of Primary Metabolites: Mechanisms and Their Roles in Plant Responses to Environmental Stimuli. Front Plant Sci **10**:157.

Candry, P., B. Abrahamson, D. A. Stahl, and M. H. Winkler. 2023. Microbially mediated climate feedbacks from wetland ecosystems. Glob Chang Biol **29**:5169–5183.

Capooci, M., A. L. Seyfferth, C. Tobias, A. S. Wozniak, A. Hedgpeth, M. Bowen, J. F. Biddle, K. J. McFarlane, and R. Vargas. 2024. High methane concentrations in tidal salt marsh soils: Where does the methane go? Glob Chang Biol **30**:e17050.

Chapman, S. K., M. A. Hayes, B. Kelly, and J. A. Langley. 2019. Exploring the oxygen sensitivity of wetland soil carbon mineralization. Biol Lett **15**:20180407.

Chari, N. R., S. J. Tumber-Dávila, R. P. Phillips, T. L. Bauerle, M. Brunn, B. D. Hafner, T. Klein, S. Obersteiner, M. K. Reay, S. Ullah, and B. N. Taylor. 2024. Estimating the global root exudate carbon flux. Biogeochemistry **167**:895–908.

Chen, H., T. Zhu, B. Li, C. Fang, and M. Nie. 2020a. The thermal response of soil microbial methanogenesis decreases in magnitude with changing temperature. Nat Commun **11**:5733.

Chen, S., L. Liu, Y. Ma, Q. Zhuang, and N. J. Shurpali. 2024. Quantifying Global Wetland Methane Emissions With In Situ Methane Flux Data and Machine Learning Approaches. Earths Future **12**:e2023EF004330.

Chen, X., H. Y. H. Chen, C. Chen, Z. Ma, E. B. Searle, Z. Yu, and Z. Huang. 2020b. Effects of plant diversity on soil carbon in diverse ecosystems: a global meta-analysis. Biol Rev Camb Philos Soc **95**:167–183.

Chen, Y., C. Thompson, and M. Collins. 2019. Controls on creek margin stability by the root systems of saltmarsh vegetation, Beaulieu Estuary, Southern England. Anthropocene Coasts **2**:21–38.

Cheng, X. L., R. H. Peng, J. Q. Chen, Y. Q. Luo, Q. F. Zhang, S. Q. An, J. K. Chen, and B. Li. 2007. CH4 and N2O emissions from Spartina alterniflora and Phragmites australis in experimental mesocosms. Chemosphere **68**:420–427.

Chmura, G. L., S. C. Anisfeld, D. R. Cahoon, and J. C. Lynch. 2003. Global carbon sequestration in tidal, saline wetland soils. Global Biogeochemical Cycles **17**.

Colmer, T. D. 2003. Long-distance transport of gases in plants: a perspective on internal aeration and radial oxygen loss from roots. Plant, Cell & Environment **26**:17–36.

Comer-Warner, S. A., S. Ullah, W. Ampuero Reyes, S. Krause, and G. L. Chmura. 2022. Spartina alterniflora has the highest methane emissions in a St. Lawrence estuary salt marsh. Environmental Research: Ecology **1**.

Connor, R. F., G. L. Chmura, and C. B. Beecher. 2001. Carbon accumulation in bay of fundy salt marshes: Implications for restoration of reclaimed marshes. Global Biogeochemical Cycles **15**:943–954.

Conrad, R. 2023. Complexity of temperature dependence in methanogenic microbial environments. Front Microbiol **14**:1232946.

Cotrufo, M. F., M. D. Wallenstein, C. M. Boot, K. Denef, and E. Paul. 2013. The Microbial Efficiency-Matrix Stabilization (MEMS) framework integrates plant litter decomposition with soil organic matter stabilization: do labile plant inputs form stable soil organic matter? Glob Chang Biol **19**:988–995.

Covey, K. R., and J. P. Megonigal. 2019. Methane production and emissions in trees and forests. New Phytol **222**:35–51.

Cui, S. H., P. F. Liu, H. A. Guo, C. K. Nielsen, J. W. M. Pullens, Q. Chen, L. Pugliese, and S. B. Wu. 2024. Wetland hydrological dynamics and methane emissions. Communications Earth & Environment **5**.

Dacey, J. W. H., and M. J. Klug. 1979. Methane Efflux from Lake-Sediments through Water Lilies. Science **203**:1253–1255.

Davidson, E. A., D. R. Monteverde, and J. D. Semrau. 2024. Viability of enhancing methanotrophy in terrestrial ecosystems exposed to low concentrations of methane. Communications Earth & Environment **5**.

Davidson, K. E., M. S. Fowler, M. W. Skov, S. H. Doerr, N. Beaumont, J. N. Griffin, and J. Bennett. 2017. Livestock grazing alters multiple ecosystem properties and services in salt marshes: a meta-analysis. Journal of Applied Ecology **54**:1395–1405.

Davidson, N. C., and C. M. Finlayson. 2019. Updating global coastal wetland areas presented in Davidson and Finlayson (2018). Marine and Freshwater Research **70**:1195–1200.

Davidson, S. J., M. Smith, E. Prystupa, K. Murray, F. C. Nwaishi, R. M. Petrone, and M. Strack. 2021. High sulfate concentrations maintain low methane emissions at a constructed fen over the first seven years of ecosystem development. Science of the Total Environment **789**.

De Cáceres, M., and P. Legendre. 2009. Associations between species and groups of sites: indices and statistical inference. Ecology **90**:3566–3574.

De Deyn, G. B., J. H. Cornelissen, and R. D. Bardgett. 2008. Plant functional traits and soil carbon sequestration in contrasting biomes. Ecol Lett **11**:516–531.

Di Bella, C. E., A. M. Rodríguez, E. Jacobo, R. A. Golluscio, M. A. Taboada, and F. Nicholson. 2015. Impact of cattle grazing on temperate coastal salt marsh soils. Soil Use and Management **31**:299–307.

Dijkema, K. S. 1990. Salt and Brackish Marshes around the Baltic Sea and Adjacent Parts of the North-Sea - Their Vegetation and Management. Biological Conservation **51**:191–209.

Dijkema, K. S., A. S. Kers, and W. E. van Duin. 2010. Salt marshes: applied long-term monitoring. Wadden Sea Ecosystem Report 26:35–40.

Dong, W., J. Zhou, C. J. Zhang, Q. Yang, and M. Li. 2024. Methylotrophic substrates stimulated higher methane production than competitive substrates in mangrove sediments. Sci Total Environ **951**:175677.

Douglas Bates, M. M., Benjamin M. Bolker, Steven C. Walker. 2018. Fitting linear mixed-effects models using lme4. Journal of Statistical Software.

Duarte, C. M. 2017. Reviews and syntheses: Hidden forests, the role of vegetated coastal habitats in the ocean carbon budget. Biogeosciences **14**:301–310.

Duarte, C. M., I. J. Losada, I. E. Hendriks, I. Mazarrasa, and N. Marbà. 2013. The role of coastal plant communities for climate change mitigation and adaptation. Nature Climate Change **3**:961–968.

Duarte, C. M., J. J. Middelburg, and N. Caraco. 2005. Major role of marine vegetation on the oceanic carbon cycle. Biogeosciences.

Duarte, C. M., and Y. T. Prairie. 2005. Prevalence of Heterotrophy and Atmospheric CO2 Emissions from Aquatic Ecosystems. Ecosystems **8**:862–870.

Dubinin, A. V., M. N. Rimskaya-Korsakova, and L. S. Semilova. 2022. Sulfate-Chlorinity Ratio in the Black Sea Water and its Variability over the Last 70 Years. MORSKOY GIDROFIZICHESKIY ZHURNAL **38**.

Duffy, J. E., C. M. Godwin, and B. J. Cardinale. 2017. Biodiversity effects in the wild are common and as strong as key drivers of productivity. Nature **549**:261–264.

Eisenhauer, N., A. Lanoue, T. Strecker, S. Scheu, K. Steinauer, M. P. Thakur, and L. Mommer. 2017. Root biomass and exudates link plant diversity with soil bacterial and fungal biomass. Sci Rep **7**:44641.

Elschot, K., J. P. Bakker, S. Temmerman, J. van de Koppel, and T. J. Bouma. 2015. Ecosystem engineering by large grazers enhances carbon stocks in a tidal salt marsh. Marine Ecology Progress Series **537**:9–21.

Elschot, K., P. Esselink, J. Frikke, K. Jensen, M. Janinhoff-Verdaat, M. Paarup Thomsen, M. Padlat, J. T. van der Wal, W. E. Duin, M. E. B. van Puijenbroek, F. Rupprecht, and M. Stock. 2024. Salt Marshes. In: Wadden Sea Quality Status Report.

Elsey-Quirk, T., and V. Unger. 2018. Geomorphic influences on the contribution of vegetation to soil C accumulation and accretion in Spartina alterniflora marshes. Biogeosciences **15**:379–397.

Envicontrol. 2023. Microportable Greenhouse Gas Analyzer - LGR ICOSTM GLA131 Series - Measurement made easy. ABB Inc. Measurement & Analytics, Quebec, Canada.

Evans, C. D., M. Peacock, A. J. Baird, R. R. E. Artz, A. Burden, N. Callaghan, P. J. Chapman, H. M. Cooper, M. Coyle, E. Craig, A. Cumming, S. Dixon, V. Gauci, R. P. Grayson, C. Helfter, C. M. Heppell, J. Holden, D. L. Jones, J. Kaduk, P. Levy, R. Matthews, N. P. McNamara, T. Misselbrook, S. Oakley, S. E. Page, M. Rayment, L. M. Ridley, K. M. Stanley, J. L. Williamson, F. Worrall, and R. Morrison. 2021. Overriding water table control on managed peatland greenhouse gas emissions. Nature **593**:548–552.

Eyre, B. D., N. Camillini, R. N. Glud, and J. A. Rosentreter. 2023. The climate benefit of seagrass blue carbon is reduced by methane fluxes and enhanced by nitrous oxide fluxes. Communications Earth & Environment **4**.

Fiedler, J., R. Fuß, S. Glatzel, U. Hagemann, V. Huth, S. Jordan, G. Jurasinski, L. Kutzbach, M. Maier, K. Schäfer, T. Weber, and D. Weymann. 2022. BEST PRACTICE GUIDELINE Measurement of carbon dioxide, methane and nitrous oxide fluxes between soil-vegetation-systems and the atmosphere using non-steady state chambers. Deutsche Bodenkundliche Gesellschaft

(German Soil Science Society), Commission IV, Working Group Soil Gases, Task Force Standardisation.

Ford, H., A. Garbutt, M. Duggan-Edwards, J. F. Pagès, R. Harvey, C. Ladd, and M. W. Skov. 2019. Large-scale predictions of salt-marsh carbon stock based on simple observations of plant community and soil type. Biogeosciences **16**:425–436.

Ford, H., A. Garbutt, L. Jones, and D. L. Jones. 2012. Methane, carbon dioxide and nitrous oxide fluxes from a temperate salt marsh: Grazing management does not alter Global Warming Potential. Estuarine, Coastal and Shelf Science **113**:182–191.

Ford, H., A. Garbutt, C. Ladd, J. Malarkey, and M. W. Skov. 2016. Soil stabilization linked to plant diversity and environmental context in coastal wetlands. J Veg Sci **27**:259–268.

Fuchs, A., I. C. Davidson, J. P. Megonigal, J. L. Devaney, C. Simkanin, G. L. Noyce, M. Lu, and G. M. Cott. 2024. Stronger increase of methane emissions from coastal wetlands by non-native Spartina alterniflora than non-native Phragmites australis. Plants, People, Planet **7**:62–79.

Gao, Y., H. Wang, F. Yang, X. Dai, S. Meng, M. Hu, L. Kou, and X. Fu. 2024. Relationships between root exudation and root morphological and architectural traits vary with growing season. Tree Physiol **44**.

Ge, M., L. J. Ren, D. Yang, X. Z. Li, Y. Huang, J. W. Tang, and H. Brix. 2025. Invasion of species enhance blue carbon functions by increasing CO2 uptake and reducing methane emissions in Chinese and Danish coastal wetlands. Journal of Cleaner Production **508**.

Girkin, N. T., A. Siegenthaler, O. Lopez, A. Stott, N. Ostle, V. Gauci, and S. Sjögersten. 2025. Plant root carbon inputs drive methane production in tropical peatlands. Scientific Reports **15**.

Gotoh, S., and W. H. Patrick Jr. 1974. Transformation of Iron in a Waterlogged Soil as Influenced by Redox Potential and pH. Soil Science Society of America Journal **38**:66–71.

Granse, D., A. Wanner, M. Stock, K. Jensen, and P. Mueller. 2024. Plant-sediment interactions decouple inorganic from organic carbon stock development in salt marsh soils. Limnology and Oceanography Letters **9**:469–477.

Graversen, A. E. L., G. T. Banta, P. Masque, and D. Krause-Jensen. 2022. Carbon sequestration is not inhibited by livestock grazing in Danish salt marshes. Limnology and Oceanography **67**.

Grybos, M., M. Davranche, G. Gruau, P. Petitjean, and M. Pédrot. 2009. Increasing pH drives organic matter solubilization from wetland soils under reducing conditions. Geoderma **154**:13–19.

Guan, Y., S. Jin, Z. Zhang, S. Chen, Y. Chen, S. Liu, M. Fan, Y. Ding, and X. Yuan. 2025. A comprehensive review of climate warming and carbon dynamics in wetland ecosystems. Discover Sustainability **6**.

Guerrero-Cruz, S., A. Vaksmaa, M. A. Horn, H. Niemann, M. Pijuan, and A. Ho. 2021. Methanotrophs: Discoveries, Environmental Relevance, and a Perspective on Current and Future Applications. Front Microbiol **12**:678057.

Gunina, A., and Y. Kuzyakov. 2015. Sugars in soil and sweets for microorganisms: Review of origin, content, composition and fate. Soil Biology and Biochemistry **90**:87–100.

Guyonnet, J. P., A. A. M. Cantarel, L. Simon, and F. E. Z. Haichar. 2018. Root exudation rate as functional trait involved in plant nutrient-use strategy classification. Ecol Evol **8**:8573–8581.

Hall, S. J., and W. L. Silver. 2015. Reducing conditions, reactive metals, and their interactions can explain spatial patterns of surface soil carbon in a humid tropical forest. Biogeochemistry **125**:149–165.

Hamer, U., and B. Marschner. 2002. Priming effects of sugars, amino acids, organic acids and catechol on the mineralization of lignin and peat. Journal of Plant Nutrition and Soil Science **165**:261–268.

Hamer, U., and B. Marschner. 2005. Priming effects in soils after combined and repeated substrate additions. Geoderma **128**:38–51.

Hansen, K., C. Butzeck, A. Eschenbach, A. Gröngröft, K. Jensen, and E.-M. Pfeiffer. 2017. Factors influencing the organic carbon pools in tidal marsh soils of the Elbe estuary (Germany). Journal of Soils and Sediments **17**:47–60.

Harvey, R. J., A. Garbutt, S. J. Hawkins, and M. W. Skov. 2019. No Detectable Broad-Scale Effect of Livestock Grazing on Soil Blue-Carbon Stock in Salt Marshes. Frontiers in Ecology and Evolution **7**.

Haviland, K. A., and G. L. Noyce. 2024. Assessing root-soil interactions in wetland plants: root exudation and radial oxygen loss. Biogeosciences **21**:5185–5198.

He, Q., A. H. Altieri, and B. S. Cui. 2015. Herbivory drives zonation of stress-tolerant marsh plants. Ecology **96**:1318–1328.

Heinzle, J., X. Liu, Y. Tian, S. Kwatcho Kengdo, B. Heinze, A. Nirschi, W. Borken, E. Inselsbacher, W. Wanek, and A. Schindlbacher. 2023. Increase in fine root biomass enhances root exudation by long-term soil warming in a temperate forest. Frontiers in Forests and Global Change **6**.

Hemingway, J. D., D. H. Rothman, K. E. Grant, S. Z. Rosengard, T. I. Eglinton, L. A. Derry, and V. V. Galy. 2019. Mineral protection regulates long-term global preservation of natural organic carbon. Nature **570**:228–231.

Hemminga, M. A., and G. J. C. Buth. 1991. Decomposition in salt marsh ecosystems of the S.W. Netherlands: the effects of biotic and abiotic factors. Vegetation **92**:73–83.

Henneberg, A., B. K. Sorrell, and H. Brix. 2012. Internal methane transport through Juncus effusus: experimental manipulation of morphological barriers to test above- and below-ground diffusion limitation. New Phytologist **196**:799–806.

Hinsinger, P., C. Plassard, and B. Jaillard. 2006. Rhizosphere: A new frontier for soil biogeochemistry. Journal of Geochemical Exploration **88**:210–213.

Hirano, S., N. Matsumoto, M. Morita, K. Sasaki, and N. Ohmura. 2013. Electrochemical control of redox potential affects methanogenesis of the hydrogenotrophic methanogen Methanothermobacter thermautotrophicus. Lett Appl Microbiol **56**:315–321.

Hopple, A. M., R. M. Wilson, M. Kolton, C. A. Zalman, J. P. Chanton, J. Kostka, P. J. Hanson, J. K. Keller, and S. D. Bridgham. 2020. Massive peatland carbon banks vulnerable to rising temperatures. Nat Commun **11**:2373.

Howard, J., A. Sutton-Grier, D. Herr, J. Kleypas, E. Landis, E. McLeod, E. Pidgeon, and S. Simpson. 2017. Clarifying the role of coastal and marine systems in climate mitigation. Frontiers in Ecology and the Environment **15**:42–50.

Hulisz, P., A. Piernik, J. Mantilla-Contreras, and T. Elvisto. 2016. Main Driving Factors for Seacoast Vegetation in the Southern and Eastern Baltic. Wetlands **36**:909–919.

Inglett, K. S., P. W. Inglett, K. R. Reddy, and T. Z. Osborne. 2011. Temperature sensitivity of greenhouse gas production in wetland soils of different vegetation. Biogeochemistry **108**:77–90.

Jeffrey, L. C., D. T. Maher, E. Chiri, P. M. Leung, P. A. Nauer, S. K. Arndt, D. R. Tait, C. Greening, and S. G. Johnston. 2021. Bark-dwelling methanotrophic bacteria decrease methane emissions from trees. Nat Commun **12**:2127.

Jenkinson, B. J., and D. P. Franzmeier. 2006. Development and Evaluation of Iron-Coated Tubes that Indicate Reduction in Soils. Soil Science Society of America Journal **70**:183–191.

Jentzsch, K., L. van Delden, M. Fuchs, and C. C. Treat. 2025. An expert survey on chamber measurement techniques and data handling procedures for methane fluxes. Earth System Science Data **17**:2331–2372.

Jones, D. L., A. Hodge, and Y. Kuzyakov. 2004. Plant and mycorrhizal regulation of rhizodeposition. New Phytol **163**:459–480.

Jones, D. L., C. Nguyen, and R. D. Finlay. 2009. Carbon flow in the rhizosphere: carbon trading at the soil–root interface. Plant and Soil **321**:5–33.

Keiluweit, M., J. J. Bougoure, P. S. Nico, J. Pett-Ridge, P. K. Weber, and M. Kleber. 2015. Mineral protection of soil carbon counteracted by root exudates. Nature Climate Change **5**:588–595.

Keiluweit, M., P. S. Nico, M. Kleber, and S. Fendorf. 2016. Are oxygen limitations under recognized regulators of organic carbon turnover in upland soils? Biogeochemistry **127**:157–171.

Keiluweit, M., T. Wanzek, M. Kleber, P. Nico, and S. Fendorf. 2017. Anaerobic microsites have an unaccounted role in soil carbon stabilization. Nat Commun **8**:1771.

Kelleway, J. J., N. Saintilan, P. I. Macreadie, and P. J. Ralph. 2016. Sedimentary Factors are Key Predictors of Carbon Storage in SE Australian Saltmarshes. Ecosystems **19**:865–880.

Keshta, A., K. Koop-Jakobsen, J. Titschack, P. Mueller, K. Jensen, A. Baldwin, and S. Nolte. 2020. Ungrazed salt marsh has well connected soil pores and less dense sediment compared with grazed salt marsh: a CT scanning study. Estuarine, Coastal and Shelf Science **245**.

Keshta, A. E., S. A. Yarwood, and A. H. Baldwin. 2023. Methane Emissions Are Highly Variable across Wetland Habitats in Natural and Restored Tidal Freshwater Wetlands. Wetlands **43**.

Khan, N. S., C. H. Vane, and B. P. Horton. 2015. Stable carbon isotope and C/N geochemistry of coastal wetland sediments as a sea-level indicator. Pages 295–311 *in* I. Shennan, A. Long, and B. P. Horton, editors. Handbook of seaVlevel research. Wiley-Blackwell.

Kim, J., D. R. Chaudhary, J. Lee, C. Byun, W. Ding, B. O. Kwon, J. S. Khim, and H. Kang. 2020a. Microbial mechanism for enhanced methane emission in deep soil layer of Phragmites-introduced tidal marsh. Environ Int **134**:105251.

Kim, J., J. Lee, J. Yun, Y. R. Yang, W. X. Ding, J. J. Yuan, and H. Kang. 2020b. Mechanisms of enhanced methane emission due to introduction of Spartina anglica and Phragmites australis in a temperate tidal salt marsh. Ecological Engineering **153**.

King, G. M., and W. J. Wiebe. 1980. Regulation of Sulfate Concentrations and Methanogenesis in Salt-Marsh Soils. Estuarine and Coastal Marine Science **10**:215–223.

Kirwan, M. L., and J. P. Megonigal. 2013. Tidal wetland stability in the face of human impacts and sea-level rise. Nature **504**:53–60.

Kirwan, M. L., S. Temmerman, E. E. Skeehan, G. R. Guntenspergen, and S. Fagherazzi. 2016. Overestimation of marsh vulnerability to sea level rise. Nature Climate Change **6**:253–260.

Knittel, K., and A. Boetius. 2009. Anaerobic oxidation of methane: progress with an unknown process. Annu Rev Microbiol **63**:311–334.

Koop-Jakobsen, K., J. Fischer, and F. Wenzhofer. 2017. Survey of sediment oxygenation in rhizospheres of the saltmarsh grass - Spartina anglica. Sci Total Environ **589**:191–199.

Koop-Jakobsen, K., R. J. Meier, and P. Mueller. 2021. Plant-Mediated Rhizosphere Oxygenation in the Native Invasive Salt Marsh Grass. Frontiers in Plant Science **12**.

Koskinen, M., K. Minkkinen, P. Ojanen, M. Kämäräinen, T. Laurila, and A. Lohila. 2014. Measurements of CO2 exchange with an automated chamber system throughout the year: challenges in measuring night-time respiration on porous peat soil. Biogeosciences **11**:347–363.

Koyama, A., N. G. Johnson, P. Brewer, C. T. Webb, and J. C. von Fischer. 2024. Biological and physical controls of methane uptake in grassland soils across the US Great Plains. Ecosphere **15**.

Koyama, T., K. L. Enggrob, J. Rasmussen, J. T. Martins, and L. Peixoto. 2025. Substrate quantity and quality affect microbial carbon use efficiency and priming effects of root exudates investigated with microdialysis. Soil Biology & Biochemistry **209**.

Kristensen, E., S. I. Ahmed, and A. H. Devol. 1995. Aerobic and anaerobic decomposition of organic matter in marine sediment: Which is fastest? Limnology and Oceanography **40**:1430–1437.

Kristjansson, J. K., and P. Schönheit. 1983. Why do sulfate-reducing bacteria outcompete methanogenic bacteria for substrates? Oecologia **60**:264–266.

Kroeger, K. D., S. Crooks, S. Moseman-Valtierra, and J. Tang. 2017. Restoring tides to reduce methane emissions in impounded wetlands: A new and potent Blue Carbon climate change intervention. Sci Rep **7**:11914.

Krüger, N., K.-H. Knorr, and P. Mueller. 2025. Opposite priming responses to labile carbon versus oxygen pulses in anoxic peat. Soil Biology and Biochemistry **202**.

Kutzbach, L., J. Schneider, T. Sachs, M. Giebels, H. Nykänen, N. J. Shurpali, P. J. Martikainen, J. Alm, and M. Wilmking. 2007. CO2 flux determination by

closed-chamber methods can be seriously biased by inappropriate application of linear regression. Biogeosciences **4**:1005–1025.
Kuzyakov, Y., and O. Gavrichkova. 2010. REVIEW: Time lag between photosynthesis and carbon dioxide efflux from soil: a review of mechanisms and controls. Global Change Biology **16**:3386–3406.
Laanbroek, H. J. 2010. Methane emission from natural wetlands: interplay between emergent macrophytes and soil microbial processes. A mini-review. Ann Bot **105**:141–153.
Lacroix, E. M., J. Frei, E. van der Loo, L. Kocsis, and M. Keiluweit. 2025. Root exudation and fine texture interact to form anoxic microsites in rhizosphere soil. Soil Biology and Biochemistry **211**.
LaCroix, R. E., M. M. Tfaily, M. McCreight, M. E. Jones, L. Spokas, and M. Keiluweit. 2019. Shifting mineral and redox controls on carbon cycling in seasonally flooded mineral soils. Biogeosciences **16**:2573–2589.
Lai, W.-L., Y. Zhang, and Z.-H. Chen. 2012. Radial oxygen loss, photosynthesis, and nutrient removal of 35 wetland plants. Ecological Engineering **39**:24–30.
Lalonde, K., A. Mucci, A. Ouellet, and Y. Gelinas. 2012. Preservation of organic matter in sediments promoted by iron. Nature **483**:198–200.
Lange, M., N. Eisenhauer, C. A. Sierra, H. Bessler, C. Engels, R. I. Griffiths, P. G. Mellado-Vazquez, A. A. Malik, J. Roy, S. Scheu, S. Steinbeiss, B. C. Thomson, S. E. Trumbore, and G. Gleixner. 2015. Plant diversity increases soil microbial activity and soil carbon storage. Nat Commun **6**:6707.
Langley, J. A., K. L. McKee, D. R. Cahoon, J. A. Cherry, and J. P. Megonigal. 2009. Elevated CO2 stimulates marsh elevation gain, counterbalancing sea-level rise. PNAS **106**:6182– 6186.
Langley, J. A., and J. P. Megonigal. 2010. Ecosystem response to elevated CO(2) levels limited by nitrogen-induced plant species shift. Nature **466**:96–99.
Le Mer, J., and P. Roger. 2001. Production, oxidation, emission and consumption of methane by soils: A review. Eur. J. Soil Biol. **37**:25–50.
Lee, J., Y. Yang, H. Kang, G. L. Noyce, and J. P. Megonigal. 2025. Climate-induced shifts in sulfate dynamics regulate anaerobic methane oxidation in a coastal wetland. Science Advances **11**.
Lehmann, J., and M. Kleber. 2015. The contentious nature of soil organic matter. Nature **528**:60–68.
Lei, X., Y. T. Shen, J. N. Zhao, J. J. Huang, H. Wang, Y. Yu, and C. W. Xiao. 2023. Root Exudates Mediate the Processes of Soil Organic Carbon Input and Efflux. Plants-Basel **12**.
Leiva-Dueñas, C., A. E. L. Graversen, G. T. Banta, J. N. Hansen, M. L. K. Schrøter, P. Masqué, M. Holmer, and D. Krause-Jensen. 2024. Region-specific drivers cause low organic carbon stocks and sequestration rates in the saltmarsh soils of southern Scandinavia. Limnology and Oceanography **69**:290–308.
Leydena, E., J. Farkaš, J. Hutsonc, and L. M. Mosleya. 2023. Controls on sulfide accumulation in coastal soils during simulated sea level rise. Geochimica et Cosmochimica Acta **347**:88–101.
Li, C., C. Liu, C. Peng, T. Li, B. Xie, and Z. Liu. 2025a. Responses of the functional traits of wetland plants to variations in water levels and regimes—A global synthesis. Ecological Informatics **90**.

Li, J., H. Zhang, W. Xie, C. Liu, X. Liu, X. Zhang, L. Li, and G. Pan. 2024. Elevated CO(2) increases soil redox potential by promoting root radial oxygen loss in paddy field. J Environ Sci (China) **136**:11–20.

Li, L., W. Han, N. Thevs, X. Jia, C. Ji, D. Jin, P. He, A. O. Schmitt, G. T. Cirella, and S. Zerbe. 2014. A comparison of the functional traits of common reed (Phragmites australis) in northern China: aquatic vs. terrestrial ecotypes. PLoS One **9**:e89063.

Li, M., F. Li, A. Malhotra, S. H. Knox, R. Stern, and R. B. Jackson. 2025b. Key Environmental and Ecological Variables of Wetland CH4 and CO2 Fluxes Change With Warming. Earth's Future **13**.

LI-COR-Environmental. 2023. LI-7810 CO_2/CH_4/H_2O Gas Analyzer Instruction Manual. LI-COR Environmental, Lincoln, NE, USA.

Liebner, S., J. Zeyer, D. Wagner, C. Schubert, E.-M. Pfeiffer, and C. Knoblauch. 2011. Methane oxidation associated with submerged brown mosses reduces methane emissions from Siberian polygonal tundra. Journal of Ecology **99**:914–922.

Lin, Y., A. N. Campbell, A. Bhattacharyya, N. DiDonato, A. M. Thompson, M. M. Tfaily, P. S. Nico, W. L. Silver, and J. Pett-Ridge. 2021. Differential effects of redox conditions on the decomposition of litter and soil organic matter. Biogeochemistry **154**:1–15.

Liu, L., D. Wang, S. Chen, Z. Yu, Y. Xu, Y. Li, Z. Ge, and Z. Chen. 2019. Methane Emissions from Estuarine Coastal Wetlands: Implications for Global Change Effect. Soil Science Society of America Journal **83**:1368–1377.

Logemann, E. L., C. Goesele, K. Jensen, and P. Mueller. 2025. Soil Organic Carbon Stocks of German Salt Marshes: A Comparative Study Along Low- and High-Energy Coastlines. Journal of Geophysical Research-Biogeosciences **130**.

Loreau, M., and A. Hector. 2001. Partitioning selection and complementarity in biodiversity experiments. Nature **412(6842)**:72–76.

Lovelock, C. E., and C. M. Duarte. 2019. Dimensions of Blue Carbon and emerging perspectives. Biol Lett **15**:20180781.

Lovelock, C. E., J. W. Fourqurean, and J. T. Morris. 2017. Modeled CO2 Emissions from Coastal Wetland Transitions to Other Land Uses: Tidal Marshes, Mangrove Forests, and Seagrass Beds. Frontiers in Marine Science **4**.

Lovelock, C. E., and R. Reef. 2020. Variable Impacts of Climate Change on Blue Carbon. One Earth **3**:195–211.

Ludwiczak, A., P. Kapusta, P. Chapko, J. Wojtasik, A. Wojciechowska, and A. Piernik. 2024. Parental environment as a factor shaping salinity tolerance in halophyte Tripolium pannonicum L. Environmental and Experimental Botany **228**.

Ma, K., and Y. Lu. 2011. Regulation of microbial methane production and oxidation by intermittent drainage in rice field soil. FEMS Microbiol Ecol **75**:446–456.

Määttä, T., and A. Malhotra. 2024. The hidden roots of wetland methane emissions. Glob Chang Biol **30**:e17127.

Macreadie, P. I., A. Anton, J. A. Raven, N. Beaumont, R. M. Connolly, D. A. Friess, J. J. Kelleway, H. Kennedy, T. Kuwae, P. S. Lavery, C. E. Lovelock, D. A. Smale, E. T. Apostolaki, T. B. Atwood, J. Baldock, T. S. Bianchi, G. L. Chmura, B. D. Eyre, J. W. Fourqurean, J. M. Hall-Spencer, M. Huxham, I. E. Hendriks, D. Krause-

Jensen, D. Laffoley, T. Luisetti, N. Marba, P. Masque, K. J. McGlathery, J. P. Megonigal, D. Murdiyarso, B. D. Russell, R. Santos, O. Serrano, B. R. Silliman, K. Watanabe, and C. M. Duarte. 2019. The future of Blue Carbon science. Nat Commun **10**:3998.

Macreadie, P. I., M. D. P. Costa, T. B. Atwood, D. A. Friess, J. J. Kelleway, H. Kennedy, C. E. Lovelock, O. Serrano, and C. M. Duarte. 2021. Blue carbon as a natural climate solution. Nature Reviews Earth & Environment **2**:826–839.

Maher, D. T., M. Call, I. R. Santos, and C. J. Sanders. 2018. Beyond burial: lateral exchange is a significant atmospheric carbon sink in mangrove forests. Biol Lett **14**.

Maher, D. T., J. Z. Sippo, D. R. Tait, C. Holloway, and I. R. Santos. 2016. Pristine mangrove creek waters are a sink of nitrous oxide. Sci Rep **6**:25701.

Maier, M., T. K. D. Weber, J. Fiedler, R. Fuß, S. Glatzel, V. Huth, S. Jordan, G. Jurasinski, L. Kutzbach, K. Schäfer, D. Weymann, and U. Hagemann. 2022. Introduction of a guideline for measurements of greenhouse gas fluxes from soils using non-steady-state chambers. Journal of Plant Nutrition and Soil Science **185**:447–461.

Mansfeldt, T. 2003. In situ long-term redox potential measurements in a dyked marsh soil. Journal of Plant Nutrition and Soil Science **166**:210–219.

Martinez-Cruz, K., M. C. Leewis, I. C. Herriott, A. Sepulveda-Jauregui, K. W. Anthony, F. Thalasso, and M. B. Leigh. 2017. Anaerobic oxidation of methane by aerobic methanotrophs in sub-Arctic lake sediments. Sci Total Environ **607-608**:23–31.

Mason, V. G., K. A. Wood, L. L. Jupe, A. Burden, and M. W. Skov. 2022. Saltmarsh blue carbon in UK and NW Europe—Evidence synthesis for a UK saltmarsh carbon code. Report to the natural environment Investment Readiness Fund. UK Centre for Ecology & Hydrology.

Maxwell, T. L., A. S. Rovai, M. F. Adame, J. B. Adams, J. Alvarez-Rogel, W. E. N. Austin, K. Beasy, F. Boscutti, M. E. Bottcher, T. J. Bouma, R. H. Bulmer, A. Burden, S. A. Burke, S. Camacho, D. R. Chaudhary, G. L. Chmura, M. Copertino, G. M. Cott, C. Craft, J. Day, C. B. de Los Santos, L. Denis, W. Ding, J. C. Ellison, C. J. Ewers Lewis, L. Giani, M. Gispert, S. Gontharet, J. A. Gonzalez-Perez, M. N. Gonzalez-Alcaraz, C. Gorham, A. E. L. Graversen, A. Grey, R. Guerra, Q. He, J. R. Holmquist, A. R. Jones, J. A. Juanes, B. P. Kelleher, K. E. Kohfeld, D. Krause-Jensen, A. Lafratta, P. S. Lavery, E. A. Laws, C. Leiva-Duenas, P. S. Loh, C. E. Lovelock, C. J. Lundquist, P. I. Macreadie, I. Mazarrasa, J. P. Megonigal, J. M. Neto, J. Nogueira, M. J. Osland, J. F. Pages, N. Perera, E. M. Pfeiffer, T. Pollmann, J. L. Raw, M. Recio, A. C. Ruiz-Fernandez, S. K. Russell, J. M. Rybczyk, M. Sammul, C. Sanders, R. Santos, O. Serrano, M. Siewert, C. Smeaton, Z. Song, C. Trasar-Cepeda, R. R. Twilley, M. Van de Broek, S. Vitti, L. V. Antisari, B. Voltz, C. N. Wails, R. D. Ward, M. Ward, J. Wolfe, R. Yang, S. Zubrzycki, E. Landis, L. Smart, M. Spalding, and T. A. Worthington. 2023. Global dataset of soil organic carbon in tidal marshes. Sci Data **10**:797.

McLeod, E., G. L. Chmura, S. Bouillon, R. Salm, M. Björk, C. M. Duarte, C. E. Lovelock, W. H. Schlesinger, and B. R. Silliman. 2011. A blueprint for blue carbon: toward an improved understanding of the role of vegetated coastal

habitats in sequestering CO2. Frontiers in Ecology and the Environment **9**:552–560.

McOwen, C. J., L. V. Weatherdon, J. V. Bochove, E. Sullivan, S. Blyth, C. Zockler, D. Stanwell-Smith, N. Kingston, C. S. Martin, M. Spalding, and S. Fletcher. 2017. A global map of saltmarshes. Biodivers Data J:e11764.

McTigue, N. D., Q. A. Walker, and C. A. Currin. 2021. Refining Estimates of Greenhouse Gas Emissions From Salt Marsh "Blue Carbon" Erosion and Decomposition. Frontiers in Marine Science **8**.

Megonigal, J. P., M. E. Hines, and P. T. Visscher. 2004. Linkages to trace gases and aerobic processes. Pages 350–362 Treatise on Geochemistry. Elsevier.

Megonigal, J. P., and W. H. Schlesinger. 2002. Methane-limited methanotrophy in tidal freshwater swamps. Global Biogeochemical Cycles **16**.

Menzel, A. C., E. J. M. Ostertag, P. Mueller, S. Nolte, R. Rich, and K. Jensen. 2025. Hydrology mediates salt marsh belowground biomass response to warming. Limnology and Oceanography **70**:1725–1739.

Metje, M., and P. Frenzel. 2005. Effect of temperature on anaerobic ethanol oxidation and methanogenesis in acidic peat from a northern wetland. Appl Environ Microbiol **71**:8191–8200.

Mitsch, W. J. G., J.G., Anderson, C.J. & Zhang, L. . 2009. Wetland Ecosystems.

Mittmann-Goetsch, J., P. Mueller, K. Jensen, S. Liebner, S. Thomsen, R. Rich, A. Bartholomaus, J. Jaitner, and V. Unger. 2025. Hydrology masks warming effects on microbial communities in salt marsh soils. FEMS Microbiol Ecol **101**.

Mittmann-Goetsch, J., M. Wilson, K. Jensen, and P. Mueller. 2024. Root-Driven Soil Reduction in Wadden Sea Salt Marshes. Wetlands **44**.

Mozdzer, T. J., J. Meschter, A. H. Baldwin, J. S. Caplan, and J. P. Megonigal. 2023. Mining of Deep Nitrogen Facilitates Phragmites australis Invasion in Coastal Saltmarshes. Estuaries and Coasts **46**:998–1008.

Mueller, P., H. T. Do, K. Jensen, and S. Nolte. 2019a. Origin of organic carbon in the topsoil of Wadden Sea salt marshes. Marine Ecology Progress Series **624**:39–50.

Mueller, P., D. Granse, S. Nolte, H. T. Do, M. Weingartner, S. Hoth, and K. Jensen. 2017. Top-down control of carbon sequestration: grazing affects microbial structure and function in salt marsh soils. Ecological Applications **27**:1435–1450.

Mueller, P., D. Granse, S. Nolte, M. Weingartner, S. Hoth, and K. Jensen. 2020a. Unrecognized controls on microbial functioning in Blue Carbon ecosystems: The role of mineral enzyme stabilization and allochthonous substrate supply. Ecol Evol **10**:998–1011.

Mueller, P., K. Jensen, and J. P. Megonigal. 2016. Plants mediate soil organic matter decomposition in response to sea level rise. Glob Chang Biol **22**:404–414.

Mueller, P., L. Kutzbach, T. J. Mozdzer, E. Jespersen, D. C. Barber, and F. Eller. 2023. Minerogenic salt marshes can function as important inorganic carbon stores. Limnology and Oceanography **68**:942–952.

Mueller, P., N. Ladiges, A. Jack, G. Schmiedl, L. Kutzbach, K. Jensen, and S. Nolte. 2019b. Assessing the long-term carbon-sequestration potential of the semi-natural salt marshes in the European Wadden Sea. Ecosphere **10**.

Mueller, P., and J. P. Megonigal. 2024. Redox control on rhizosphere priming in wetlands. Nature Geoscience **17**:1209–1217.

Mueller, P., T. J. Mozdzer, J. A. Langley, L. R. Aoki, G. L. Noyce, and J. P. Megonigal. 2020b. Plant species determine tidal wetland methane response to sea level rise. Nat Commun **11**:5154.

Murray, R. H., D. V. Erler, and B. D. Eyre. 2015. Nitrous oxide fluxes in estuarine environments: response to global change. Glob Chang Biol **21**:3219–3245.

Myhre, G., D. Shindell, F.-M. Bréon, W. Collins, J. S. Fuglestvedt, J. Huang, D. Koch, J.-F. Lamarque, D. Lee, B. Mendoza, T. Nakajima, A. Robock, G. Stephens, T. Takemura, and H. Zhang. 2013. Anthropogenic and natural radiative forcing. Pages 659–740 *in* T. F. Stocker, D. Qin, G.-K. Plattner, M. Tignor, S. K. Allen, J. Boschung, A. Nauels, Y. Xia, V. Bex, and P. M. Midgley, editors. Climate Change 2013: The Physical Science Basis. Cambridge University Press, Cambridge, UK.

Nahlik, A. M., and M. S. Fennessy. 2016. Carbon storage in US wetlands. Nat Commun **7**:13835.

Needelman, B. A., I. M. Emmer, S. Emmett-Mattox, S. Crooks, J. P. Megonigal, D. Myers, M. P. J. Oreska, and K. McGlathery. 2018. The Science and Policy of the Verified Carbon Standard Methodology for Tidal Wetland and Seagrass Restoration. Estuaries and Coasts **41**:2159–2171.

Neiske, F., M. Seedtke, A. Eschenbach, M. Wilson, K. Jensen, and J. N. Becker. 2025. Soil organic carbon stocks and stabilization mechanisms in tidal marshes along estuarine gradients. Geoderma **456**.

Nellemann, C., E. Corcoran, C. M. Duarte, L. Valdes, C. De Young, L. Fonseca, and G. Grimsditch. 2009. Blue carbon. A rapid response assessment. United Nations Environment Programme, GRID-Arendal.

Neubauer, S. C., and J. P. Megonigal. 2015. Moving Beyond Global Warming Potentials to Quantify the Climatic Role of Ecosystems. Ecosystems **18**:1000–1013.

Neubauer, S. C., and J. P. Megonigal. 2021. Biogeochemistry of wetland carbon preservation and flux. Pages 33–71 *in* K. W. Krauss, Z. Zhu, and L. Camille, editors. Wetland Carbon and Environmental Management. Wiley.

Ning, Z. H., T. Xie, Z. Z. Liu, J. H. Bai, and B. S. Cui. 2019. Native herbivores enhance the resistance of an anthropogenically disturbed salt marsh to invasion. Ecosphere **10**.

Nolte, S., P. Esselink, J. P. Bakker, and C. Smit. 2014. Effects of livestock species and stocking density on accretion rates in grazed salt marshes. Estuarine, Coastal and Shelf Science **152**:109–115.

Nolte, S., E. C. Koppenaal, P. Esselink, K. S. Dijkema, M. Schuerch, A. V. De Groot, J. P. Bakker, and S. Temmerman. 2013a. Measuring sedimentation in tidal marshes: a review on methods and their applicability in biogeomorphological studies. Journal of Coastal Conservation **17**:301–325.

Nolte, S., F. Müller, M. Schuerch, A. Wanner, P. Esselink, J. P. Bakker, and K. Jensen. 2013b. Does livestock grazing affect sediment deposition and accretion rates in salt marshes? Estuarine, Coastal and Shelf Science **135**:296–305.

Noyce, G. L., and J. P. Megonigal. 2021. Biogeochemical and plant trait mechanisms drive enhanced methane emissions in response to whole-ecosystem warming. Biogeosciences **18**:2449–2463.

Noyce, G. L., A. J. Smith, M. L. Kirwan, R. L. Rich, and J. P. Megonigal. 2023. Oxygen priming induced by elevated CO2 reduces carbon accumulation and methane emissions in coastal wetlands. Nature Geoscience **16**:63–68.

O'Leary, M. H. 1998. Carbon Isotopes in Photosynthesis. BioScience **38**:328–336.

Oburger, E., and D. L. Jones. 2018. Sampling root exudates – Mission impossible? Rhizosphere **6**:116–133.

Olff, H., J. De Leeuw, J. P. Bakker, R. J. Platerink, and H. J. van Wijnen. 1997. Vegetation Succession and Herbivory in a Salt Marsh: Changes Induced by Sea Level Rise and Silt Deposition Along an Elevational Gradient. Journal of Ecology **85**:799–814.

Oremland, R. S., L. M. Marsh , and S. Polcin. 1982. Methane production and simultaneous sulphate reduction in anoxic, salt marsh sediments.

Oremland, R. S., and S. Polcin. 1982. Methanogenesis and Sulfate Reduction: Competitive and Noncompetitive Substrates in Estuarine Sediments. Applied and Environmental Microbiology **Vol. 44**:1270–1276.

Ouyang, X., and S. Y. Lee. 2014. Updated estimates of carbon accumulation rates in coastal marsh sediments. Biogeosciences **11**:5057–5071.

Pan, Y., J. Liu, M. Zhang, P. Huang, M. Hipesy, L. Dai, Z. Ma, F. Zhang, Z. Zhang, and Z. Ning. 2024. The below-ground biomass contributes more to wetland soil carbon pools than the above-ground biomass—a survey based on global wetlands. Journal of Plant Ecology **17**.

Panchal, P., C. Preece, J. Penuelas, and J. Giri. 2022. Soil carbon sequestration by root exudates. Trends Plant Sci **27**:749–757.

Parmentier, F. J. W., J. van Huissteden, N. Kip, H. J. M. Op den Camp, M. S. M. Jetten, T. C. Maximov, and A. J. Dolman. 2011. The role of endophytic methane-oxidizing bacteria in submerged Sphagnum in determining methane emissions of Northeastern Siberian tundra. Biogeosciences **8**:1267–1278.

Pavelka, M., M. Acosta, R. Kiese, N. Altimir, C. Brümmer, P. Crill, E. Darenova, R. Fuß, B. Gielen, A. Graf, L. Klemedtsson, A. Lohila, B. Longdoz, A. Lindroth, M. Nilsson, S. M. Jiménez, L. Merbold, L. Montagnani, M. Peichl, M. Pihlatie, J. Pumpanen, P. S. Ortiz, H. Silvennoinen, U. Skiba, P. Vestin, P. Weslien, D. Janous, and W. Kutsch. 2018. Standardisation of chamber technique for CO2, N2O and CH4 fluxes measurements from terrestrial ecosystems. International Agrophysics **32**:569–587.

Pezeshki, S. R., and R. D. DeLaune. 2012. Soil oxidation-reduction in wetlands and its impact on plant functioning. Biology (Basel) **1**:196–221.

Philippot, L., S. Hallin, G. Börjesson, and E. M. Baggs. 2008. Biochemical cycling in the rhizosphere having an impact on global change. Plant and Soil **321**:61–81.

Phillips, R. P., A. C. Finzi, and E. S. Bernhardt. 2011. Enhanced root exudation induces microbial feedbacks to N cycling in a pine forest under long-term CO2 fumigation. Ecol Lett **14**:187–194.

Poffenbarger, H. J., B. A. Needelman, and J. P. Megonigal. 2011. Salinity Influence on Methane Emissions from Tidal Marshes. Wetlands **31**:831–842.

Pollmann, T., M. E. Böttcher, and L. Giani. 2021. Young soils of a temperate barrier island under the impact of formation and resetting by tides and wind. Catena **202**.

Qiu, S., Z. Wang, J. Xu, E. Cui, and L. Yan. 2023. Influence of Vegetation Dynamics on Soil Organic Carbon and Its Fractions in a Coastal Wetland. Ecosystem Health and Sustainability **9**.

Rabenhorst, M. C. 2013. Using Synthesized Iron Oxides as an Indicator of Reduction in Soils. Methods in Biogeochemistry of Wetlands **10**:723–740.

Rabenhorst, M. C., R. R. Bourgault, and B. R. James. 2008. Iron Oxyhydroxide Reduction in Simulated Wetland Soils: Effects of Mineralogical Composition of IRIS Paints. Soil Science Society of America Journal **72**:1838–1842.

Rabenhorst, M. C., and S. N. Burch. 2006. Synthetic iron oxides as an indicator of reduction in soils (IRIS). Soil Science Society of America Journal **70**:1227–1236.

Rafalska, A., A. Walkiewicz, B. Osborne, K. Klumpp, and A. Bieganowski. 2023. Variation in methane uptake by grassland soils in the context of climate change - A review of effects and mechanisms. Sci Total Environ **871**:162127.

Raghoebarsing, A. A., A. J. Smolders, M. C. Schmid, W. I. Rijpstra, M. Wolters-Arts, J. Derksen, M. S. Jetten, S. Schouten, J. S. Sinninghe Damste, L. P. Lamers, J. G. Roelofs, H. J. Op den Camp, and M. Strous. 2005. Methanotrophic symbionts provide carbon for photosynthesis in peat bogs. Nature **436**:1153–1156.

Redelstein, R., T. Dinter, D. Hertel, and C. Leuschner. 2018. Effects of Inundation, Nutrient Availability and Plant Species Diversity on Fine Root Mass and Morphology Across a Saltmarsh Flooding Gradient. Front Plant Sci **9**:98.

Rich, R. L., P. Mueller, M. Fuß, S. Gonçalves, E. Ostertag, S. Reents, H. Tang, A. Tashjian, S. Thomsen, L. Kutzbach, K. Jensen, and S. Nolte. 2023. Design and Assessment of a Novel Approach for Ecosystem Warming Experiments in High-Energy Tidal Wetlands. Journal of Geophysical Research: Biogeosciences **128**.

Ritter, A., P. J. Becker, K. Möller, D. Granse, K. Jensen, I. C. Meier, and H. J. Subrahmaniam. 2025. Targeting the untargeted: Uncovering the chemical complexity of root exudates. Plant and Soil.

Rolando, J. L., M. Kolton, T. Song, and J. E. Kostka. 2022. The core root microbiome of Spartina alterniflora is predominated by sulfur-oxidizing and sulfate-reducing bacteria in Georgia salt marshes, USA. Microbiome **10**:37.

Rosentreter, J. A., A. N. Al-Haj, R. W. Fulweiler, and P. Williamson. 2021a. Methane and Nitrous Oxide Emissions Complicate Coastal Blue Carbon Assessments. Global Biogeochemical Cycles **35**.

Rosentreter, J. A., A. V. Borges, B. R. Deemer, M. A. Holgerson, S. Liu, C. Song, J. Melack, P. A. Raymond, C. M. Duarte, G. H. Allen, D. Olefeldt, B. Poulter, T. I. Battin, and B. D. Eyre. 2021b. Half of global methane emissions come from highly variable aquatic ecosystem sources. Nature Geoscience **14**:225–230.

Rosentreter, J. A., D. T. Maher, D. V. Erler, R. H. Murray, and B. D. Eyre. 2018. Methane emissions partially offset "blue carbon" burial in mangroves. Science Advances **4**.

Ruiz-Fernandez, A. C., V. Carnero-Bravo, J. A. Sanchez-Cabeza, L. H. Perez-Bernal, O. A. Amaya-Monterrosa, S. Bojorquez-Sanchez, P. G. Lopez-Mendoza, J. G.

Cardoso-Mohedano, R. B. Dunbar, D. A. Mucciarone, and A. J. Marmolejo-Rodriguez. 2018. Carbon burial and storage in tropical salt marshes under the influence of sea level rise. Sci Total Environ **630**:1628–1640.

Ruiz-Fernández, A. C., J.-A. Sanchez-Cabeza, T. Cuéllar-Martínez, L. H. Pérez-Bernal, V. Carnero-Bravo, E. Ávila, and J. G. Cardoso-Mohedano. 2020. Increasing salinization and organic carbon burial rates in seagrass meadows from an anthropogenically-modified coastal lagoon in southern Gulf of Mexico. Estuarine, Coastal and Shelf Science **242**.

Rupprecht, F., G. Reichert, B. Merling, and B. Oltmanns. 2023. Renaturierung von Salzwiesen im Nationalpark Niedersächsisches Wattenmeer. Nationalpark Niedersächsisches Wattenmeer.

Saintilan, N., K. Rogers, D. Mazumder, and C. Woodroffe. 2013. Allochthonous and autochthonous contributions to carbon accumulation and carbon store in southeastern Australian coastal wetlands. Estuarine Coastal and Shelf Science **128**:84–92.

Sapkota, Y., C. Duball, K. Vaughan, M. C. Rabenhorst, and J. F. Berkowitz. 2022. Indicator of Reduction in Soil (IRIS) devices: A review. Sci Total Environ **852**:158419.

Saunois, M., A. R. Stavert, B. Poulter, P. Bousquet, J. G. Canadell, R. B. Jackson, P. A. Raymond, E. J. Dlugokencky, S. Houweling, P. K. Patra, P. Ciais, V. K. Arora, D. Bastviken, P. Bergamaschi, D. R. Blake, G. Brailsford, L. Bruhwiler, K. M. Carlson, M. Carrol, S. Castaldi, N. Chandra, C. Crevoisier, P. M. Crill, K. Covey, C. L. Curry, G. Etiope, C. Frankenberg, N. Gedney, M. Hegglin, L. Hoglund-Isaksson, G. Hugelius, M. Ishizawa, A. Ito, G. Janssens-Maenhout, K. M. Jensen, F. Joos, T. Kleinen, P. B. Krummel, R. L. Langenfelds, G. G. Laruelle, L. C. Liu, T. Machida, S. Maksyutov, K. C. McDonald, J. McNorton, P. A. Miller, J. R. Melton, I. Morino, J. Müller, F. Murguia-Flores, V. Naik, Y. Niwa, S. Noce, S. O. Doherty, R. J. Parker, C. H. Peng, S. S. Peng, G. P. Peters, C. Prigent, R. Prinn, M. Ramonet, P. Regnier, W. J. Riley, J. A. Rosentreter, A. Segers, I. J. Simpson, H. Shi, S. J. Smith, L. P. Steele, B. F. Thornton, H. Q. Tian, Y. Tohjima, F. N. Tubiello, A. Tsuruta, N. Viovy, A. Voulgarakis, T. S. Weber, M. van Weele, G. R. van der Werf, R. F. Weiss, D. Worthy, D. Wunch, Y. Yin, Y. Yoshida, W. X. Zhang, Z. Zhang, Y. H. Zhao, B. Zheng, Q. Zhu, Q. A. Zhu, and Q. L. Zhuang. 2020. The Global Methane Budget 2000-2017. Earth System Science Data **12**:1561–1623.

Savage, K., R. Phillips, and E. Davidson. 2014. High temporal frequency measurements of greenhouse gas emissions from soils. Biogeosciences **11**:2709–2720.

Schlesinger, W. H., and E. S. Bernhardt. 2020. Biogeochemistry: An Analysis of Global Change. 4 edition. Academic Press (Elsevier).

Schmidt, H., T. Eickhorst, and R. Tippkötter. 2010. Monitoring of root growth and redox conditions in paddy soil rhizotrons by redox electrodes and image analysis. Plant and Soil **341**:221–232.

Schrama, M., P. Heijning, J. P. Bakker, H. J. van Wijnen, M. P. Berg, and H. Olff. 2013. Herbivore trampling as an alternative pathway for explaining differences in nitrogen mineralization in moist grasslands. Oecologia **172**:231–243.

Schulze, D., K. Jensen, and S. Nolte. 2021. Livestock grazing reduces sediment deposition and accretion rates on a highly anthropogenically altered marsh island in the Wadden Sea. Estuarine, Coastal and Shelf Science **251**.

Segers, R. 1998. Methane production and methane consumption: a review of processes underlying wetland methane fluxes. Biogeochemistry **41**:23–51.

Seitz, V. A., Bridget B. McGivern, Rebecca A. Daly, Jacqueline M. Chaparro, Mikayla A. Borton, Amy M. Sheflin, Stephen Kresovich, Lindsay Shields, Meagan E. Schipanski, Kelly C. Wrighton, and J. E. Prennia. 2022. Variation in Root Exudate Composition In Microbiome Membership and Function. Applied and Environmental Microbiology.

Sela-Adler, M., Z. Ronen, B. Herut, G. Antler, H. Vigderovich, W. Eckert, and O. Sivan. 2017. Co-existence of Methanogenesis and Sulfate Reduction with Common Substrates in Sulfate-Rich Estuarine Sediments. Front Microbiol **8**:766.

Seyfferth, A. L., F. Bothfeld, R. Vargas, J. W. Stuckey, J. Wang, K. Kearns, H. A. Michael, J. Guimond, X. Yu, and D. L. Sparks. 2020. Spatial and temporal heterogeneity of geochemical controls on carbon cycling in a tidal salt marsh. Geochimica et Cosmochimica Acta **282**:1–18.

Sha, C., W. J. Mitsch, Ü. Mander, J. Lu, J. Batson, L. Zhang, and W. He. 2011. Methane emissions from freshwater riverine wetlands. Ecological Engineering **37**:16–24.

Shahzad, A., and H. Gul. 2025. Sensing the dry: Redox-regulated auxin repression shapes root plasticity. Advanced Agrochem.

Sica, Y. V., R. D. Quintana, V. C. Radeloff, and G. I. Gavier-Pizarro. 2016. Wetland loss due to land use change in the Lower Parana River Delta, Argentina. Science of the Total Environment **568**:967–978.

Smith, S. W., S. J. Woodin, R. J. Pakeman, D. Johnson, and R. van der Wal. 2014. Root traits predict decomposition across a landscape-scale grazing experiment. New Phytol **203**:851–862.

Sogin, E. M., D. Michellod, H. R. Gruber-Vodicka, P. Bourceau, B. Geier, D. V. Meier, M. Seidel, S. Ahmerkamp, S. Schorn, G. D'Angelo, G. Procaccini, N. Dubilier, and M. Liebeke. 2022. Sugars dominate the seagrass rhizosphere. Nat Ecol Evol **6**:866–877.

Spivak, A. C., J. Sanderman, J. L. Bowen, E. A. Canuel, and C. S. Hopkinson. 2019. Global-change controls on soil-carbon accumulation and loss in coastal vegetated ecosystems. Nature Geoscience **12**:685–692.

Spohn, M., B. Babka, and L. Giani. 2013. Changes in soil organic matter quality during sea-influenced marsh soil development at the North Sea coast. Catena **107**:110–117.

Stagg, C. L., D. R. Schoolmaster, K. W. Krauss, N. Cormier, and W. H. Conner. 2017. Causal mechanisms of soil organic matter decomposition: deconstructing salinity and flooding impacts in coastal wetlands. Ecology **98**:2003–2018.

Stark, J., T. Van Oyen, P. Meire, and S. Temmerman. 2015. Observations of tidal and storm surge attenuation in a large tidal marsh. Limnology and Oceanography **60**:1371–1381.

Steinberg, L. M., and J. M. Regan. 2008. Phylogenetic comparison of the methanogenic communities from an acidic, oligotrophic fen and an

anaerobic digester treating municipal wastewater sludge. Appl Environ Microbiol **74**:6663–6671.

Stepniewska, Z., W. Goraj, A. Kuzniar, A. Szafranek-Nakonieczna, A. Banach, A. Górski, A. Pytlak, and D. Urban. 2018. Methane Oxidation by Endophytic Bacteria Inhabiting Sphagnum sp. and Some Vascular Plants. Wetlands **38**:411–422.

Steudel, B., Y. Hautier, A. Hector, and M. Kessler. 2011. Diverse marsh plant communities are more consistently productive across a range of different environmental conditions through functional complementarity. Journal of Applied Ecology **48**:1117–1124.

Stewart, G. A., S. J. Sharp, A. K. Taylor, M. R. Williams, and M. A. Palmer. 2024. High spatial variability in wetland methane fluxes is tied to vegetation patch types. Biogeochemistry **167**:1589–1607.

Suchrow, S., and K. Jensen. 2010. Plant Species Responses to an Elevational Gradient in German North Sea Salt Marshes. Wetlands **30**:735–746.

Sulman, B. N., F. M. Yuan, T. O'Meara, B. H. Gu, E. M. Herndon, J. Q. Zheng, P. E. Thornton, and D. E. Graham. 2022. Simulated Hydrological Dynamics and Coupled Iron Redox Cycling Impact Methane Production in an Arctic Soil. Journal of Geophysical Research-Biogeosciences **127**.

Sutton-Grier, A. E., J. K. Keller, R. Koch, C. Gilmour, and J. P. Megonigal. 2011. Electron donors and acceptors influence anaerobic soil organic matter mineralization in tidal marshes. Soil Biology & Biochemistry **43**:1576–1583.

Sutton-Grier, A. E., and J. P. Megonigal. 2011. Plant species traits regulate methane production in freshwater wetland soils. Soil Biology & Biochemistry **43**:413–420.

Suzuki, R. O., and S. N. Suzuki. 2011. Facilitative and competitive effects of a large species with defensive traits on a grazing-adapted, small species in a long-term deer grazing habitat. Plant Ecology **212**:343–351.

Szubryt, M. B., K. Skinner, E. J. O'Loughlin, J. Koval, S. M. Greenwald, S. M. Owens, K. M. Kemner, and P. B. Weisenhorn. 2020. Wetland plant evolutionary history influences soil and endophyte microbial community composition. Preprint.

Taillardat, P., B. S. Thompson, M. Garneau, K. Trottier, and D. A. Friess. 2020. Climate change mitigation potential of wetlands and the cost-effectiveness of their restoration. Interface Focus **10**:20190129.

Tang, H., S. Nolte, K. Jensen, R. Rich, J. Mittmann-Goetsch, and P. Mueller. 2023. Warming accelerates belowground litter turnover in salt marshes – insights from a Tea Bag Index study. Biogeosciences **20**:1925–1935.

Tang, H., S. Nolte, K. Jensen, Z. Yang, J. Wu, and P. Mueller. 2020. Grazing mediates soil microbial activity and litter decomposition in salt marshes. Sci Total Environ **720**:137559.

Temmink, R. J. M., L. P. M. Lamers, C. Angelini, T. J. Bouma, C. Fritz, J. van de Koppel, R. Lexmond, M. Rietkerk, B. R. Silliman, H. Joosten, and T. van der Heide. 2022. Recovering wetland biogeomorphic feedbacks to restore the world's biotic carbon hotspots. Science **376**:eabn1479.

Tessier, M., J. P. Vivier, A. Ouin, J. C. Gloaguen, and J. C. Lefeuvre. 2003. Vegetation dynamics and plant species interactions under grazed and ungrazed

conditions in a western European salt marsh. Acta Oecologica-International Journal of Ecology **24**:103–111.

Turner, J. C., C. J. Moorberg, A. D. Wong, K. Shea, M. P. Waldrop, M. R. Turetsky, and R. B. Neumann. 2020. Getting to the Root of Plant-Mediated Methane Emissions and Oxidation in a Thermokarst Bog. Journal of Geophysical Research-Biogeosciences **125**.

Van de Broek, M., S. Temmerman, R. Merckx, and G. Govers. 2016. Controls on soil organic carbon stocks in tidal marshes along an estuarine salinity gradient. Biogeosciences **13**:6611–6624.

van den Berg, M., E. van den Elzen, J. Ingwersen, S. Kosten, L. P. M. Lamers, and T. Streck. 2020. Contribution of plant-induced pressurized flow to CH(4) emission from a Phragmites fen. Sci Rep **10**:12304.

Van der Nat, F. J., and J. J. Middelburg. 2000. Methane emission from tidal freshwater marshes. Biogeochemistry **49**:103–121.

Van Hulzen, J. B., R. Segers, P. M. Van Bodegom, and P. A. Leffelaar. 1999. Temperature effects on soil methane production: An explanation for observed variability. Soil Biology and Biochemistry **31**:1919–1929.

Visser, E. J. W., T. D. Colmer, C. W. P. M. Blom, and L. A. C. J. Voesenek. 2008. Changes in growth, porosity, and radial oxygen loss from adventitious roots of selected mono- and dicotyledonous wetland species with contrasting types of aerenchyma. Plant, Cell & Environment **23**:1237–1245.

Vroom, R. J. E., M. van den Berg, S. R. Pangala, O. E. van der Scheer, and B. K. Sorrell. 2022. Physiological processes affecting methane transport by wetland vegetation - A review. Aquatic Botany **182**.

Waldo, N. B., B. K. Hunt, E. C. Fadely, J. J. Moran, and R. B. Neumann. 2019. Plant root exudates increase methane emissions through direct and indirect pathways. Biogeochemistry **145**:213–234.

Wang, Q., L. Chen, H. Xu, K. Ren, Z. Xu, Y. Tang, and J. Xiao. 2021. The effects of warming on root exudation and associated soil N transformation depend on soil nutrient availability. Rhizosphere **17**.

Wang, W., C. Zeng, J. Sardans, C. Wang, C. Tong, and J. Peñuelas. 2018. Soil Methane Production, Anaerobic and Aerobic Oxidation in Porewater of Wetland Soils of the Minjiang River Estuarine, China. Wetlands **38**:627–640.

Wanner, A. 2009. Management, biodiversity and restoration potential of salt grassland vegetation of the Baltic Sea: Analyses along a complex ecological gradient. Dissertation. Universität Hamburg, Hamburg, Germany.

Wen, Z., P. J. White, J. Shen, and H. Lambers. 2022. Linking root exudation to belowground economic traits for resource acquisition. New Phytol **233**:1620–1635.

Weston, N. B., and S. B. Joye. 2005. Temperature-driven decoupling of key phases of organic matter degradation

in marine sediments. Proceedings of the National Academy of Sciences of the United States of America **102**:17036–17040.

Whitaker, K., K. Rogers, N. Saintilan, D. Mazumder, L. Wen, and R. J. Morrison. 2015. Vegetation persistence and carbon storage: Implications for environmental water management for Phragmites australis. Water Resources Research **51**:5284–5300.

Whiting, G., and J. Chanton. 1993. Primary production control of methane emission from wetlands. Nature.

Wilson, A. M., M. Shanahan, and E. M. Smith. 2021. Salt Marshes as Groundwater Buffers for Development: A Survey of South Carolina Salt Marsh Basins. Frontiers in Water **3**.

Wilson, R. M., A. M. Hopple, M. M. Tfaily, S. D. Sebestyen, C. W. Schadt, L. Pfeifer-Meister, C. Medvedeff, K. J. McFarlane, J. E. Kostka, M. Kolton, R. K. Kolka, L. A. Kluber, J. K. Keller, T. P. Guilderson, N. A. Griffiths, J. P. Chanton, S. D. Bridgham, and P. J. Hanson. 2016. Stability of peatland carbon to rising temperatures. Nat Commun **7**:13723.

Wilson, S. J., B. Bond-Lamberty, G. Noyce, R. Bittencourt Peixoto, and J. P. Megonigal. 2024. fluxfinder: An R Package for Reproducible Calculation and Initial Processing of Greenhouse Gas Fluxes From Static Chamber Measurements. Journal of Geophysical Research: Biogeosciences **129**.

Wiszniewska, A., A. Kozminska, E. Hanus-Fajerska, M. Dziurka, and K. Dziurka. 2019. Insight into mechanisms of multiple stresses tolerance in a halophyte Aster tripolium subjected to salinity and heavy metal stress. Ecotoxicol Environ Saf **180**:12–22.

Witte, S., and L. Giani. 2016. Greenhouse Gas Emission and Balance of Marshes at the Southern North Sea Coast. Wetlands **36**:121–132.

Wolf, A. A., B. G. Drake, J. E. Erickson, and J. P. Megonigal. 2007. An oxygen-mediated positive feedback between elevated carbon dioxide and soil organic matter decomposition in a simulated anaerobic wetland. Global Change Biology **13**:2036–2044.

Xiao, K. Q., F. Beulig, H. Roy, B. B. Jorgensen, and N. Risgaard-Petersen. 2018. Methylotrophic methanogenesis fuels cryptic methane cycling in marine surface sediment. Limnology and Oceanography **63**:1519–1527.

Yang, D., A. B. Jensen, B. K. Sorrell, H. Brix, and F. Eller. 2024. Rising water levels increase CH4 emissions and decrease CO2 exchange in a temperate salt marsh. Limnology and Oceanography **70**:291–304.

Yarwood, S. A. 2018. The role of wetland microorganisms in plant-litter decomposition and soil organic matter formation: a critical review. FEMS Microbiol Ecol **94**.

Yin, S., S. An, Q. Deng, J. Zhang, H. Ji, and X. Cheng. 2015. Spartina alterniflora invasions impact CH4 and N2O fluxes from a salt marsh in eastern China. Ecological Engineering **81**:192–199.

Yuan, J., D. Liu, Y. Ji, J. Xiang, Y. Lin, M. Wu, W. Ding, and G. Bielefeld Nardoto. 2019. Spartina alterniflora invasion drastically increases methane production potential by shifting methanogenesis from hydrogenotrophic to methylotrophic pathway in a coastal marsh. Journal of Ecology **107**:2436–2450.

Yvon-Durocher, G., A. P. Allen, D. Bastviken, R. Conrad, C. Gudasz, A. St-Pierre, N. Thanh-Duc, and P. A. del Giorgio. 2014. Methane fluxes show consistent temperature dependence across microbial to ecosystem scales. Nature **507**:488–491.

Zhai, X., N. Piwpuan, C. A. Arias, T. Headley, and H. Brix. 2013. Can root exudates from emergent wetland plants fuel denitrification in subsurface flow constructed wetland systems? Ecological Engineering **61**:555–563.

Zhang, Q., J. J. Acuna, N. G. Inostroza, M. L. Mora, S. Radic, M. J. Sadowsky, and M. A. Jorquera. 2019. Endophytic Bacterial Communities Associated with Roots and Leaves of Plants Growing in Chilean Extreme Environments. Sci Rep **9**:4950.

Zhang, Y., X. Zhang, W. Fang, Y. Cai, G. Zhang, J. Liang, J. Chang, L. Chen, H. Wang, P. Zhang, Q. Wang, and Y. Zhang. 2025. Carbon sequestration potential of wetlands and regulating strategies response to climate change. Environ Res **269**:120890.

Zhang, Z., and A. Furman. 2021. Soil redox dynamics under dynamic hydrologic regimes - A review. Sci Total Environ **763**:143026.

Zhou, Y., T. O'Meara, Z. G. Cardon, J. Wang, B. N. Sulman, A. E. Giblin, and I. Forbrich. 2024. Simulated plant-mediated oxygen input has strong impacts on fine-scale porewater biogeochemistry and weak impacts on integrated methane fluxes in coastal wetlands. Biogeochemistry **167**:945–963.

Zhu, G., Y. Wang, A. Huang, and Y. Qin. 2025. Research Status and Development Trend of Greenhouse Gas in Wetlands: A Bibliometric Visualization Analysis. Ecol Evol **15**:e70938.

ACKNOWLEDGEMENTS

Danksagung

Zunächst gilt mein aufrichtiger Dank meinen Betreuern Kai Jensen und Peter Müller. Ich danke euch für die Unterstützung und Begleitung während der vergangenen acht Jahre. Ihr habt meinen Weg in die Wissenschaft geprägt und mich wachsen lassen. Ich freue mich sehr auf die weitere Zusammenarbeit. Auch danke ich euch beiden dafür, dass ihr mir mehrere Auslandsaufenthalte ermöglicht habt, die mich wissenschaftlich bereichert und meinen Horizont entscheidend erweitert haben.

Mein herzlicher Dank gilt außerdem der gesamten Arbeitsgruppe Angewandte Pflanzenökologie, in der ich all meine Studien abschließen durfte. Ich bin unglaublich dankbar, Teil dieser offenen, hilfsbereiten und herzlichen Gruppe zu sein, und freue mich auf gemeinsame Projekte in der Zukunft.

Ein besonderer Dank geht an Claudia Mählmann und Anna Knöpfle für ihre stete organisatorische Unterstützung, ihre Geduld und ihren unermüdlichen emotionalen Rückhalt.

Ebenso danke ich Viktoria und Monica, meinen Co-Betreuerinnen, für ihre wertvolle Unterstützung, insbesondere bei der Zusammenstellung dieser Dissertation, und für die vielen inspirierenden Brainstorming-Sitzungen.

Liebe Caroline, meine unermüdliche Partnerin in Feldarbeit, ohne dich gäbe es diese Arbeit wohl nur zur Hälfte. Wie schön, dass du im Dezember 2023 geblieben bist und auch im Dezember 2025 immer noch mit mir zusammenarbeitest. Am wichtigsten ist die Freundschaft, die daraus entstanden ist.

Mein Dank gilt auch meinen Freundinnen und Kolleginnen Ella, Julian und Diana für die wunderbare Arbeitsatmosphäre, die wir gemeinsam geschaffen haben und weiterhin schaffen werden.

Von Herzen danke ich schließlich meiner Familie – insbesondere Katrin und Claus – sowie all meinen Freundinnen und Freunden für ihr Verständnis, ihre Geduld und ihre bedingungslose Unterstützung. Ihr habt mir den Freiraum gegeben, meinen eigenen Weg zu gehen, so zu arbeiten und zu sein, wie ich bin.

Eidesstattliche Versicherung

Hiermit versichere ich an Eides statt, die vorliegende Dissertationsschrift selbst verfasst und keine anderen als die angegebenen Hilfsmittel und Quellen benutzt zu haben. Sofern im Zuge der Erstellung der vorliegenden Dissertationsschrift generative Künstliche Intelligenz (gKI) basierte elektronische Hilfsmittel verwendet wurden, versichere ich, dass meine eigene Leistung im Vordergrund stand und dass eine vollständige Dokumentation aller verwendeten Hilfsmittel gemäß der Guten wissenschaftlichen Praxis vorliegt. Ich trage die Verantwortung für eventuell durch die gKI generierte fehlerhafte oder verzerrte Inhalte, fehlerhafte Referenzen, Verstöße gegen das Datenschutz- und Urheberrecht oder Plagiate.

Affidavit

I hereby declare and affirm that this doctoral dissertation is my own work and that I have not used any aids and sources other than those indicated. If electronic resources based on generative artificial intelligence (gAI) were used in the course of writing this dissertation, I confirm that my own work was the main and value-adding contribution and that complete documentation of all resources used is available in accordance with good scientific practice. I am responsible for any erroneous or distorted content, incorrect references, violations of data protection and copyright law or plagiarism that may have been generated by the gAI.

Hamburg, den 15.12.2025 Clarisse Gösele